Bulletin
of
The Geological Society of America

VOLUME 70 August 1959 NUMBER 8

CONTENTS

Pages

Igneous rocks and constituent hornblendes of the Henry Mountains, Utah. By Celeste G. Engel 951–980

Origin of the ultramafic complex at Union Bay, southeastern Alaska. By John C. Ruckmick and James A. Noble 981–1018

Fused-quartz extensometer for secular, tidal, and seismic strains. By Hugo Benioff 1019–1032

History of Imuruk Lake, Seward Peninsula, Alaska. By David M. Hopkins 1033–1046

Gravity tectonics in the Naukluft Mountains of South West Africa. By Hermann Korn and Henno Martin (Translated by John G. Dennis) 1047–1078

Thrust faulting in Sinking Valley, Blair and Huntingdon counties, Pennsylvania. By N. N. Moebs and R. B. Hoy 1079–1088

Turbidites in flysch of the Polish Carpathian Mountains. By S. Dzulynski, M. Ksiazkiewicz, and Ph. H. Kuenen 1089–1118

Short Note

Chemistry of granophyres from Wichita lopolith, Oklahoma. By Warren Hamilton 1119–1126

Subscription $15.00 per year.

Printing Office: Mt. Royal & Guilford Aves., Baltimore 2, Md.

Communications for publications should be addressed to The Geological Society of America, Dr. H. R. Aldrich, Secretary, 419 West 117 Street, New York 27, N. Y.

Please give notice of change of address 4 weeks in advance. Claims for nonreceipt of the Bulletin of a given month must be sent to the Secretary of the Society before the end of the second succeeding month.

Second-class postage paid at Baltimore, Md.
Accepted for mailing at special rate of postage provided for in Section 1103
Act of October 3, 1917, authorized on July 8, 1918.

PAPERS IN PRESS FOR FORTHCOMING ISSUES

Geologic Evolution of the Beartooth Mountains, Montana and Wyoming. Part 3. Gardner Lake Area, Wyoming. By Rae L. Harris, Jr.

Geochemical Table of the Elements for 1959. By Jack Green

Stratigraphic-Sedimentary Significance of Contemporary Climate and Relief in Four Regions of the Andes Mountains. By H. F. Garner

Precambrian Rocks of the Hall Valley Area, Front Range, Colorado. By Ernest E. Wahlstrom and Ok Joon Kim

Inspissation of Post-Oligocene Sediments in Southern Louisiana. By Robert W. Crouch

Geology of Continental Shelf off Louisiana: Its Influence on Offshore Foundation Design By Harold N. Fisk and Bramlette McClelland

BULLETIN OF THE GEOLOGICAL SOCIETY OF AMERICA
VOL. 70, PP. 951-980, 4 FIGS. AUGUST 1959

IGNEOUS ROCKS AND CONSTITUENT HORNBLENDES OF THE HENRY MOUNTAINS, UTAH

BY CELESTE G. ENGEL

ABSTRACT

The dominant intrusive igneous rock in the Henry Mountains is diorite porphyry. This rock is chemically and mineralogically montonous through the stocks, laccoliths, bysmaliths, and dikes. The aggregate volume exceeds 16 cubic miles. Locally the diorite porphyry is cut by and grades into monzonite porphyry which is more variable in composition but constitutes only 5 per cent of the exposed rock.

Most hornblende phenocrysts in the diorite porphyry are also chemically alike, with molecular proportions of FeO/MgO of about 0.9 to 1.1. In one coarse-grained laccolith the large hornblende phenocrysts have a molecular proportion of FeO/MgO of about 0.4. This more magnesian hornblende is compositionally similar to most hornblendes from the hornblendite and amphibolite inclusions in the diorite porphyry.

Except for relatively high Na content, the diorite porphyry of the Henry Mountains could have been derived by the tapping of the upper portions of a typical andesitic parent magma from which early formed crystals of hornblende and pyroxene have settled. The monzonitic variant appears to represent a differentiate of the diorite. The inclusions are interpreted to be early formed mafic hoods or crystal segregates from the parent magma. Possibly, however, they are xenoliths of amphibolite or basaltic crust.

CONTENTS

TEXT

	Page
Introduction and acknowledgments	952
General geology	952
Present investigation	954
Sampling	954
General program	954
Sample collection	954
Petrographic analytical methods	955
Preparation of rock samples	955
Chemical analytical methods	955
Wet chemical analyses	955
Spectrographic analyses	956
Rock composition	956
Introduction	956
Mt. Ellen complex	957
Mt. Pennell complex	964
Mt. Hillers complex	965
Petrology	968
Hornblendes	971
Introduction	971
Sample preparation	971
Optical properties	973
Chemical composition	973
Wet chemical analyses	973
Spectrographic analyses	974
Comparisons with other hornblendes	976
Origin	978
References cited	980

ILLUSTRATIONS

Figure	Page
1. Generalized geologic map of part of the Henry Mountains, Utah	953
2. Vertical section along Bull Creek laccolith showing location of samples cited in Table 4	959
3. Composition of average diorite porphyry from the Henry Mountains plotted on a variation diagram derived from Daly's average basalt, andesite, dacite, rhyolite	968
4. Relations of hornblendes from the Henry Mountains to hornblendes from various rock types	979

TABLES

Table	Page
1. Size range of hornblende phenocrysts separated for chemical analyses	955
2. Limits of detection for semiquantitative spectrographic analyses by Myers and Oda	956
3. Modal and chemical analyses of diorite porphyries of the Henry Mountains, Utah	958
4. Modal and chemical analyses of diorite porphyry from the Bull Creek laccolith	960
5. Modal and chemical analyses of diorite porphyry from the Bull Mountain bysmalith	963
6. Modal and spectrographic analyses of diorite porphyries from the Mt. Ellen stock and shattered zone	964
7. Modal and chemical analyses of monzonite porphyry, Mt. Pennell complex	966
8. Variations in trace-element composition of diorite and monzonite porphyries	967

Table		Page
9.	Modal and spectrographic analyses of diorite porphyry from intrusive bodies in the northeast portion of the Mt. Hillers complex	967
10.	Average diorite porphyry from the Henry Mountains and hypothetical rock derived by adding 13 per cent hornblende (by weight)	969
11.	Igneous rocks of western United States similar in composition to diorite porphyry of the Henry Mountains	970
12.	Analyses of hornblendes	972
13.	Structural formulae of hornblendes	973
14.	Spectrographic and partial chemical analyses of hornblendes from diorite porphyries and inclusions	975
15.	Spectrographic analyses of identical hornblende samples, made in different laboratories	976
16.	Chemical analyses of hornblendes from other igneous rocks, inclusions and amphibolites, compared with composition of hornblende from the Henry Mountains, Utah	977

Introduction and Acknowledgments

This investigation is part of a program of the United States Geological Survey to determine the composition of igneous rocks. The porphyritic rocks of the Henry Mountains, Utah, were chosen because they are definitely igneous and include a variety of hypabyssal intrusive bodies closely related in space and time of development. The intrusive bodies are stocks, laccoliths, bysmaliths, and dikes and sills that are well exposed. Their form and distribution have been carefully determined (Hunt, 1953). The rocks are almost entirely diorite porphyry with rare monzonite porphyry.

The study reported herein had two major objectives. One of these was to determine the variations in physical properties and chemical composition of the porphyries from place to place within a single intrusive body and between bodies. A second objective, only partly accomplished, was to learn more of the properties of the hornblendes that are the principal mafic mineral in both porphyries and inclusions in the porphyries. This phase of the work has been limited because of widespread, although not extreme, alteration of the hornblendes.

Chemical analyses are reported for five hornblende phenocrysts and for one hornblende from a hornblende inclusion. Partial chemical data are reported for nine other hornblendes from hornblendite and amphibolite inclusions.

The manuscript has been read and greatly improved by the constructive comments of A. F Buddington, M. F. Fleischer, Charles B. Hunt, and A. T. Miesch. Miss Priscilla Patton contributed editorial assistance in the assembly of the paper. I wish to thank my husband, A. E. Engel, for assistance throughout the work.

General Geology

The general geology of the Henry Mountains region is well known from Gilbert's pioneer work (1877) and later studies by Hunt (1953). The Henry Mountains are a series of structural domes that lie within a broad structural basin in the Colorado Plateau. The basin is diamond-shaped, measuring roughly 100 miles long and 50 miles wide. Its axis trends in a general northward direction in accordance with associated structural uplifts and depressions of the Colorado Plateau in southeastern Utah.

There are five Henry Mountain domes. Each of the four southern domes is 6–8 miles in diameter. The northern dome, the Mt. Ellen complex, is about 10 miles in diameter. Each of the domes has a structural relief of several thousand feet. They occur on the gentle east flank of the surrounding structural basin. The basin was developed probably in late Cretaceous or early Tertiary time. The intrusions and doming of the Henry Mountains appear to have followed the development of the basin, possibly in the early or middle Tertiary (Hunt, 1953, p. 88).

Each of the domes of the Henry Mountains consists of a central stock around which laccoliths, dikes, sills, and bysmaliths are clustered. All these intrusions were formed by the injection of magma into the sedimentary strata with little or no stoping, incorporation, or assimilation of the wall rock. The larger stocks contain minor deposits of metal sulfides that are rare or absent in the other intrusive bodies. Each stock is surrounded by a shattered zone of the enclosing sedimentary rocks variously injected by igneous rock. The laccoliths radiate from the central stocks and the surrounding shattered zone and are roughly concordant with the bedding in the intruded sedimentary rocks. Gilbert (1877) noted that the laccoliths raised the overlying sedimentary rocks by arching the beds. The outermost intrusive types, the bysmaliths, raised their roofs by faulting (Hunt, 1953, p. 90). Evidence assembled by Hunt suggests that the laccoliths and bysmaliths were injected radially from conduits now filled by the

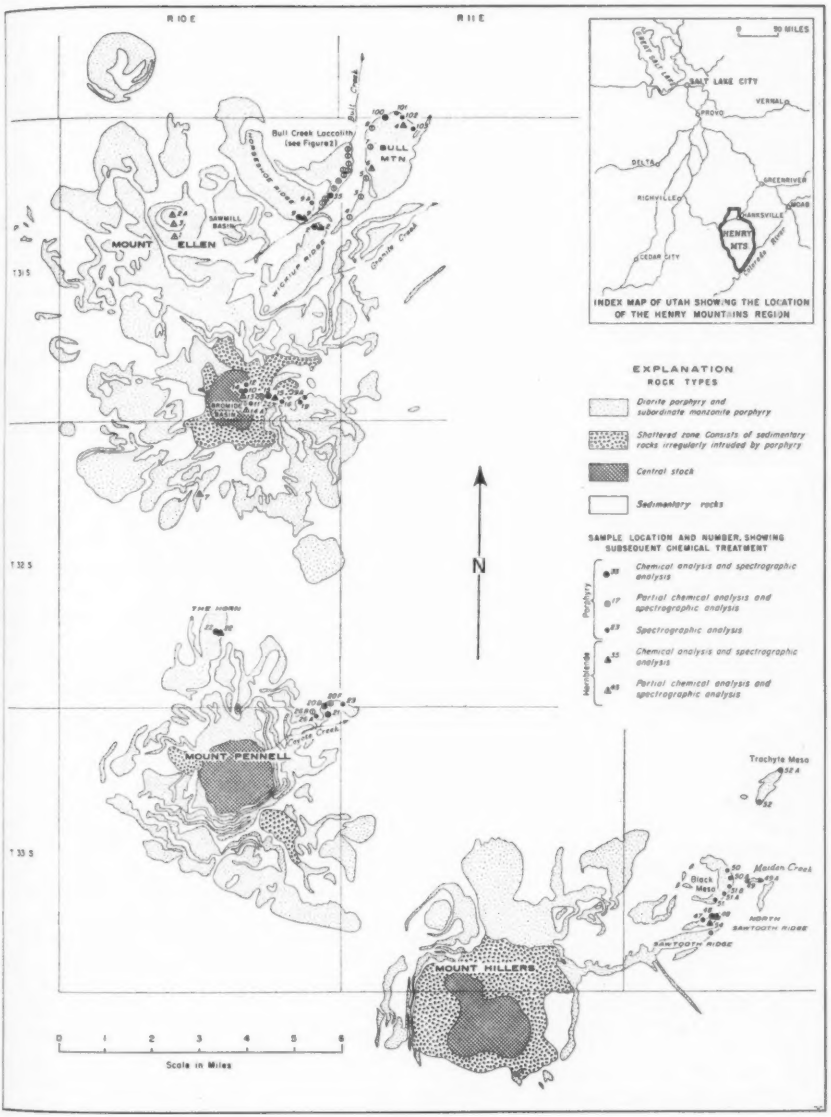

FIGURE 1.—GENERALIZED GEOLOGIC MAP OF PART OF THE HENRY MOUNTAINS, UTAH (After Hunt, 1953) Showing location and type of samples and subsequent chemical treatment.

central stocks. Metamorphism of the sediments adjacent to the intrusive bodies is very slight. Some of the shales and siltstones appear to be slightly baked and reconstituted at and within a few feet of the contact. Grain size of the sediments is not appreciably increased by the metamorphism.

Throughout the Henry Mountains the dominant intrusive rock (95 per cent by volume) is diorite porphyry. Subordinate monzonite

porphyry occurs on Mt. Pennell and very locally on Mt. Ellen (Fig. 1). Other igneous rock types, a few aplite and basalt dikes, total a fraction of 1 per cent of the total igneous rocks (Hunt, 1953, p. 152).

All the igneous rocks of the Henry Mountains show alteration effects which are either deuteric or hydrothermal. This alteration is manifested principally in sericitization of the feldspars and the replacement of hornblende by chlorite, calcite, epidote, iron oxides, and minor amounts of serpentine. The amount of alteration varies but reaches a maximum in parts of the stocks and shattered zones, in the roofs of laccoliths, and in some dikes which form outlying intrusive bodies. Alteration is only slight to moderate in many internal parts of the stocks, laccoliths, and bysmaliths.

Present Investigation

The present investigation of the igneous rocks in the Henry Mountains was begun in July 1956 when Charles B. Hunt and T. S. Lovering accompanied me on a tour of the Henry Mountains and the La Sal Mountains. Hunt's maps and detailed knowledge of the geology and geography of the Henry Mountains were used as a basis for evaluating the intrusive rocks as a source of samples suitable for more detailed study of rock composition. After this trip my husband and I worked 5 weeks in the field, walking out the intrusive bodies and sampling them. The northern part of the area was revisited in September 1957 for additional samples. Hunt contributed samples of hornblende-rich inclusions from several relatively inaccessible areas which I did not visit.

Sampling

General Program

In the sampling program, an attempt was made to obtain least altered samples of igneous rock from the following occurrences: (1) central stocks, (2) peripheral shattered zones that envelop the stocks, (3) laccoliths radiating outward from the central stocks, (4) bysmaliths associated with the outlying laccoliths, and (5) outlying dikes and sills.

Specimens of hornblende, the dominant mafic mineral in the igneous rocks, were obtained from laccoliths and the Mt. Ellen shattered zone of the Henry Mountains. In addition hornblendes were obtained from the hornblendite and amphibolite inclusions which are fairly abundant in the igneous rocks. The location of samples and description of chemical work employed are shown in Figure 1. The selection of sample sites was controlled by the abundance of altered rocks, by limited exposures, and by relative inaccessibility of many intrusives.

Most rock samples were taken from the Mt. Ellen intrusive complex[1] which is well exposed, not highly altered, and by far the most accessible. Within the Mt. Ellen complex studies were made of the major and minor element composition of the stock, its shattered zone, and intrusive bodies radiating to the northeast. These include the Wickiup Ridge, Horseshoe Ridge, and Bull Creek laccoliths and the Bull Mountain bysmalith (Fig. 1). Variations of composition within the Bull Creek laccolith were also studied. It was sampled from proximal to distal end and from exposures near the inferred floor to its roof.

Specimens of porphyry containing hornblende phenocrysts were obtained from the following intrusive bodies: (1) Mt. Ellen complex: Wickiup Ridge laccolith, Horseshoe Ridge laccolith, and shattered zone enveloping the central stock; (2) Mt. Pennell complex: Horn laccolith; (3) Mt. Hillers complex: North Sawtooth Ridge laccolith. Specimens of hornblende from hornblendite and amphibolite inclusions were obtained from the Mt. Ellen, Mt. Pennell, and Mt. Hillers complexes.

Sample Collection

Most of the porphyries are devoid of obvious planar and linear elements, although locally one or both of these features are well developed. Two types of samples were collected: (1) samples weighing approximately 2 pounds for petrographic study and chemical analyses, and (2) larger samples, weighing 10-20 pounds. The large samples were taken at localities where both total rock composition and the composition of the constituent hornblendes were to be studied. Many larger samples were rejected later because of alteration effects in the hornblendes not detected in the field.

All samples were collected at least 4 inches below exposed surfaces of rock. At each locality least altered rock types were sought, because the object of the study was to investigate primary differences in composition. As already

[1] The word complex is used to designate the variety of intrusive forms such as laccoliths, bysmaliths, dikes, and sills associated with each of the central stocks in the Henry Mountains.

noted, however, most of the rocks of the Henry Mountains have been altered by deuteric or hydrothermal processes, and in some places such as the upper parts of several laccoliths, unaltered rock is rare or nonexistent.

Petrographic Analytical Methods

Petrographic study of all samples was made to select those best suited for further analysis. From two to five thin sections were cut from each sample, depending upon its size and textural features. One section of each sample was etched with hydrofluoric acid, and the K feldspars were stained with a 50 per cent solution of sodium cobaltinitrite as described by Chayes (1952). Other sections were unstained. Although much of the K feldspar in the groundmass is less than .02 mm in diameter it acquired a faint yellow tint as a result of the staining. Inasmuch as the feldspar grains are dispersed almost uniformly through the groundmass it became more readily distinguished from coarser plagioclase and other phenocrysts. In several samples the groundmass is coarse—many grains between .009 and .02 mm—and in these stained sections about 30 per cent of the groundmass is K feldspar. Presumably rocks with finer groundmass but with the same amounts and kinds of phenocrysts and the same bulk chemical composition have about this same amount of K feldspar in the groundmass.

Phenocrysts of K feldspar appear principally in what Hunt (1953, p. 155) defines as monzonite porphyry. They acquire a bright yellow stain and are readily differentiated from plagioclase and from quartz.

Modal analyses of the minerals in thin section were made with a point counter. The amounts of each mineral were tabulated on a laboratory counter. Normally 1000–1500 counts were made per section. In coarser-grained samples, especially those from which hornblende was extracted, as many as five thin sections were counted. The sections were cut at intervals of about 2 inches in the rock specimens, and the remaining fragments were ground for chemical analysis and mineral separation.

In most specimens there is no sharp break in size between those grains defined as phenocrysts and groundmass. In the tabulated modes "groundmass" invariably includes grains less than .01 mm in size. The cutoff between groundmass and phenocrysts is not, however, precisely the same in all specimens. In many specimens where the groundmass is relatively coarse-grained and involves a subtle transition in grain size to "phenocrysts", the cutoff between the two textural types is closer to .02 or .04 mm.

Table 1.—Size Range of Hornblende Phenocrysts Separated for Chemical Analyses

(In millimeters)

	1 (HM 15)	2 (HM 22)	3 (HM 9)	4 (HM 48)	5 (HM 2)
Maximum...	1.20	1.00	1.80	1.60	28.00
Minimum...	.04	.04	.04	.04	.04
Mean.....	.20	.15	.40	.35	1.00

1. (HM 15) Diorite porphyry, shattered zone, Mt. Ellen complex.
2. (HM 22) Diorite porphyry, Horn laccolith, Mt. Pennell complex.
3. (HM 9) Diorite porphyry, Horseshoe Ridge laccolith, Mt. Ellen complex.
4. (HM 48) Diorite porphyry, North Sawtooth Ridge laccolith, Mt. Hillers complex.
5. (HM 2) Diorite porphyry, Wickiup Ridge laccolith, Mt. Ellen complex.

Hornblende crystals were easily counted except where the hornblende is appreciably altered by iron oxides. In general hornblendes less than .04 mm are included in the groundmass. Grain size and locations of hornblende phenocrysts that have been analyzed chemically are given in table 1.

Grains of opaque minerals, largely magnetite and hematite, were counted if they were .02 mm or larger.

Preparation of Rock Samples

Representative chips were crushed to approximately a quarter of an inch in a jaw crusher and pulverized on ceramic plates to −100 mesh. About 20 grams of the −100-mesh fraction was split off for chemical analyses of major and minor elements. Approximately 5 grams of the −100 mesh was pulverized to −200 mesh for spectrographic analysis of trace elements. The remainder of the −100-mesh sample (3–5 pounds) was used to obtain a hornblende separation where possible.

Chemical Analytical Methods

Wet Chemical Analyses

Wet chemical analyses of rocks and hornblendes were made by me. Analytical proce-

dures employed were largely classical gravimetric techniques slightly modified after Shapiro and Brannock (1956). A complete description of methods of analysis is published elsewhere (Engel and Engel, 1958).

During the analytical work on the rock specimens, the standard G-1 (Fairbairn *et al.*, 1951) also was partly analyzed as a means of establishing reproducibility and error.

The determinations for Na_2O, K_2O, TiO_2, and MnO of the hornblende samples were run with the standard W-1. These determinations and the adjusted mean values of W-1 (Fairbairn, 1953), are given at the bottom of Table 12.

Spectrographic Analyses

Spectrographic analyses of rocks and hornblendes listed in Tables 3 and 15 were done twice, once by U. Oda and E. F. Cooley of the U. S. Geological Survey and independently by Elisabeth Godijn at the California Institute of Technology. All other rock and mineral samples were analyzed by Oda and Cooley.

The analytical method used by Oda and Cooley was largely designed by Alfred T. Myers (Personal communication). It is a semiquantitative method used for the rapid scanning of samples for many elements, where the spectral lines of the unknown samples are visually compared with the same spectral lines on standard films. Both sample and standard powders are weighed and arced under standardized conditions in the presence of added graphite powder. Ten mg of the samples or standard was mixed with 20 mg of graphite powder and arced for a 90-second exposure time on a 20-inch strip of film in the spectrograph to record the spectra. The spectral region from 2060 to 4840 Å is recorded in the second order. Each film is exposed to 16–18 samples. The spectrum of each sample is compared with standard spectra by means of a projection-type visual comparator, for the estimation of element concentration. Table 2 indicates the limits of detection of the analytical methods employed by Oda and Cooley.

Spectrographic analyses were made on 70 specimens. Fifteen of the analyses were made in duplicate at different times as one means of establishing reproducibility of the spectrographic analyses.

In general, the spectrographic analyses done at different times in the Denver laboratory are reproducible within 25–50 per cent of the number reported for all elements except Cu, Pb, and Zr. Values for Cu from the same rock analyzed 2 months apart vary as much as 500 per cent. The Pb and Zr values differ by about 100 per cent.

TABLE 2.—LIMITS OF DETECTION FOR SEMIQUANTITATIVE SPECTROGRAPHIC ANALYSES BY MYERS AND ODA
(In parts per million)

Ag	1	Cr	20	Sc	20
As	500	Cu	5	Sn	10
B	10	Ga	10	Sr	20
Ba	10	Ge	10	Ti	10
Be	1	La	50	V	10
Bi	5	Mo	10	Y	10
Cd	20	Mn	10	Zn	200
Co	10	Ni	5	Zr	10
		Pb	10		

Spectrographic analyses employed by the California Institute of Technology are described in Engel and Engel (1958).

ROCK COMPOSITION

Introduction

The chemical and mineralogical composition of the rocks in the Henry Mountains has been reported by Hunt, who published 22 chemical analyses (1953, p. 154). Although these chemical analyses were not accompanied by modes, they suggest a remarkable uniformity in composition of the rocks within the several bodies of a single intrusive complex as well as between complexes. It seemed useful to attempt a more extended study of the chemistry and mineralogy of the igneous rocks to evaluate these compositional relations in more detail.

In this work about 80 specimens of igneous rocks have been studied. About 50 of these specimens come from the Mt. Ellen complex, and the remaining specimens are from the Mt. Pennell and Mt. Hillers complexes. The distribution of these rocks in the various intrusives is shown in Figure 1. Detailed modal analyses were made on all the specimens. Thirty-nine modal analyses appear in Tables 3, 4, 5, 6, 7, and 9.

Most of the work was done on diorite porphyry. The only other rock type studied was monzonite porphyry.

The following generalizations may be made on the basis of the present investigation. The

diorite porphyry averages about 55 per cent groundmass, although variations from 35 to 63 per cent are recorded. Plagioclase feldspar (32 per cent) and hornblende (10 per cent) occur as phenocrysts in the groundmass. The remaining 3 per cent is composed of augite, rounded quartz grains, iron oxides, calcite, chlorite, epidote, sphene, biotite, zircon, and locally serpentine, allanite, and clinozoisite. The groundmass is dense, light gray, and contains abundant, evenly distributed large white phenocrysts of plagioclase and smaller amounts of dark, finer-grained hornblende. A few crystals of sphene are large enough to identify in the hand specimens. Marked variations in texture are common within some of the porphyries, and in a few cases important textural variations occur within a single intrusive body. These variations coincide locally, in both abrupt and subtle transitions to a more monzonitic rock that contains phenocrysts of augite and K feldspar as well as plagioclase. Hunt (1953, p. 91, 115) concludes that the monzonite is confined to the Mt. Pennell complex, but two samples that I collected in the Mt. Ellen stock contain phenocrysts of K feldspar and are similar to the monzonite from Mt. Pennell in total mineralogical composition. Within the diorite porphyry measurable variations are found in: (1) amount and grain size of the groundmass and phenocrysts; (2) mineralogy, especially the local appearance of augite or quartz as phenocrysts; (3) texture, from the widespread massive rocks to slightly foliated and lineated types; (4) degree of alteration of the rock.

Most variations in texture and mineralogy in the diorite porphyries are not large enough to cause systematic variations in the bulk composition of the rock that can be detected by conventional analytical methods. Slight to moderate alteration of the rock, unless obvious in the hand specimen, cannot be correlated with most changes in the measured compositions. An exception is the systematic increase in the Fe_2O_3:FeO ratio with increasing alteration, although total iron content remains constant. The most important textural changes introduced by alteration are a decrease in grain size resulting from the appearance of microcrystalline sericite, chlorite, and iron oxides.

The monzonite porphyry is much less uniform than the diorite porphyry. Some samples of monzonite contain abundant, coarse phenocrysts of K feldspar, whereas in others the K feldspar is confined to the groundmass. Hornblende and augite phenocrysts are present in about equal amounts, but locally augite may be absent (Table 7). In general, the groundmass and feldspar and hornblende phenocrysts are more altered than in the diorite porphyries. Most phenocrysts of augite are fresh.

Mt. Ellen Complex

The bulk compositions of five diorite porphyries from the Mt. Ellen complex are given in Table 3. The samples are HM 9, HM2, HM 15, HM 100, and HM 35. Three of these samples were chosen for analysis of constituent hornblendes because they were texturally and compositionally like the bulk of the diorite porphyry, and the hornblende phenocrysts were unaltered. The other two analyses are of samples of diorite porphyry from the Bull Creek laccolith and the adjacent Bull Mountain bysmalith.

BULL CREEK LACCOLITH: The Bull Creek lacolith, at the northeast edge of Mt. Ellen, is exposed for about 9000 feet along Bull Creek, in a valley about 900 feet deep at the bulged northeast end of the intrusion. Samples were collected along the entire exposed length of the laccolith, and two vertical traverses were made from the creek floor to the roof of the laccolith. Additional samples were collected throughout the body. Figure 2 is a generalized vertical section drawn approximately along Bull Creek, showing the form of the laccolith and the sample locations. The rock specimens collected from this laccolith were taken principally for studies of the compositional variations within a single intrusive. The mineralogic and chemical data are given in Table 4.

The porphyry in this intrusive has a uniformly fine-grained groundmass containing large phenocrysts of plagioclase, hornblende, and minor quartz. Both groundmass and phenocrysts are partially replaced by sericite and calcite. This alteration is similar to that in nearby laccoliths but greater and more pervasive than in the adjoining Bull Mountain bysmalith. Hornblende throughout the Bull Creek laccolith is more altered than that in the adjacent Wickiup Ridge and Horseshoe Ridge laccoliths but is like that in the Bull Mountain bysmalith. Hornblende is replaced mainly by iron oxides (principally magnetite) that rim and corrode the margins of the hornblende crystals and are speckled throughout the grains.

Quartz is faily abundant in samples collected along the floor of Bull Creek and consists of round grains large enough to be seen in hand specimens. Maximum quartz content exclusive

TABLE 3.—MODAL AND CHEMICAL ANALYSES OF DIORITE PORPHYRIES OF THE HENRY MOUNTAINS, UTAH

	1 (HM 9)	2 (HM 2)	3 (HM 15)	4 (HM 48)	5	6 (HM 100)	7 (HM 35)	8 (HM 22)	9	10
Modal Analyses										
Groundmass	62.0	36.6	56.5	61.8	...	52.0	61.3	59.9	53.8	...
Plagioclase phenocrysts	25.2	46.9	30.3	22.1	...	35.4	27.2	33.0	32.0	...
Hornblende	11.6	10.1	10.7	13.1	...	10.6	7.0	4.7	11.2	...
Augite	....	1.2	....	....	...	....	....	tr	.2	...
Quartz	....	1.0	.7	....	...	....	1.9	....	.4	...
Calcite	.7	.1	.5	1.4	...	.5	.7	....	.6	...
Opaque minerals	.4	3.4	.5	1.2	...	.5	.4	1.9	1.2	...
Others*	.1	.7	.8	.4	...	1.0	1.5	.5	.6	...
Total	100.0	100.0	100.0	100.0	...	100.0	100.0	100.0	100.0	...
Chemical Analyses										
SiO_2	62.45	61.63	63.52	62.22	62.88	62.51	65.03	67.65	62.47	62.58
Al_2O_3	18.01	18.29	17.95	17.82	17.13	18.60	17.60	17.05	18.13	18.00
Fe_2O_3	1.37	1.69	1.35	2.49	1.86	1.50	1.77	1.09	1.68	2.27
FeO	2.79	2.68	2.55	2.10	2.58	2.11	1.20	1.35	2.45	2.12
MgO	1.29	1.33	1.32	1.42	1.48	1.06	.88	.82	1.28	1.21
CaO	5.58	5.75	5.50	5.94	5.39	5.86	5.24	2.93	5.73	5.28
N_2O	4.84	4.92	4.71	4.66	4.50	5.11	4.78	5.79	4.85	4.91
K_2O	1.96	1.97	1.72	1.88	2.25	1.97	1.70	2.82	1.90	2.11
H_2O+	.76	.77	.54	.63	.58	.49	.88	.44	.64	.84
H_2O-	.20	.20	.13	.07		.06	.18	.02	.13	
TiO_2	.48	.45	.47	.50	.51	.29	.40	.21	.44	.39
P_2O_5	.18	.27	.16	.18	n.d.	.25	.16	.15	.21	n.d.
MnO	.18	.14	.15	.10	.16	.16	.12	.06	.15	.09
Total	100.09	100.09	100.07	100.01	99.32	99.97	99.94	100.38	100.06	99.80

Trace-Element Analyses

Analyst	A	B	A	B	A	B	A	B		A	B	A	A	B	A	B	
Ba	750	1300	750	1250	1000	1150	1000	1300	...	1000	1350	750	1500	2200	900	1300	...
Co	<10	8	<10	7	<10	6	<10	6	...	<10	5	<10	<10	3	<10	6	...
Cr	<20	11	<20	9	<20	7	<20	8	...	<20	6	<20	<20	5	<20	8	...
Cu	10	30	5	21	5	12	15	16	...	3	8	3	15	28	8	17	...
Mn	1500	1100	2000	1100	1000	900	1500	1100	...	1500	940	1500	500	380	1500	1000	...
Ni	<5	4	<5	3	<5	2	<5	3	...	<5	2	<5	<5	tr	<5	3	...
Pb	10	..	10	..	10	..	10	tr	...	10	tr	10	35	40	10	..	...
Sc	<20	10	<20	9	<20	9	<20	9	...	<20	7	n.d.	<20	..	<20	~9	...
Sr	1500	790	1500	790	1500	830	1500	730	...	1500	970	1500	2000	1200	1500	820	...
Ti	2000	2100	1500	2100	1500	2300	2000	1900	...	2000	1700	3500	750	760	1800	2000	...
V	100	117	75	96	75	92	75	90	...	100	93	100	75	93	80	100	...
Y	35	32	35	32	15	tr	15	20	...	20	25	15	10	..	24	~20	...
Zr	150	150	200	140	100	120	100	140	...	150	130	350	75	71	140	140	...

Analyst A—U. Oda, U. S. Geological Survey; analyst B—Elisabeth Godijn, California Institute of Technology.

* Chiefly chlorite, apatite, epidote, sphene, zircon, and microcrystalline sericite and limonite.

1. (HM 9) Horseshoe Ridge laccolith, Mt. Ellen complex (average of 5 samples). Analyst, C. G. Engel.
2. (HM 2) Wickiup Ridge laccolith, Mt. Ellen complex (average of 3 samples). Analyst, C. G. Engel.
3. (HM 15) Shattered zone, Mt. Ellen complex. Analyst, C. G. Engel.
4. (HM 48) North Sawtooth Ridge laccolith, Mt. Hillers complex. Analyst, C. G. Engel.
5. Black Mesa bysmalith, Mt. Hillers complex. The bysmalith is adjacent to No. 4 above. (Analysis taken from Hunt, 1953, Table 7, col. 11) Analyst, J. F. Fairchild.
6. (HM 100) Bull Mountain bysmalith, Mt. Ellen complex. Analyst, C. G. Engel.
7. (HM 35) Bull Creek laccolith, Mt. Ellen complex. Analyst, C. G. Engel.
8. (HM 22) Horn laccolith, Mt. Pennell complex. Analyst, C. G. Engel.
9. Mean of samples 1, 2, 3, 4, and 6 (least altered porphyries).
10. Mean of 7 diorite porphyries cited by Hunt (1953, p. 154). Analysts, R. E. Stevens and J. F. Fairchild.

of groundmass is 3.5 per cent in the specimens collected. Accessory minerals are green spherulitic chlorite, iron oxides, apatite, sphene, epidote, calcite, and rare allanite.

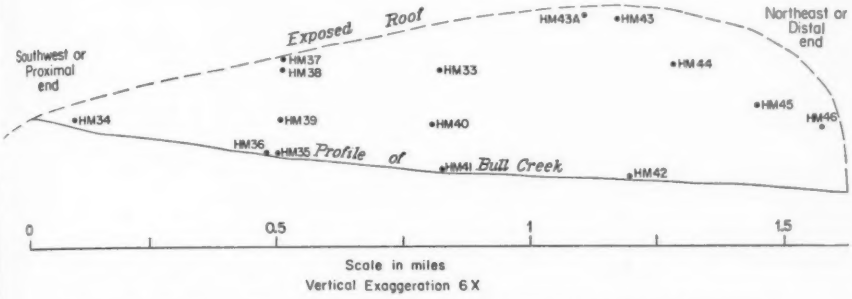

FIGURE 2.—VERTICAL SECTION ALONG BULL CREEK LACCOLITH SHOWING LOCATION OF SAMPLES CITED IN TABLE 4
The floor of the laccolith is not exposed.

The modal analyses of rocks from the Bull Creek laccolith indicate moderate variations in texture and mineralogy but that all the primary rock is diorite porphyry. The composition of the one specimen analyzed in detail is only slightly different from the average diorite porphyry of the Henry Mountains (Table 3; compare column 7 with columns 9 and 10). The Bull Creek laccolith contains somewhat more groundmass and fewer phenocrysts (including hormblende and opaques) than the average diorite. The slightly lower content of mafic minerals is reflected in a decrease in total Fe.

The trace-element composition of the Bull Creek laccolith is, within the limits of analytical error, essentially that of the average diorite porphyry of the Henry Mountains.

The groupings in Table 4 of samples from the Bull Creek laccolith are based upon the location of the samples in the body. Group I consists of samples along or within 50 feet of the exposed floor of the laccolith. Group II consists of samples collected from internal parts of the laccolith. Group III consists of samples collected at or within 100 feet of the roof of the laccolith. The only differences appear in the rocks very near the roof (Group III), which contain hornblendes that are especially "bleached" and altered to iron oxides. Two samples taken within 15 feet of the contact of porphyry with overlying sedimentary rock (roof) contain only small relics and crystal outlines of hornblende which have been almost completely replaced by iron oxides and calcite. The groundmass of the samples at or near the roof contain colorless, spherulitic serpentine.

The alteration of the porphyry is reflected in the chemical analyses of the samples. Although the total Fe content is approximately constant throughout the laccolith the ratio of Fe_2O_3/FeO increases abruptly, by a factor of 5, in the rocks within 15 feet of the roof (Table 4, samples 43 and 37). This ratio also seems slightly greater in the internal parts of the laccolith (Group II) than in the lower part (Group I). These changes in the valency of Fe reflect the mineralogical alteration of hornblende and spinels to hematite and limonite. The development of iron oxides is accompanied by the appearance of some chlorite and serpentine as well as calcite. The development of chlorite and serpentine suggests that the alteration is either deuteric or hydrothermal. The arched apical area of the laccolith is an obvious locus for rising deuteric or hydrothermal fluids.

The spectrographic analyses of the samples taken from the Bull Creek laccolith show no significant variations from floor to roof or from proximal to distal ends (Table 4; Fig. 2).

BULL MOUNTAIN BYSMALITH: The Bull Mountain bysmalith, a very prominent landmark at the northeast corner of the Mt. Ellen complex, stands isolated between Bull Creek on the west and Granite Creek on the southeast. The summit is about 2000 feet above the creeks. Along the west side of Bull Mountain the contact of the intrusive porphyry with the sedimentary rock is poorly exposed. Along the steep north face of the intrusive, the porphyry is emplaced against steeply dipping beds of the Morrison formation. The floor of the bysmalith is not exposed. Most of the samples were collected along the west and north sides of

TABLE 4.—MODAL AND CHEMICAL ANALYSES OF DIORITE PORPHYRY IN THE BULL CREEK LACCOLITH

	Group I (Lowermost exposures of laccolith, floor hidden)						Group II (Internal parts of the lacccolith)							Group III (At or within 100 feet of roof of laccolith)				
	1 (HM 34)	2 (HM 36)	3 (HM 35)*	4 (HM 41)	5 (HM 42)	6 Mean	7 (HM 39)	8 (HM 40)	9 (HM 33)	10 (HM 44)	11 (HM 45)	12 (HM 46)	13 Mean	14 (HM 38)	15 (HM 43)	16 (HM 37)	17 (HM 43A)	18 Mean
Modal Analyses																		
Groundmass	63.7	62.2	61.3	64.4	68.5	....	66.9	65.6	64.3	63.6	69.7†	65.8	....	68.4	64.0	69.7	66.1	....
Plagioclase phenocrysts	29.5	28.4	27.2	26.8	22.5	....	23.5	23.1	24.6	28.6	21.9	25.2	....	23.8	28.3	18.9	23.8	....
Hornblende	4.5	7.4	7.0	6.9	7.1	....	6.1	5.9	6.2	6.2	7.1	6.7	....	5.4	4.4	.....	3.0	....
Quartz	....	tr	1.9	.5	.4	....	.9	3.5	2.2	.8	....	2.0	....	tr	....	.....	.....	....
Calcite	.4	....	.7	.5	tr	....	.1	.3	.2	....	tr	tr	....	....	.2	.8	1.0	....
Opaque minerals	.8	.5	.4	.3	1.1	....	1.9	1.1	1.7	.4	1.0	.1	....	1.6	2.6	10.2††	4.7††	....
Others**	1.1	1.5	1.5	.6	.4	....	.6	.5	.8	.4	.3	.2	....	.8	.5	.4	1.4	....
Total	100.0	100.0	100.0	100.0	100.0	....	100.0	100.0	100.0	100.0	100.0	100.0	....	100.0	100.0	100.0	100.0	....
Partial Chemical Analyses (Analyst, C. G. Engel)																		
Total Fe*** (as Fe_2O_5)	2.99	3.09	3.09	2.84	3.11	3.02	3.03	2.99	3.00	3.06	2.90	2.99	3.00	2.90	2.71	2.90	2.01	2.88
Fe_2O_3	1.76	1.77	1.77	1.52	1.67	1.70	2.15	2.15	1.89	2.14	1.58	1.81	1.95	1.89	2.31	2.37	2.23	2.20
FeO	1.12	1.20	1.20	1.20	1.32	1.21	.80	.76	1.00	.84	1.20	1.05	.94	.92	.36	.48	.70	.61
Na_2O	4.76	4.78	4.78	4.67	4.87	4.77	4.87	4.87	4.72	5.11	5.00	5.07	4.94	4.91	5.14	4.98	5.01	5.01
K_2O	1.71	1.72	1.70	1.68	1.73	1.71	1.68	1.72	1.69	1.71	1.64	1.71	1.69	1.72	1.71	1.17	1.69	1.57
MnO	.13	.14	.12	.12	.13	.13	.13	.12	.13	.13	.11	.12	.13	.12	.13	.12	.12	.12

Trace-Element Analyses (ppm) (Analyst, U. Oda)

MnO	.13	.14	.12	.12	.13	.13	.13	.12	.13	.13	.11	.12	.13	.12	.13	.12	.12	.12

Trace-Element Analyses (ppm) (Analyst, U. Oda)

Ba	1000	1000	750	1000	1500	....	1500	1000	1000	1500	750	750	....	1000	1000	1000	750	....
Co	<10	<10	<10	<10	<10	....	<10	<10	<10	10	<10	10	....	10	10	10	<10	....
Cr	<20	<20	<20	<20	<20	....	<20	<20	<20	20	<20	20	....	20	20	20	<20	....
Cu	10	5	3	35	3	....	10	3	5	3	2	15	....	3	3	5	5	....
Mn	2000	1500	1000	1500	1000	....	1500	1500	1000	1000	1000	1500	....	1500	1500	1000	1500	....
Ni	<5	<5	<5	<5	<5	....	<5	<5	5	5	<5	5	....	5	5	5	<5	....
Pb	15	10	10	75	10	....	10	10	10	10	<10	10	....	10	10	10	10	....
Sn	10	<10	10	<10	<10	....	10	<10	<10	10	<10	10	....	10	10	10	10	....
Sr	3500	2000	1500	1500	1500	....	2000	1500	1500	1500	1500	1500	....	1500	1500	1000	1500	....
Ti	3500	1500	3500	2000	1500	....	3500	3500	3000	1500	3500	2000	....	2000	3500	2000	2000	....
V	75	50	75	75	75	....	75	50	50	75	35	75	....	50	50	75	75	....
Y	10	10	15	20	15	....	20	15	15	20	10	20	....	10	10	20	15	....
Zr	350	200	350	350	200	....	350	350	200	150	150	350	....	350	200	350	200	....

* For complete chemical analysis *see* column 7 of Table 3.

† Includes 0.6 per cent K-feldspar grains larger than .2 mm.

** Chiefly chlorite, apatite, epidote, sphene, biotite, and microcrystalline sericite and limonite.

†† Iron-oxide stains penetrate and obscure identity of other minerals.

*** Determinations of total Fe were made in succession using G-1 as a reference. (*See* Fairbairn *et al.*, 1951.)

Bull Mountain, at intervals of about a quarter of a mile, along the exposed length (2⅝ miles) of the intrusive.

The Bull Mountain porphyry consists of large, zoned, and twinned plagioclase crystals, hornblende, and accessory minerals in a very fine-grained groundmass. The groundmass is stained in thin sections treated with sodium cobaltinitrite but is too fine-grained to permit an estimate of K feldspar content. The plagioclase is rather fresh with a few intergrowths of K feldspar. The hornblende is highly altered. It is chloritic, embayed by groundmass, and surrounded and riddled by small opaque grains. Quartz is present in most of the sections, usually as one or two large, round grains per thin section. Veinlets of quartz are present in some sections. Calcite is present as irregular films replacing the groundmass and as discrete grains replacing the hornblende and groundmass. Rare biotite appears as shreds in the hornblende crystals. Euhedral sphene and apatite are also present.

Studies of the Bull Mountain bysmalith were confined to the total rock because of the extreme alteration of hornblende. The data on rocks from the Bull Mountain bysmalith are in Table 5.

Modal analyses indicate a remarkable uniformity in mineral composition and texture throughout the Bull Mountain bysmalith. The average of nine modal analyses (Table 5) indicates a mineralogical composition and texture very close to the average for diorite porphyry collected from the Henry Mountains.

Spectrographic analyses and partial chemical analyses for TiO_2, total Fe, Na_2O and K_2O substantiate the modes: within the limits of analytical error, there appear to be no differences in the composition of the bysmalith from one end to the other.

HORSESHOE RIDGE AND WICKIUP RIDGE LACCOLITH: The Horsehoe Ridge laccolith adjoins the Bull Creek laccolith on the west but is not so well exposed and is less accessible. The Wickiup Ridge laccolith lies between the Mt. Ellen stock and the Horseshoe Ridge and Bull Creek laccoliths (Fig. 1).

Samples were collected from the Horseshoe Ridge and Wickiup Ridge laccoliths where they converge with the southwestern part of the Bull Creek laccolith (Fig. 1). Modal and chemical analyses of the three intrusions and chemical analyses of hornblende from them offer a means of comparing the properties of the three laccoliths at points separated by only a few hundred feet of sedimentary wall rock.

Texturally and mineralogically the Horseshoe Ridge laccolith is like the Bull Creek laccolith except that its hornblendes are relatively fresh. An average modal analysis of 5 thin sections of the Horseshoe Ridge laccolith cut from specimens collected approximately 10 feet apart is given in column 1 of Table 3. This average is slightly higher in groundmass and lower in plagioclase phenocrysts than the mean modal composition of Henry Mountain diorite porphyries. The chemical composition (Table 3, column 1) is similar to that of the average of Henry Mountain diorite porphyries (Table 3, columns 9, 10).

Hunt (1953, p. 105) noted that the Wickiup Ridge laccolith is petrographically different from the other laccoliths. This is partly because the phenocrysts of hornblende are very large; a few are 28 mm long. These hornblendes also contain a higher Mg/Fe ratio than hornblende analyzed from other intrusives in the Henry Mountains (Table 12). The phenocrysts of plagioclase and groundmass also are coarser-grained than most other diorite porphyries of the Henry Mountains. Commonly a little augite is present, and locally it is more abundant than hornblende. The rock at the northeast end of the laccolith is coarsely crystalline and contains very little augite. The hornblendes average about 1 mm in length (Table 1). An average modal analysis of 3 thin sections of rocks collected about 20 feet apart is given in column 2 of Table 3. The small amount of groundmass (36.6 per cent) reflects the coarse texture of diorite porphyry in the Wickiup Ridge laccolith.

The variations in petrography of the Wickiup Ridge diorite porphyry from the mean diorite porphyry are not reflected in chemical composition. The chemical analyses of major, minor, and trace elements of a typical Wickiup Ridge porphyry (Table 3, column 2) are approximately those of the average of diorite porphyries in the Henry Mountains.

CENTRAL STOCK AND SHATTERED ZONE: The Mt. Ellen stock and shattered zone occur along the southern part of the Mt. Ellen complex at altitudes up to 11,000 feet. As Hunt notes (1953, p. 91) the stock is roughly circular in plan and consists of diorite porphyry. It is surrounded by a shattered zone that consists of sedimentary breccias variously injected by igneous rocks. The proportions of sedimentary to igneous rocks vary widely in the shattered zone. In general, however, large masses of igneous rock are most abundant in the inner part of the shattered zone, whereas most of

TABLE 5.—MODAL AND CHEMICAL ANALYSES OF DIORITE PORPHYRY FROM THE BULL MOUNTAIN BYSMALITH

	Proximal ← 2½ miles → Distal									
	1 (HM 4)	2 (HM 3)	3 (HM,5)	4 (HM 7)	5 (HM 8)	6 (HM 100)*	7 (HM 101)	8 (HM 102)	9 (HM 103)	10 Mean
Modal Analyses										
Groundmass	51.3	47.9	48.0	49.9	50.8	52.0	49.7	50.5	48.6	49.9
Plagioclase phenocrysts	40.5	39.2	40.9	38.6	35.6	35.4	38.0	36.9	39.0	38.2
Hornblende	6.4	9.4	8.7	8.3	11.3	10.6	8.7	10.1	9.9	9.3
Calcite	.2	.4	.7	.7	.6	.5	.7	.7	.5	.5
Opaque minerals	.3	.7	.8	.6	.8	.5	.7	.6	.6	.6
Others†	1.3	2.4	.9	1.9	.9	1.0	2.2	1.2	1.4	1.5
Total	100.0	100.0	100.0	100.0	100.0	100.0	100.0	100.0	100.0	100.0
Partial Wet Chemical Analyses (Analyst, C. G. Engel)										
Total Fe (as Fe_2O_3)	3.88	3.88	4.21	3.91	3.80	3.78	n.d.	n.d.	n.d	3.91
Na_2O	5.00	5.04	4.83	4.89	5.01	5.11	n.d.	n.d.	n.d.	4.98
K_2O	1.97	1.94	2.15	2.00	2.01	1.97	n.d.	n.d.	n.d.	2.06
TiO_2	.31	.35	.29	.32	.30	.29	n.d.	n.d.	n.d.	.31
Trace-Element Analyses (ppm) (Analyst, U. Oda)										
Ba	1500	1500	1000	1500	1000	1000	1000	1000	1000	1200
Co	<10	<10	10	<10	<10	<10	<10	<10	<10	<10
Cr	<20	<20	<20	<20	<20	<20	<20	<20	<20	<20
Cu	5	3	10	5	3	3	2	2	5	5
Mn	1500	1000	1500	1500	1500	1500	1500	1500	1500	1500
Ni	<5	<5	5	<5	<5	<5	<5	<5	<5	<5
Pb	20	20	35	20	20	10	20	20	35	20
Sn	<10	<10	<10	<10	10	<10	<10	<10	<10	<10
Sr	1500	1500	2000	1500	1500	1500	1500	1500	1500	1500
Ti	3500	1500	1500	1500	1500	2000	3500	3500	3500	2500
V	100	75	75	100	75	100	75	100	75	85
Y	20	20	20	20	20	20	15	20	20	20
Zr	150	200	200	350	350	150	350	500	500	300

* For complete chemical analysis *see* column 6 of Table 3.

† Chiefly biotite, chlorite, apatite, epidote, sphene, zircon, and microcrystalline sericite and limonite.

the outer part is broken sedimentary rock. Exposures of the central stock and shattered zone are locally good, but large areas are poorly exposed or unexposed.

Alteration of the igneous rocks in the stock and in the shattered zones is well developed and widespread. The alteration involves sericitization of the plagioclase and extensive replacement of the hornblende by magnetite, epidote, and chlorite. Veinlets and disseminated masses of pyrite, chalcopyrite, and other sulfides occur in the central stock in the Bromide Basin area. Specimens that show little effect of alteration may be obtained, however, as is indicated by porphyry HM 15 (Table 3). This rock is relatively unaltered and is the source of the hornblende HM 15 (Table 12). Hunt concluded (1953, p. 93) that diorite porphyry and quartz-bearing diorite porphyry within the stock were separate intrusive masses. However, field and

TABLE 6.—MODAL AND SPECTROGRAPHIC ANALYSES OF DIORITE PORPHYRIES FROM THE MT. ELLEN STOCK AND SHATTERED ZONE

	1 (HM 10)*	2 (HM 11)	3 (HM 12)	4 (HM 14)	5 (HM 15)	6 (HM 19)
Modal Analyses						
Groundmass	..	46.3	36.6	48.2	56.5	2.0
Plagioclase phenocrysts	..	44.0	46.1	40.9	30.3	70.8
Hornblende	..	1.8	5.6	5.5	10.7	20.0
Augite	..	...	.8	...	...	...
Quartz	..	1.0	2.8	4.0	.7	1.6
Calcite	..	3.0	...	...	.5	...
K-feldspar	..	.6	3.0	...	...	...
Epidote	..	...	1.5	.5	.2	4.2
Opaques	..	1.4	2.9	.6	.5	.8
Others†	..	1.9	.7	.3	.6	.6
Total	..	100.0	100.0	100.0	100.0	100.0
Trace-Element Analyses (ppm) (Analyst, U. Oda)						
Ba	500	1000	1000	1000	1000	750
Co	20	<10	<10	<10	<10	20
Cr	75	<20	<20	<20	<20	75
Cu	150	750	15	15	5	75
Mn	2000	750	1500	1500	1000	1000
Ni	20	<5	<5	<5	<5	20
Pb	10	35	10	10	<10	10
Sn	<10	<10	<10	<10	<10	<10
Sr	1000	1500	1500	2000	1500	1500
Ti	3500	2000	3500	2000	1500	5000
V	350	100	75	75	75	500
Y	15	15	35	20	15	20
Zr	350	350	350	350	100	200

* Very chloritic, epidotic porphyry. Coarse-grained like HM 19 with very little Groundmass. Hornblende abundant like HM 19 but is "bleached" and altered to chlorite.

† Chiefly chlorite, sphene, zircon, sericite.

HM 10, HM 11, HM 12, HM 14. Mt. Ellen stock, Bromide Basin.

HM 15. Shattered zone, Mt. Ellen. (Chemical analysis of this sample appears in column 3 of Table 3.)

HM 19. Laccolith 1 mile east of the Mt. Ellen stock.

petrographic studies show that in some parts of the stock there are all gradations between diorite porphyry and porphyry with almost 7 per cent quartz. The relative proportions of quartz-bearing and quartz-free samples of porphyry are unknown.

Modal analyses of four porphyries from the central stock and two from the shattered zone (Table 6) indicate some interesting compositional features in the central stock. The low hornblende content and the local appearance of orthoclase phenocrysts indicates "monzonitic" rock types much like those found in the Mt. Pennell complex. For example, specimen HM 12 (Table 6) contains only 5.6 per cent hornblende but contains 3 per cent orthoclase phenocrysts. Some of the rocks on Mt. Pennell that Hunt refers to as monzonites approximate this composition (Table 7, specimen HM 21). The dominant diorite porphyry of the Henry Mountains shows no orthoclase as phenocrysts and contains approximately 10 per cent hornblende.

The concentrations of trace-elements in the rocks from the stock and the shattered zone (Table 6) are essentially like those from other parts of the Henry Mountains except that two of the samples show a high Cu content. This is a reflection of minor chalcopyrite disseminated through the rock.

Mt. Pennell Complex

Mt. Pennell, like Mt. Ellen, consists of a central stock and shattered zone surrounded by laccoliths and numerous dikes and sills. As at Mt. Ellen, most laccoliths radiate from the central stock. Hunt (1953, p. 115) notes several rock types in the Mt. Pennell complex. He states that the central stock consists of diorite porphyry, monzonite porphyry intrusive into the diorite porphyry, and aplitic dikes. The Horn laccolith north of Mt. Pennell is described by Hunt as a "biotite-bearing" porphyry. Many dikes and sills in the Mt. Pennell complex are reported to be composed of monzonite porphyry. A brief investigation was undertaken of the biotite-bearing porphyry in the Horn laccolith and of the monzonite porphyries in the Coyote Creek laccolith. The rocks in the central stock were not studied.

HORN LACCOLITH: The Horn laccolith is the most northerly intrusion in the Mt. Pennell complex. Its component igneous rocks are more widely and extensively altered than those in the other intrusive rocks studied in the Henry Mountains. This is especially true of the plagioclase phenocrysts and groundmass which have a soft, pithy texture and are partly replaced by hydrous sheet-structure silicates. In contrast, some of the hornblende phenocrysts are little altered. One specimen of hornblende

(Table 12, specimen HM 22) is from altered porphyry of the Horn laccolith. Modal and chemical analyses of this rock are given in column 8 of Table 3. This rock and numerous other specimens studied from the Horn laccolith do not contain biotite.

The groundmass of the Horn porphyries when etched and stained with sodium cobaltinitrite appears to be more deeply colored in thin section than most porphyries, which suggests a higher percentage of K feldspar. Hornblende is less abundant than in typical diorite porphyry. There is little or no quartz. The chemical analysis of the rock from the Horn laccolith differs from the other porphyries I studied and from those described by Hunt (1953, p. 154, Table 7, specimens 16, 17). The Na and K content of the rock analyzed from the Horn laccolith appears to be intermediate in amount between that in typical diorite porphyry and the rocks of the Mt. Pennell complex that Hunt refers to as monzonite. Unfortunately, Hunt's analyses on monzonite are of rock with some of the large crystals of K feldspar removed (1953, p. 157). Therefore detailed comparisons between Hunt's analyses and analyses given in this report are not appropriate.

COYOTE CREEK LACCOLITH: The Coyote Creek laccolith extends northeast from Mt. Pennell to the perimeter of the exposed igneous complex. Hunt noted the presence of monzonite porphyry along the southeast flank of the laccolith, although other parts of it are diorite porphyry. Six specimens of the monzonite were studied in detail (Table 7), and thin sections of 11 others were examined. In general the monzonitic rocks contain less hornblende and more augite than typical diorite porphyries. Most of them contain large phenocrysts of K feldspar and opal-filled vugs with associated subhedral crystals of calcite, clinozoisite, and sphene. The hornblende and augite phenocyrsts show interesting differences. Most of the augite is in large euhedral crystals that are only slightly altered even in the most altered host rocks. Most of the hornblendes are partly replaced by groundmass and are riddled and surrounded by opaque minerals.

Two types of monzonitic porphyry are present, one in which there is little or no K feldspar as phenocrysts, the other in which K feldspar is present as large phenocrysts. In a few specimens of the first type phenocrysts of plagioclase have an outer rim or sheath of K feldspar. In samples of the second type, K feldspar embays the plagioclase phenocrysts. In the rocks where K feldspar either sheaths the plagioclase or embays it, K feldspar is a relatively late-forming mineral.

The textural variations, especially the appearance of large phenocrysts of K feldspar, make it difficult to obtain representative samples. The modal and chemical analyses in Table 7 are of less coarse-textured monzonites and are fairly representative of these types. In general, the chemical composition of the monzonite porphyries is not so uniform as the diorite porphyries. The monzonites are lower in Si, Ca, and Mg, although these constituents, especially Si and Ca, show wide variations; Na, K, and Al are highly concentrated in the monzonites. The Na_2O/K_2O ratio in the monzonite porphyry is about 1.50. It should be noted that the monzonite rock devoid of K feldspar phenocrysts contains almost as much K_2O as monzonites with 9 per cent K feldspar phenocrysts (Table 7, columns 2, 4).

The mean and range in concentrations of trace elements in the monzonitic rocks from Mt. Pennell are compared with analagous data on diorites from the Henry Mountains (Table 8). Trace elements Cu, V, Pb, Sr, and Ba are more abundant in the monzonite porphyry than in the diorite porphyry. In the monzonite, Cu is 6 times more abundant, V 4 times more abundant, Pb and Sr about 3 times more abundant, and Ba twice as abundant. These seemingly significant differences in means were checked statistically, using the Student's T-test (Mood, 1950, Chap. 9). The results show that for each of the elements Cu, Pb, V, Sr, and Ba the probability of the means being due to chance is less than 0.01. The enrichment of the monzonite in Pb, Sr, and Ba is consistent with its higher content of K feldspar. The enrichment in Cu and V suggests that these elements were concentrated in the liquid fractions of the Henry Mountain magma types during the early stages of their differentiation.

Mt. Hillers Complex

The Mt. Hillers complex is the most southerly dome from which samples were obtained. Samples were obtained from the North Sawtooth Ridge laccolith, the Black Mesa bysmalith, the Maiden Creek laccolith, and the Trachyte Mesa laccolith in the northeast part of the complex (Fig. 1). The samples from the North Sawtooth Ridge laccolith are about 5 miles northeast of the central stock. Those collected from the Trachyte Mesa laccolith are about 8 miles northeast of the central stock. Both the Maiden Creek laccolith and the

TABLE 7.—MODAL AND CHEMICAL ANALYSES OF MONZONITE PORPHYRY, MT. PENNELL COMPLEX

	1 (HM 26A)	2 (HM 26B)	3 (HM 20D)	4 (HM 20F)	5 (HM 21)	6 (HM 23)
Modal Analyses						
Groundmass	58.5	61.7	53.9	44.1	46.7	65.3
Plagioclase phenocrysts	28.1	27.0	32.5	42.0	42.0	28.4
Hornblende	2.2	1.4	4.5	3.0	5.0	1.7
Augite	4.8	6.1	2.0	1.2	?	2.1
K-feldspar phenocrysts	.....	.....	4.3	8.7	3.3	.....
Opal (vugs)*	3.7	2.2	.....	.....	.....	1.5
Opaque minerals	1.0	1.1	.5	.1	.1	.5
Others†	1.7	.5	2.3	.9	2.9	.5
Total	100.0	100.0	100.0	100.0	100.0	100.0
Chemical Analyses (Analyst, C. G. Engel)						
SiO_2	.....	.....	59.21	.....	57.01	.....
Al_2O_3	.....	.....	19.43	.....	19.11	.....
Fe_2O_3	.....	1.53	1.03	1.22	2.30	.....
FeO	.....	2.02	2.98	1.59	3.00	.....
MgO	.....	.....	.90	.....	1.37	.....
CaO	.....	.....	3.78	.....	5.01	.....
Na_2O	.....	6.40	6.20	6.33	6.50	.....
K_2O	.....	3.89	4.18	4.40	3.80	.....
H_2O+	.....	.....	.80	.....	.75	.....
H_2O-	.....	.....	.49	.....	.06	.....
TiO_2	.....	.....	.49	.....	.57	.....
P_2O_5	.....	.....	.20	.....	.15	.....
MnO	.....	.....	.18	.....	.23	.....
Total	.....	.....	99.87	.....	99.86	.....
Trace-Element Analyses (ppm) (Analyst, U. Oda)						
Ba	.....	.....	2000	2000	2000	2000
Co	.....	.....	<10	<10	<10	<10
Cr	.....	.....	<20	<20	<20	<20
Cu	.....	.....	50	75	75	75
Mn	.....	.....	1000	1500	1500	1500
Ni	.....	.....	<5	<5	<5	<5
Pb	.....	.....	20	100	35	75
Sn	.....	.....	10	10	10	10
Sr	.....	.....	3500	7500	3500	3500
Ti	.....	.....	3500	3500	3500	3500
V	.....	.....	350	200	150	750
Y	.....	.....	35	20	20	35
Zr	.....	.....	350	350	350	350

* Includes clinozoisite in vugs.

† Chiefly calcite, quartz, biotite, apatite, epidote, sphene, chlorite and microcrystalline sericite and limonite.

1. (HM 26A) Augite monzonite, 2½ miles northeast of Mt. Pennell.
2. (HM 26B) Augite monzonite, 2½ miles northeast of Mt. Pennell.
3. (HM 20D) Monzonite, Coyote Creek laccolith.
4. (HM 20F) Monzonite, Coyote Creek laccolith.
5. (HM 21) Monzonite, Coyote Creek laccolith.
6. (HM 23) Monzonite, Coyote Creek laccolith.

Trachyte Mesa laccoliths are sill-like bodies 80-100 feet thick with bulged roofs and leading edges. The form and interrelations as reconstructed by Hunt are shown in his Figure 51

TABLE 8.—VARIATIONS IN TRACE-ELEMENT COMPOSITION OF DIORITE AND MONZONITE PORPHYRIES

	Group I Diorite porphyry (54 samples)			Group II Monzonite porphyry (18 samples)		
	Minimum	Maximum	Mean	Minimum	Maximum	Mean
	(in parts per million)			(in parts per million)		
Ba	750	1500	1100	1500	2000	1900
Co	<10	15	<10	<10	10	<10
Cr	<20	<20	<20	<20	<20	<20
Cu	2	35	9	10	75	57
Mn	500	3500	1500	1000	2000	1500
Ni	<5	5	<5	<5	5	<5
Pb	<10	75	15	10	150	59
Sn	<10	10	<10	<10	<10	<10
Sr	1500	3500	1600	1500	7500	4600
Ti	1500	7500	2800	1500	5000	3300
V	35	100	80	100	750	300
Y	10	50	20	15	35	26
Zr	100	500	340	200	500	360

Group I. Diorite porphyries from stocks, laccoliths, bysmaliths, dikes, and sills in the Mt. Ellen, Mt. Pennell, and Mt. Hillers complexes.

Group II. Monzonite porphyries from sills and laccoliths in the Mt. Pennell complex.

(1953, p. 126). All these rocks are diorite porphyry.

Samples from the North Sawtooth Ridge laccolith are the least altered diorite porphyries collected in this investigation. Both total rock (Table 3, column 4) and hornblende phenocrysts (Table 12, column 4) were analyzed. Most other specimens from the Mt. Hillers complex are moderately to highly altered. Modal analyses of porphyries from Mt. Hillers are shown in Table 9. Their primary mineral composition varies greatly, but the mean composition is approximately that of diorite porphyry throughout the Henry Mountains. There are no well-defined differences in composition between specimens of diorite porphyry collected in the Mt. Hillers complex and specimens collected in the northern part of the Mt. Ellen complex some 18 miles distant.

TABLE 9. MODAL AND SPECTROGRAPHIC ANALYSES OF DIORITE PORPHYRY FROM INTRUSIVE BODIES IN THE NORTHEAST PORTION OF THE MT. HILLERS COMPLEX

	1 (HM 48)*	2 (HM 47)	3 (HM 50)	4 (HM 51)	5 (HM 49)	6 (HM 52)
Modal Analyses						
Groundmass	61.8	51.3	45.3	42.8	52.6	65.6
Plagioclase phenocrysts	22.1	34.7	38.9	39.8	32.2	18.7
Hornblende	13.1	13.2	9.9	12.5	5.5	11.4
Augite	...	tr	1.9	.8	...	.1
Quartz	...	...	.8	.8	...	...
Calcite	1.4	.3	.2	.3	3.3	1.2
Opaque minerals	1.2	.3	2.3	1.9	3.0	.8
Others†	.4	.2	.7	1.1	3.4	2.2
Total	100.0	100.0	100.0	100.0	100.0	100.0
Trace-Element Analyses (ppm) (Analyst, U. Oda)						
Ba	1000	1500	1500	750	1500	750
Co	<10	<10	<10	<10	<10	<10
Cu	15	20	5	15	10	20
Mn	1500	1500	1500	1500	1500	1500
Ni	<5	<5	<5	<5	<5	<5
Pb	10	10	10	15	15	15
Sr	1500	1500	1500	1500	2000	1500
Ti	2000	2000	5000	3500	2000	3500
V	75	100	100	100	75	100
Y	15	35	35	20	20	15
Zr	100	200	350	350	350	350

* For complete chemical analysis *see* column 4 of Table 3.

† Chiefly chlorite, apatite, epidote, sphene, zircon, and sericite.

1. (HM 48) North Sawtooth Ridge laccolith.
2. (HM 47) North Sawtooth Ridge laccolith.
3. (HM 50) Black Mesa bysmalith.
4. (HM 51) Black Mesa bysmalith.
5. (HM 49) Maiden Creek laccolith.
6. (HM 52) Trachyte Mesa laccolith.

The trace-element composition of rocks from the Mt. Hillers complex (Table 9) appears to be essentially like that of other diorite porphyries in the Henry Mountains. Any differences in trace-element content within the diorite porphyries can be demonstrated only with

much more precise sampling and analytical techniques.

Petrology

Hunt concluded from stratigraphic and structural reconstructions in the Henry Mountains that the porphyries were emplaced at a depth of about 1 mile (1953, p. 146). The total volume of the exposed intrusive igneous rocks is calculated by him (1953, p. 152) to be about 16 cubic miles. The textural features of the porphyries are consistent with this assumption of a hypabyssal environment. They are unquestionably igneous. There is no evidence of stoping or assimilation of wall rock; magma was forcefully intruded in those parts of the porphyry now exposed. Presumably the plagioclase and hornblende phenocrysts in the porphyries began to grow as intratelluric crystals in a deep-seated magma chamber from which the porphyries were derived. Later stages in the growth of these phenocrysts and the development of the groundmass occurred as the porphyries were emplaced in their present position.

The dominant rock type (95 per cent by volume) is referred to as diorite porphyry by most investigators, but this designation may be misleading. The name "diorite porphyry" for these rocks is derived from their mineralogical and textural features rather than from their bulk chemical composition. Comparison of the chemical composition of the average diorite porphyry from the Henry Mountains (Table 3, columns 9, 10) with an average diorite such as that tabulated by Osann, Washington, and Daly (Daly, 1914, p. 26) indicates the following differences: the diorite porphyry from the Henry Mountains contains more Si and Al and much more Na but is deficient in Fe and Mg

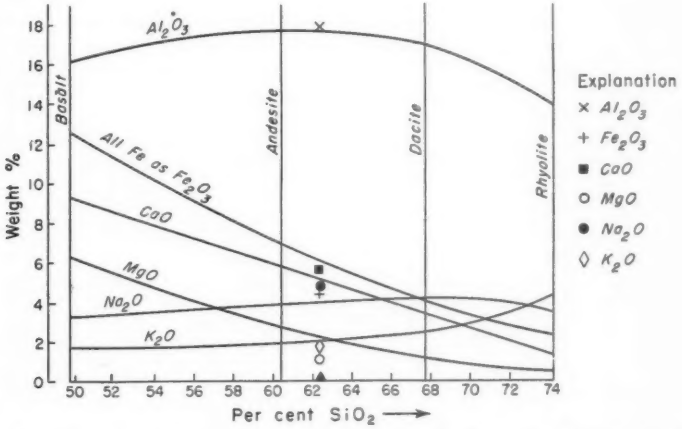

FIGURE 3.—Composition of Average Diorite Porphyry from the Henry Mountains Plotted on a Variation Diagram Derived from Daly's Average Basalt, Andesite, Dacite, Rhyolite (After Bowen, 1928, Fig. 37)

(Fig. 3). There the concentration of major elements in the "average" diorite porphyry from the Henry Mountains is plotted on a variation diagram based upon Daly's average basalt, andesite, dacite, and rhyolite. The diorite porphyry of the Henry Mountains is more felsic than Daly's average andesite, but its composition is not widely divergent from the curves drawn for Daly's average rocks. Assuming that the curves in Figure 3 represent a liquid line of descent during magmatic differentiation, the divergences that exist are of considerable interest. The Henry Mountain porphyries could have been derived by the tapping of the upper part of a deep magma chamber of andesitic composition in which the first-forming mafic crystals were slowly settling. A chamber of this type, at the onset of cooling, would contain crystals of plagioclase with either augite or hornblende. The density of the plagioclase crystals would be very close to that of the liquid, and the crystals would not sink rapidly to the base of the chamber. In contrast, the augite or hornblende crystals would tend to sink and be concentrated in the lower half of the reservoir. Even if they tended to be redissolved

or recirculated, a gradient in composition probably existed from bottom to top of the reservoir: the base relatively enriched in Fe and Mg, the top in Si, Na, and K, and (because of the suspended plagioclase) Ca and Al. The high Na content of the Henry Mountain rocks seems difficult to explain by a simple, reasonable hypothesis.

Tapping the upper portions of this magma reservoir would yield a magma analogous to that predominant in the intrusive forms (especially the laccoliths, bysmaliths, and dikes) of the Henry Mountains. This interpretation may be visualized from inspection of Table 10. In column 1 is the composition of the average diorite porphyry from the Henry Mountains which contains about 10 per cent hornblende. If another 10 volume per cent hornblende (13 per cent by weight) of compositon HM 48 (Table 12) is added to this rock the result (Table 10, column 2) is a rock very similar in composition to Daly's average andesite (Table 10, column 3). These relations suggest that crystal settling of about half of the hornblende formed in a parental andesitic magma could have produced a rock like the porphyry of the Henry Mountains. Many andesitic flows in western North America contain about 20 per cent hornblende or hornblende and pyroxene. The abundance of hornblendite inclusions in the Henry Mountains porphyries may represent early formed hornblende crystals which have settled out of the magma.

The diorite porphyry of the Wickiup Ridge laccolith is slightly less siliceous and more mafic than the average diorite porphyry, and the included hornblendes are much more magnesian than the average. The ratio of Fe/Mg in the hornblende in the Wickiup Ridge laccolith is 1.5, whereas the average for hornblendes in most other porphyries is consistently about 2.5 (Table 12). Moreover, the hornblendes of the Wickiup Ridge laccolith are five times larger than most hornblendes in the Henry Mountains (Table 1). The high Mg content and the large size of the hornblende crystals suggest that they may have been some of the earliest hornblendes to crystallize or that the laccolith may have been derived from intermediate rather than upper parts of the parent magma reservoir.

Within the Mt. Ellen stock and shattered zone there are wide variations in the percentage of groundmass to coarse (largely intratelluric ?) phenocrysts in the diorite porphyry. There the "porphyries" contain as little as 2 per cent groundmass and more than 70 per cent plagioclase (Table 6, column 6). Other porphyries not far removed in space and transitional with the above type contain more than 56 per cent groundmass and about 30 per cent plagioclase phenocrysts. These features are consistent with field relations that suggest that the porphyries richest in phenocrysts represent clusters of crystal-rich magma trapped in breccia pockets during the intrusion and cooling of the stock. The rocks impoverished in phenocrysts appear to represent liquid-rich magma filtered through breccias and crystal mats.

TABLE 10.—AVERAGE DIORITE PORPHYRY FROM THE HENRY MOUNTAINS AND HYPOTHETICAL ROCK DERIVED BY ADDING 13 PER CENT HORNBLENDE (BY WEIGHT)

Compared with Daly's average andesite

	1	2	3
SiO_2	62.47	59.72	59.59
Al_2O_3	18.13	17.43	17.31
Fe_2O_3	1.68	2.19	3.33
FeO	2.45	3.31	3.13
MgO	1.28	2.70	2.75
CaO	5.73	6.51	5.80
Na_2O	4.85	4.51	3.58
K_2O	1.90	1.75	2.04
H_2O	.77	.93	1.26
TiO_2	.44	.64	.77
MnO	.15	.18	.18
P_2O_5	.21	.19	.26
Total	100.06	100.06	100.00

1. Average of five diorite porphyries from column 9 of Table 3.

2. Hypothetical rock derived by adding 13 per cent hornblende; hornblende analysis from column 5 of Table 12.

3. Average composition of 87 andesites from Daly (1914, p. 26).

The rocks designated as monzonite also appear to have compositional peculiarities. If the specimens analyzed during this study are typical, the monzonite contains less Si than the diorite but more Al, Na, and K.

The monzonite variant in the central stock of Mt. Pennell may represent magma derived from the uppermost portions of the parent magma reservoir both during and after the emplacement of the diorite porphyry. This mon-

TABLE 11.—IGNEOUS ROCKS OF WESTERN UNITED STATES SIMILAR IN COMPOSITION TO DIORITE PORPHYRY OF THE HENRY MOUNTAINS

Column	1	2	3	4	5	6	7	8	9	10	11	12	13	14	15	16
Location	Henry Mtns. Utah	Henry Mtns. Utah	Henry Mtns. Utah	Sierra el Late Colo.	La Plata Mtns., Colo.	Mt. Shasta, Calif.	Mt. Shasta, Calif.	Northern Calif.	Crater Lake, Ore.	Sierra Carriso, Ariz.	Yellow-stone, Wyo.	Yellow-stone, Wyo.	Absaroka Range. Wyo.	Southern Calif.	Sierra Nevada, Calif.	British Columbia, Canada
Rock	Porphyry	Porphyry	Porphyry	Porphyry	Porphyry	Andesite	Porphyry	Andesite	Andesite	Porphyry	Diorite	Porphyry	Andesite	Tonalite	Quartz diorite	Porphyry
Number of samples	5	7	3	1	1	3	1	3	4	1	2	2	3	3	1	1
SiO_2	62.47	62.58	62.34	62.65	60.44	64.50	64.24	62.82	60.64	63.18	63.41	60.00	63.01	60.65	59.70	65.44
Al_2O_3	18.13	18.00	17.81	16.68	16.65	18.80	18.67	17.19	17.79	16.47	16.88	17.06	18.10	18.18	18.18	16.83
Fe_2O_3	1.68	2.27	2.02	2.35	2.31	1.15	1.40	2.01	2.01	2.36	1.98	4.26	2.71	.83	1.71	1.49
FeO	2.45	2.12	2.01	2.63	3.09	2.15	1.96	2.80	3.34	2.28	2.67	1.73	1.80	4.91	4.58	2.72
MgO	1.28	1.21	1.13	1.43	2.18	2.00	1.48	2.69	3.12	1.33	2.85	2.19	2.04	2.40	2.95	1.29
CaO	5.73	5.28	5.11	4.96	4.22	5.09	4.11	5.53	5.99	4.77	4.59	5.62	4.37	5.89	5.63	4.18
Na_2O	4.85	4.91	5.30	4.45	5.18	4.53	4.14	3.94	4.21	4.40	4.42	3.73	4.05	3.77	3.57	4.14
K_2O	1.90	2.11	2.54	2.75	2.71	1.19	1.71	1.76	1.43	2.93	2.16	1.44	2.40	1.54	2.16	1.88
H_2O	.77	.84	.73	.93	1.43	.13	1.18	.80	.41	.87	.52	2.44	1.25	.65	.52	1.02
TiO_2	.44	.39	.36	.42	.60	n.d.	.76	.40	.57	.66	.68	tr	.26	.75	.83	.50
P_2O_5	.21	n.d.	.16	.28	.29	n.d.	.08	.12	.20	.28	.21	1.15	.23	.08	.18	.22
MnO	.15	.09	.10	.16	.16	n.d.	tr	.10	tr	.15	tr	.12	.04	.07	.07	.06

1. Diorite porphyry (Table 3, column 9). Analyst, C. G. Engel.
2. Diorite porphyry (Table 3, column 10; data taken from Hunt, 1953, p. 154). Analysts, R. E. Stevens and F. G. Fairchild.
3. Diorite porphyry (Clarke, 1900, p. 165). Analyst, W. F. Hillebrand.
4. Hornblende porphyry. Contains hornblende, plagioclase, rare quartz and biotite (Cross, 1894, p. 227). Analyst, W. F. Hillebrand.
5. Diorite porphyry (Clarke, 1900, p. 161). Analyst, W. F. Hillebrand.
6. Hornblende-hypersthene andesite (Diller, 1898, p. 221, 227). Analyst, W. F. Hillebrand.
7. Dacite porphyry, contains phenocrysts of plagioclase, hornblende, biotite, quartz in fine-grained groundmass (Clarke, 1900, p. 177). Analyst, J. E. Whitfield.
8. Andesites (Clarke, 1900 p. 180–183). Analysts, J. E. Whitfield and W. F. Hillebrand.
9. Andesites, dikes and flows (Clarke, 1900, p. 222–223). Analyst, H. N. Stokes.
10. Hornblende porphyry, contains phenocrysts of hornblende and plagioclase in fine-grained groundmass (Cross, 1894, p. 227). Analyst, W. F. Hillebrand
11. Quartz, mica diorite (Iddings, 1891, p. 627). Analyst, W. H. Melville.
12. Hornblende, mica porphyry (Iddings, 1891, p. 627). Analyst, W. H. Melville.
13. Hornblende-andesite dikes (Clarke, 1900, p. 97–99). Analysts, H. N. Stokes and W. F. Hillebrand.
14. Tonalite, southern California Batholith (Larsen, 1948, p. 66, 73). Analyst, F. S. Gonyer.
15. Quartz diorite, contains feldspar, biotite, hornblende and quartz (unpublished). Analyst, C. G. Engel.
16. Biotite porphyrite, contains plagioclase, hornblende, biotite in microcystalline groundmass (Phemister, 1945, p. 58). Analyst, W. H. Herdsman.

zonite contains phenocrysts of orthoclase, plagioclase, some augite, and minor amounts of altered hornblende. There is slightly less Fe and Mg and more Na and K than in the average diorite porphyry. The augite phenocrysts appear, from the geometry of textures in thin sections, to have formed late in the paragenetic sequence. The presence of augite suggests that water and halogens necessary for the formation of hornblende escaped through the thin roof of sedimentary rocks.

The field relations of the monzonite and diorite porphyry differ from place to place. Hunt noted (1953, p. 115) that many bodies of monzonite intrude the diorite with fairly sharp contacts. At other places noted during the present study contacts between the two rocks are gradational, suggesting a close genetic relationship.

Read (1948, p. 3–4) states that intrusive igneous rocks approximating diorite in composition are invariably of hybrid origin. This comment of Read's was prompted by the fact that both hypabyssal and plutonic diorite intrusives that presumably were derived from primary magmas are rare in the exposed Precambrian terranes and uncommon in younger terranes in most parts of the world. An important exception exists in the Cordilleran and Coast ranges of western North America. There both plutonic and hypabyssal diorites and quartz diorites are abundant. Plutonic diorites having a composition very close to that of the porphyries in the Henry Mountains occur from Alaska to Mexico. Perhaps the best known plutonic rocks analogous to the Henry Mountains porphyries are the quartz diorites (tonalities) described by Larsen (1948) from the Southern California batholith. (*See* Table 11, column 14.) Almost identical quartz diorites occur southward throughout Baja (Lower) California and northward into Alaska.

Hypabyssal porphyritic rocks analagous to those in the Henry Mountains are common in other laccolithic mountains throughout the Colorado Plateau. These are described by Hunt (1958) and by Eckel (1949). The great similarity in composition, mode of intrusion, and proximity of these intrusive rocks suggests that they are all derived from the same parent magma. Analogous porphyritic quartz diorites emplaced near the surface and erupted as flows are abundant also in the Yellowstone Plateau, the Absaroka Range of Wyoming, the volcanic centers of Mt. Lassen and Mt. Shasta in California, Crater Lake in Oregon, and throughout the Sierran complex from Northern California to Baja California (Table 11).

Hornblendes

Introduction

The diorite porphyry of the Henry Mountains contains phenocrysts of hornblende and inclusions that are rich in hornblende. In the following discussion the phenocrysts are called hornblende phenocrysts, and hornblendes from inclusions are referred to as inclusion hornblendes.

Five samples of hornblende phenocrysts were extracted from various diorite porphyry intrusions. Ten samples of hornblende were obtained from inclusions. Brief descriptions of the inclusions appear in Table 14. All the hornblendes were analyzed spectrographically by U. Oda and E. F. Cooley in the Denver Laboratories of the U. S. Geological Survey. Six of these same samples were analyzed spectrographically by Elisabeth Godijn at the California Institute of Technology, to test the precision between the two laboratories. Wet chemical analyses were made of five hornblende phenocrysts and one inclusion hornblende. In addition, partial wet chemical analyses of Fe, Ti, and Mn were made on the remaining nine inclusion hornblendes. The wet chemical analyses and optical determinations were made by me.

The six hornblendes analyzed in detail fall into the femaghastingsite and magnesiohastingsite subdivisions of the hastingsite group, as defined by Billings (1928), on the basis of the molecular proportions of FeO/MgO: ferrohastingsite, FeO/MgO > 2; femaghastingsite, FeO/MgO < 2 but $> .5$; and magnesiohastingsite FeO/MgO $< .5$.

Sample Preparation

Hornblendes were separated from the -100-mesh sample of porphyries and from hornblendite and amphibolite inclusions in the porphyries. Hornblende concentrates from inclusions were obtained from a -120-mesh and $+150$-mesh fraction. A single exception required crushing to -150- and $+200$-mesh size. Hornblendes from the porphyries were crushed to a -100 and $+150$ mesh. However, one sample required crushing to a -150- and $+200$-mesh fraction before a hornblende separation was possible. Hornblende concentrates were obtained by the combined use of heavy liquids

16. Biotite porphyrite, contains plagioclase, hornblende, biotite in microcrystalline groundmass (Phemister, 1943, p. 36). Analyst, W. H. Herdsman.

TABLE 12.—ANALYSES OF HORNBLENDE

All chemical determinations made together with W-1 run as a reference (*See* Fairbairn, 1953, Table 1, p. 146.) (Analyst, C. G. Engel)

	1 (HM 9)	2 (HM 15)	3 (HM 22)	4 (HM 48)	5 (HM 2)	6 (HM 54)
SiO_2	39.65	40.30	41.53	39.50	41.34	40.14
Al_2O_3	13.94	14.17	12.49	14.14	12.76	13.92
Fe_2O_3	4.60	5.86	5.63	6.98	5.65	6.49
FeO	15.46	13.24	13.22	13.66	9.12	9.56
MgO	7.68	8.48	9.30	7.33	12.27	10.94
CaO	11.19	10.93	11.07	11.04	11.68	11.93
Na_2O*	2.19	1.83	1.79	2.06	2.20	2.01
K_2O†	.98	.95	.96	1.02	.77	.79
H_2O+	1.68	1.86	1.88	1.40	1.86	1.83
H_2O-	.08	.05	.00	.05	.00	.01
TiO_2**	1.57	1.32	1.40	1.52	1.99	1.98
P_2O_5	.17	.16	.13	.12	.10	.16
MnO††	.59	.53	.63	.55	.36	.26
F	.32	.21	.20	n.d.	.20	.22
	100.10	99.89	100.23	99.37	100.30	100.24
Less O for F	.13	.09	.08		.08	.09
	99.97	99.80	100.15		100.22	100.15
FeO/MgO (Mol. prop.)	1.13	.88	.80	1.04	.42	.49
Nx	1.682	1.677	1.669	1.675	1.666	1.675
Ny	1.693	1.688	1.686	1.690	1.679	1.688
Nz	1.700	1.696	1.693	1.698	1.686	1.694
Nz − Nx	.018	.019	.024	.023	.020	.019

Hornblende from	Pleochroism		
	X	Y	Z
1. Horseshoe Ridge laccolith, diorite porphyry, Mt. Ellen complex	pale yellow green	green	blue green
2. Shattered zone, diorite porphyry, Mt. Ellen complex	pale greenish yellow	yellow green	bluish green
3. Horn laccolith, diorite porphyry, Mt. Pennell complex	yellow green	green	blue green
4. North Sawtooth Ridge laccolith, diorite porphyry, Mt. Hillers complex, 15 miles SE of No. 1	pale greenish yellow	green	bluish green
5. Wickiup Ridge laccolith, diorite porphyry, Mt. Ellen complex	pale greenish yellow	pale brownish yellow	green
6. Hornblendite inclusion in No. 4	yellow green	green	blue green

* Na_2O determined for W-1, 2.27 per cent. Adjusted mean for W-1, 2.00 per cent.
† K_2O determined for W-1, 0.69 per cent. Adjusted mean for W-1, 0.63 per cent.
** TiO_2 determined for W-1, 1.09 per cent. Adjusted mean for W-1, 1.10 per cent.
†† MnO determined for W-1, 0.16 per cent. Adjusted mean for W-1, 0.165 per cent.

and the Frantz isodynamic separator. Samples were first run through bromoform, tetrabromoethane, and diiodomethane, and final cleaning was made with the magnetic separator. The hornblende concentrates used for analysis ranged from 96 to more than 99 per cent pure. The contaminants are chiefly feldspar and pyroxene with very minor amounts of apatite

and biotite (Table 14). The feldspar occurs as tiny grains that have not broken free from the hornblende. Most of the pyroxene occurs as free grains but has about the same density and magnetic properties as the hornblende and could not be completely separated from it. Some workers claim 99.5–99.9 per cent purity for hornblendes extracted from equigranular rocks although no evidence is offered to demonstrate this purity. In the diorite porphyries a sample with less than 0.5 per cent impurity is rarely possible even after exhaustive hand picking. This is due to the fact that crystals are partly altered or replaced by calcite, chlorite, and epidote, and some contain clouds or clusters of minute inclusions. I found that about 60 hours of hand picking under the microscope was required to purify only 2 grams of a sample of approximately 99 per cent pure hornblende.

TABLE 13.—STRUCTURAL FORMULAE OF HORNBLENDES*

	1 (HM 9)		2 (HM 15)		3 (HM 22)		4 (HM 48)		5 (HM 2)		6 (HM 54)	
K	.18		.18		.18		.20		.14		.14	
(W) Na	.64	2.64	.54	2.49	.52	2.48	.61	2.62	.62	2.61	.62	2.61
Ca	1.82		1.77		1.78		1.81		1.85		1.85	
Mg	1.73		1.91		2.09		1.67		2.70		2.39	
(X) Fe^{++}	1.96	3.76	1.67	3.64	1.66	3.83	1.75	3.49	1.13	3.87	1.17	3.60
Mn	.07		.06		.08		.07		.04		.04	
Al	.50		.61		.47		.66		.35		.47	
(Y) Fe^{+++}	.53	1.21	.67	1.43	.63	1.26	.81	1.64	.62	1.19	.72	1.41
Ti	.18		.15		.16		.17		.22		.22	
(Z) Si	6.01	8.00	6.09	8.00	6.25	8.00	6.05	8.00	6.12	8.00	6.06	8.00
Al	1.99		1.91		1.75		1.95		1.88		1.94	
OH	1.69	1.84	1.87	1.97	1.88	1.98	1.43		1.83	1.93	1.80	1.91
F	.15		.10		.10		n.d.		.10		.11	

*The structural type is taken as W_{2-3} $(XY)_5$ $(Z_4O_{11})_2$ (OH, F, Cl)$_2$.

1. (HM 9) Horseshoe Ridge laccolith, diorite porphyry.
2. (HM 15) Shattered zone, Mt. Ellen, diorite porphyry.
3. (HM 22) Horn laccolith, diorite porphyry.
4. (HM 48) North Sawtooth Ridge laccolith, diorite porphyry.
5. (HM 2) Wickiup Ridge laccolith, diorite porphyry.
6. (HM 54) Hornblendite inclusion in North Sawtooth Ridge laccolith (HM 48 above).

Optical Properties

All the hornblendes are green, and all show faint to well-developed zonal growth. The indices of refraction determined on each sample (Table 12) are those of fragments crushed from numerous crystals. The indices were determined in sodium light and also in white light in oils graduated on .002 intervals. The determinations made in sodium light and white light were in fair agreement (usually .002), and I believe that white light is the better medium for deeply colored minerals with high absorption, such as hornblende. There seems to be no simple correlation between chemical composition and optical properties of hornblendes. A lack of obvious correlations of optics and composition of hornblende is implicit in most modern studies (Deer, 1938; Buddington and Leonard, 1953; Larsen and Draisen, 1950) although there is little discussion of the fact, and Winchell's elaborate diagrams (1951, p. 434, Fig. 325) suggest precise, sympathetic relations between optics and composition that cannot be demonstrated.

Chemical Composition

Wet chemical analyses.—The chemical analyses of five hornblende phenocrysts and one

inclusion hornblende appear in Table 12. These analyses are computed to the structural formula in Table 13. The inclusion hornblende HM 54 was extracted from an inclusion at the locality from which phenocrysts HM 48 was obtained. The inclusion was collected about 5 feet from the sample of porphyry HM 48 and hornblende phenocryst HM 48. This is the only instance where it was possible to obtain fresh phenocryst and inclusion hornblendes from the same intrusive body and locality.

The compositions of porphyries from which these hornblendes were obtained appear in Table 3. Rocks and phenocrysts have the same sample numbers. The hornblendite inclusion from which hornblende HM 54 was obtained was not analyzed. The textural and mineralogical composition of the hornblendite and amphibolite inclusions is given in Table 14. Locations of rock and hornblende samples are shown in Figure 1.

Four of the 5 hornblende phenocrysts analyzed (HM 9, HM 15, HM 22, HM 48) are very similar in composition even though two (HM 9 and HM 48) are from localities 15 miles apart in separate intrusive complexes. The hornblende phenocrysts, HM 9 and HM 2, that are from adjacent laccoliths of approximately the same composition, showing striking differences especially in the molecular proportions of FeO/MgO (Table 12). Hornblende HM 2, the "aberrant" hornblende phenocryst, is 5 times larger than other phenocrysts in the Henry Mountains (Hunt, 1953, p. 155). The rock in which it occurs is much coarser-grained than the average porphyry and contains much less groundmass. Phenocryst HM 2 is almost identical in composition to the inclusion hornblende HM 54 but is unlike the hornblende phenocryst HM 48 from which the inclusion came.

Billings' study (1928) of hornblendes from the Paleozoic igneous intrusive complex of northeastern United States and southeastern Canada led him to suggest that the molecular proportions of the ratio FeO/MgO increases with decreasing temperature of crystallization of the parent rock. If this generalization is valid for hornblende phenocrysts and inclusion hornblendes in the Henry Mountains, then the coarsely crystalline phenocryst HM 2 and the inclusion hornblende HM 54 were crystallized at higher temperatures than the rest of the hornblende in Table 12. In an effort to determine whether other inclusion hornblendes were enriched in Mg relative to Fe, analyses were made of total Fe on nine other inclusion hornblendes (Table 14). These analyses were undertaken on the assumption that the total Fe content of the hornblendes would offer an approximate index of its Mg content. As a further test of this assumption, the approximate Mg content of each hornblende was determined spectrographically (Table 14). The data show that hornblendes relatively enriched in total Fe contain about 50,000 ppm Mg (5 per cent); hornblendes relatively low in Fe contain about 70,000 ppm Mg (7 per cent). Most of the inclusion hornblendes are what Billings classified as magnesiohastingsite and may reflect a more mafic environment and higher temperature of crystallization than most hornblende phenocrysts in the diorite porphyry. The inclusions are probably not formed by the clustering of crystals formed in equilibrium with porphyry enclosing the inclusion. Presumably the inclusions are either xenoliths or crystal aggregates formed in another part of the magma or at an earlier stage in its differentiation. These problems are considered in the succeeding section on origin of the hornblendes.

Spectrographic analyses.—The concentrations of elements obtained spectrographically by Oda and Cooley are listed in Table 14, which also contains data on Fe, Mn, and Ti obtained using wet methods. All analyses of a given type were done at the same time to limit the errors in precision as much as possible. Elisabeth Godijn repeated trace-element analyses of six of the same samples of hornblende at the California Institute of Technology, and the results of independent analyses of the two laboratories are listed in Table 15. Studies of analyses of masked replicate samples show variations up to 50 per cent from the posted values for most elements. This error increases appreciably if the analyses are made at different times, even in the same laboratory by the same analyst.

In Table 14 the spectrographic analyses of hornblende phenocrysts constitute Group I; analyses of inclusion hornblendes form Group II. Arithmetic means for the concentrations of each element in each group are listed in the right-hand column of Table 14. The analyses of trace elements in the two types of hornblendes corroborate the general conclusion drawn from the data on major elements; both hornblende phenocrysts and inclusion hornblendes show moderate variations in composition with essentially complete compositional overlap. Eight of the inclusion hornblendes are magnesiohastingsite with more Cr, Ni, and Mg and possibly less Ti and Mn than four of the five hornblende phenocrysts. In the inclusion horn-

TABLE 14.—SPECTROGRAPHIC AND PARTIAL CHEMICAL ANALYSES OF HORNBLENDE FROM DIORITE PORPHYRIES AND INCLUSIONS

	Group I Hornblende phenocrysts from diorite porphyry					Group II Hornblende from inclusions in diorite porphyry					
	HM 9	HM 15	HM 22	HM 48	Mean	HM 2	HM 54	HM 55	HM 56	HM 57	Mean
Fe	10.0	10.0	10.0	10.0	10.0	10.0	10.0	10.0	10.0	10.0	10.0
Mn	0.3	0.3	0.3	0.3	0.3	0.3	0.3	0.3	0.3	0.3	0.3
Ti	0.3	0.3	0.3	0.3	0.3	0.3	0.3	0.3	0.3	0.3	0.3
Mg	5.0	5.0	5.0	5.0	5.0	7.0	7.0	7.0	7.0	7.0	7.0
Cr	0.0015	0.0015	0.0015	0.0015	0.0015	0.0070	0.0070	0.0070	0.0070	0.0070	0.0070
Ni	0.0015	0.0015	0.0015	0.0015	0.0015	0.0070	0.0070	0.0070	0.0070	0.0070	0.0070
Co	0.0015	0.0015	0.0015	0.0015	0.0015	0.0015	0.0015	0.0015	0.0015	0.0015	0.0015
Cu	0.0015	0.0015	0.0015	0.0015	0.0015	0.0015	0.0015	0.0015	0.0015	0.0015	0.0015
Zn	0.0070	0.0070	0.0070	0.0070	0.0070	0.0070	0.0070	0.0070	0.0070	0.0070	0.0070
Ga	0.0015	0.0015	0.0015	0.0015	0.0015	0.0015	0.0015	0.0015	0.0015	0.0015	0.0015
Ba	0.15	0.15	0.15	0.15	0.15	0.15	0.15	0.15	0.15	0.15	0.15
Sr	0.0070	0.0070	0.0070	0.0070	0.0070	0.0070	0.0070	0.0070	0.0070	0.0070	0.0070
Zr	0.0070	0.0070	0.0070	0.0070	0.0070	0.0070	0.0070	0.0070	0.0070	0.0070	0.0070
Y	0.0015	0.0015	0.0015	0.0015	0.0015	0.0015	0.0015	0.0015	0.0015	0.0015	0.0015
Yb	0.0003	0.0003	0.0003	0.0003	0.0003	0.0003	0.0003	0.0003	0.0003	0.0003	0.0003
Be	0.0003	0.0003	0.0003	0.0003	0.0003	0.0003	0.0003	0.0003	0.0003	0.0003	0.0003
Mo	0.0003	0.0003	0.0003	0.0003	0.0003	0.0003	0.0003	0.0003	0.0003	0.0003	0.0003
Ag	0.0003	0.0003	0.0003	0.0003	0.0003	0.0003	0.0003	0.0003	0.0003	0.0003	0.0003
Pb	0.0015	0.0015	0.0015	0.0015	0.0015	0.0015	0.0015	0.0015	0.0015	0.0015	0.0015
Sn	0.0003	0.0003	0.0003	0.0003	0.0003	0.0003	0.0003	0.0003	0.0003	0.0003	0.0003
V	0.0070	0.0070	0.0070	0.0070	0.0070	0.0070	0.0070	0.0070	0.0070	0.0070	0.0070
Sc	0.0015	0.0015	0.0015	0.0015	0.0015	0.0015	0.0015	0.0015	0.0015	0.0015	0.0015
Ca	10.0	10.0	10.0	10.0	10.0	10.0	10.0	10.0	10.0	10.0	10.0
Na	0.7	0.7	0.7	0.7	0.7	0.7	0.7	0.7	0.7	0.7	0.7
K	0.3	0.3	0.3	0.3	0.3	0.3	0.3	0.3	0.3	0.3	0.3
Si	10.0	10.0	10.0	10.0	10.0	10.0	10.0	10.0	10.0	10.0	10.0
Al	1.5	1.5	1.5	1.5	1.5	1.5	1.5	1.5	1.5	1.5	1.5
B	0.0003	0.0003	0.0003	0.0003	0.0003	0.0003	0.0003	0.0003	0.0003	0.0003	0.0003
Li	0.0015	0.0015	0.0015	0.0015	0.0015	0.0015	0.0015	0.0015	0.0015	0.0015	0.0015
Ti	0.3	0.3	0.3	0.3	0.3	0.3	0.3	0.3	0.3	0.3	0.3
Mn	0.3	0.3	0.3	0.3	0.3	0.3	0.3	0.3	0.3	0.3	0.3
Fe	10.0	10.0	10.0	10.0	10.0	10.0	10.0	10.0	10.0	10.0	10.0
Mg	5.0	5.0	5.0	5.0	5.0	7.0	7.0	7.0	7.0	7.0	7.0

TABLE 14.—SPECTROGRAPHIC AND PARTIAL CHEMICAL ANALYSES OF HORNBLENDE FROM DIORITE PORPHYRIES AND INCLUSIONS

	Group I: Hornblende phenocrysts from diorite porphyry					Group II: Hornblende from inclusions in diorite porphyry												
						Hornblende from inclusions that consist of very coarse-grained, randomly oriented crystals of hornblende with minor amounts of feldspar, pyroxene, and magnetite				Hornblendes from inclusions that consist of about equal amounts of hornblende and feldspar. This type of inclusion has a crude layering and orientation of crystals.					Hornblende from amphibolite gneiss with alternate feldspar-and hornblende-rich layers	Group I	Group II	
	HM 9	HM 15	HM 22	HM 48	HM 2	HM 54	HM 13	HM 16	HM 7	HM 14A	HM 1	HM 3	HM 6	HM 4	HM 2A	Mean	Mean	
	ppm*																	
Ba	150	150	300	200	150	150	150	150	150	150	150	150	100	100	100	200	150	Ba
Co	20	50	50	30	50	50	50	50	70	50	70	30	70	50	70	40	50	Co
Cr	50	50	30	20	<20	150	20	150	20	1000	100	700	300	1000	300	~30	400	Cr
Cu	5	7	7	30	7	150	20	5	300	7	7	5	5	5	10	10	20	Cu
Mn	3000	3000	3000	3000	3000	1500	3000	2000	2000	3000	3000	3000	3000	3000	3000	3000	3000	Mn
Ni	30	15	20	20	20	70	20	50	70	300	50	100	100	300	70	20	120	Ni
Sc	50	70	70	50	70	70	70	70	100	50	150	50	70	50	100	70	70	Sc
Sr	150	150	300	200	300	150	100	300	300	100	<50	200	50	100	<50	200	~150	Sr
Ti	7000	5000	5000	7000	7000	7000	5000	7000	7000	3000	7000	5000	3000	3000	7000	7000	5000	Ti
V	300	300	500	500	300	500	300	300	500	300	500	300	300	300	500	300	300	V
Y	30	30	30	50	30	20	30	20	15	50	30	30	15	30	30	30	30	Y
Zn	300	200	200	200	<200	<200	200	<200	<200	<200	<200	<200	<200	<200	<200	~200	<200	Zn
Zr	150	200	200	150	100	100	100	70	50	100	100	70	50	70	70	150	70	Zr
Mg	50,000	50,000	50,000	30,000	70,000	70,000	50,000	70,000	70,000	70,000	70,000	70,000	70,000	70,000	50,000	50,000	70,000	Mg
	Weight per cent†																	
Fe	15.22	14.38	14.20	15.49	11.04	11.97	13.73	11.92	11.11	8.80	13.60	12.40	12.84	9.60	14.81	14.1	12.1	Fe
Mn	.46	.41	.49	.43	.28	.20	.39	.21	.25	.40	.25	.28	.32	.25	.29	.41	.28	Mn
Ti	.94	.79	.84	.91	1.19	1.19	.74	.91	.87	.40	.97	.91	.41	.53	.90	.93	.78	Ti
Mg	4.63	5.12	5.61	4.42	7.40	6.60	n.d.	n.d.	n.d.	n.d.	n.d.	n.d.	n.d.	n.d.	n.d.	5.44	n.d.	Mg
Estimated purity of sample (%)	99	97	98	98+	99	99+	98	96	97	97	99	98	98	99+	98			
Impurities**	f	f	f	f, p	f	f, a	f, a	f, p	f, p	o	f, a	f, a	f, b	o	f, p			

* Semiquantitative spectrographic analyses by U. Oda and E. F. Cooley, U. S. Geological Survey.
† Wet chemical analyses by C. G. Engel.
** f = feldspar, p = pyroxene, a = apatite, o = opaque inclusions, b = biotite.

blendes Zn may be less abundant but this is not positively demonstrated. The differences in Ba and Sr probably reflect the unequal distribution of feldspar impurities but may be intrinsic differences in the amounts of these elements in hornblendes.

The enrichment of Cr and Ni in the more magnesian inclusion hornblendes is established; Cr shows a maximum enrichment—by a factor of 5—as the molecular proportions of FeO/MgO are halved (decreasing from 1 to about 0.5). The enrichment of Cr is accompanied by a fivefold increase in Ni. There is little or no increase in Co.

The absence of adequate data on Fe^{++} and Mg in the inclusion hornblendes prevents a more rigorous correlation between the concentrations of Co, Cr, and Ni with these major elements.

Most of the hornblendes contain about 6 ppm Cu. The much higher values in several specimens (up to 160 ppm) are probably correct, although the reasons for the abrupt differences are not apparent. The two inclusion hornblendes that show the highest concentrations of Cr and Ni have a "bleached" appearance and contain numerous oriented opaque inclusions. These inclusions seem to be spinels that may have exsolved from the hornblende during cooling and aging.

TABLE 15.—SPECTROGRAPHIC ANALYSES OF IDENTICAL HORNBLENDE SAMPLES, MADE IN DIFFERENT LABORATORIES

(In parts per million)

	HM 9		HM 15		HM 22		HM 48		HM 2		HM 54	
Ba	150	160	150	170	300	330	200	280	150	185	150	290
Co	20	25	50	26	50	33	30	26	50	36	50	29
Cr	50	33	50	47	30	45	20	40	<20	6	150	245
Cu	5	17	7	17	7	29	30	28	7	17	150	56
Mn	3000	3200	3000	2000	3000	2300	3000	2400	3000	2100	1500	830
Ni	30	16	15	15	20	20	20	15	20	14	70	48
Sc	50	39	70	42	70	41	50	41	70	65	70	46
Sr	150	330	150	310	300	330	200	320	300	410	150	310
Ti	7000	6300	5000	4800	5000	4800	7000	6900	7000	7700	7000	5100
V	300	440	300	420	500	610	500	550	300	320	500	470
Y	30	69	30	77	30	43	50	63	30	52	20	pt
Zr	150	108	200	135	200	145	150	114	100	51	100	28
Analyst	A	B	A	B	A	B	A	B	A	B	A	B

Analyst A. Analyses run independently by U. Oda and E. F. Cooley, U. S. Geological Survey. The figures reported are an average of the two runs.

Analyst B. Analyses by Elisabeth Godijn, California Institute of Technology.

HM 9. Horseshoe Ridge laccolith, diorite porphyry, Mt. Ellen complex.

HM 15. Shattered zone, diorite porphyry, Mt. Ellen complex.

HM 22. Horn laccolith, diorite porphyry, Mt. Pennell complex.

HM 48. North Sawtooth Ridge laccolith, diorite porphyry, Mt. Hillers complex.

HM 2. Wickiup Ridge laccolith, diorite porphyry, Mt. Ellen complex.

HM 54. Hornblendite inclusion in HM 48, Mt. Hillers complex.

Comparisons with Other Hornblendes

Hornblendes from igneous rocks compositionally like the diorite porphyry of the Henry Mountains have been described by Larsen and Draisen (1950), Deer (1938), and others. Analyses of similar hornblendes from metamorphosed granitic rocks have been published by Buddington and Leonard (1953). Older analyses of hornblendes from dioritic rocks are discussed by Hallimond (1943). Hornblendes from inclusions like those in the porphyry are discussed by Deer (1938) and Hurlbut (1935). Hornblendes similar in composition to inclusion

TABLE 16.—CHEMICAL ANALYSES OF HORNBLENDES FROM OTHER IGNEOUS ROCKS, INCLUSIONS, AND AMPHIBOLITES, COMPARED WITH COMPOSITION OF HORNBLENDE FROM THE HENRY MOUNTAINS, UTAH

	1	2	3	4	5	6	7
SiO_2	40.30	43.72	42.11	38.92	39.78	41.25	40.14
Al_2O_3	14.17	12.40	10.05	12.68	11.39	13.26	13.92
Fe_2O_3	5.86	3.32	2.82	7.42	5.93	3.56	6.49
FeO	13.24	14.22	15.14	14.64	14.21	13.50	9.56
MgO	8.48	9.86	11.48	7.86	9.62	10.27	10.94
CaO	10.93	11.64	11.34	11.24	9.68	10.22	11.93
Na_2O	1.83	.86	1.01	2.38	1.57	1.82	2.01
K_2O	.95	.77	1.43	1.58	1.60	.83	.79
H_2O+	1.86	1.69	2.02	.93	2.59	1.48	1.83
H_2O-	.05	n.d.	.06	n.d.	.25	.06	.01
TiO_2	1.32	1.44	2.76	1.51	1.47	2.96	1.98
P_2O_5	.16	n.d.	n.d.	n.d.	n.d.	n.d.	.16
MnO	.53	.08	.24	.09	.68	.47	.26
F	.21	.18	n.d.	1.20	1.29	.11	.22
	99.89	100.18	100.46	100.45	100.64*	99.79	100.24
Less O for F	.09	.08		.51	.67	.05	.09
	99.80	100.10		99.94	99.97	99.74	100.15
FeO/MgO (Mol. prop)	.88	.80	.74	1.04	.83	.75	.49
MRM/MRR†	.93	.96					
N_x	1.677	1.667	1.662	1.690	1.666	1.666	1.675
N_y	1.688	1.680	1.673	1.702	1.689		1.688
N_z	1.696	1.685	1.680	1.705	1.693	1.689	1.694

*The original analysis published by Buddington and Leonard (1953) contains 0.58 Cl. The Cl is deducted from this table but is included in the total.

†Ratio $\frac{FeO+MnO+Fe_2O_3}{FeO+MnO+Fe_2O_3+MgO}$ in hornblende to $\frac{FeO+MnO+Fe_2O_3}{FeO+MnO+Fe_2O_3+MgO}$ in rock.

1. Hornblende phenocryst from diorite porphyry, Mt. Ellen shattered zone. Analyst, C. G. Engel.
2. Hornblende from Lakeview Mountain tonalite, southern California batholith (Larsen and Draisen, 1950, p. 71, Table 3, column 8). Analyst, F. A. Gonyer.
3. Hornblende from Glen Tilt diorite, Scotland (Deer, 1938, p. 58, Table 1, column 1). Analyst, W. A. Deer.
4. Hornblende in vug (miarolitic cavity) in monzonite dike, Bearpaw Mountains, Montana (Pecora and Fisher, 1946, p. 379). Analyst, F. A. Gonyer.
5. Hornblende from microcline granite gneiss, northwest Adirondack Mountains, New York (Buddington and Leonard, 1953, p. 894, Table 1, column 1). Analyst, E. K. Oslund.
6. Hornblende from garnet-bearing amphibolite, northwest Adirondack Mountains, New York (Buddington, 1952, p. 42, Table 3, column 7), Analyst, Lee C. Peck.
7. Hornblende from, hornblendite inclusion in diorite porphyry, North Sawtooth Ridge laccolith, Henry Mountains, Utah. Analyst C. G. Engel.

hornblendes occur in metagabbro of the Adirondack Mountains (Buddington, 1952).

The similarities in composition between the plutonic tonalites from the southern California batholith (Larsen, 1948, p. 67, columns 3, 4, 7) and the diorite porphyry made comparisons of their constituent hornblendes especially interesting. Hornblende is the most widespread femic mineral in the southern California batholith and is the chief dark mineral in the tonalite. Analysis of one of the hornblendes from the Lakeview Mountain tonalite (Larsen and Draisen, 1950, p. 71) is given in column 2 of Table 16. Analyses of hornblendes from the

Henry Mountains, the Glen Tilt complex of Scotland, a monzonite dike in the Bearpaw Mountains, and the Adirondack Mountains are also given in Table 16.

The hornblendes in the Lakeview Mountain tonalite and in the diorite porphyry are alike in composition. Larsen and Draisen (1950, p. 74–75) note that the ratio of FeO + MnO + Fe_2O_3/FeO + MnO + Fe_2O_3 + MgO is about the same for the rock as for the mafic minerals (*e.g.*, hornblende). This is also true for the hornblende phenocrysts and enclosing porphyry of the Henry Mountains (Table 16, columns 1, 2). The hornblendes in the southern California batholith appear to have concentrations of the oxides Fe_2O_3, MgO, and FeO + MnO systematically related to the composition of the parent rock. As plotted against ½ SiO_2 + K_2O-FeO-MgO-CaO in the rock, Fe_2O_3 and FeO + MnO in the constituent hornblendes seems to increase, whereas MgO decreases (Larsen and Draisen, 1950, Fig. 2).

Hornblende-rich inclusions are abundant in the tonalites of the southern California batholith. Hurlbut (1935, p. 609) interprets these inclusions to be xenoliths of associated gabbro, variously modified by interaction with the tonalite. There are no chemical analyses of the inclusion hornblendes, but Hurlbut states (1935, p. 622) that their optical properties (N_x 1.64–1.664, N_z 1.662–1.682) "indicate that the hornblendes of the inclusions are higher in Mg and lower in Fe than those of the tonalite." If the optical data are diagnostic, there are obvious analogies between the hornblendes of the Henry Mountains and those in the tonalites of the batholith.

The hornblende-bearing diorites of the Glen Tilt complex, Scotland, also contain hornblende-rich inclusions derived from the Perthshire Series of the Dalradian (Precambrian). Hornblendes from both rock types have been analyzed by Deer (1938, p. 58). He reports that the intrusive diorites (appinites) commonly contain two hornblendes. One, the first formed, is brown; the later generation is green. Neither hornblende is interpreted by Deer as having formed in equilibrium with magma. The hornblende from "typical Glen Tilt diorite" (Table 16, column 3) is much richer in Ti and Mg and much poorer in Fe_2O_3 than the hornblende phenocrysts in the Henry Mountains (Table 16, column 1).

The hornblendes analyzed by Deer (1938) from the xenoliths have a higher content of silica (44.2–49.0 per cent SiO_2) than those from the diorites. The molecular proportions of FeO/MgO in the xenolithic hornblendes range from 0.29 to 0.49, as compared to 0.49 for the inclusion hornblende HM 54 in the Henry Mountains.

The constituent hornblendes in metamorphosed granitic rocks of the northwest Adirondack Mountains are of interest in that several of them are very like the hornblende phenocrysts in the Henry Mountains. An analysis of hornblende from microcline granite gneiss as reported by Buddington and Leonard (1953) is listed in column 5 of Table 16. It differs from the hornblende phenocrysts from Mt. Pennell only in its slightly lower Al and Ca content and very high F content.

The hornblendes described by Buddington (1952) from metamorphosed and granitized gabbros of the Adirondack Mountains also are noteworthy because of their similarity to the inclusion hornblendes from the Henry Mountains (Table 16, columns 6, 7). Except for the differences in F and in the oxidation state of Fe, these hornblendes are remarkably alike. Buddington suggested a correlation between Ca content of the hornblendes and that of the enclosing rocks. This relationship does not seem to exist, however, for the rocks and constituent hornblendes in the southern California batholith (Larsen and Draisen, 1950; this report, Table 16). The ratio of CaO in parent rock to CaO in the constituent hornblende decreases markedly with decreasing basicity of the rocks in the calc-alkaline line of descent.

Another hornblende essentially like the phenocryst hornblendes has been described by Pecora and Fisher (1946). The analysis is listed in column 4 of Table 16. This hornblende occurs in vugs in a monzonite dike in the Bearpaw Mountains, Montana.

Most analyses of hornblendes published before 1943 are tabulated by Hallimond (1943). He attempted to correlate their Si content and "excess" (more than 2 atoms) of Na + K + Ca with the origin and composition of the host rock. Both phenocrysts and inclusion hornblendes from the Henry Mountains fall in the field of "diorite" hornblendes, near its mutual boundary with hornblendes from basalts (Fig. 4). Hallimond's elaborate diagram is liable to criticism if only because of the probable lack of precision between many of the analysts involved and the impurities of the samples analyzed.

Origin

The similarity in composition of four of the five hornblende phenocrysts is expectable in view of the constancy in composition of the

parent diorite porphyry. The one hornblende phenocryst from the Wickiup Ridge laccolith is compositionally unlike the others, and its parent rock is abnormally coarse-grained. This portion of the magma chamber and intruded with more initial heat or volatiles, these conditions would enable hornblende crystals to grow larger, to acquire a higher ratio of Mg/Fe,

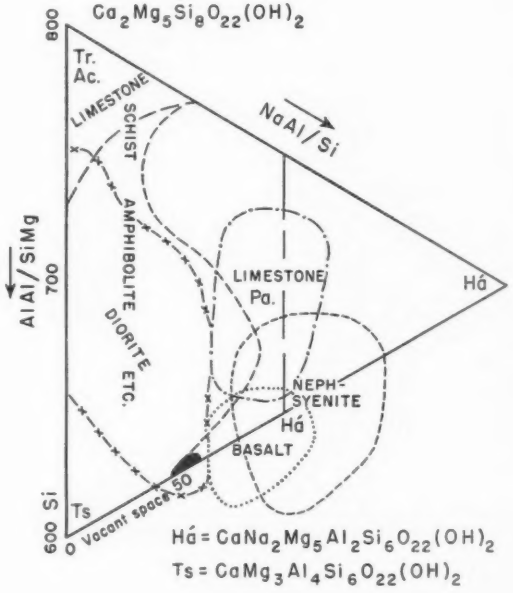

FIGURE 4.—RELATIONS OF HORNBLENDES FROM THE HENRY MOUNTAINS (SOLID AREA) TO HORNBLENDES FROM VARIOUS ROCK TYPES

(After Hallimond, 1943) Total Si content of the hornblendes is plotted against "excess" (more than 2 atoms) of Na + K + Ca.

hornblende also replaces pyroxene. Elsewhere, pyroxene replaces hornblende. Both the textural and paragenic differences at Wickiup Ridge are stated by Hunt (1953, p. 105) to be unique in the Henry Mountains. One possible explanation of the paragenic, textural, and compositional differences is that the Wickiup Ridge hornblende and associated plagioclase began growth in the parent magma before most of the phenocrysts in the exposed porphyries. If the Wickiup Ridge type phenocrysts were crystals formed early in the paragenetic sequence they may have settled to a different level in the magma chamber than that supplying most of the intrusive rocks in the Henry Mountains. This implies that part of the Wickiup Ridge laccolith with very coarse-grained crystals was tapped from deeper levels of the parent magma than the rest of the exposed porphyry. If the coarse-grained porphyry at Wickiup Ridge was derived from a deeper, hotter, and more mafic and to prevent late pyroxenes from forming at the expense of hornblendes.

The origin of the inclusion hornblendes is obscure because of the enigmatic nature of the inclusions themselves. Hunt (1953, p. 164) suggested that "... the inclusions may be altered fragments of diverse wall rock floated from great depths, or rock fragments from early differentiates in the magma reservoir or fragments of marginal unfused layers of the substratum from which the magma was derived." The possibility that these inclusions represent early hornblende-rich segregations is appealing because this would readily explain (1) the overlap in composition of phenocrysts and inclusion hornblendes, (2) the relative enrichment of Mg, Cr, and Ni in most of the inclusion hornblendes, and (3) the constancy of mineralogy in the inclusions, and (4) their abnormally high hornblende content (80–95 per cent in many inclusions). Inclusions of other rock types are

extremely rare in the porphyries of the Henry Mountains (Hunt, 1953, p. 164), whereas hornblendite and amphibolite inclusions are numerous.

References Cited

Billings, M. P., 1928, The chemistry, optics, and genesis of the hastingsite group of amphiboles: Am. Mineralogist, v. 13, p. 287–296

Bowen, N. L., 1928, The evolution of the igneous rocks: Princeton Univ. Press, 322 p.

Buddington, A. F., 1952, Chemical petrology of some metamorphosed Adirondack gabbroic, syenitic and quartz syenitic rocks: Am. Jour. Sci., Bowen Volume, pt. 1, p. 37–84

Buddington, A. F., and Leonard, B. F., 1953, Chemical petrology and mineralogy of hornblendes in northwest Adirondack granitic rocks: Am. Mineralogist, v. 38, p. 891–902

Chayes, Felix, 1952, Notes on the staining of potash feldspar with sodium cobaltinitrite in thin sections: Am. Mineralogist, v. 37, p. 336–340

Clarke, F. W., 1900, Analyses of rocks: U. S. Geol. Survey Bull. 168, 305 p.

Cross, Whitman, 1894, The laccolithic mountain groups of Colorado, Utah and Arizona: U. S. Geol. Survey 14th Ann. Rept., pt. 2, p. 157–241

Daly, R. A., 1914, Igneous rocks and their origin: N. Y., McGraw-Hill Book Co., 563 p.

Deer, W. A., 1938, The composition and paragenesis of the hornblendes of the Glen Tilt complex, Perthshire (Scotland): Mineralog. Mag. v. 25, p. 56–74

Diller, J. S., 1898, The rock specimens collected by the U. S. Geological Survey: U. S. Geol. Survey Bull. 150, 400 p.

Eckel, E. B., 1949, Geology and ore deposits of the La Plata district, Colorado: U. S. Geol. Survey Prof. Paper 219, 179 p.

Engel, A. E. J., and Engel, Celeste G., 1958, Progressive metamorphism and granitization of the major paragneiss, northwest Adirondack Mountains, New York. Part I. Total rock: Geol. Soc. America Bull., v. 69, p. 1369–1414

Fairbairn, H. W., 1953, Precision and accuracy of chemical analyses of silicate rocks: Geochim. et Cosmoschim. Acta, v. 4, p. 143–156

Fairbairn, H. W. *et al.*, 1951, A cooperative investigation of precision and accuracy in chemical, spectrochemical, and modal analysis of silicate rocks: U. S. Geol. Survey Bull. 980, 71 p.

Gilbert, G. K., 1877, Report on the geology of the Henry Mountains: U. S. Geog. and Geol. Survey, Rocky Mtn. Region, 160 p.

Hallimond, A. F., 1943, On the graphical representations of the calciferous hornblendes: Am. Mineralogist, v. 28, p. 65–89

Hunt, Charles B., 1953, Geology and geography of the Henry Mountain region Utah: U. S. Geol. Survey Prof. Paper 228, 234 p.

—— 1958, Structural and igneous geology of the La Sal Mountains, Utah: U. S. Geol. Survey Prof. Paper 294-I, p. 305–364

Hurlbut, Cornelius, 1935, Dark inclusions in a tonalite of Southern California: Am. Mineralogist, v. 20, p. 609–630

Iddings, J. P., 1891, The eruptive rocks of Electric Peak and Sepulchre Mountain, Yellowstone National Park: U. S. Geol. Survey 12th Ann. Rept., pt. 1, p. 569–664

Larsen, Esper S., 1948, Batholith and associated rocks of Corona, Elsinore, and San Luis Rey quadrangles, Southern California: Geol. Soc. America Mem. 29, 182 p.

Larsen, Esper S., and Draisen, W. M., 1950, Composition of the minerals in the rocks of the southern California batholith: London, 18th Internat. Geol. Cong. Rept., Pt. 2, Problems of geochemistry, p. 66–79

Mood, A. M., 1950, Introduction to the theory of statistics: N. Y., McGraw-Hill Book Co., 325 p.

Pecora, W. T., and Fisher, Bernard, 1946, Drusy vugs in a monzonite dike, Bearpaw Mountains, Montana: Am. Mineralogist, v. 31, p. 370–385

Phemister, T. C., 1945, The Coast Range batholith near Vancouver, British Columbia: Geol. Soc. London Quart. Jour., v. 101, p. 37–88

Read, H. H., 1948, Granites and granites, p. 1–19 *in* Gilluly, James, *Chairman*, Origin of granites: Geol. Soc. American Mem. 28, 140 p.

Shapiro, Leonard, and Brannock, W. W., 1956, Rapid analysis of silicate rocks: U. S. Geol. Survey Bull. 1036-C, 56 p.

Winchell, A. N., and Winchell, Horace, 1951, Elements of optical mineralogy: N. Y., John Wiley & Sons, 551 p.

California Institute of Technology, Pasadena, Calif.

Manuscript Received by the Secretary of the Society, July 8, 1958

Published by Permission of the Director, U. S. Geological Survey

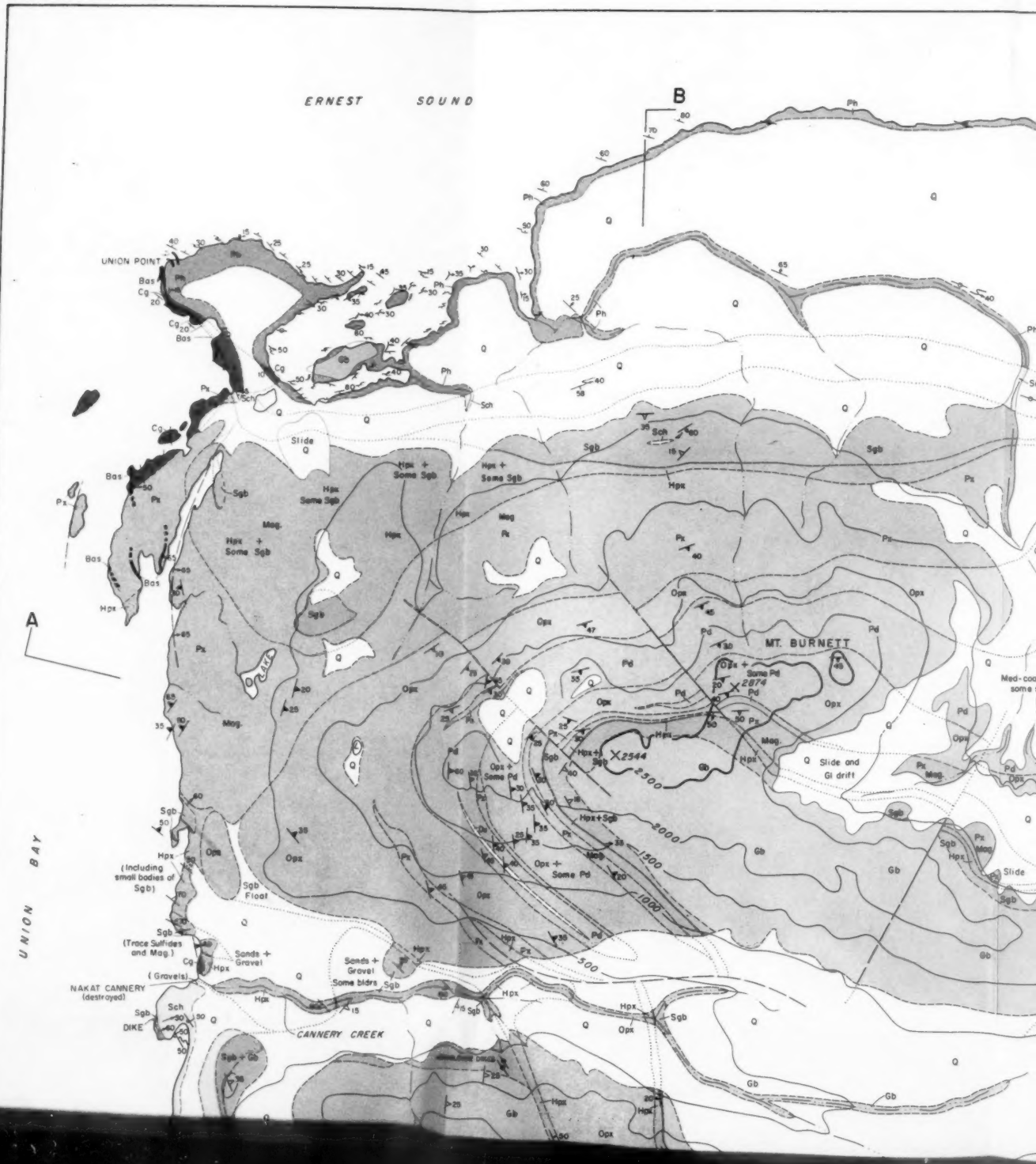
ERNEST SOUND
UNION POINT
Bas
Cg
Ph
Px
Sch
Slide
Q
Sgb
Hpx + Some Sgb
Mag.
Opx
Pd
MT. BURNETT
2874
2544
Opx + Some Pd
Slide and Gl drift
Gb
2500
2000
1500
1000
500
A
B
UNION BAY
(Including small bodies of Sgb)
Sgb Float
(Trace Sulfides and Mag.)
Sands + Gravel
(Gravels)
NAKAT CANNERY (destroyed)
DIKE
CANNERY CREEK
Sands + Gravel Some blds
Med-coa some

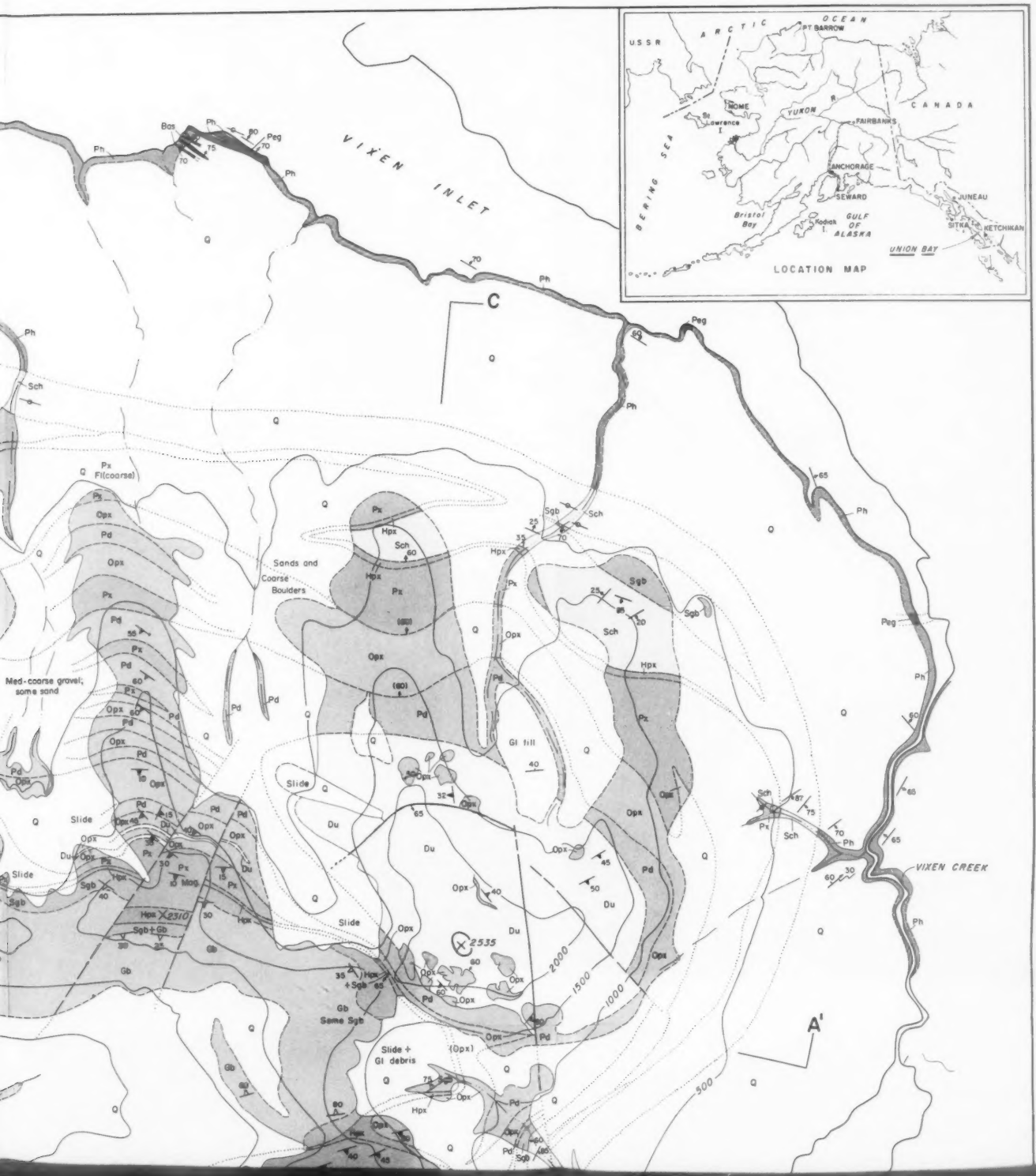
VIXEN INLET
Ph
Bas
Peg
Q
Px
Fl(coarse)
Opx
Pd
Hpx
Sch
Sgb
Gb
Du
Mog
Sands and
Coarse
Boulders
Med-coarse gravel;
some sand
Slide
Gl till
Same Sgb
Slide +
Gl debris
(Opx)
2310
2535
2000
1500
1000
500
C
A'
VIXEN CREEK
ARCTIC OCEAN
PT BARROW
U.S.S.R.
NOME
St Lawrence I.
YUKON R.
CANADA
FAIRBANKS
BERING SEA
ANCHORAGE
SEWARD
JUNEAU
Bristol Bay
Kodiak I.
GULF OF ALASKA
SITKA
KETCHIKAN
UNION BAY
LOCATION MAP

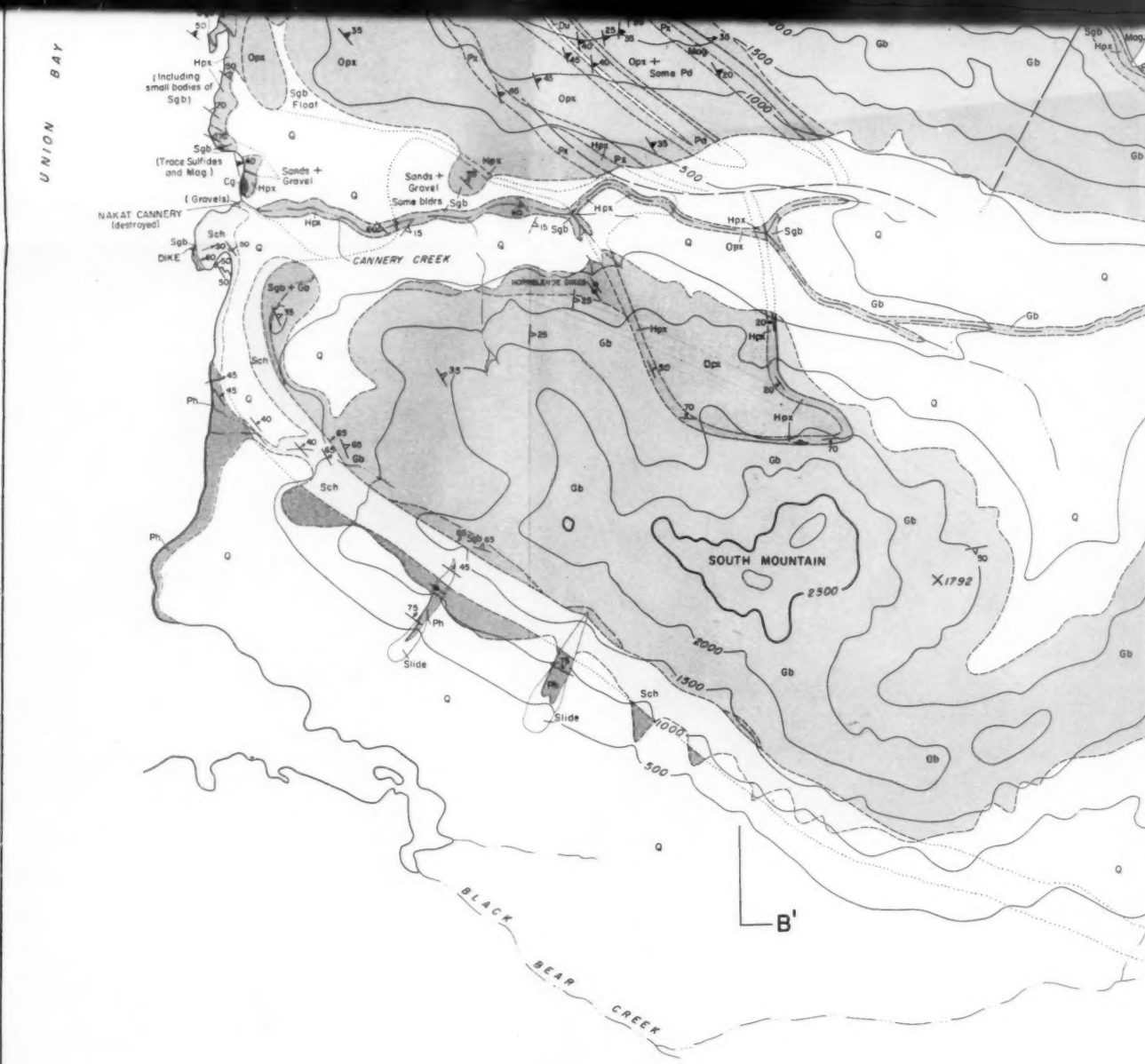

INTRUSIVE ROCKS

Du	Dunite	< 10% Pyroxene
Pd	Peridotite	> 40% < 90% Olivine
Opx	Olivine Pyroxenite	> 10% < 40% Olivine
Px	Pyroxenite	< 10% Olivine
Hpx	Hornblende Pyroxenite	
Gb	Gabbro	
Sgb	Saussuritized Gabbro	
Bas	Basaltic Dikes	
	Pegmatitic Dikes	
Mag	Rocks containing notable Magnetite	

METAMORPHIC ROCKS

Sch	Schist
Ph	Phyllite

SEDIMENTARY ROCKS

Q	Quaternary (Alluvium & Glacial drift)
	Conglomerate

STRUCTURE SY

- 60 Mineral band
- 80 Strike and d
- Vertical bed
- 34 Plunge of lin
- 60 20 Strike and di
- 60 Predominant
- 60 Foliation in

GEOLOGY OF THE UNION BAY

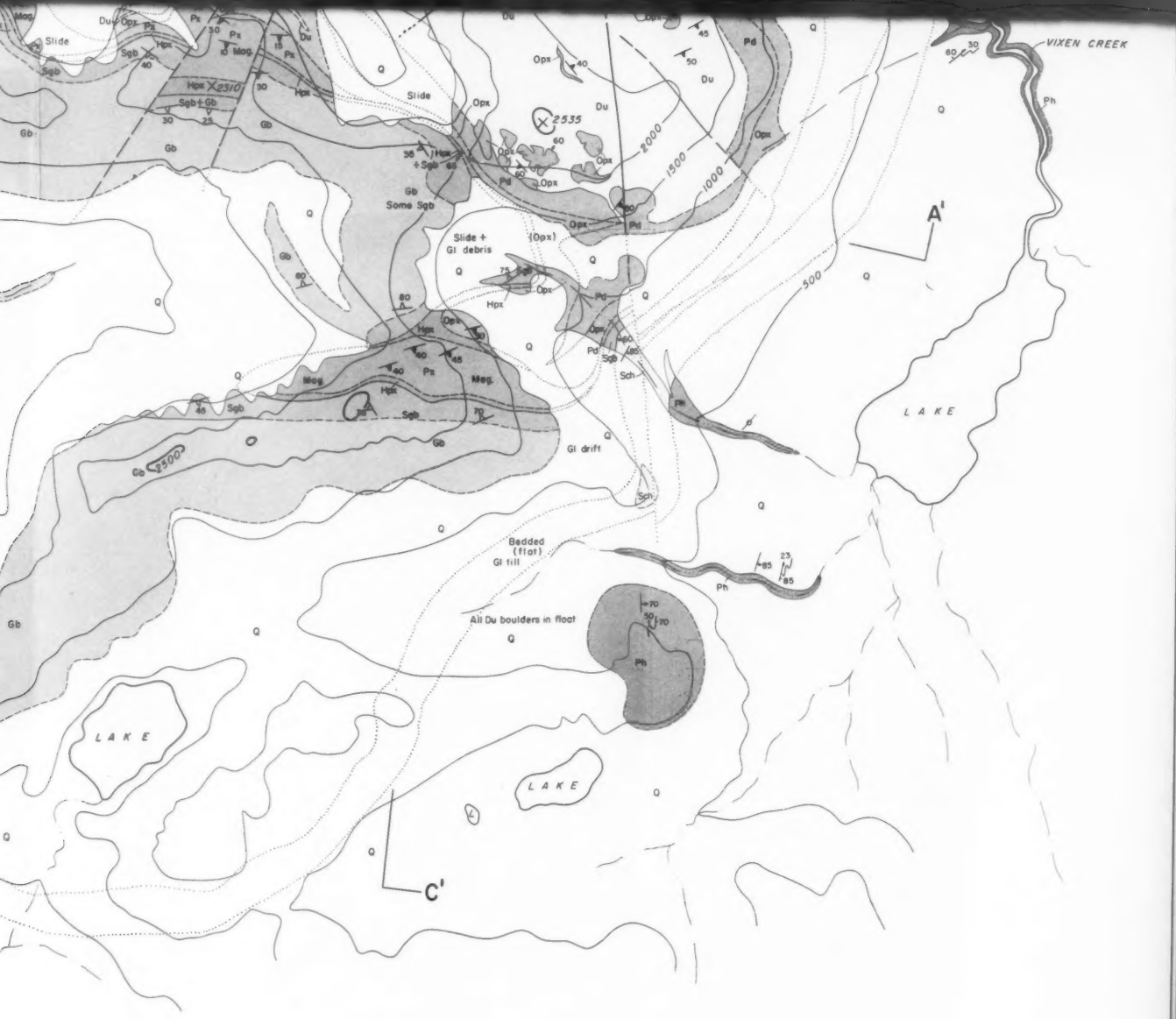

E SYMBOLS

- al banding in intrusive rocks
- and dip of bedding
- al bedding
- e of lineation
- and dip and plunge of folds
- minant foliation in metamorphic rocks
- on in intrusive rocks

CONTACTS

- Well exposed
- Poorly exposed; approximately located
- Covered
- Dip of contacts

GEOLOGY BY JOHN C. RUCKMICK

1954 – 1956

N

SCALE IN FEET

1320 660 0 1320 2640 3960 5280 6600

CONTOUR INTERVAL 500 FEET

AY AREA, SOUTHEASTERN ALASKA

BULLETIN OF THE GEOLOGICAL SOCIETY OF AMERICA
VOL. 70, PP. 981–1018, 5 FIGS., 4 PLS. AUGUST 1959

ORIGIN OF THE ULTRAMAFIC COMPLEX AT UNION BAY, SOUTHEASTERN ALASKA

BY JOHN C. RUCKMICK AND JAMES A. NOBLE

ABSTRACT

An ultramafic complex at Union Bay, in southeastern Alaska, is an exceptionally well-exposed example of a series of similar complexes forming a belt parallel to the Coast batholith.

A body of gabbro, approximately circular in plan and about 6 miles in diameter, intrudes folded sedimentary rocks of probably Triassic and Cretaceous age. A moderately low grade of regional metamorphism in the sedimentary rocks is increased to almandite-zone grade adjacent to the gabbroic contact. Intrusive into the gabbro is a remarkable ultramafic complex which comprises a vertical pipe approximately 1 mile in diameter, to which is attached a lopolithic offshoot approximately 5 miles long and 3 miles wide. The ultramafic units range through hornblende pyroxenite, pyroxenite, olivine pyroxenite, peridotite, and dunite, and both the pipe and the lopolith show a well-developed concentric zoning with dunite in the center and pyroxenite or hornblende pyroxenite on the periphery. Magnetite is a primary constituent of the pyroxenite unit.

The most plausible explanation of the structure and petrology of the ultramafic complex is a hypothesis of successive injections of an ultramafic magma changing in composition with time and intruded in reverse of the order of crystallization of the component minerals. It has not been possible to explain the gabbro (which is olivine-free) by the same mechanism, yet the space and time relationships here, as elsewhere in the world, are probably not accidental. It is proposed, therefore, that a body of gabbro was emplaced, and into this was injected a plug and associated lopolith first of diopside-magnetite magma with minor olivine, then diopside-olivine magma, and finally olivine magma, each new magma intruding the central, incompletely solidified portion of the earlier magma. Minor mixing and melting explain the composition and distribution of the intermediate units of the complex. Lack of contact metamorphism of grade that might be expected to accompany intrusions of such high temperature is explained first by the fact that the ultramafic magmas were almost everywhere in contact with gabbro, not sedimentary rocks, and second by the fact that, being anhydrous, the ultramafic magmas absorbed, rather than expelled, volatiles.

The only likely source for magmas of these compositions would be melting portions of the mantle, but no proposed mechanism for supplying the energy for this process is suggested herein. With an available source of energy, however, it can be postulated that magmas would be generated in the succession proposed. The gabbroic magma probably would originate as a result of melting at a shallower level.

CONTENTS

TEXT

	Page
Introduction	982
Geology of Union Bay	982
Metasedimentary rocks	982
Gabbro	982
Ultramafic intrusive complex	982
Tertiary rocks	983
Description of formations	983
Metasedimentary rocks	983
Gabbro and saussurite gabbro	986
Ultramafic intrusive rocks	989
Definitions	989
Pyroxenite	989
Hornblende pyroxenite	997
Olivine pyroxenite	999
Peridotite	1000
Dunite	1002
Magnetite	1003
Origin of ultramafic rocks	1005
Relationships between gabbro and ultramafic rocks	1005
Nature of the ultramafic magma	1006
Distribution of ultramafic rock types	1006
Origin of the magnetite	1011
Problem of metamorphism	1012
Source of the magmas	1014
References cited	1016

ILLUSTRATIONS

Figure	Page
1. Contact between ultramafic and gabbroic intrusive bodies, (generalized)	987
2. Correlation of indices and composition for olivine and diopside in ultramafic rock units	996
3. Chemical composition of monoclinic pyroxenes in terms of percentages of Ca, Mg, and Fe	997
4. Sketch of two dunite sills	1000
5. Equilibrium diagrams of the system diopside-forsterite	1009

Plate	Facing page
1. Geology of Union Bay area	98
2. Photomicrographs of thin sections	99
3. Photomicrographs of thin sections	99
4. Interpretive geological sections	100

TABLES

Table	Page
1. Chemical and mineralogical analyses of specimens	98
2. Definitions of ultramafic rock units	99
3. Correlation of optical indices and composition of specimens	99

Introduction

Many separate bodies of ultramafic intrusions occur in the coastal belt of islands and mainland of southeastern Alaska, between the open Pacific Ocean and the granodioritic masses of the Coast batholith. The ultramafic complex of Mount Burnett, at Union Bay, 35 miles north of Ketchikan, is one of the best exposures (Pl. 1). This area is mentioned in Buddington and Chapin (1929), Kennedy and Walton (1946), and Walton (1951).

Assistance and advice in the field were given by S. P. Clark, T. N. Irvine, G. C. Kennedy, W. F. Slawson, R. H. Stebbins, and H. P. Taylor, Jr. The manuscript has been reviewed critically by A. F. Buddington, Ian Campbell, H. H. Hess, J. W. Peoples, H. P. Taylor, Jr., C. E. Tilley, and G. J. Wasserburg, to whom the authors are indebted for many suggestions.

Geology of Union Bay

Metasedimentary Rocks

The ultramafic and gabbroic intrusive bodies at Union Bay crop out 12 miles west of the western contact of the Coast batholith and intrude a belt of metasedimentary rocks mapped and referred to as the Wrangell-Revillagigedo metamorphic series by Buddington and Chapin (1929, p. 49–74). These rocks have undergone low-grade regional metamorphism to marbles, slates, phyllites, and chloritic and amphibolitic volcanic greenstones. At Union Bay the intrusive rocks are emplaced in a sequence of phyllites with a very few intercalated tuffs.

Problems of correlation of the Wrangell-Revillagigedo members leave their age uncertain, and Buddington refers to the sequence as "probably Ordovician to Jurassic or later." The Union Bay metamorphic rocks are probably best correlated with the belt of slates, graywackes, and greenstones in the vicinity of Ketchikan. Here Triassic slates and Cretaceous greenstones have been dated with fair certainty on the basis of lithologic, structural, and some paleontological evidence.

Gabbro

Although the main body of gabbro lies south of the ultramafic body, a portion of it crops out along most of the high east-west ridge north of Cannery Creek, forming a relatively thin cap over part of the ultramafic complex. Different-sized areas of gabbro also crop out along or near portions of the north, northeast, and southwest margins of the ultramafic body. In many places along the margin of the main body of gabbro, where it is in contact with metasedimentary or ultramafic rocks, the gabbro has been partially saussuritized. All the smaller bodies of gabbro which are separate from the main body of gabbro are completely saussuritized.

Ultramafic Intrusive Complex

The over-all form of the ultramafic complex is interpreted herein to be that of a spoon-shaped lopolith with a feeder (Pl. 4). At the east end of the intrusive body, a cylindrical plug of dunite, 1 mile in diameter, constitutes the feeder conduit. On the north, east, and south, the dunite plug is enclosed in peridotite, olivine pyroxenite, and pyroxenite (in that order) dipping steeply away from the dunite core. To the west, the dunite passes gradationally through peridotite into the central portion of the main body of the lopolith. The spoon-shaped lobe, which forms the main

body of the lopolith, exhibits a pronounced, subhorizontal, compositional layering; layers measure from inches to hundreds of feet in thickness. The layering is a primary feature that expresses the difference between layers in the relative proportions of the two principal minerals, diopside and olivine. The more olivine-rich rocks, dunite and peridotite, are involved in the most conspicuous layering and constitute the more central portions of the lopolith. These units pass outward gradationally (in three dimensions) through olivine pyroxenite to pyroxenite, constituting a continuous shell or envelope encasing the olivine-rich rocks. Hornblende is important in the outer margin of the pyroxenite shell, forming a hornblende pyroxenite rock. This rock lies between pyroxenite and saussurite gabbro or schist, and it constitutes the outermost ultramafic unit in most places.

The hornblende pyroxenite, pyroxenite, and much of the olivine pyroxenite are essentially devoid of primary layering, with the exception of one feature. Locally in the pyroxenite and in the olivine pyroxenite, regular, parallel bands of magnetite from a fraction of an inch to several inches in thickness and from an inch to 1 foot apart are present. These magnetite bands or layers are especially prevalent in the western portion of the pyroxenite and in places are continuous for 100 feet or more along the strike. The most continuous exposures are in the higher, more central region of the lower pyroxenite unit on the western slopes. Here the attitude of the magnetite bands is concordant with the attitude of the peridotite layering higher in the intrusive body.

Some primary magnetite is present in all the igneous rock units at Union Bay. However, the most concentrated occurrence is in the pyroxenite unit. The most notable concentration of magnetite lies in a zone in the lower pyroxenite and hornblende pyroxenite units along the west and northwest sides of the ultramafic body, where, over a considerable area, the magnetite content of the rock is remarkably constant.

Chromite occurs as a minor constituent of the dunite, and there are minor amounts of sulfide minerals, mostly pyrite with some chalcopyrite and pyrrhotite, sporadically distributed throughout the peripheral rocks of the ultramafic intrusive mass. None of these products of mineralization appear to be of economic interest.

Tertiary Rocks

The ultramafic rocks and the Wrangell-Revillagigedo metamorphic rocks are unconformably overlain in some places by a coarse conglomerate which has been correlated with the Port Camden basal Eocene unit by Buddington and Chapin (1929, p. 263). The conglomerate, metamorphic, and ultramafic rocks are cut by basaltic dikes and sills. Acidic rocks of pegmatitic nature crop out in the metamorphic rocks north and east of the ultramafic complex.

Description of the Formations

Metasedimentary Rocks

With the exception of a very few tuff beds, the Wrangell-Revillagigedo series is represented at Union Bay by the low-grade metamorphic equivalents of pelitic sediments, most probably shales and fine-grained graywackes. Beyond the aureole of contact metamorphism the dominant rock type is a very fine-grained phyllite composed of quartz, sericite, penninite, and albite (An_{10}), with some graphite and traces of apatite, pyrite, and magnetite (specimen 400 of Table 1).

Fairly continuous sections across the contact-metamorphic aureole are rare, but enough are found to illustrate the grade of metamorphism. The first notable change, generally at about 1000 feet from the igneous contact, is to quartz-oligoclase-almandite-biotite schist, at first without increase in average grain size or foliation, but gradually increasing in grain to a schist, with marked metamorphic segregation and generally strong contortion. In a typical exposure of coarse-grained, foliated, and highly contorted schist within 500 feet of the igneous contact, the foliation consists of biotite-rich bands between bands of recrystallized, granulose quartz and oligoclase (An_{28} to An_{30}). The leucocratic bands also contain a few subhedral crystals of epidote and sphene, a few ragged, anhedral grains of hornblende, and traces of interstitial orthoclase. In thin section, the regular orientation of the biotite is deflected around medium-grained, fractured, subhedral garnets and, to a lesser degree, around larger grains of quartz and andesine. Garnets also include circular or spiral patterns of fine-grained biotite typical of porphyroblastic crystal development. The garnets are deep red in hand specimen and, on the basis of very high indices and complete lack

TABLE 1.—CHEMICAL AND MINERALOGICAL ANALYSES OF SPECIMENS

Chemical analyses by W. H. Herdsman, Glasgow, Scotland. Abbreviations as follows: Ph, phyllite; Sch, schist; Gb, gabbro; Sgb, saussurite gabbro; Hpx, hornblende pyroxenite; Px, pyroxenite; Opx, olivine pyroxenite; Pd, peridotite; Du, dunite. Blank boxes indicate mineral was not observed.

Components	Specimen No.																			
	400 Ph	111 Sch	192c Sch	222 Sch	160 Gb	164 Sgb	223 Sgb	130 Sgb	193 Sgb	192a Hpx	95 hb min. sep.	32a diop. min. sep.	32a Px	109 diop. min. sep.	183b diop. min. sep.	9 Opx	200 Pd	6 Du	183a Du	231 Du
SiO_2	66.34	58.66	59.36	60.14	49.94	48.70	48.76	45.96	52.34	43.57	39.82	47.42	37.54	48.66	51.94	49.24	39.06	37.25	38.48	40.22
Al_2O_3	15.08	17.68	17.94	17.93	20.24	18.14	17.54	19.38	18.58	17.13	16.64	5.98	5.35	5.88	1.52	2.42	1.42	.97	1.06	1.69
FeO	4.95	6.96	7.08	6.12	7.63	6.61	4.94	6.42	5.85	7.83	8.93	3.96	9.64	5.43	2.79	6.75	7.24	12.34	8.42	9.28
Fe_2O_3	.64	.92	.94	.74	2.58	4.58	5.66	5.17	2.86	3.16	4.37	2.48	15.52	2.33	.83	2.00	5.75	4.58	1.08	.88
TiO_2	.65	.90	.72	.88	.56	.96	.68	.88	.66	.56	1.24	.86	2.23	.38	.13	.21	tr.	..	..	tr.
MnO	.07	.13	.14	.14	.18	.20	.19	.24	.18	.24	.18	.13	.16	.19	.14	.19	.23	.27	.17	.18
CaO	1.56	1.83	2.88	3.92	9.46	9.54	10.36	11.35	9.46	18.42	12.09	23.36	17.40	23.02	22.82	18.90	4.78	.38	.19	..
MgO	2.88	3.69	3.72	2.93	5.13	5.06	5.74	5.22	3.72	4.83	12.63	14.62	11.85	13.63	18.56	19.12	34.39	39.42	46.88	47.46
K_2O	1.48	2.49	1.68	1.74	.62	.95	.43	.83	.39	tr.	.96	tr.	tr.	.06	.04	.07	tr.	.11	..	tr.
Na_2O	3.34	3.05	3.54	3.58	2.74	2.23	3.87	2.74	3.48	1.04	1.62	tr.	tr.	.18	.09	.18	.12	.36	..	.04
H_2O, −105°C.	.23	.24	.42	.10	.05	.34	.06	.06	.24	.25	.26	.20	.32	.09	.19	.19	.49	.48	.68	.09
H_2O, +105°C.	2.80	2.95	1.23	1.35	.35	2.44	1.30	1.04	1.87	1.82	1.38	.76	.28	.31	.62	.64	6.31	3.96	2.94	.30
CO_2	..	..	..	..	..	..	..	..	..	..	..	..	..	..	..	..	..	..	..	..
P_2O_5	.23	.22	.13	.17	.33	.37	.27	.53	.56	1.31	tr.	tr.	tr.	tr.	tr.	tr.	tr.	tr.	tr.	tr.
Cr	n.d.	n.d.	..	..	n.d.	n.d.	tr.	..	n.d.	n.d.	n.d.	n.d.	n.d.	..	.22	.26	..	.26	n.d.	..
Total	100.25	99.72	99.78	99.74	99.81	100.12	99.80	99.82	100.19	100.16	100.12	99.77	100.29	100.16	99.89	100.17	99.79	100.12	99.90	100.14
Olivine																				
Diopside					12					16	tr.	98	72	93	3	16	57	80	92	97
Hornblende															92	80	12	4		

Total	100.25	99.72	99.78	99.74	99.81	100.12	99.80	99.82	100.19	100.16	100.12	99.77	100.29	100.16	99.89	100.17	99.79	100.12	99.90	100.14

Olivine															3	16	57	80	92	97
Diopside					12					16	tr.	98	72	93	92	80	12	4		
Hornblende				6		21	45	33	12	30	97	tr.	4	2	1	1		tr.		
Hypersthene					14															
Actinolite								tr.	10	5	2									
Biotite		31	29	42	4	3	tr.	tr.												
Chlorite (penninite)	26	4				12		10	8	3										
Serpentine																				
Epidote and clinozoisite				1		37	20	36	35	32					1	tr.	28	15	6	
Plagioclase	12	18	38	25	64	16	28	18	22	10										
Comp. of plagioclase	An_{10}	An_{30}	An_{15-40}	An_{28-30}	An_{55}	An_{5}	An_{5}	An_{5}	An_{5}	An_{5}										
Quartz	27	12	28	18		2	5		10											
Sericite	32	34	tr.	3		6	tr.	tr.	1											
Orthoclase				tr.	tr.															
Carbonate			1				tr.													
Almandite (garnet)			3	3																
Apatite	?					1		tr.		tr.										
Hercynite													2							
Sphene						1	1			tr.										
Magnetite	tr.	tr.			5	tr.	tr.			tr.	tr.	1	21	5	2	2	2	tr.	1	2
Ilmenite													1							
Chromite															tr.		tr.	tr.	1	1
Sulfides	tr.	1	tr.	1		tr.	tr.	2	1	3										
Total	99+	100	99+	99+	99+	99+	99+	99+	99	99+	99+	99+	100	100	99+	99+	99+	99+	100	100

of birefringence, are judged to be almandite. The mineralogy and a chemical analysis of a typical specimen of this rock (no. 222) appear in Table 1.

The inner part of the metamorphic aureole is well exposed just south of Cannery Creek at the abandoned cannery. Here, a considerable range in composition of plagioclase is present in transitional textures. The largest grains (1–2 mm) are zoned from An_{40} (center) to An_{25} (rim). The smallest grains (*ca.* 0.3 mm) are subhedra of the composition An_{32} to An_{25}. Medium to large (up to 0.8 mm), very irregular, interstitial areas are An_{25} to An_{15}. The mineralogy and a chemical analysis of a representative specimen of this schist (specimen no. 192c) appear in Table 1. At another location about a mile to the south, relatively large (0.7–2 mm) almandite garnets, quartz, and zoned plagioclase grains show porphyroblastic development with inclusions and local deflection of the biotite orientation. The porphyroblastic plagioclase is zoned from An_{37} (center) to An_{30} (rim), probably indicating a steep temperature gradient at the contact and reflecting the related lack of equilibrium during metamorphism.

In many places saussuritization has been superimposed on the thermal metamorphism, converting almandite to aggregates of penninite and magnetite, and oligoclase to aggregates of clinozoisite, epidote, albite, and quartz. Sphene is common in these zones, and green hornblende is locally abundant, in places poikilitically enclosed in quartz.

Gabbro and Saussurite Gabbro

With the exception of marginal areas of one to several hundred feet in width, the main body of gabbro constituting South Mountain and its northward extension capping the ultramafic intrusion are essentially homogeneous texturally and mineralogically. An average composition is 60 per cent plagioclase (An_{56} to An_{43}), 15 per cent hypersthene (En_{67} Fs_{33}), 10 per cent diopside, 5 per cent biotite, 5 per cent magnetite, and traces of orthoclase, clays, sericite, apatite, and hydrous iron oxides. The rock is everywhere medium-grained, plagioclase crystals ranging from 1 mm to 4 mm and pyroxene crystals from 0.5 mm to 2 mm. Most outcrops exhibit subparallel orientation of pyroxene and plagioclase crystals. This foliation is more continuous in marginal areas than toward the center of the intrusive body, where it either shows local variation or is too inconspicuous to map. The chemical composition and mineralogy of a specimen representative of the central portion of the main body of gabbro underlying South Mountain are given in Table 1 (specimen no. 160).

The marginal portions of the main gabbro intrusive body are dioritic for several hundred feet adjacent to the contacts with schist on the west, southwest, and south slopes of South Mountain. In these areas the mafic minerals are hornblende and biotite, and the composition of the plagioclase ranges from An_{50} to An_{36}. A specimen collected from the contact with schist at a landslide scar on the west flank of South Mountain has the following composition: 60 per cent andesine, 15 per cent biotite, 10 per cent quartz, 10 per cent tremolite and actinolite, 2 per cent penninite, a few anhedral garnets, and traces of magnetite, apatite, and carbonate. Many of the larger plagioclase grains are zoned from An_{47} (center) to An_{31} (rim). Tremolite and actinolite occur together in clusters, probably as a replacement of hornblende. The actinolite is intimately associated with small, anhedral grains of magnetite.

The indices of refraction of both monoclinic and orthorhombic pyroxenes from four selected specimens were compared in an attempt to study the variation in composition throughout the gabbroic intrusive body. The variation in composition of the monoclinic pyroxene was found to be very small, almost within the limits of error of the oil-immersion method. The hypersthene, however, showed the following variation: in two specimens collected from the cap of gabbro overlying the ultramafic body, 3½ miles apart, but both within 500 feet of the contact with the ultramafic body, the composition of the hypersthene is En_{67} Fs_{33}. The composition of the hypersthene in a specimen collected from the central portion of the main gabbroic intrusive body is En_{64} Fs_{36}; hypersthene in a specimen collected 500 feet from the contact with schist on the west slope of South Mountain is En_{54} Fs_{46}. This trend of decreasing percentage of the magnesian molecule (enstatite) from the ultramafic contact (to the north) to the contact with metasedimentary rocks (to the southwest) is difficult to interpret unless the ultramafic body is younger and has intruded the gabbro.

The only clean, but very limited, exposure of the contact between the main body of gabbro and the ultramafic intrusive body occurs in Cannery Creek one-half mile east of tidewater. Nowhere has been found a well-exposed contact where the cap of gabbro overlies the ultramafic body, although many outcrops of both

intrusive bodies occur at higher elevations near (within 200 or 300 feet of) the contact. All the field evidence indicates that the contact relationships between these two intrusive bodies are similar everywhere. Figure 1 is a graphic generalization of these contact relationships.

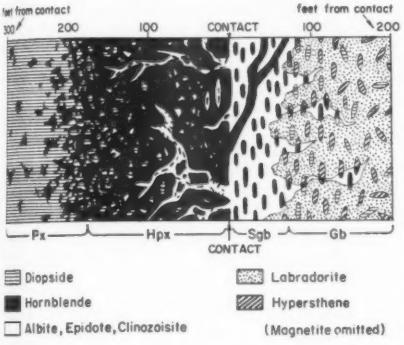

FIGURE 1.—CONTACT BETWEEN ULTRAMAFIC AND GABBROIC INTRUSIVE BODIES (GENERALIZED)

The scale of the veins and mineral grains is much larger than the scale of the distance, in feet, from the contact.

In all areas, the ultramafic rock in contact with the gabbro is hornblende pyroxenite, in which the relative amount of hornblende increases toward the contact to such proportions (over 75 per cent) that the rock can be termed hornblendite. Generally within 100 to 200 feet of the gabbro, the hornblende pyroxenite exhibits many irregular veinlets of all sizes up to several feet in width composed of clinozoisite, epidote, and albite, with or without elongate prisms of black hornblende (generally partially or wholly actinolitized). Some quartz, carbonate, and sericite are commonly present in the veins. At the contact with gabbro, the texture and relative proportions of minerals change abruptly to the rock unit mapped and referred to as saussurite gabbro (25–50 per cent hornblende and actinolite, 50–75 per cent albite, clinozoisite and epidote).

The saussurite gabbro commonly exhibits a foliation parallel to the contact and concordant with foliation in the gabbro near by. Saussuritization of the gabbro disappears inward, away from the ultramafic contact, through a system of veins and pods in which the orientation of the hornblende is parallel to the orientation of plagioclase and pyroxene in the adjacent, unaltered rock (Fig. 1).

Because continuous exposures are rare, the extent of saussuritization around the margins of the main body of gabbro in contact with the ultramafic body cannot be accurately determined. The distribution of saussurite appears to be sporadic, and, in a number of places near the periphery of the gabbro cap overlying the ultramafic body, unaltered gabbro crops out within 100 to 200 feet of the ultramafic rocks (Pl. 1).

One specimen of unaltered gabbro collected 100 feet from the ultramafic contact near Mount Burnett contains, besides the normal plagioclase and pyroxenes, an unusual amount of orthoclase (15 per cent of the rock). At the northeastern extremity of the main body of gabbro, in the vicinity of the dunitic core of the ultramafic body, the gabbro is unusually mafic and contains up to 60 per cent pyroxene (approximately equal amounts of diopside and hypersthene).

On both sides of Cannery Creek ½ to 1 mile east of tidewater, the gabbro is saussuritized over an area of ½ square mile, extending several thousand feet away from the ultramafic contact. The structure sections suggest that this portion of the gabbro may have been just under the floor of the ultramafic intrusion before erosion.

Southeast of the contact in Cannery Creek, the saussurite gabbro is cut by several hornblendite dikes approximately 3 feet wide. These dikes are vertical and strike N. 40° W. The saussurite gabbro in this area also contains many podlike segregations from 1 inch to 10 feet in diameter of magnetite surrounded by successive rims of diopside and hornblende, in that order.

The marginal portions of the dioritic gabbro in contact with schist on the west and southwest slopes of South Mountain exhibit minor areas of saussuritization. However, the distribution of saussurite gabbro around this contact is not continuous. Some saussuritization is evident near the contact of gabbro and schist 1½ miles southeast of the cannery. Otherwise most outcrops along the west and southwest periphery of the gabbro, including one clean exposure of the contact at the landslide scar previously mentioned, show no evidence of saussuritization.

The development of saussurite gabbro in the main body of gabbro can be considered essentially, but not entirely, a marginal feature. In two or three places in the more central portions of the unaltered gabbro, small veins and patches of saussurite gabbro were observed.

At the southeastern extremity of the ultramafic intrusion, the main gabbro body pinches out between ultramafic rocks and schist. The gabbro here is a medium-coarse-grained albite-clinozoisite-epidote-hornblende schist, briefly mentioned in the preceding section of the text. The mineralogy and a chemical analysis of this rock (specimen no. 223) appear in Table 1. The chemical analysis of this schist is very similar to that of unaltered gabbro (specimen no. 160).

Included in the hornblende pyroxenite in some places within 200 feet of the contact with the overlying cap of gabbro are tabular bodies of saussurite gabbro from 6 inches to 20 feet in length oriented parallel to the contact. These inclusions are best exposed near the western extremity of the gabbro cap.

Bodies of saussurite gabbro of all sizes from several inches to several hundred feet long appear to be included in the hornblende pyroxenite along the shore for 1 mile north of the cannery site. The larger inclusions are lenticular in plan, dip steeply, and trend northwest (Pl. 1). The largest of these inclusions crops out 500 feet north of the mouth of Cannery Creek. At the southeastern extremity of the outcrop, the rock is fine-grained, well indurated, and vaguely exhibits a thin banding. This rock is composed of hornblende partly altered to actinolite, clinozoisite, epidote, quartz, albite (An_5), penninite, and minor amounts of sericite, apatite, and pyrite. The amount of quartz ranges from less than 5 per cent to 20 per cent of the rock in different specimens. The mineralogy and a chemical analysis of a representative specimen of this outcrop are given in Table 1 (specimen no. 193).

Although the exposure is interrupted by 200 feet of stream gravel, the fine-grained, banded rock appears to grade, over a distance of 600 feet along the shore, through a coarsely banded, gneissic rock into medium to coarse-grained saussurite gabbro without any change in mineralogy other than a decrease in the amount of quartz.

Specimen no. 130 was collected from a strongly banded, fine-grained, granular inclusion of saussurite gabbro in hornblende pyroxenite three-quarters of a mile north of Cannery Creek. The mineralogy and a chemical analysis of this rock are given in Table 1.

There are three other areas at Union Bay where bodies of saussurite gabbro are distinct from each other and separated from the main gabbro intrusive body at the present level of erosion (Pl. 1). They are: (1) two bodies approximately 1300 feet in the longest dimension which crop out within the northwestern portion of the hornblende pyroxenite south of Union Point; (2) an elongate, lenticular body 3 miles long and as much as ½ mile wide which crops out along the northern margin of the ultramafic body, and separates that intrusive body from the metasedimentary rocks to the north; (3) an outlying, lenticular body 1 mile long and as wide as 1000 feet which crops out in the metasedimentary rocks one-quarter mile northeast of the ultramafic body near Vixen Inlet.

All these bodies of saussurite gabbro exhibit essentially identical mineralogy, textures, and contact relationships (against the same rock types). An average composition for all saussurite gabbro is approximately 30 per cent hornblende, 30 per cent epidote and clinozoisite, 15 per cent albite (An_3 to An_{10}), and minor and variable amounts of diopside, quartz, actinolite, apatite, carbonate (ankerite), sphene, chlorite (penninite), biotite, sericite, magnetite, sulfides (pyrite, chalcopyrite, pyrrhotite), and hydrous iron oxides. Except for some fine-grained inclusions north of Cannery Creek, the rock is generally composed of relatively coarse grains of hornblende and fine-grained albite, epidote, clinozoisite, and minor constituents. Foliation is pronounced only in some inclusions, or within approximately 100 feet of the contact with ultramafic rocks.

In most specimens hornblende exhibits elongate, subprismatic form, although in thin section even the best-developed prisms have ragged, interlocking boundaries. Many hornblende grains poikilitically enclose fine-grained quartz and apatite. Where diopside grains are observed, they are very ragged remnant grains almost completely replaced by hornblende. Two generations of albite are commonly present. Medium-grained anhedra constitute 30 to 60 per cent of the area of a thin section. These grains contain many fine-grained subhedral to anhedral clinozoisite and epidote crystals and commonly some sericite. A later generation of fine-grained, unaltered albite commonly cuts across and rims the larger grains of albite and hornblende. Both clinozoisite and epidote are present in most specimens. Clinozoisite is the more widespread of the two and occurs as very fine grains in albite. Although epidote also occurs in this way in some specimens, it is more commonly developed as larger, individual, subhedral grains associated with hornblende and magnetite. In fields of fine-grained clinozoisite, there is an invariable increase in birefringence and pleochroism of

the clinozoisite to that of epidote adjacent to grains of hornblende and magnetite. Grains of anhedral quartz generally make up 3 to 5 per cent of the rock. Subhedral to euhedral sphene is commonly observed in intimate association with grains of magnetite. Paragenetically, the sphene is the later mineral, rimming and cutting the magnetite.

The mineralogy and a chemical analysis of a representative specimen (no. 164), collected from the saussurite gabbro marginal to the north side of the ultramafic body, appear in Table 1.

In all specimens of saussurite gabbro studied, albite (An_3 to An_{10}) is the only plagioclase present. Therefore, if this mineral assemblage is representative of saussuritization of a gabbroic rock originally containing a more calcic plagioclase, the metamorphism has been so complete that no relict grains of the original plagioclase are evident in thin section.

The contact relationships between saussurite gabbro and metasedimentary rock have been presented in the preceding section of the text. In a stream channel midway along the north side of the ultramafic body, and along the shore north of the cannery, contacts between saussurite gabbro and ultramafic rocks are exposed. These outcrops, plus other less continuous exposures in other places, show that the contact relationships between the separate bodies of saussurite gabbro and ultramafic rocks are identical to the relationships which have been described between the margin of the main body of gabbro and the ultramafic complex (Fig. 1). However, the main gabbro intrusive body exhibits only peripheral saussuritization over a distance of several hundred feet against the ultramafic body, whereas the outlying bodies are completely saussuritized.

At the time of the ultramafic intrusions, the outlying bodies of gabbro, which now crop out along the north and northeast margins of the ultramafic body, probably were not completely saussuritized, and therefore contained less water than the surrounding metasedimentary rocks. The complete saussuritization of these gabbros may be due to the diffusion of water into them from the relatively wet metasedimentary rocks when temperatures were raised by the ultramafic intrusions. Such a possibility has been recently suggested by Thompson (1955, p. 98–99). On the other hand, the contact between the ultramafic intrusive masses and the main body of gabbro would have been a relatively dry environment.

The possibility is not precluded that some portions of the rocks mapped as saussurite gabbro represent sedimentary rocks highly metamorphosed and mobilized by the ultramafic intrusions, especially the fine-grained, banded inclusions in hornblende pyroxenite near the mouth of Cannery Creek. However, the following evidence supports the conclusion that individual bodies of saussurite gabbro are saussuritized portions of a single gabbroic intrusion, having been separated from the main body of gabbro by the ultramafic intrusions:

(1) Except for 1.5 to 2 per cent water, the chemical analyses of all specimens of saussurite gabbro (130, 164, 193, and 223, Table 1) are essentially identical to the chemical analysis of a specimen from the unaltered portion of the main gabbroic intrusion (specimen no. 160).

(2) The texture and mineralogy of outlying bodies of saussurite gabbro are identical with that of the portion of the main body of gabbro which has been saussuritized along the ultramafic contacts.

(3) The contact relationships between outlying bodies of saussurite gabbro and ultramafic rocks are identical with contact relationships between the main gabbro intrusive body and ultramafic rocks.

(4) The texture and mineralogy of the saussurite gabbro at Union Bay is similar to that of metamorphosed mafic intrusive rocks in other regions, such as the albite-epidote-hornblende schists or "epidiorites" of the Scottish Highlands described by Harker (1932, p. 278–280) and others. Most authors assign these rocks to the albite-epidote amphibolite facies, embracing a grade of metamorphism corresponding to the almandine zone as defined for pelitic schists (Turner, 1948, p. 88). Therefore, the saussurite gabbro at Union Bay can be considered correlative in metamorphic rank with the zone of garnetiferous biotite schist which has been developed in the metasedimentary rocks around the gabbroic and ultramafic intrusive rocks.

Ultramafic Intrusive Rocks

Definitions.—The ultramafic rock units at Union Bay are defined in Table 2. Distinctions between units are purely mineralogical, and the terminology employed is intended to be descriptive of the mineralogy. Divisions between the units are based upon the best distinctions that can be made in the field.

Pyroxenite.—The pyroxenite is a peripheral unit, encasing the spoon-shaped, lopolithic portion of the ultramafic body. However, the thickness of the pyroxenite shell is not sym-

metrical about the lopolith. The largest areas of pyroxenite outcrop and the greatest thickness of the unit lie around the north and west margins of the intrusive mass. The upper portion of the pyroxenite shell, under the cap of gabbro, is thinner in section than the lower portion but has the same texture and mineralogy. With an increase in amount of hornblende, the pyroxenite grades outward to hornblende pyroxenite in many areas, and with an increase in the amount of olivine it grades inward to olivine pyroxenite everywhere. Except for thin bands of magnetite (generally 1–5 cm thick) in some areas, the pyroxenite exhibits no structure other than joints and is of monotonous composition over large areas. It is essentially

TABLE 2.—DEFINITIONS OF ULTRAMAFIC ROCK UNITS

All figures are estimated volume per cent.

Rock units	Mineral components					
	Diopside	Hornblende	Olivine	Albite, clinozoisite, epidote	Magnetite	Serpentine minerals
Pyroxenite (Px)	45–95	0–15	0–10 locally	0–10 locally	1–40+	tr.
mode	75	5	..	..	5–20 variable	..
Hornblende pyroxenite (Hpx)	10–85	15–90	0–10 locally	0–30+	tr.–20	tr.
mode	40	40	..	10	10	...
Olivine-pyroxenite (Opx)	40–90	tr.–10	10–40	..	tr.–10	tr.–20
mode	75	tr.	20	..	3–5	2-3
Peridodite (Pd)	10–60	tr.	40–90	..	1–5	tr.–30
mode	45	tr.	45	..	1–2	5
Dunite (Du)	0–10	tr.	90+	..	tr.–3*	0-30
mode	2	..	95	..	1*	3-5

* magnetite and chromite

PLATE 2.—PHOTOMICROGRAPHS OF THIN SECTIONS

FIGURE 1.—Photomicrograph of a thin section of magnetiferous pyroxenite from the magnetite-bearing zone (×25). Plain light. Subhedral to euhedral grains of diopside with interstitial magnetite (black areas). A narrow rim of antigorite is commonly developed between diopside and magnetite. A, antigorite; D, diopside; E, epidote; H, hornblende.

FIGURE 2.—Photomicrograph of a thin section cut across a band of magnetite in pyroxenite (×25). Plain light. The black areas are magnetite at the edge of the band. The remainder of the field is diopside with traces of hornblende. Note the granulation around the large grain of diopside and the tiny, oriented inclusions of magnetite near the center of the grain.

FIGURE 3.—Photomicrograph of a thin section of hornblende pyroxenite (×25). Plain light. In this section, a relatively large, anhedral, interstitial area of hornblende (gray mineral) encloses a euhedral crystal of diopside (transparent). Two 100 traces of twin planes are evident in this crystal. The black mineral is magnetite. Penninite and some epidote occur at the borders between magnetite and hornblende.

FIGURE 4.—Photomicrograph of a thin section cut from a small dunite sill in olivine pyroxenite (×25). Plain light. The fractured, but undisturbed, subhedral olivine grains enclose an aggregate of anhedral diopside grains. The black, opaque mineral associated with the diopside is magnetite. The olivine grains are approximately 1 mm in size. The fractures, which curve around the inclusions of diopside grains, contain bowlingite.

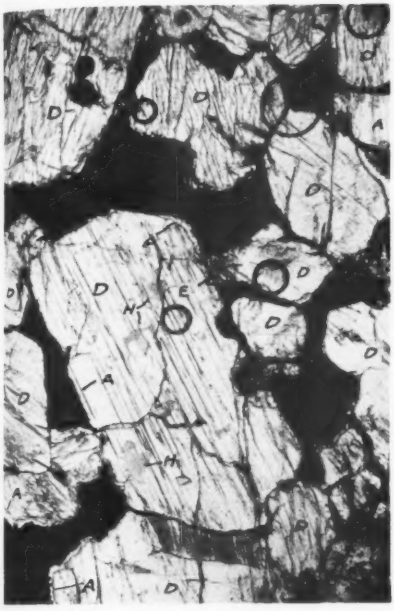
D
D
D

FIGURE 1

FIGURE 2

FIGURE 3

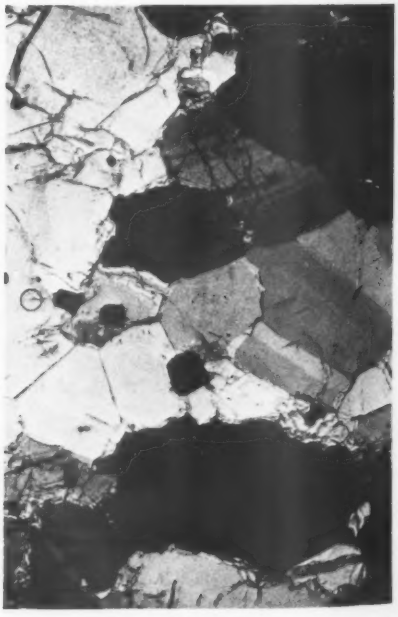

FIGURE 4

PHOTOMICROGRAPHS OF THIN SECTIONS

composed of diopside with some hornblende and magnetite. Fresh surfaces of the rock show dark-green, vitreous grains of diopside and black, metallic grains of magnetite. Weathered surfaces are medium gray-green with blue-gray, metallic magnetite standing out in relief. The grain size of the rock ranges locally from medium (1 mm) to coarse (1–3 cm). Pyroxene grains as large as 10 cm are not unusual, but these very coarse grains are generally in irregular clots or veins which cut the finer-grained pyroxenite. The rock is typically equigranular with randomly oriented, equant, subhedral grains of diopside. The grain sizes of magnetite and diopside generally vary directly because the magnetite is interstitial to the pyroxene grains.

Grains of different size in the pyroxenite unit are randomly distributed. From lack of adequate exposures, it is not known whether there are textures in the pyroxenite and hornblende pyroxenite units that could be interpreted as chilled margins where these rocks are in contact with schist. However, there are enough exposures of medium- to coarse-grained hornblende pyroxenite at or near contacts with gabbro and saussurite gabbro to permit the inference that there is no chilled zone between the ultramafic and gabbroic rocks.

Although some thin sections of pyroxenite contain two or three grains of diopside that exhibit undulatory extinction or strain shadows, more than 90 per cent of the grains studied in thin section show sharp extinctions. Features that could be interpreted as mortar texture (granulated and sutured grain boundaries) are rare. Thin sections of two specimens collected from within 300 feet of the upper contact between the ultramafic body and the overlying gabbroic cap do show a mortar texture. This feature is not typical of the contact zone of the ultramafic body. The majority of specimens collected along the outer margin of the pyroxenite exhibit no evidence of strain. Mortar textures are evident in all thin sections of pyroxenite intimately associated with bands of magnetite. These are discussed in more detail under the heading "Magnetite."

A photomicrograph of a representative thin section of pyroxenite appears in Plate 2, figure 1. Some specimens show considerable diallage twinning on the 100 plane. Most of the magnetite occurs in the interstices between diopside grains, but many grains of diopside exhibit tiny, brownish, translucent inclusions of magnetite regularly oriented parallel to the 100, 001, 011, and $\bar{1}22$ crystallographic directions in the pyroxene. These inclusions, which in some grains are so concentrated that the pyroxene has a dusty appearance in thin section, are clustered in the central portions of the pyroxene grains and are absent from the periphery (see Pl. 2, fig. 2). It can be deduced from this feature that the magnetite inclusions are not replacement phenomena but rather represent ferric and ferrous iron trapped in the diopside lattice at the time and temperature of crystallization of the pyroxene and later exsolved as magnetite at lower temperature as the diopside grains cooled.

In almost all cases, a few small (0.2 mm) anhedral grains of hercynite spinel are present in the magnetite that is interstitial to diopside grains. Also invariably associated with the

---

PLATE 3.—PHOTOMICROGRAPHS OF THIN SECTIONS

FIGURE 1.—Photomicrograph of a thin section of textural peridotite (×25). Plain light. Anhedral diopside (D) interstitial to subhedral and euhedral crystals of forsteritic olivine (Ol). All the diopside in this photograph has parallel extinction. Several of the olivine crystals contain bands of bowlingite and tiny, graphic grains of magnetite (see arrows). One olivine crystal contains a small, euhedral crystal of chromite (Cr).

FIGURE 2.—Photomicrograph of a thin section of peridotite (×75). Plain light. A small, euhedral crystal of olivine (Ol) is poikilitically enclosed in a larger grain of diopside (D). The black mineral in the olivine crystals is either magnetite or chromite.

FIGURE 3.—Photomicrograph of a thin section of partially serpentinized peridotite (×25). Plain light. A subhedral crystal of olivine (Ol) has been partly altered to antigorite (A) and bowlingite (B). Diopside (D) containing much very fine-grained magnetite is interstitial to the olivine. Fractures filled with chrysotile (C) occur radially distributed in the diopside around the olivine crystal. Black areas are magnetite.

FIGURE 4.—Photomicrograph of a thin section of fresh dunite (×25). Crossed nicols. Strain shadows are evident in several of the olivine grains in the right-center portion of the photograph. Note that others exhibit euhedral crystal faces.

magnetite is some hornblende, black in hand specimen and pleochroic green to brown in thin section. In sections containing only a very small amount of hornblende (1 or 2 per cent of the rock), this mineral occurs as a fine-grained deuteric alteration of diopside, typically at the contact between diopside and magnetite but in some instances in the interior and along the c-axis directions of the pyroxene grains. With an increase in the amount of hornblende (5–15 per cent of the rock), the hornblende also appears as medium- to coarse-grained, anhedral, ophitic patches in the interstices between diopside grains with, in thin section, many separate anhedral areas of hornblende in parallel orientation. In such rocks, a narrow (0.05 mm) rim of very fine-grained antigorite is common as an alteration of diopside grain boundaries in contact with interstitial magnetite. Narrow rims of penninite are also common between magnetite and hornblende in the same rocks.

In places small, secondary veins of ankerite, generally 3 mm–10 mm wide, cut through the pyroxenite and hornblende pyroxenite. Diopside and hornblende grains exhibit local alteration to actinolite, and magnetite shows secondary development of earthy hematite adjacent to these carbonate veins.

All pyroxenite hand specimens and thin sections studied contain magnetite in amounts from 1 to more than 50 per cent. However, as previously mentioned, the magnetite content of the rock is constant throughout large areas of outcrop. The largest areal concentration of magnetite crops out around the west and northwest exposures of the lower pyroxenite and hornblende pyroxenite units.

The portions of the lower pyroxenite unit that crop out around the north, northwest, and west sides of the ultramafic body and the upper pyroxenite unit under the gabbro cap contain essentially no olivine 200 feet or so away from the olivine pyroxenite unit. In these portions of the pyroxenite, olivine is found in amounts up to 10 per cent of the rock in only a very few small areas, and its occurrence cannot be traced for more than 100 feet or so in any direction.

The pyroxenite around the northeast, east, and south periphery of the ultramafic body in the vicinity of the dunite core contains generally 5 per cent and locally 8–10 per cent olivine. Due south of the dunite core the outer margin of the ultramafic body is olivine pyroxenite which contains 15–20 per cent olivine at the contact with albite-clinozoisite-epidote-hornblende schist.

Olivine in the pyroxenite unit has the same optical properties and textural relationships as the olivine of the olivine pyroxenite unit. However, the olivine in the olivine pyroxenite is relatively fresh, and that in the pyroxenite unit is considerably altered to antigorite, chrysotile, and bowlingite, especially within several hundred feet of the outer margin of the ultramafic body. A specimen of pyroxenite collected at the contact between the ultramafic body and wall rock due east of the dunite core contained 72 per cent diopside, 20 per cent magnetite, and 8 per cent olivine completely altered to antigorite, chrysotile, and bowlingite. The alteration of this rock has been highly selective. All the diopside grains are fresh and unaltered.

The indices of refraction of 30 diopside specimens collected from various parts of the ultramafic intrusive body were determined by immersion oils. The relative proportions of the diopside and hedenbergite molecules (D_nH_{100-n}) were established from charts correlating this relative molecular composition and optical properties published by Hess (1949, p. 641). These determinations are listed in Table 3. The results of this study indicate a regular pattern of variation in the composition of the diopside throughout the ultramafic body. The two extremes in composition in Table 3 are represented by specimen no. 156 ($D_{70}H_{30}$) collected from the peripheral hornblende pyroxenite unit and specimen no. 183b ($D_{99}H_1$) collected from the dunite core. The average molecular composition of the diopside in each ultramafic unit in the order: hornblende pyroxenite, pyroxenite, olivine pyroxenite, peridotite, dunite, is successively richer in $CaMgSi_2O_6$ and poorer in $CaFeSi_2O_6$. This is illustrated in Figure 2, which also indicates a parallel trend in the relative proportions of MgO and FeO in the olivine of the olivine pyroxenite, peridotite, and dunite units.

Of the 30 diopside specimens in Table 3, 13 were collected from the pyroxenite unit and show a variation in composition from $D_{78}H_{22}$ to $D_{86}H_{14}$. The variation within the magnetiferous areas is from $D_{78}H_{22}$ to $D_{80}H_{20}$. The lowest value for the diopside molecule ($D_{73}H_{27}$, specimen no. 109) was collected from within 50 feet of the schist contact at the northwest edge of the ultramafic body. The more hedenbergitic pyroxenes in every portion of the pyroxenite sampled are those which are associated with

TABLE 3.—CORRELATION OF OPTICAL INDICES AND COMPOSITIONS OF SPECIMENS
Correlations according to charts published by Hess (1941) and Kennedy (1949).

Rock Type	Specimen No.	Mineral	Indices	Composition	Remarks
Px (plus magnetite)	109	Diopside	Z 1.713 Y 1.693 X 1.684	$D_{73}H_{27}$	2V = 58°
Px (plus magnetite)	76b	Diopside	Z 1.712 Y 1.690 X 1.684	$D_{74}H_{26}$	
Px (plus magnetite)	150	Diopside	Z 1.712 Y 1.691 X 1.684	$D_{74}H_{26}$	
Px (plus magnetite)	218	Diopside	Z 1.710 Y 1.688 X 1.682	$D_{77}H_{23}$	
Px (plus magnetite)	309	Diopside	Z 1.710 Y 1.688 X 1.682	$D_{77}H_{23}$	
Px (plus magnetite)	233a	Diopside	Z 1.710 Y 1.688 X 1.682	$D_{77}H_{23}$	
Px (plus magnetite)	32a	Diopside	Z 1.710 Y 1.688 X 1.682	$D_{77}H_{23}$	2V = 58½°
Px (plus magnetite)	126a	Diopside	Z 1.708 Y 1.687 X 1.679	$D_{80}H_{20}$	2V = 59°
Px (plus magnetite)	316	Diopside	Z 1.709 Y 1.686 X 1.679	$D_{80}H_{20}$	
Px (plus magnetite)	161	Diopside	Z 1.705 Y 1.683 X 1.676	$D_{86}H_{14}$	
Px	235	Diopside	Z 1.710 Y 1.688 X 1.682	$D_{77}H_{23}$	
Px	46	Diopside	Z 1.708 Y 1.687 X 1.680	$D_{80}H_{20}$	
Px	168	Diopside	Z 1.707 Y 1.684 X 1.677	$D_{84}H_{16}$	
Hpx	98	Diopside	Z 1.713 Y 1.692 X 1.684	$D_{73}H_{27}$	
Hpx	51	Diopside	Z 1.713 Y 1.692 X 1.684	$D_{73}H_{27}$	
Hpx	156	Diopside	Z 1.714 Y 1.693 X 1.686	$D_{70}H_{30}$	2V = 60°
Opx	144	Diopside	Z 1.710 Y 1.690 X 1.682	$D_{77}H_{23}$	
Opx	305	Diopside	Z 1.710 Y 1.688 X 1.682	$D_{77}H_{23}$	From ore zone; specimen associated with 20 per cent magnetite, some hematite
Opx	155	Diopside	Z 1.707 Y 1.686 X 1.678	$D_{82}H_{18}$	From structural Pd unit; specimen assoc. with 20 per cent magnetite
Opx	8	Diopside	Z 1.705 Y 1.683 X 1.676	$D_{86}H_{14}$	

TABLE 3.—*Continued*

Rock Type	Specimen No.	Mineral	Indices	Composition	Remarks
Opx	9	Diopside	Z 1.705 Y 1.684 X 1.676	$D_{86}H_{14}$	2V = 58°
Opx	85a	Diopside	Z 1.705 Y 1.682 X 1.676	$D_{86}H_{14}$	Specimen contains more than 10 per cent hornblende
Opx	87a	Diopside	Z 1.705 Y 1.682 X 1.676	$D_{86}H_{14}$	Specimen contains more than 10 per cent hornblende
Opx	226	Diopside	Z 1.703 Y 1.681 X 1.674	$D_{88}H_{12}$	2V = 57°
Opx	224	Diopside	Z 1.702 Y 1.679 X 1.673	$D_{90}H_{10}$	All olivine serpentinized
Pd	200	Diopside	Z 1.699 Y 1.677 X 1.670	$D_{94}H_{6}$	Textural Pd
Pd	225	Diopside	Z 1.698 Y 1.677 X 1.670	$D_{94}H_{6}$	Structural Pd
Pd	183d	Diopside	Z 1.698 Y 1.675 X 1.669	$D_{96}H_{4}$	Textural Pd
Du	183a	Diopslde	Z 1.696 Y 1.672 X 1.667	$D_{99}H_{1}$	
Du	183b	Diopside	Z 1.696 Y 1.672 X 1.667	$D_{99}H_{1}$	2V = 59°
Opx	8	Olivine	Z 1.714 Y 1.696 X 1.676	$Fo_{78}Fa_{22}$	Opx wall rock adjacent to dunite sill; see Pd specimen no. 8; optically negative
Opx	9	Olivine	Z 1.714 Y 1.696 X 1.676	$Fo_{78}Fa_{22}$	2V = 88°; optically negative
Opx	87a	Olivine	Z 1.713 Y 1.696 X 1.676	$Fo_{79}Fa_{22}$	Specimen contains more than 10 per cent hornblende. Optically negative
Opx	144	Olivine	Z 1.713 Y 1.695 X 1.675	$Fo_{79}Fa_{21}$	Optically negative
Opx	305	Olivine	Z 1.713 Y 1.695 X 1.675	$Fo_{79}Fa_{21}$	Optically negative; from ore zone; associated with magnetite and hematite
Opx	6	Olivine	Z 1.713 Y 1.695 X 1.675	$Fo_{79}Fa_{21}$	Opx wall rock adjacent to dunite sill; compare with Pd spec. no. 6
Opx	226	Olivine	Z 1.693 Y 1.677 X 1.658	$Fo_{88}Fa_{12}$	Optically negative
Pd	8	Olivine	Z 1.710 Y 1.692 X 1.672	$Fo_{81}Fa_{19}$	Specimen of dunite sill intrusive into specimen no. 8 (pyroxenite wall rock). Optically negative
Pd	155	Olivine	Z 1.709 Y 1.692 X 1.672	$Fo_{81}Fa_{19}$	Optically negative; from dunite sill in structural Pd

TABLE 3.—*Concluded*

Rock Type	Specimen No.	Mineral	Indices	Composition	Remarks
Pd	6	Olivine	Z 1.703 Y 1.686 X 1.666	$Fo_{83}Fa_{17}$	Specimen of dunite sill intrusive into specimen no. 6 (pyroxenite wall rock). Optically negative
Pd	200	Olivine	Z 1.694 Y 1.678 X 1.660	$Fo_{87}Fa_{13}$	Textural Pd.; Optically negative
Pd	225	Olivine	Z 1.695 Y 1.679 X 1.661	$Fo_{87}Fa_{13}$	Textural Pd.; Optically negative
Pd	227	Olivine	Z 1.695 Y 1.679 X 1.661	$Fo_{87}Fa_{13}$	Textural Pd.; Optically negative
Pd	183d	Olivine	Z 1.686 Y 1.667 X 1.650	$Fo_{93}Fa_{7}$	Textural Pd.; Optically positive
Du	231	Olivine	Z 1.690 Y 1.671 X 1.654	$Fo_{90}Fa_{10}$	Optically positive; ZV = 88°
Du	183a	Olivine	Z 1.688 Y 1.670 X 1.654	$Fo_{91}Fa_{9}$	Optically positive
Du	220	Olivine	Z 1.685 Y 1.668 X 1.651	$Fo_{93}Fa_{7}$	2V = 90°
Du	210	Olivine	Z 1.687 Y 1.669 X 1.650	$Fo_{93}Fa_{7}$	2V = 90°
Hpx	115	Apatite	N_e 1.634 N_o 1.638		Biaxial, small 2V
Sch	205	Garnet	N > 1.770	Probably almandite	Red; isotropic
Px	316	Ankerite	N_e 1.516 N_o 1.696		In veins in Px
Spb	203	Diopside	Z 1.714 Y 1.693 X 1.686	$D_{70}H_{30}$	
Gb	189	Hypersthene	Z 1.713 Y 1.710 X 1.699	$En_{64}Fs_{36}$	Central portion of main body of gabbro. 2V = 52°
Gb	221	Diopside	Z 1.718 Y 1.697 X 1.690	$D_{64}H_{36}$	Specimen from within 900 ft. of ultramafic contact near dunite core
Gb	189	Diopside	Z 1.715 Y 1.695 X 1.687	$D_{68}H_{32}$	Central portion of main body of gabbro
Gb	159	Diopside	Z 1.715 Y 1.695 X 1.687	$D_{68}H_{32}$	From within 500 ft. of ultramafic contact on ridge west of Mt. Burnett
Gb	206	Diopside	Z 1.717 Y 1.696 X 1.688	$D_{65}H_{35}$	Collected 300 ft. from contact with Sch south of Cannery Creek
Gb	159	Hypersthene	Z 1.708 Y 1.706 X 1.695	$En_{67}Fs_{33}$	See 159 above
Gb	206	Hypersthene	Z 1.725 Y 1.723 X 1.712	$En_{54}Fs_{46}$	See 206 above

approximately 20 per cent or more magnetite and which are closest to the outer margin of the ultramafic body. No more detailed pattern of variation in composition of the diopside within the pyroxenite unit could be determined from the specimens collected.

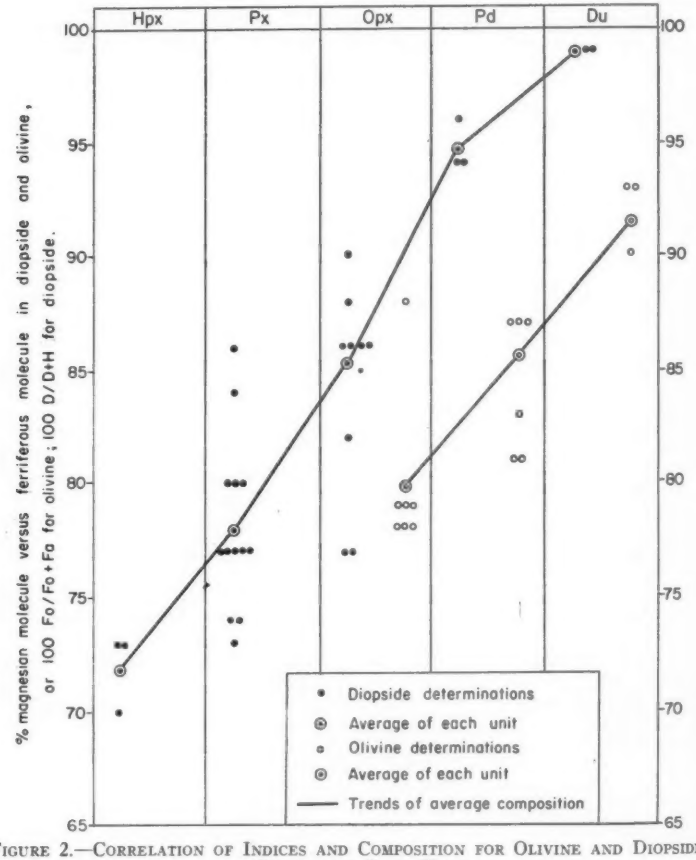

FIGURE 2.—CORRELATION OF INDICES AND COMPOSITION FOR OLIVINE AND DIOPSIDE IN ULTRAMAFIC ROCK UNITS

Per cent determined by correlation of indices and charts by Hess (1949, p. 641) and Kennedy (1949, p. 567).

Mineral and chemical analyses of a pyroxenite specimen collected from the central part of the magnetiferous area are given in Table 1 (specimen no. 32a). The diopside of this specimen and of specimen 109 were separated, except for approximately 3 per cent contamination by magnetite and some hornblende, and were analyzed. The atomic percentages of Ca, Mg, and Fe were calculated from these two diopside separates plus one other diopside separate from the dunite core (specimen no. 183b). These determinations are plotted on a ternary diagram (Fig. 3). Amounts of FeO and Fe_2O_3 were subtracted from the chemical analyses to correspond with the amount of magnetite contamination in the separates. Remaining Fe_2O_3 was assumed to be in octahedral (sixfold) coordination in the diopside lattice and was recalculated as ferrous iron in the diagram.

Specimens no. 183b and 109 represent respectively the magnesian and ferriferous ends of the spectrum of composition of diopside in the ultramafic body. Curve *A* in Figure 3 is drawn through the plots of specimens 183b, 32, and

109 to represent the trend of composition of the diopside in the intrusive mass. Curve *B* in Figure 3 represents the trend of composition of the monoclinic pyroxene in the Blashke Island

crepancy must be due to the amount of Al_2O_3 in the diopside, which increases the indices of refraction.

Chemical analyses of the diopside in the

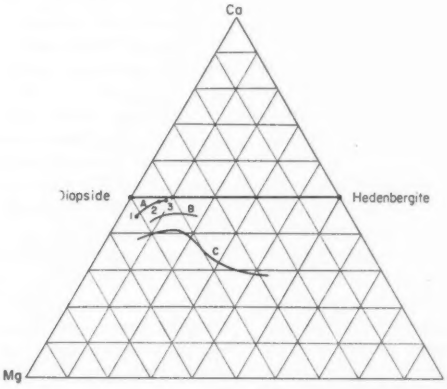

FIGURE 3.—CHEMICAL COMPOSITION OF MONOCLINIC PYROXENES IN TERMS OF PERCENTAGES OF CA, MG, AND FE

Points: 1, Specimen 183b (diopside from the dunite core); 2, Specimen 32a (diopside from the magnetite rich zone); 3, Specimen 109 (diopside from outer ultramafic contact with schist near the magnetite-rich zone). Curves: *A*, Trend of composition of diopside in the Union Bay ultramafic complex, as determined by chemical analyses; *B*, Trend of composition of monoclinic pyroxenes in the Blashke Islands ultramafic complex, after M. S. Walton, Jr. (1951, PhD thesis, Columbia Univ.); *C*, Trend of composition of monoclinic pyroxenes crystallizing from common mafic magmas, after Hess (1941, p. 585).

ultramafic body determined by M. S. Walton, Jr. (1951, PhD thesis, Columbia Univ.). Curve C shows the trend of composition of monoclinic pyroxenes crystallizing from the more common mafic magmas (gabbro, norite, and diorite) according to Hess (1941, p. 585). The trend of composition of diopside at Union Bay is 7–8 per cent more calcic than the trend in the more common mafic magmas (curve *C*) and 3–5 per cent more calcic than the monoclinic pyroxenes at the Blashke Islands (curve *B*). Curve *A* does fall within the relatively limited range of composition for porphyritic pyroxenes in many basaltic rocks (Barth, 1931, p. 195).

An increase in the amount of Al_2O_3 from the dunite core to the pyroxenite unit of the lopolith is conspicuous in the chemical analyses of diopside separates from specimens no. 109, 32, and 183b.

A discrepancy is exhibited in Figure 3 between the plots by atomic per cent of the more alumina-rich diopsides of the pyroxenite unit (specimens no. 32a and 109) and their relative position on the diopside-hedenbergite line according to the position on the line predicted by Hess's optical data (1949, p. 641). This dis-

pyroxenite unit at Union Bay indicate less SiO_2 and more Al_2O_3, Fe_2O_3, and CaO than most chemical analyses of diopsides in the literature (Hess, 1949, p. 645–666). Analyses of chromian diopsides from periodotitic inclusions in basalts (Ross, Foster, and Myers, 1954, p. 709) are very similar to analyses of the Union Bay diopsides, especially with respect to the relatively high Al_2O_3 content. Analyses of the pyroxenite and diopside, as well as other ultramafic rocks, at Union Bay are practically identical to analyses published by Camsell (1913, p. 53, 61) for the Lodestone Mountain ultramafic body near Tulameen, British Columbia. The Lodestone ultramafic body crops out near the southern extremity of the Coast Range batholith. It does not exhibit lopolithic structure but is similar to the Union Bay ultramafic body in most other respects.

Hornblende pyroxenite.—The hornblende pyroxenite unit is a compositional modification of the pyroxenite unit at the contact between pyroxenite and wall rock (schist, gabbro, and saussurite gabbro) around the perimeter of the lopolithic portion of the ultramafic intrusion. The essential compositional and textural

relationships between pyroxenite and hornblende pyroxenite in contact with gabbro have been diagrammatically summarized in Figure 1.

Specimens of pyroxenite representative of the more central portions of the pyroxenite unit contain an average of approximately 5 per cent hornblende. The amount of hornblende associated with pyroxenite commonly increases outward toward the wall-rock contact to the extent (up to 90 per cent of the rock) that in some places the rock can be termed hornblendite. Also associated with the hornblende pyroxenite near the contact are veins and dikes composed primarily of hornblende and clinozoisite. For these reasons the mineralogical definition of the hornblende pyroxenite unit in Table 2 shows the most variation in composition of any of the ultramafic rock units.

Because it is gradational (Fig. 1), the contact between pyroxenite and hornblende pyroxenite is the most ambiguous contact mapped within the ultramafic body. The relative composition of approximately 15 per cent hornblende and 85 per cent diopside was found to be the most convenient mineralogical field boundary between these two rock types.

The width of the hornblende pyroxenite generally ranges from 200 to 500 feet and is relatively uniform around most of the perimeter of the lopolith (Pl. 1). Only traces of hornblende (1–2 per cent, or less, of the rock) are present locally in the pyroxenite around the eastern periphery of the ultramafic body in the vicinity of the dunite core, and there is no hornblende pyroxenite in this area. Hornblende pyroxenite, enclosing small areas of saussurite gabbro, crops out over approximately 1 square mile along the northern portion of the magnetiferous area at the northwest periphery of the lopolith. That this relatively large area of hornblende pyroxenite outcrop is close to the floor of the intrusion (within 1000 vertical feet) is an interpretation suggested by the structure cross sections (Pl. 4).

Hornblende pyroxenite at or near contacts with schist around the northeastern periphery of the ultramafic body is generally composed of approximately 40 per cent hornblende, 40 per cent diopside, 15 per cent magnetite, and a few small veins from 1 mm to several cm in thickness of hornblende, clinozoisite, epidote, and albite. In areas in contact with gabbro or saussurite gabbro, the hornblende pyroxenite contains more hornblende relative to pyroxene than in other areas, and generally 20–30 per cent of the rock is composed of hornblende-clinozoisite-epidote-albite veins and dikes up to several feet in thickness. Good exposures of hornblende pyroxenite of this nature crop out along the shore line for a distance of one-half mile north of the cannery site at the southwest edge of the ultramafic body. The rock in this area locally contains 70–90 per cent coarse hornblende and 10–30 per cent clinozoisite, epidote, and albite which are either interstitial to the hornblende crystals or in separate veins, and only traces of diopside and magnetite. The veins and dikes that cut the hornblende pyroxenite in this area are composed primarily of ragged hornblende crystals, interstitial clinozoisite with some epidote and albite, and minor amounts of apatite, carbonate, sericite, quartz, magnetite, and sulfides (mostly pyrite with some chalcopyrite and pyrrhotite). The porphyritic hornblende crystals are commonly randomly oriented, but radiating groups of crystals and crystals oriented perpendicular to the walls of the veins or dikes also occur. Some of the hornblende in the vein material is partially or completely altered to actinolite and penninite. These veins and dikes cannot be distinguished mineralogically from saussurite gabbro rock in either hand specimen or thin section.

Hornblende pyroxenite exposures at the cannery site, on the southwest margin of the ultramafic complex, are separated from the closest exposures of metasedimentary schist by approximately 250 feet of stream gravel. Hornblende pyroxenite that crops out in the bed of Cannery Creek is unusually fine-grained (largest grains are hornblende, approximately 1 mm) and may be within a few feet of the metasedimentary contact. The mineralogy and a chemical analysis of this fine-grained rock (specimen 192a) are given in Table 1.

On the weathered surface of a typical hornblende pyroxenite specimen, the black hornblende contrasts with the gray-green weathered surfaces of diopside grains. However, on a freshly broken surface of medium- or fine-grained rock, the hornblende can be distinguished from the dark-green diopside in most cases only with a hand lens. In thin section the hornblende exhibits all the features of common black hornblende and is pleochroic: X = pale yellow brown; Y = medium brownish green; Z = dark brownish green; absorption $X < Y < Z$. Approximately 10 per cent of the hornblende grains studied in thin section are twinned on the 100 crystallographic plane.

The textural association between hornblende and diopside in all the hornblende pyroxenite specimens studied indicates that the hornblende

crystallized after diopside. In specimens containing more diopside than hornblende, the hornblende occurs both as a fine-grained replacement of diopside, generally along the c-axis directions and around the perimeter of diopside grains and as relatively coarse, anhedral patches interstitial to diopside grains. In a typical specimen of hornblende pyroxenite of this composition that contains medium-grained diopside (grains up to 1 cm), ophitic, interstitial patches of hornblende exhibit parallel cleavage surfaces over areas as large as 15 cm in the longest dimension. The hornblende commonly encloses subhedral and euhedral crystals of diopside as illustrated in Plate 2, figure 3. In many thin sections in which hornblende encloses diopside grains, the diopside grains are peripherally altered to actinolite, occurring either as a fine-grained separate mineral phase or as a gradational, compositional variation of the enclosing hornblende crystal.

Textural relationships between hornblende and diopside indicate that only a very minor portion of the hornblende is a deuteric alteration formed at the expense of diopside grains. The majority of the hornblende can be considered primary in that it has crystallized in the interstices between diopside crystals. Therefore, exclusive of gabbroic veins and dikes, hornblende, plus some magnetite, represents the last ultramafic fraction to crystallize in the peripheral regions of the lopolith.

The chemical analysis of a hornblende separate of hornblendite appears in Table 1 (no. 95).

Olivine pyroxenite.—Through an increase in the amount of forsteritic olivine, the pyroxenite unit everywhere grades inward toward the central portions of the ultramafic body to olivine pyroxenite. This contact is transitional, generally over a distance of approximately 200 feet measured approximately perpendicular to the main structure of the intrusive body. In the lopolithic portion of the intrusive body, erosion has exposed upper and lower segments of the olivine pyroxenite that exhibit subhorizontal attitudes and are essentially symmetrical above and below the peridotitic central portion of the lopolith. The general distribution of the olivine pyroxenite unit throughout the lopolith reflects the spoon-shaped structure of the intrusive body. In the eastern portion of the ultramafic body, the olivine pyroxenite crops out as a sheath, dipping steeply outward, around the dunite feeder but separated from the dunite by peridotite. Several relatively small, isolated areas of olivine pyroxenite crop out as inclusions in the dunite core. Relationships between these inclusions and the dunite are discussed in the description of the dunite unit. Much of the rock included in the peridotite unit, described in the next section of the text, is of the same composition as olivine pyroxenite.

The olivine pyroxenite is generally composed of approximately 80 per cent diopside and 20 per cent forsteritic olivine, and this composition is remarkably constant throughout the intrusive mass. The variation in composition expressed in the definition of the unit in Table 2 is confined to the margins of the olivine pyroxenite where it grades into peridotite with an increase in the olivine content or into pyroxenite with a decrease in the olivine content.

Olivine weathers more rapidly than diopside and appears as brownish-yellow depressions on the weathered surfaces of olivine pyroxenite outcrops. The rock is generally medium-grained and equigranular (grains from 1 to 8 mm). In hand specimen and thin section the textural relationships between diopside and olivine are the same. Individual grains and clusters of several grains of olivine are scattered evenly throughout the rock. Grains of both diopside and olivine range from anhedral to euhedral, and no convincing age relationships can be deduced from observations of their mutual boundaries. Both the general texture and the relative mineralogical composition of the olivine pyroxenite strongly suggest that the diopside and the olivine crystallized simultaneously along a cotectic curve.

The olivine grains in the olivine pyroxenite are generally altered to bowlingite along fractures and around grain boundaries. Many olivine grains are also partly or completely altered to antigorite, chrysotile, talc, and very fine-grained, secondary magnetite, especially where the olivine pyroxenite constitutes, or is close to, the periphery of the ultramafic body, around the eastern and southwestern portions of the intrusion. Although minor amounts of bowlingite follow fractures in the diopside grains, particularly where they are adjacent to partly or completely serpentinized grains of olivine, the pyroxene is relatively fresh and unaltered. In thin section, relatively unaltered grains of olivine in a few specimens exhibit regular bands of bowlingite which do not follow fractures and which contain very fine-grained "graphic" magnetite oriented parallel to crystallographic directions in the olivine.

The indices of refraction of the diopside and the olivine from several specimens of olivine

pyroxenite are listed in Table 3 and Figure 2. The range in molecular composition of diopside and olivine is from D_{77} H_{23} in specimen no. 144 to D_{90} H_{10} in specimen no. 224 and from Fo_{78} Fa_{22} in specimens no. 8 and 9 to Fo_{88} Fa_{12} in specimen no. 226. In the cases of both diopside and olivine, the relatively ferriferous minerals were collected from the western portion of the lopolith and the relatively magnesian specimens from within 300 feet of the southeastern contact of the ultramafic body in the vicinity of the dunite core.

A chemical and mineralogical analysis of a representative specimen of olivine pyroxenite collected from the western portion of the lopolith, specimen no. 9 (D_{86} H_{14}; Fo_{78} Fa_{22}), appears in Table 1.

Peridotite.—The peridotite unit constitutes the central section of the lopolithic portion of the ultramafic body and crops out as a sheath, dipping steeply outward, around the north, east, and south periphery of the dunite core. Along the axis of the lopolith to the west of the dunite core, the peridotite grades to the east, with decreasing amount of diopside, into dunite. In the lopolith, the over-all structure of the peridotite unit and smaller-scale structures within the unit generally exhibit subhorizontal attitudes and reflect the spoon-shaped structure of the intrusive body.

The mineralogical definition of the peridotite unit is given in Table 2. Rocks mapped in the field as peridotite fall into two categories: (1) "textural peridotite," rocks composed of evenly scattered grains of forsteritic olivine and diopside in approximately equal proportions; and (2) "structural peridotite," rocks which have the composition and texture of olivine pyroxenite but which are host to many irregular and sill-like intrusions of dunitic material such that the bulk mineralogical composition of the rock, over an outcrop area of several hundred square feet, is within the limits prescribed for the peridotite unit.

Most of the peridotite unit that crops out around the dunite core is textural peridotite. Structural peridotite is typical of the lopolithic portion of the intrusive body and constitutes most of the primary structural features mapped within the lopolith.

Individual bodies of dunitic material in the structural peridotite are of all sizes and shapes. Many have the dimensions and attitudes of sills with somewhat irregular but knife-sharp contacts and attitudes displaying considerable continuity in both vertical and horizontal directions within the peridotite unit. The thickness of these sills ranges from less than an inch to more than 50 feet. In several places sills of dunite approximately 75 feet thick were considered large enough to map as individual units on the scale employed. Figure 4 is a sketch of a photograph of two parallel sills of this size that crop out in olivine pyroxenite across the crest of a ridge 1 mile west of the dunite core. The uppermost of these relatively large sills separates pyroxenite from olivine pyroxenite and creates an anomaly in the usual gradational sequence of these two units.

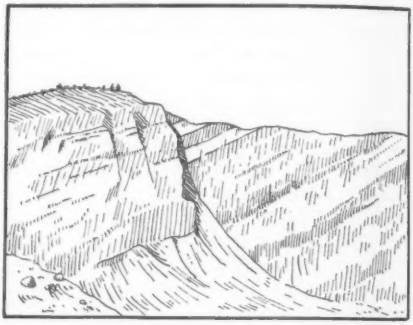

FIGURE 4.—SKETCH OF TWO DUNITE SILLS

Traced from photograph. The sills are approximately 75 feet thick and crop out across the top of the ridge in center of the illustration. Large bands (less clearly defined in the photograph) of pyroxenite, olivine pyroxenite, and peridotite can also be seen; the peridotite makes the lighter bands in the sketch.

Many outcrops of peridotite along the north and west flanks of the lopolith contain many relatively small sill-like and veinlike bodies of dunitic material from less than 1 inch to several feet in thickness. Although many of the smallest of these exhibit regular continuity along the strike, many are in the form of irregular veins which may or may not follow the general attitude of the larger sills in the area. In a few of the smaller sills and veins, small veins of diopside, generally one or two crystals or 5–10 cm thick, cut across the dunitic sills from wall to wall and create contradictory age relationships.

The pyroxene-rich portion of the structural peridotite is generally composed of approximately 80 per cent diopside and 20 per cent forsteritic olivine and cannot be distinguished in either hand specimen or thin section from specimens of the olivine pyroxenite unit. The dunitic material is composed of 85–95 per cent

forsteritic olivine and 5–15 per cent diopside. Some fine-grained, disseminated magnetite is generally present in the rocks, especially in the pyroxene-rich rocks. Locally magnetite is concentrated in irregular patches or veins up to several feet long in either rock type, and in some places the larger veins cut across both. Traces of hornblende (generally less than 1 per cent of the rock) occur in all portions of the peridotite as alteration of diopside grains.

The texture of the dunitic material is more constant than that of the pyroxene-rich rocks. The grain size of olivine ranges between 0.2 and 1.5 mm, and diopside ranges from approximately 1 mm to 2 cm in the olivine pyroxenite rock. In the dunitic material, grains of olivine are generally equant and display anhedral to generally subhedral crystal outlines. Diopside in this portion of the rock ranges from anhedral to subhedral and occurs either as individual grains or clusters of several grains in most specimens. Practically all the magnetite in the dunitic material is concentrated in these clusters of diopside grains (Pl. 2, fig. 4).

Most of the individual bodies of dunitic rock exhibit patterns of closely spaced, parallel fractures in which one or two directions are predominant. In most of the more regular sills, the predominant set of fractures is parallel to the walls of the sills. Megascopically these fracture patterns flow around inclusions of olivine pyroxenite and bear a remarkable, but false, similarity to flow lines. In thin section, the fractures cross through olivine grains in all directions without disrupting the orientation of individual portions of each grain. The predominant set of fractures is deflected around grains of diopside in thin section in the same manner as around the megascopic olivine pyroxenite inclusions (Pl. 2, fig. 4).

The dunitic portion of the structural peridotite is serpentinized to different degrees in different places. In general, the rock is relatively fresh, with only minor alteration of olivine to bowlingite along fractures. However, in some specimens as much as 50 per cent of the olivine has been altered to antigorite, chrysotile, bowlingite, and secondary magnetite along fractures.

Seven thin sections (including the section illustrated in Pl. 2, fig. 4) were cut at various orientations across three specimens of small, regular dunitic sills. A study of these sections indicates that the olivine grains in these specimens show no preferred crystallographic orientation with respect to the dimensions of the sills.

Periodotite of the relative composition and texture designated as the textural type occurs in places in the central portions of the lopolith but is especially typical of the peridotite which crops out around the dunite core. The textural relationships between diopside and olivine in this rock are identical to the relationships between hornblende and diopside in the hornblende pyroxenite unit. Diopside grains are typically irregular, anhedral, and interstitial to equant, subhedral, and euhedral crystals of olivine (Pl. 3, fig. 1). In most specimens the olivine is medium-grained (1–5 mm), and interstitial, ophitic patches of diopside commonly display parallel crystallographic orientation over areas as large as 10 cm in the longest dimension. In some local pyroxene-rich facies of the textural peridotite near the dunite core, the diopside is even coarser-grained and exhibits subhedral crystal shapes. Both the coarse, subhedral grains and the interstitial grains of diopside poikilitically enclose euhedral crystals of olivine (Pl. 3, fig. 2). The poikilitic inclusions of olivine exhibit more perfect crystal development and are finer-grained than most of the olivine in the rock.

In many places in the structural peridotite where dunitic material exhibits a rounded, convex contact against the olivine pyroxenite, radial fracture patterns occur in the pyroxene-rich rock adjacent to the contact. This feature is especially obvious where small bodies of dunitic rock show a circular cross section. The nature of this secondary (post-solidification) fracture pattern indicates either that the olivine has increased in volume or that the pyroxene has decreased in volume. Because the coefficient of expansion with temperature is greater for olivine than for diopside (Birch, Schairer, and Spicer, 1942, p. 32–33), the fractures were probably not caused by differential contraction as the intrusion cooled. All the dunitic rocks associated with this feature contain approximately 10 per cent or more of serpentine minerals, and possibly the fractures were caused by relative expansion of the dunitic material during serpentinization of the olivine. The same fracture pattern is seen in thin section where interstitial areas of diopside enclose partially serpentinized grains of olivine. This is illustrated in Plate 3, fig. 3, in which the olivine is moderately serpentinized, and radial fractures in the diopside are filled with chrysotile.

The indices of refraction and relative molecular compositions were determined for several specimens of olivine and diopside collected from both textural and structural types of peridotite from various portions of the ultra-

mafic body (Table 3 and Fig. 2). The indices indicate that the olivine and diopside in the textural peridotite near the dunite core contain more of the magnesian molecule relative to the ferriferous molecule than specimens from the structural peridotite of the lopolith.

Specimens no. 6 and 8 (Table 3) are specimens of structural peridotite collected from the western portion of the lopolith and consist of olivine pyroxenite wall rock and small, regular sills of dunitic material approximately 1 inch thick. Two determinations of the olivine constituent were made of each specimen: one from the sill of dunitic material and one from the olivine pyroxenite wall rock. The olivine of the dunitic portions of specimens 6 and 8 contains respectively 4 and 3 per cent more of the forsterite molecule than does the olivine of the wall rock in the same specimen. This difference definitely exceeds the limits of error of the oil-immersion method and suggests the possibility of a hiatus between the olivine of the wall rock and the olivine in the dunitic sills.

A chemical and mineralogical analysis of a specimen of textural peridotite (specimen no. 200) collected from near the dunite core appears in Table 1 (see also Pl. 3, fig. 3). Also in Table 1 is a chemical and mineralogical analysis of specimen no. 6, which is dunitic material collected from a sill in structural peridotite in the western portion of the lopolith. An approximate average composition of the structural peridotite in this area can be calculated from an average between the analyses of specimens no. 6 and 9 (the latter is olivine pyroxenite from this area) using a one-to-one ratio.

Dunite.—The dunite core, cropping out over an area slightly larger than 1 square mile, constitutes the predominant feature of the eastern portion of the ultramafic intrusive body. The general shape of the dunite outcrop is that of a vertical plug essentially circular in plan, although it grades to the west into the peridotitic, central portion of the lopolith. Judged from its intersection with the topography, the outer contact of the dunite is either vertical or steeply dipping outward to the north, east, and south. This contact is everywhere abruptly gradational to peridotite through an increase in the amount of diopside relative to olivine in the rock.

The mineralogical definition of the dunite unit is given in Table 2. The bulk mineralogical composition of the dunite plug is approximated by the mode given in the table. The olivine is generally equant and subhedral and is medium-grained throughout the entire unit (grains from 1 mm to 5 mm). Diopside ranges from medium- to coarse-grained and generally occurs as scattered anhedral grains interstitial to the olivine. In some places veins of diopside from less than an inch to several inches in width cut the dunite. The diopside crystals in these veins are medium- to coarse-grained and are generally subhedral. In one locality in the northern part of the dunite core, the dunite contains many closely spaced, parallel layers of subhedral, medium-grained diopside crystals. These layers, which range from one-quarter inch (one or two crystals) to several inches in thickness, exhibit a remarkable continuity over a distance of 300 feet along their strike. The layers strike north-south and dip 38° west. In places the layers show a gradation upward in the amount of diopside relative to olivine (which decreases upward) but not in the size of the diopside crystals. These features resemble the primary layering described in a number of basic intrusive bodies such as the Skaergaard (Wager and Deer, 1939), and they imply gravitational settling of crystals from a crystallizing magma.

Both chromite and magnetite occur in the dunite in finely disseminated, subhedral to euhedral grains, many of which are poikilitically included in grains of both olivine and diopside. In a few places in the dunite plug, chromite is concentrated in small, irregular veins from 6 inches to 3 feet in the long dimension.

Fifteen separate bodies of olivine pyroxenite, large enough to be mapped on the scale employed, crop out within the dunite core. These appear to be inclusions. The largest body of olivine pyroxenite is approximately 650 feet in the longest dimension exposed. One of the olivine pyroxenite inclusions is tabular and dips northeast at 40°. The other bodies are irregular. Contacts between the olivine pyroxenite and the dunite are sharp and highly irregular, with many irregular apophyses of dunite extending into the olivine pyroxenite around the perimeters of the inclusions.

The dunite is serpentinized to different degrees in different places, but the majority of the rock is relatively fresh, as indicated in Table 2. Two distinct colors of weathered surfaces are seen throughout the dunite core. Olivine partially altered to serpentine minerals weathers a light brownish yellow, and that which is fresh and unaltered weathers to a darker reddish brown. Probably 60 per cent of the exposed surface of the dunite plug has been partially serpentinized and weathers yellow, and approximately 40 per cent is fresh and weathers brown. The irregular areas of different-colored rock vary in size but are

generally as large as 500 to several thousand feet in one dimension. There is no pattern to their distribution except that the periphery of the plug and the areas of dunite surrounding the olivine pyroxenite inclusions are invariably somewhat serpentinized for a distance of 200 feet or more away from the contact.

In a typical specimen of partially serpentinized dunite, only 5–10 per cent of the olivine has been altered to bowlingite, antigorite, chrysotile, and secondary magnetite along fractures. In a few specimens, the serpentine minerals constitute 20–30 per cent of the rock. In thin sections of fresh dunite, many of the olivine grains have subhedral to euhedral outlines. Some grains have irregular, interlocking boundaries and exhibit wavy extinctions or strain shadows (Pl. 3, fig. 4). One or two grains in each thin section generally exhibit true mortar texture with granulated grain boundaries.

The depth of weathering of the dunite is approximately the same, about 1 cm, in all outcrops of both fresh and partially serpentinized rock. Freshly broken surfaces of the dunite are black, but the edges of olivine grains are clear and vitreous under a hand lens. The diopside associated with the dunite core and the peridotite in the vicinity of the core is a brighter green and can be distinguished from the dark-green diopside of other portions of the ultramafic body. As indicated in the chemical analysis of specimen no. 183b in Table 1, a chromium content of approximately 0.2 per cent is at least partly responsible for the brighter green color.

Both the diopside and the olivine in the dunite plug are the most magnesium-rich varieties collected from the ultramafic body. The relative molecular composition of two specimens of diopside collected from the dunite core is $D_{99}H_1$, as determined from their indices of refraction (specimens no. 183a and 183b in Table 3). The range in composition of four specimens of olivine collected from various parts of the dunite core is from $Fo_{90}Fa_{10}$ (specimen no. 231) to $Fo_{93}Fa_7$ (specimens no. 183d, 210, and 220, Table 3).

A chemical analysis of a pyroxene mineral separate from specimen no. 183b is given in Table 1. Also given in Table 1 are chemical and mineralogical analyses of a specimen of fresh, unaltered dunite (specimen no. 231) and a specimen of partly serpentinized dunite (specimen no. 183a), both collected from the dunite plug.

Magnetite

As the preceding descriptions have indicated, all the ultramafic rock units and most portions of the gabbro and saussurite gabbro units contain some magnetite. However, the most notable concentration of magnetite crops out around the west and northwest portions of the lower pyroxenite and hornblende pyroxenite units.

Twenty-five polished section mounts of various types of magnetite distributions were studied. Of these 25 mounts, 16 were made from specimens collected from the magnetiferous area. The textures and distribution of the magnetite throughout the ultramafic body clearly indicate that the magnetite is a primary constituent of the ultramafic rocks, except for magnetite which results from serpentinization of olivine.

The textural relationships between magnetite and rocks with which it is associated are of four types: (1) fine-grained, euhedral magnetite disseminated in, but constituting only a very minor amount of, the dunite core; (2) regular, closely spaced, parallel bands; (3) large, irregular clots and irregular veins up to several feet in the longest dimension; and (4) disseminated fine- to coarse-grained, anhedral magnetite interstitial to diopside and commonly evenly distributed throughout the rock.

The first type of textural association is present only in specimens collected from dunitic material in the vicinity of the dunite plug. Chromite is found in the same specimens in the same texture and in approximately the same amounts. Because most of the magnetite in the ultramafic body is associated with pyroxenite in textures that indicate that most of the magnetite has crystallized after the diopside, different physicochemical conditions are indicated by the fine-grained magnetite that has crystallized euhedrally and apparently either before or contemporaneously with the olivine in the vicinity of the dunite core.

Regular, thin bands or layers of magnetite crop out in only a few places in the pyroxenite and olivine pyroxenite units. They are generally 0.5–4.0 cm thick and are remarkably parallel and continuous over distances of several hundred feet. In some places near the periphery of the intrusive body, the bands exhibit undulations or open folds. The diopside grains near the bands show granulation and some irregular extinctions or strain shadows. Diopside grains immediately adjacent to or included in the bands are anhedral and generally less than

0.5 mm in size. Plate 2, figure 2 is a photomicrograph of a thin section cut perpendicular to a band of magnetite.

Probably 90 per cent or more of the magnetite in the ultramafic intrusive body is present in the pyroxenite and hornblende pyroxenite units in the fourth type of textural association. In a representative specimen of fine-grained rock from the magnetite-rich zone, the pyroxene grains range from 1 to 4 mm and the magnetite grains from 0.07 to 2 mm. In the coarser-grained rock, pyroxene grains range from 2 to 15 mm and the magnetite grains from 1 to 10 mm. Magnetite that exceeds 1 mm is almost invariably composed of several irregular grains, rarely larger than 3 mm. The pyroxene grains in all grain sizes range from anhedral to euhedral but are generally subhedral and equant. The interstitial magnetite is very irregular and inequant (Pl. 2, fig. 1). The primary textural relationship indicates that the most of the magnetite has crystallized in the interstices between diopside grains.

In several specimens of pyroxenite collected from, or near, the contacts between pyroxenite and schist, most of the magnetite is irregular and interstitial to diopside, but grains of diopside poikilitically enclose small, subhedral grains of magnetite. This texture indicates that some magnetite had commenced crystallization during crystallization of diopside. This texture is peculiar to these specimens and is probably the result of especially rapid crystallization of the rock at the contact with schist.

Most of the polished mounts of magnetite contain some ilmenite, both as independent grains and as exsolution lamellae in the magnetite. Independent ilmenite grains are generally irregular, anhedral, and peripheral to larger grains of magnetite. The textures in some mounts indicate that ilmenite has replaced magnetite along crystallographic directions in the latter. Individual grains of ilmenite compose approximately 1–3 per cent of the opaque minerals in those mounts in which they occur and range in size from 0.06 mm to 0.6 mm. The most common size is 0.15 mm. Approximately 75 per cent of the magnetite grains exhibit exsolved blades of ilmenite along octahedral directions in the magnetite. In a typical example, there are a few larger blades which may run the length of the magnetite grain (up to 3 mm) but are not more than 0.005 mm in width, plus swarms of smaller, oriented blades grading in size from 0.04 mm in length down to the limits of resolution of the microscope. The ilmenite present as blades of all sizes is visually estimated to compose 2–5 per cent of the opaque material. Small (0.02 mm) blades of a gangue mineral are also present in amounts of approximately 1–2 per cent, oriented along cubic directions in the magnetite. The identification of this mineral in polished mounts is difficult, but extrapolation from thin-section studies indicates that it is most probably hercynite spinel.

Since there are all gradations in size of ilmenite blades in the magnetite, there is reason to believe that there are ilmenite blades below the limits of resolution of the microscope. Approximately 20 per cent of the magnetite grains appear slightly anisotropic. This probably indicates that TiO_2 is present either as submicroscopic lamellae or actually substituting for Fe_2O_3 in the magnetite lattice.

Local and minor amounts of earthy hematite are associated with ankerite veinlets in some areas of hornblende pyroxenite and pyroxenite. Both megascopic and microscopic textural relationships show that this is a secondary alteration of magnetite. There are also minor amounts of sulfide minerals around the periphery of the ultramafic body. Most of the sulfide minerals are in the ultramafic rocks, generally hornblende pyroxenite, but minor concentrations occur locally in saussurite gabbro. The sulfides are mostly pyrite with some pyrrhotite and chalcopyrite and traces of marcasite. Some magnetite is intimately associated with the sulfide minerals.

The sulfides generally occur as individual grains disseminated throughout portions of the rock, but there are a few irregular and discontinuous veins. In the ultramafic rocks, pyrite is the only sulfide mineral which shows euhedral crystal development. Pyrrhotite and chalcopyrite occur as irregular grains, generally interstitial to silicate minerals. The texture studies in polished mounts indicate the following general paragenetic relationships:

ilmenite$_I$* (exsolution) magnetite$_I$ –ilmenite$_{II}$*–pyrrhotite–?–pyrite**–marcasite

chalcopyrite–magnetite$_{II}$

magnetite$_I$ = primary magnetite.

magnetite$_{II}$ = secondary magnetite, a product of serpentinization.

* exsolved ilmenite and peripheral grains of ilmenite are most logically explained by two separate generations.

** only definite relationship between pyrite and other opaque minerals is that chalcopyrite veins pyrite. Chalcopyrite also veins pyrrhotite.

Origin of Ultramafic Rocks

Relationships Between Gabbro and Ultramafic Rocks

In other localities in southeastern Alaska, and in other regions of the world, relatively small, intrusive ultramafic bodies of the type exposed at Union Bay invariably show space relationships with gabbro intrusions generally similar in size and mineralogy with the rocks described here (Aho, 1956; Camsell, 1913; Dresser, 1913; Grout, 1918; Hjelmqvist, 1949; Ingerson, 1935; Little, 1949; Walton, 1951; Zaveritsky and Betekhtin, 1937).

From his study of the ultramafic complex at the Blashke Islands, southeastern Alaska, M. S. Walton, Jr. (1951, PhD thesis, Columbia Univ.) concludes that the "gabbro ring" peripheral to that ultramafic plug, although discontinuous, has been developed by fusion and mobilization of metasedimentary wall rock by the ultramafic intrusion. This hypothesis fails to explain the relationships at Union Bay. The igneous textures, intrusive relationships, and peripheral metamorphism of metasedimentary wall rocks around the main body of gabbro at Union Bay indicate that the gabbro was emplaced as a magma. The ultramafic magma probably did not contain enough heat in excess of the latent heat of fusion to melt a volume of wall rock approximately equal to or possibly even greater than the volume of the ultramafic body. There is no evidence at contacts between ultramafic rocks and schist that more than minor amounts of a few components of the wall rocks, mostly water, were mobilized by heat from the ultramafic intrusion.

Although the composition of the mineral diopside, as determined by refractive indices, and the general chemical composition of the rocks are somewhat similar on both sides of the contacts between hornblende pyroxenite and saussurite gabbro (Table 1), there is no other evidence that the ultramafic and gabbroic rocks could have been differentiated from a common magma, either in the site of intrusion or anywhere else. Any mechanism of differentiation would fail to explain the distribution of the gabbro around the ultramafic body, the intrusive relationships between the ultramafic body and gabbro, and the absence of complementary, intermediate, or gradational rock types. Except for inclusions of saussurite gabbro and veins of material similar to saussurite gabbro in the hornblende pyroxenite, which are marginal, essentially contact, features, not one plagioclase grain has been observed in 7 square miles of outcrop within the ultramafic intrusive body.

The only tenable explanation of the relationships between ultramafic and gabbroic rocks at Union Bay must incorporate a hypothesis of two intrusions separated by enough time to allow the earlier intrusive body to become largely or wholly crystalline. The lack of chilled margins in either gabbroic or ultramafic rocks at their mutual contacts implies that the time gap separating the two intrusions was relatively short.

Age relationships between gabbroic (and saussurite gabbro) and ultramafic rocks are not obvious from their contact relationships (Fig. 1). Veins of albite, clinozoisite, epidote, and hornblende that cut through the hornblende pyroxenite at or near the contact cannot be taken as criteria that the gabbro is the younger of the two intrusions. Dikes of hornblendite that cut the gabbro near the contact are contradictory evidence, and the development of saussuritization of gabbro along the ultramafic contact is a feature clearly superimposed upon the main gabbroic intrusive body. Furthermore, in the general case of an ultramafic magma intruding hot, gabbroic rocks, a eutectic or cotectic mixture of the least refractory constituents of the gabbro would be the first material (if any) to be mobilized by temperature and pressure conditions at the contact, with or without the presence of water, and these would normally be expected to recrystallize after the more refractory minerals of the ultramafic body had crystallized, in which case the apparent age relationships would be reversed and misleading.

A conclusion that the gabbro is earlier than, and intruded by, the ultramafic body is preferable. The alternative hypothesis that the gabbro is later than the ultramafic body would fail to explain the following features:

(1) Inclusions of saussurite gabbro in the hornblende pyroxenite, in some cases close to and oriented parallel to the contact with the main body of gabbro.

(2) Dikes of hornblendite cutting the gabbro at or near the contact with hornblende pyroxenite.

(3) Mineralogical asymmetry of the main gabbro intrusive mass: the apparent interruption by the ultramafic body of both the general trend toward a dioritic periphery and the trend of composition of the mineral hypersthene (see the detailed description of the gabbroic rocks).

(4) The pattern of distribution of the gabbroic rocks around the ultramafic body and the

three-dimensional symmetry of the ultramafic intrusion against the gabbro contacts. Nowhere can it be demonstrated that the gabbro has cut out or cut across a unit of the ultramafic intrusive mass.

Nature of the Ultramafic Magma

In the geologic literature of the past 30 years, there has been considerable discussion about the physical nature of ultramafic magmas. The experimental work of Bowen and Schairer (1935) with the system MgO-FeO-SiO_2 indicates that magnesian olivine of the type commonly occurring in intrusive bodies of peridotite and dunite only begins to melt at approximately 1600° C. and becomes completely molten at approximately 1800° C. In spite of these high temperatures, an anomalous lack of high-grade metamorphism of the adjacent wall rocks is commonly associated with the ultramafic intrusions. Consideration of this problem has forced Bowen and Schairer (1935) and others to conclude that there must be a special mechanism of solid intrusion for peridotitic and dunitic rocks. However, many observers have found it difficult or impossible to reconcile a great deal of field evidence with any hypothesis other than intrusion of a relatively liquid magma of peridotitic or dunitic composition (Camsell, 1913; Cooke, 1937; Hess, 1938; Walton, 1951; and others).

The abundance of igneous relationships associated with both large- and small-scale features of the ultramafic rocks at Union Bay definitely precludes any mechanism of solid intrusion. Briefly summarized are features of the ultramafic rocks that have been described in detail in earlier portions of the text, and that can be explained only by an intrusion of a liquid magma:

(1) General intrusive relationships such as dikes of hornblendite cutting the gabbro around the margin of the ultramafic body.

(2) Regular sills of dunitic rock of all sizes from 75 feet to less than 1 inch thick with sharp contacts and a great deal of continuity.

(3) The general unsheared and ungranulated allotriomorphic texture of all the rock types, plus detailed textures which can be explained only by crystallization of the rock in place.

(4) Evidence of crystal settling in peridotitic rocks.

Distribution of Ultramafic Rock Types

Although local features of some of the ultramafic rocks at Union Bay require explanation by crystal settling, a mechanism of differentiation by crystal settling cannot explain the general petrologic structure of the ultramafic intrusive body. As Wager and Deer (1939, p. 117–123) have pointed out, a crystal accumulation from a crystallizing magma contains approximately 20 per cent of interstitial material representing the composition of the magma from which the crystals have separated. A hypothesis explaining crystallization of all the ultramafic rocks from a single magma would fail to explain the presence of a large body of dunite, essentially a monomineralic rock. This rock requires a separation of mineral phases that is more complete than is possible by crystal accumulation from a compound magma represented by the total composition of all the ultramafic rock types or the ultramafic plus the gabbroic rocks.

If differentiation by crystal accumulation had controlled the distribution of ultramafic rock types, the lopolithic portion of the intrusive body should show a definite gradation in composition from bottom to top. Assuming that the initial composition of the magma was on the olivine side of a binary eutectic mixture of diopside and olivine, dunite, the early crystallizing phase, should be concentrated near the floor of the lopolith with an increasing amount of diopside (in cotectic proportion) near the roof. There is no mechanism of differentiation by a gravity controlled crystal accumulation that can explain the fact that the most refractory ultramafic rocks, dunite and peridotite, constitute the central portion of the intrusive complex and are surrounded on all sides (above and below) by the less refractory pyroxenite and hornblende pyroxenite units.

As an explanation of the concentric zoning of the Blashke Islands ultramafic intrusive plug, Walton (1951) advanced a hypothesis of differentiation by thermal diffusion in part, or wholly, in a supercritical gas (water vapor) phase, and operating along strong thermal and concentration gradients within the magma. Many portions of the ultramafic rocks and the wall rocks at Union Bay do not show evidence of a sufficient quantity of water, or any other volatile component, for the large-scale operation of a mechanism of this type.

There is no field or experimental evidence that rates of diffusion through the liquid state are sufficient to operate as a mechanism of differentiation throughout an intrusive body as large as the ultramafic body at Union Bay. From experimental work, Bowen (1921) calculated the rate of diffusion of liquid diopside through liquid plagioclase (An_{66}) at a tempera-

ture of 1500° C. to be 2.31×10^{-6} cm²/sec. At this rate, the diffusion of diopside through plagioclase would take over 300 years to be significant (half saturation) over a linear distance of 2 meters.

Any hypothesis based upon a mechanism of differentiation of the ultramafic magma in the site of intrusion appears to be further burdened with the necessity for explaining the crystallization of the intrusive body from the center outward. The most refractory minerals (olivine and chromite) are concentrated in the central portions of the intrusive body, and the less refractory minerals (hornblende and diopside) occur peripherally. This distribution is the reverse of that which would be expected assuming a single-stage intrusion of ultramafic magma and realistic temperature gradients between intrusive body and wall rock. The expected differentiation is illustrated by one peridotite dike, in which most of the olivine has crystallized along the walls of the dike, and most of the diopside occurs in the center.

A mechanism based upon water-vapor pressure gradients has been proposed by Kennedy (1955) whereby sufficient quantities of water vapor and other volatile components may concentrate around the periphery of a magma chamber to reduce the melting points of local components far enough below the existing temperature gradient to promote crystallization of an intrusive magma from the center outward. This plausible mechanism may help to explain the peripheral concentration of magnetite and hornblende, but it is doubtful that the ultramafic intrusive body ever contained enough water, or other volatiles, for this mechanism to control crystallization of the whole body. Furthermore, crystallization from the center outward is a phenomenon that is mechanically unstable in a gravity field and would imply accumulation of the first material to crystallize (dunite) on the floor of a subhorizontal lopolith. Therefore, it is impossible to explain the concentric petrology of the lopolith at Union Bay by any mechanism requiring crystallization of the ultramafic body from the center outward.

The most plausible explanation of the structure and petrology of the Union Bay ultramafic complex is a hypothesis of successive injections of an ultramafic magma changing in composition with time and intruded in reverse of the order of crystallization of the component minerals.

The proposed history of the ultramafic intrusions is outlined herein. In the most simplified form, the successive intrusions may be considered to constitute essentially a three-stage phenomenon.

(1) Lopolithic, or probably initially sill-like, intrusion into metasedimentary rocks and a part of the completely, or almost completely, crystalline gabbro of a relatively liquid magma equal in composition to approximately 80 per cent diopside (approximately $D_{75}H_{25}$), 15 per cent magnetite, and 5 per cent forsteritic olivine (approximately $Fo_{80}Fa_{20}$).

(A) Some peripheral contaminations of this magma by H_2O, SiO_2, Al_2O_3, and Na_2O, mostly from gabbroic wall rock, and minor amounts, mostly H_2O, and possibly some SiO_2 from metasedimentary wall rocks.

(B) Almost complete crystallization of this magma to form the hornblende pyroxenite unit and magnetiferous portions of the pyroxenite unit.

(2) Intrusion into the hot, still crystallizing, central portions of the first intrusive body of a relatively liquid magma approximately equal in composition to a binary eutectic mixture of diopside (approximately $D_{80}H_{20}$) and forsteritic olivine (approximately $Fo_{80}Fa_{20}$): probably 80 per cent diopside and 20 per cent forsteritic olivine, but probably also containing several per cent ferric iron.

(A) Some remobilization of the still hot, crystalline, magnetiferous pyroxenite rocks. Some assimilation of the still liquid, initial magma and mixing with the second intrusive body.

(B) Almost complete crystallization of the second magma to form the olivine pyroxenite rock and some less magnetiferous portions of the pyroxenite unit.

(3) Intrusions of relatively liquid dunitic material into the central portions of the lopolith, exhibiting generally concordant, but some crosscutting, intrusive relationships with other ultramafic units.

(A) Some remobilization and assimilation of the recently crystallized and hot olivine pyroxenite rocks, and local contamination of the dunite to form textural peridotite rocks.

(B) Crystallization of peridotitic and dunitic rocks and subsequent cooling of the intrusive body. Local formation of serpentine minerals when the cooling intrusive body reached the temperature range of 500°–600° C. (Bowen and Tuttle, 1949).

The authors know of no physicochemical data on any system approximating the composition of the initial magma postulated. On the basis of the assumptions outlined it must be further assumed that there are binary and ternary eutectic relationships between diopside and

magnetite and diopside, olivine, and magnetite. The texture and composition of the pyroxenite unit indicate that the eutectic point between diopside and magnetite lies toward the magnetite side of the system. If this inference is correct, and if the initial magma was of the composition assumed, most of the diopside would have crystallized before any magnetite began to crystallize at the eutectic point, creating the textural relationships between diopside and magnetite observed in the pyroxenite unit.

Because of heterogeneity of the source of material, the initial magma must have been composed of diopside and magnetite with some olivine. In most of those portions of the pyroxenite unit which contain from 10 to 20 per cent magnetite, there is no olivine. Therefore, a local mechanism must be postulated to change the composition of the melt away from the stability field of olivine. Such a mechanism may have been furnished by contamination of the magma by material derived from the wall rocks, especially H_2O and SiO_2.

Water diffusing into the magma from the wall rocks would have been partially dissociated at the temperature of the environment and probably would have oxidized proportional amounts of ferrous iron in the melt according to the equation (Goldschmidt, 1954, p. 657):

$$Fe^{++} + H_2O \rightarrow Fe^{+++} + H_2 + OH^-.$$

Olivine can be converted to magnetite and pyroxene (enstatite or clinoenstatite) by water according to the equation (R. N. Clayton, 1955, unpub. PhD thesis, California Institute of Technology):

$$3Fe_2SiO_4 + 3Mg_2SiO_4 + 2H_2O \rightarrow 2Fe_3O_4 + 2H_2 + 6MgSiO_3.$$

For this reaction, the calculated change in free energy at 298° C. is −59,000 cal, and at 1000° C. is −95,000 cal. These data indicate that, with increasing temperature, water is increasingly capable of oxidizing ferrous iron in olivine to ferric iron in magnetite. To simulate the composition of the initial magma postulated, the solid-solution series diopside-hedenbergite would have to be added to both sides of the reaction, complicating it considerably. However, there is solid solution between diopside and clinoenstatite (Bowen, 1928, p. 49), and quite probably any addition of water to the ultramafic magma would have favored the formation of proportional amounts of diopside and magnetite and may have prevented the crystallization of olivine.

The reaction probably means that oxidation of ferrous iron on the left-hand side of the equation has increased the ratio (relative saturation) of SiO_2 to MgO beyond the field of stability of olivine. Because ferric iron would not have been stable in the silicate lattice in amounts of more than a few per cent, oxidation of ferrous iron in the ultramafic melt would have increased the stoichiometric proportions, and relative saturation, of SiO_2 in the melt, inhibiting the crystallization of olivine.

In the course of experimental work, Bowen and Tuttle (1949) and Kennedy (1950) have noted the facility with which silica has been transported in supercritical water vapor at temperatures above the critical temperature of water and pressures above 140 atmospheres. Therefore, water diffusing into the ultramafic magma from the wall rocks may have carried some silica. This phenomenon plus the oxidation of ferrous iron by water constitute additive mechanisms that may have increased the relative saturation of SiO_2 in some portions of the initial ultramafic magma, locally inhibiting the precipitation of olivine and causing the crystallization of bimineralic rock composed of diopside and magnetite.

It is not entirely clear whether the chemical components of the mineral hornblende and the gabbroic veins in the hornblende pyroxenite represent primary constituents of the ultramafic magmas concentrated in late, pegmatitic phases of intrusion, or whether this material largely represents contamination of the ultramafic body by material derived from wall rocks, or both. However, the absolute confinement of the hornblende pyroxenite unit to the periphery of the complex and the intimate association between hornblende pyroxenite and inclusions of both schist and gabbroic material strongly indicate that the H_2O, Al_2O_3, Na_2O, K_2O, and much of the SiO_2 were derived from the wall rocks.

If a relatively short time separated the crystallization of the gabbro and the initial intrusion of ultramafic material, the minerals of the gabbro would have remained very close to (just below) the temperature of crystallization. In this case, only a relatively small contribution of heat energy from the ultramafic magma would have caused mobilization of a eutectic liquid of the least refractory constituents of the gabbroic wall rock, and, as previously discussed, this material would have crystallized after the more refractory minerals of the ultramafic body had crystallized.

The equilibrium diagram of Bowen (1914, p. 212) shows that eutectic proportions of pure

diopside and pure forsterite are 87.5 per cent diopside and 12.5 per cent forsterite (Fig. 5). The diopside and olivine of the olivine pyroxenite rocks contain approximately 20–25 per

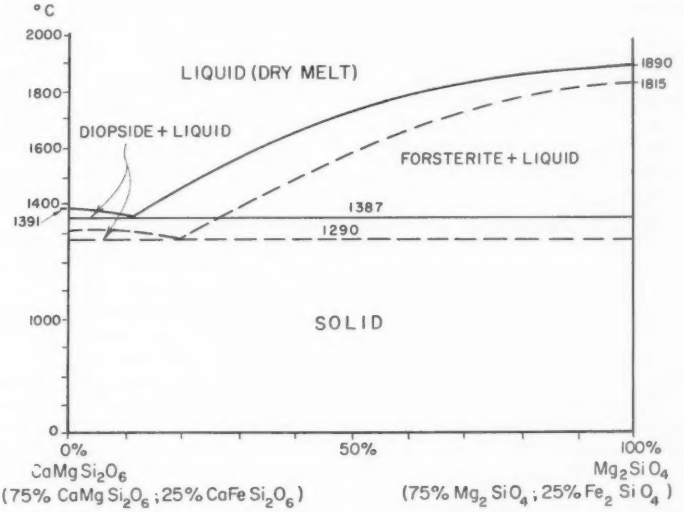

FIGURE 5.—EQUILIBRIUM DIAGRAMS OF THE SYSTEM DIOPSIDE-FORSTERITE

Solid lines: the binary system diopside-forsterite, after Bowen (1914, p. 212). Dashed lines: proposed binary system diopside-forsterite, each mineral containing 25 per cent of the ferriferous molecule, hedenbergite and fayalite, respectively.

cent of the respective iron molecules, hedenbergite and fayalite. The general composition of the rock indicates that eutectic proportions of this mineralogy are in the range of 80–85 per cent diopside and 15–20 per cent olivine (Fig. 5).

The composition of the second stage of ultramafic intrusion must have approximated the lower-temperature eutectic point in Figure 5 but in addition probably contained 1–3 per cent ferric iron. The invasion of this material would have found the hotter, probably still crystallizing, central portion of the preceding intrusion the most accessible locus for intrusion. This phenomenon has been outlined by Harker (1932) and Bowen (1928, p. 157–158) as a mechanism of intrusion for composite dikes in the Hebrides.

At the time of intrusion of the second ultramafic magma (olivine pyroxenite), crystalline portions of the initial intrusive body (diopside and magnetite) must have been just below the temperature of crystallization. Therefore, in addition to some mixing of still-liquid portions of the initial magma in the second magma, there would have been some remobilization and assimilation of diopside and magnetite by the second magma. If this assumption is correct, and if magnetite is neglected in order to simplify the system, the composition of the second magma would have shifted away from the eutectic point (Fig. 5) toward the diopside portion of the system. In this case, only diopside would have crystallized around the periphery of the second magma until the composition of the liquid returned to the eutectic point. Then the central portions of the magma would have precipitated eutectic proportions of diopside and olivine, forming the olivine pyroxenite unit.

Because of assimilation and mixing phenomena, the possibility of precipitation of some pyroxenite by the second stage of intrusion, and the lack of chilled boundaries within the ultramafic complex, it is not possible to make sharp distinctions in the field between the first and second stages of intrusion. The second intrusion probably extended laterally in some places beyond the limits of the initial intrusion, and it is probable that less magnetiferous portions of the pyroxenite unit around the north and northeast periphery of the ultramafic body

represent crystallization from the second stage of intrusion.

The olivine pyroxenite unit was probably mostly, but not entirely, crystalline at the time of the third stage of intrusion of peridotitic or dunitic material, and the arriving magma again must have found the hottest, still crystallizing, central portions of the olivine pyroxenite the most accessible locus of intrusion. Some of the olivine pyroxenite wall rock must have been mobilized and assimilated by the dunitic magma. Therefore, owing to assimilation of liquid portions of the olivine pyroxenite magma and remobilization and assimilation of some crystalline olivine pyroxenite, portions of the dunitic magma, probably the earlier of a succession of dunitic intrusions, may have been locally contaminated to peridotitic composition. It is possible that the initial injections of the final, dunitic stage of intrusion were originally peridotitic in composition, but there are no criteria from which to determine the relative importance of this possibility versus effects of contamination of dunitic material by remobilization and assimilation of olivine pyroxenite.

Dunitic rocks locally contain as much as 10 per cent diopside, and rocks of the textural peridotite type range from 10 per cent diopside and 90 per cent olivine to 60 per cent diopside and 40 per cent olivine (Table 2). According to the equilibrium diagram in Figure 5, melts with a composition to the right (forsterite side) of the eutectic point (12.5 per cent forsterite and 87.5 per cent diopside) would have precipitated only olivine until eutectic proportions were reached in the liquid, at which stage both diopside and olivine would have crystallized in eutectic proportion. This requisite physicochemical behavior explains such features as crosscutting peridotite dikes and diopside-rich veins in dunite.

Evidence of local crystal settling in some peridotitic rocks implies rhythmic precipitation of eutectic proportions of diopside and forsterite in quiescent portions of the intrusive mass. These residual pockets of liquid must have been surrounded by more dunitic material which crystallized at a higher temperature. No diopside would have precipitated from the residual liquid until the composition and temperature of the eutectic point was reached, at which point both diopside and forsterite crystallized together in eutectic proportion. It is proposed that diopside settled through the liquid faster than forsterite due to a higher density at that temperature and a more rapid rate of crystal growth.

The densities of pure diopside and pure forsterite at ordinary temperature are 3.275 and 3.216 respectively (Birch, Schairer, and Spicer, 1942, p. 15). This difference is negligible, but the coefficient of thermal expansion is greater for olivine than for diopside. At 1000° C. the density of diopside is approximately 10 per cent greater than that of olivine (Birch, Schairer, and Spicer, 1942, p. 32–33). Although no data are available for higher temperatures, the density of diopside at the eutectic temperature (1387° C.) must be more than 10 per cent greater than the density of olivine.

The mechanism responsible for the rhythmic precipitation of the multiple layers is not clear. Similar mineral layering has been described in many less mafic igneous rocks such as the Bushveld (Lombaard, 1934), Stillwater (Peoples, 1936), Duluth gabbro (Grout, 1918), and Skaergaard (Wager and Deer, 1939) intrusive bodies and the Keweenawan lava flows (Cornwall, 1951). The most plausible explanation of this type of layering has been advanced by Wager and Deer (1939, p. 332), who attribute the banding in the Skaergaard intrusive body to magmatic convection currents:

> "It is believed that downward currents were formed along the walls of the intrusion due to the greater density of the cooled, and partly crystallized magma which occurred there. Compensating currents are considered to have swept across the floor of the intrusion; then to have risen at the centre to the top of the intrusion where cooling and concomitant increase in density again took place causing the circulation to continue . . . The minerals denser than the magma . . . would sink through the current and be deposited at the bottom of the liquid . . . The rhythmic layering must have been produced by a rhythmic variation in the conditions of deposition, and it is suggested that changes in velocity of the convection currents were responsible."

This type of mechanism may have been operative locally in the ultramafic intrusive body at Union Bay, but it is very doubtful that rhythmic magmatic currents could have caused extensive banding in peridotitic rocks exposed on Duke Island, southeastern Alaska (now under study as a separate research project.) The great continuity and planar character of the layers on Duke Island, plus the lack of features such as "trough banding" or channel cutting within the layered rock, are difficult to explain by a mechanism of convective currents. Although no satisfactory alternative explanation is proposed here, it is believed that the rhythmic precipitation of the multiple

layers in both the Union Bay and the Duke Island ultramafic intrusions must be due to the fluctuation of a delicate physicochemical balance between temperature, pressure, and composition.

Origin of the Magnetite

All petrologic features of the magnetite in the ultramafic rocks at Union Bay clearly indicate that the magnetite is a primary crystalline product of the ultramafic magmas and is not material which has been added to, or which has replaced portions of, the already crystalline ultramafic rocks by secondary processes (excluding magnetite formed as a product of serpentinization).

In differentiated basic igneous bodies such as the Palisades sill (Walker, 1940) and the Skaergaard (Wager and Deer, 1939), magnetite has formed a major constituent of the rocks during the later stages of crystallization in the intrusion. This relationship is reversed at Union Bay relative to the whole ultramafic complex. Most of the magnetite is concentrated in portions of the peripheral pyroxenite unit and has to be considered a product of an early stage of crystallization relative to the olivine pyroxenite, peridotite, and dunite rocks in the more central portions of the complex.

In the pyroxenite unit, most of the magnetite is anhedral and interstitial to subhedral diopside crystals and is evenly distributed throughout large portions of the rock. The distribution and textural relationships indicate that the magnetite crystallized in equilibrium with the diopside, probably at a eutectic point in the binary system magnetite-diopside. If this assumption is correct, the eutectic point must lie close to the magnetite portion of the system, and the composition of the melt which precipitated the magnetiferous pyroxenite rock must have been close to the diopside side of the system, perhaps 80 to 85 per cent diopside and 15 to 20 per cent magnetite, because textures indicate that most of the diopside was crystalline before magnetite began to crystallize. The amount of magnetite precipitated must have been directly proportional to the amount of ferric iron in the melt.

Three possible explanations of the ferric iron in the melt, or the magnetite in the rock, may be considered: (1) assimilation of ferric iron-rich material by the initial ultramafic magma; (2) the oxidation of a portion of the ferrous iron in the magma to ferric iron by water derived from any source; and (3) proportional amounts of ferrous and ferric iron in excess of diopside and olivine contained in the original magma and derived at the source of the magma.

Residual portions of the gabbro intrusive body which were still liquid or least refractory portions remobilized and assimilated at the time of the initial intrusion of ultramafic magma may have contained Fe_2O_3 and FeO, but probably not in excess of other molecules, because there is no evidence that the gabbroic intrusive body had differentiated toward a ferrogabbro in the manner of the Skaergaard intrusive mass. Furthermore, a mechanism of assimilation of iron-rich material by the ultramafic body fails to explain the concentration of magnetite at contacts with schist containing approximately 5 per cent total iron.

Therefore, it is doubtful that much, if any, iron was contributed to the formation of magnetite in the initial ultramafic magma by assimilation of foreign material. It is proposed that all the iron now present as magnetite was an original constituent of the initial ultramafic magma, but that the ratio of ferric to ferrous iron in the melt was increased to some extent by locally derived water.

Water diffusing into the relatively dry magma from the wall rocks would have oxidized proportional amounts of ferrous iron in the melt as previously discussed. There is good evidence that some water did migrate into the intrusive body from both schist and gabbroic wall rocks, but it is not possible to explain the derivation of all, or most of, the magnetite concentrated in the pyroxenite unit in this way without assuming an unrealistic and complicated circulatory mechanism carrying water relatively great distances into the magma and circulating both water and ferric iron back to the periphery of the intrusive mass.

The chemical analysis of a specimen of magnetiferous pyroxenite from the northwest portion of the lower pyroxenite unit shows 19 per cent total iron (11.2 per cent ferric, 7.8 per cent ferrous), of which 14.5 per cent (9.7 per cent ferric, 4.8 per cent ferrous) is in magnetite, and 4.5 per cent (1.5 per cent ferric, 3 per cent ferrous) is in diopside (see analyses of specimen 32a and pyroxene mineral separate from specimen 32a in Table 1). Unless a concentrating mechanism is postulated for iron, the magma from which this rock crystallized must have contained 19 per cent total iron. If all the iron had been in the ferrous state, the magma, without any oxidation of the ferrous iron by water or other volatiles, would have precipitated a pyroxene containing approximately 70 per cent

of the hedenbergite molecule, or pyroxene and olivine containing approximately 70 per cent of the hedenbergite and fayalite molecules respectively. The diopside and olivine of the ultramafic complex range in composition only from 30 to 1 per cent of the hedenbergite molecule for diopside, and from 22 to 7 per cent of the fayalite molecule for olivine. Therefore, it is highly improbable that the original magma contained only ferrous iron, and equally improbable that oxidation of ferrous iron by water or other volatile material could have been the controlling process responsible for the formation or concentration of magnetite.

If any process of concentration of iron, such as circulating volatile material in the magma, had been a dominant factor in the concentration of magnetite around the periphery of the ultramafic body, there is no reason why magnetite should not have been locally concentrated to 90 per cent or more, as commonly observed in contact-metamorphic magnetite deposits. In a few places in the pyroxenite at Union Bay, the concentration of magnetite is as high as approximately 50 per cent of the rock over small areas of outcrop of approximately 100 square feet or less. However, there are no masses of magnetiferous pyroxenite containing more than approximately 25 per cent magnetite that would exceed 400 or 500 tons each.

The most plausible explanation of the magnetite is that proportional amounts of ferric and ferrous iron were contained in the initial ultramafic magma. This assumption is the only satisfactory explanation of the even distribution of the magnetite throughout large volumes of pyroxenite, and requires no concentrating mechanism. However, there is good evidence that some water migrated from the wall rocks into portions of the initial intrusive body, and the state of oxidation of the iron in the melt and the amount of magnetite in the rock must have been increased accordingly.

It has been proposed that the composition of the initial ultramafic magma approximated 80 per cent diopside ($D_{75}H_{25}$), 15 per cent magnetite, and 5 per cent olivine ($Fo_{80}Fa_{20}$). If this mixture (containing 19 per cent total iron) had crystallized without further oxidation of the iron, the distribution of the iron should have been: 7.5 per cent in diopside and olivine, 11.5 per cent in magnetite. However, specimen 32a contains 20 per cent magnetite (14.5 per cent total iron), and the diopside ($D_{77}H_{23}$) contains only 4.5 per cent total iron. Therefore, it is proposed that approximately 14 per cent of the iron now present as magnetite in specimen 32a has been oxidized by water diffusing into the magma from the wall rocks, either in the site of intrusion or en route, but most probably both.

Although they are much smaller features, the regular bands of magnetite found in a few places in the pyroxenite and olivine pyroxenite units at Union Bay bear an interesting similarity to the oxide bands of the Bushveld (Lombaard, 1934). Bateman (1951) has explained the oxide bands of the Bushveld complex by a mechanism of "gravitative liquid accumulation" whereby the heavy oxide liquid, under great hydraulic pressure, has accumulated on a floor and floated the silicates with such force that the adjacent silicate crystals have become strained, bent, and granulated. This explanation may be applicable to the magnetite bands at Union Bay, where, at a late stage in the crystallization of the rock, most of the diopside had crystallized, and the residual, heavy, oxide-rich liquid locally settled into layers. However, an alternative explanation for the magnetite bands at Union Bay seems to be more tenable.

At a late stage in the crystallization of the pyroxenite, when most the the diopside but little of the magnetite had crystallized, the whole may have had enough rigidity to respond to stress as a solid. In this case, stress created by subsequent intrusion may have caused the almost wholly crystalline mass to fail along regular fractures. Following local pressure gradients created by the fracturing, the still-liquid portion of the magma (mostly magnetite) would then have accumulated along the fractures according to the principles of dilatency outlined by Mead (1925). The bifurcation and close spacing of many magnetite bands and the granulation of adjacent diopside crystals are best explained by this type of mechanism.

Problem of Metamorphism

One of the principal objections to the assumption of liquid ultramafic magmas has been the lack of high-grade metamorphic effects in the wall rocks corresponding to the high temperatures which must be assumed for melts of ultramafic, especially dunitic, composition. Because there are no plausible mechanisms for reducing the temperature of the magmas, the problem at Union Bay is clearly one of accepting the necessary temperatures and attempting to explain the lack of high-grade metamorphism.

At atmospheric pressure the melting points

of pure diopside and magnetite are 1391° C. and 590° C. respectively. The melting point of diopside containing 25 per cent of the hedenbergite molecule must be approximately 1300° C., and the eutectic temperature between diopside of this composition and magnetite must be below 1300° C. The eutectic temperature of the system diopside-forsterite is 1387° C. (Fig. 5), and the eutectic temperature between diopside and forsterite, each containing 25 per cent of the ferriferous molecule, must be approximately 1290° C. (Fig. 5).

According to calculations of Bowen and Schairer (1935, p. 208), the change in volume from the solid to the liquid state is relatively small for forsterite. Other data indicate that the change in volume from the solid to the liquid state is less for diopside than it is for olivines (Birch, Schairer, and Spicer, 1942, p. 15). Therefore, the effect of pressure upon the melting point is relatively small for both minerals $\left(\frac{dT}{dp} = \frac{\Delta V}{\Delta H} T\right)$. Bowen and Schairer (1935, p. 208) calculated the increase in melting point of forsterite as 4.7° C. per 1000 atmospheres, an increase of approximately 20° C. corresponding to a depth of 15 Km in the crust. Therefore, the temperatures of the magmas during the first two stages of ultramafic intrusion at Union Bay, unless superheated, probably were between 1250° C. and 1350° C.

The temperatures of the later stages of dunitic intrusion must have been approximately 1800° C. However, the dunitic material included the central portions of the ultramafic complex, and no peridotite or dunite rocks are in contact with either schist or gabbro.

Temperature distributions, as a function of time, in and around cooling igneous bodies of simple geometric shapes, have been determined from Fourier's classical theories of heat conduction in solids and have been presented by several authors (Lovering, 1935, 1936; Larsen, 1945). This work incorporates assumptions concerning the uniformity of thermal properties in hot and cold rocks and neglects the effects of convection in the magma and dissipation of heat by radiation. Solution of problems for infinite, planar igneous bodies of finite thickness indicate: (1) that the temperature of the wall rocks at the igneous contact rises rapidly to a maximum of approximately 60 per cent of the original difference in temperature between the wall rocks and the magma and remains at this figure until the igneous body is completely crystalline; (2) that the maximum reached during the progressive rise and fall of temperature, for points in the wall rocks beyond the igneous contact, travels outward from the contact with constantly decreasing value (H. P. Taylor, Jr., personal communication).

The simplifying assumptions made in the course of the work render its strict application to natural phenomena improbable. However, it is the best means available to estimate the order of magnitude of the temperatures in the wall rocks at Union Bay.

If the regional temperature of the wall rocks at the time of ultramafic intrusion was 200° C., and if the temperatures of the first two stages of ultramafic intrusion were 1300°, the solution of the heat equation used by Taylor suggests a maximum temperature of 850° in the wall rocks at the ultramafic contact. The final stages of intrusion of dunitic magma would have raised this temperature at least 100° C. locally. These temperatures, plus a lithostatic pressure of several thousand atmospheres, definitely satisfy the temperature-pressure conditions for the highest grade of contact metamorphism. However, it is improbable that the reactions involved in contact metamorphism proceed at a significant rate at any temperature without the catalytic effect of the presence of aqueous fluids.

The importance of water as an agent in processes of metamorphism has been particularly emphasized recently by Yoder (1952, 1955), but even classic theories of contact metamorphism attribute mineralogical changes within contact aureoles to relatively brief periods of accelerated chemical reaction controlled by the coincidence of high temperatures with the passage of catalyzing waves of aqueous fluids expelled from the crystallizing magmas (Turner and Verhoogen, 1951, p. 241, 567).

At Union Bay there is no evidence associated with either the ultramafic or surrounding rocks that any volatile, fluid phases were expelled from the ultramafic magmas during crystallization. The occurrence of magnetite, probably the last mineral phase to crystallize in the peripheral portions of the ultramafic body, is entirely confined to the ultramafic rocks and is not transgressive into the wall rocks, as in the case of contact-metamorphic deposits. Even the minor concentrations of sulfide minerals, occurring around the periphery of the complex, are largely confined to ultramafic rocks. These features, plus the pattern of serpentinization and the peripheral disposition of the hornblende pyroxenite unit, suggest that the ultramafic magmas, instead of emanating volatiles during

crystallization, absorbed some aqueous fluids from the wall rocks.

Because of the temperature gradient across the contact between magma and wall rock, only nonequilibrium conditions could have prevailed. A quantitative solution of the problem of water distribution under these conditions has not yet been obtained. However, Kennedy (1955, p. 491) has considered the case of a hot, dry magma intruding cool, wet sediments in a qualitative manner and has concluded:

"The temperature of the sediments close to the magma will rise very rapidly, and in consequence the partial pressure of water in the sediments may increase at a rapid rate, provided the water is in pore spaces which do not communicate readily with the surface of the earth. Suppose the sediments are initially at 200° and have interstitial water at a partial pressure of 100 atmospheres. If the sediments are heated to 400° by the magma, and the water cannot escape, the partial pressure of the water will increase from 100 atmospheres to more than 3400 atmospheres. The water may then escape by diffusing into the magma. The marginal portions of the melt may thus become greatly enriched in water. . . ."

Therefore, it is proposed that the lack of high-grade metamorphic effects in the wall rocks around the ultramafic complex at Union Bay is not a reflection of low temperatures of intrusion but rather is a result of the invasion of hot, but unusually dry, magmas, probably containing 0.3 per cent or less water. Owing to the anhydrous state of the magmas, they did not exude waves of volatile material during any stage of crystallization but rather absorbed some aqueous fluid from the adjacent wall rocks. The metasedimentary wall rocks probably were not "wet" at the time of ultramafic intrusion but must have contained approximately 3 per cent water as a constituent of crystalline phases, as indicated by the chemical analysis of specimen 400 in Table 1. It is proposed that a portion of this water was mobilized through partial fusion by heat energy from the crystallizing magmas and diffused from the wall rocks into the anhydrous magmas, as proposed by Kennedy.

These conditions, which must be the antithesis of contact phenomena adjacent to more hydrous magmas, must have inhibited high-grade metamorphism in the wall rocks adjacent to both the gabbroic and ultramafic intrusive bodies at Union Bay and may apply to the explanation of anomalously low-grade metamorphic effects associated with some basic and ultrabasic intrusions in other regions.

Source of the Magmas

The world-wide restriction of peridotitic intrusive rocks, or their serpentinized equivalents, to orogenic belts indicates that mechanisms of generation and intrusion of ultramafic magmas are related to the broader phenomena of orogeny. The regional distribution of peridotitic intrusive rocks in various parts of the world is summarized by Hess (1955), who concludes that their emplacement occurs during the early stages of deformation in mountain belts.

The most probable source of ultramafic magmas is a ubiquitous peridotite layer, the upper boundary of which may constitute the Mohorovičič discontinuity. Many geologists accept the existence of this layer in the earth on the basis of geophysical evidence. The only geologic evidence suggesting a layer of this composition is the occurrence of the ultramafic intrusive bodies themselves, and the occurrence, in some basaltic lavas, of blocks of ultramafic rock that are plausibly explained as exotic inclusions derived from the peridotitic mantle (Ross, Foster, and Meyers, 1954). The mineralogy and chemical analyses of many of these inclusions, especially those collected from the Hawaiian volcanic province, are practically identical with ultramafic rocks at Union Bay.

The intimate space association of the gabbroic intrusive mass and the ultramafic complex at Union Bay would be most simply explained by the derivation of both magma types by the same process at the same place in the mantle. Washington (1925), Bowen (1928), and Buddington (1943) have assumed that the peridotite shell of the earth is composed largely of olivine and pyroxene with approximately 20–30 per cent feldspar, a composition approaching that of chondritic meteorites. Both Bowen and Buddington have emphasized that if such material were subjected to fusion there would be a stage at which the liquid, constituting approximately 40 per cent of the mass, would be basaltic, or gabbroic, in composition (Bowen, 1928, p. 316; Buddington, 1943, p. 139).

However, the composition of any system similar to the composition proposed herein for the peridotitic mantle is analogous to the ternary system diopside-anorthite-forsterite presented by Osborn and Tait (1952, p. 419). The eutectic point in this system is 49 per cent diopside, 44 per cent anorthite, and 7 per cent forsterite. Any liquid derived from this, or any similar, system should, upon crystallization, precipitate some olivine, unless the composition of the melt was extraneously changed. The

gabbro at Union Bay contains no olivine, and therefore it is improbable that the gabbroic magma was generated from the same material as the ultramafic magmas.

Because none of the ultramafic rocks contain any feldspar at Union Bay, exclusive of some peripheral portions of the hornblende pyroxenite unit, a further complication is imposed upon the hypothesis of a mutual source for both the gabbro and ultramafic rocks, in that a mechanism is required for complete separation of the two magma types. No physicochemical mechanism at the source, or gravity controlled mechanism en route to the site of emplacement, appears capable of such complete separation of the two liquids.

In all fairness to the hypothesis of a mutual source for both the gabbroic and ultramafic magmas, it must be parenthetically noted that some ultramafic intrusions of size and association similar to the complex at Union Bay, notably the complex at Taberg, Sweden, studied by Hjemlqvist (1949), seem to be quite amenable to explanation by this hypothesis. Most of the "olivinite" intrusive rock at Taberg contains some plagioclase (labradorite) identical in composition with the plagioclase of the associated gabbro. The gabbro also contains an unusual, pleochroic olivine identical with the olivine of the ultramafic rocks. These features suggest a close genetic relationship between the gabbroic and ultramafic rocks, which could be plausibly explained by fusion of material similar in composition to that proposed by Washington, Bowen, and Buddington for the peridotite shell of the earth.

However, the evidence at Union Bay favors the more complex explanation that the gabbroic and ultramafic magmas, although probably generated or tapped by the same process, were probably derived from different levels within the earth. In this case, the same orogenic process may have tapped or generated the gabbroic magma at a high level in the mantle, or in the crust above the Mohorovičič discontinuity, and generated the ultramafic magmas at greater depth in the mantle.

Although the precise nature of the process has remained unsolved, the generation of fluid magma from crystalline material at depth within the earth appears to depend upon a mechanism for either the focus of heat energy or the release of pressure, or, most probably, both. Such a mechanism, localized along a major fracture, or in a zone of weakness that transected the Mohorovičič discontinuity, may have been responsible for the rise of the gabbroic and ultramafic magmas along the same route and their close association in space at the site of emplacement.

If it is assumed that the gabbroic and ultramafic magmas originated at different levels within the earth, as indicated by the evidence at Union Bay, explanations of their origins constitute two separate problems. The genesis of basaltic, or gabbroic, magmas has received a great deal of attention in the literature, and current thought is summarized by Turner and Verhoogen (1951, p. 194–200, 223). More recently Waters (1955) has discussed the problem.

The simplest approach to the composition of the peridotite shell at the source of the ultramafic rocks at Union Bay is based upon the assumption that the mineralogy of the source material is directly reflected by the mineralogy of the ultramafic complex, exclusive of portions of the hornblende pyroxenite unit which are, in part, composed of foreign material locally derived from the wall rocks. On the basis of this assumption, the source material may have been composed largely of forsteritic olivine and diopside, with some magnetite, chromite, and other spinels. These minerals may have been, in part, randomly distributed throughout some portions of the source, constituting relatively homogeneous rock, and, in some places, may have been segregated into olivine-rich and diopside-rich bodies or layers.

If these assumptions are made concerning the composition of the source material, and if a local mechanism capable of focusing increasing amounts of heat energy is postulated, the following results are proposed, in chronological order:

(1) From approximately 1250° C. to 1350° C.: rock composed of diopside, olivine, and magnetite produces a liquid of the composition of the eutectic point between magnetite and the most ferriferous diopside and olivine fractions. Concomitantly, rock composed of diopside and magnetite produces a liquid of the composition of the eutectic point between magnetite and the most ferriferous diopside fraction. These events would be accompanied and followed (overlapped in time) by fusion, in rocks composed only of diopside, first of the most ferriferous diopside fraction, followed by fusion of progressively more magnesian diopside. In rock containing less magnetite than eutectic proportions (probably the general case), the temperature would remain at the eutectic temperature between magnetite and diopside

(or olivine, or both) until all the magnetite had been melted.

(2) From approximately 1350° C. to 1450° C.: continued fusion of progressively more magnesian diopside in rock composed of that mineral only, and, in rock composed of diopside and olivine, fusion of eutectic proportions of progressively more magnesian fractions of both minerals. At approximately 1450° C., the probable eutectic temperature of the system diopside-forsterite at this depth, the temperature would remain constant in rock composed of both minerals until all the diopside in rock at this temperature had been melted (assuming that, at this stage, the composition of the system lies to the right, or forsterite, side of the eutectic point).

(3) From approximately 1450° C. to 1800° C.: fusion of eutectic proportions of olivine and magnetite and olivine and chromite, where these minerals are in contact, until all the magnetite and chromite had been melted. Production of dunitic liquid by fusion of progressively more magnesian olivine.

This sequence of progressive fusion of the source material provides a tentative explanation of the sequence of ultramafic rocks in the complex at Union Bay. The evidence further indicates a periodicity of the processes responsible for the generation and migration of the magmas such that time gaps occurred between the three stages.

An important, and possibly the controlling, force responsible for the ascent of magma, once generated, must be the difference in density between the liquid and the surrounding rock, both being subject to lithostatic pressure. The densities of diopside and olivine glasses are 2.830 and 2.831 respectively (Birch, Schairer, and Spicer, 1942, p. 15), and the density of liquid diopside at its temperature of crystallization (1391°) is 2.671 (Birch, Schairer, and Spicer, 1942, p. 36). The densities of dry ultramafic magmas, devoid of a gaseous phase and equivalent in composition to the ultramafic rocks at Union Bay, are probably less than crystalline basalt or gabbro (approximately 2.95) and greater than crystalline granite (approximately 2.65). Therefore, ultramafic magmas may have the ability to rise into, but not through, the sialic portion of the crust, due to the relative densities. This inference, that it may be physically impossible for ultramafic magma to rise to the surface of the earth, is the most plausible explanation of the absence of effusive ultramafic rocks.

References Cited

Aho, A. E., 1956, Geology and genesis of ultrabasic nickel-copper-pyrrhotite deposits at the Pacific Nickel property, southwestern British Columbia: Econ. Geology, v. 51, p. 444–481

Barth, T. F. W., 1931, Crystallization of pyroxene from basalts: Am. Mineralogist, v. 16, p. 195–208

Bateman, A. M., 1951, The formation of late magmatic oxide ores: Econ. Geology, v. 46, p. 404–426

Birch, F., Schairer, J. F., and Spicer, H. C., 1942, Handbook of physical constants: Geol. Soc. America Special Paper 36, 325 p.

Bowen, N. L., 1914, The system: diopside-forsterite-silica: Am. Jour. Sci., v. 38, p. 207–264

—— 1921, Diffusion in silicate melts: Jour. Geology, v. 29, p. 295–317

—— 1928, Evolution of the igneous rocks: Princeton, Princeton Univ. Press, 332 p.

Bowen, N. L., and Schairer, J. F., 1935, The system MgO-FeO-SiO_2: Am. Jour. Sci., v. 29, p. 151–217

Bowen, N. L., and Tuttle, O. F., 1949, The system MgO-SiO_2-H_2O: Geol. Soc. America Bull., v. 60, p. 439–460

Buddington, A. F., 1943, Some petrological concepts and the interior of the earth: Am. Mineralogist, v. 28, p. 119–140

Buddington, A. F., and Chapin, T., 1929, Geology and mineral deposits of southeastern Alaska: U. S. Geol. Survey Bull. 800, 398 p.

Camsell, C., 1913, Geology and mineral deposits of the Tulameen District, British Columbia: Geol. Survey Canada Mem. 26, 188 p.

Cooke, H. C., 1937, Thetford, Disraeli, and eastern half of Warwick Map-Areas, Quebec: Geol. Survey Canada Mem. 211, 160 p.

Cornwall, H. R., 1951, Differentiation in lavas of the Keweenawan series, and the origin of the copper deposits of Michigan: Geol. Soc. America Bull., v. 62, p. 159–202

Dresser, J. A., 1913, Preliminary report on the serpentine and associated rocks of southern Quebec: Geol. Survey Canada Mem. 22, 103 p.

Goldschmidt, V. M., 1954, Geochemistry: Oxford, Clarendon Press, 730 p.

Grout, F. F., 1918, Internal structures of igneous rocks; their significance and origin; with special reference to the Duluth gabbro: Jour. Geology, v. 26, p. 439–458

Harker, A., 1932, Metamorphism: London, Methuen and Co., 360 p.

Hess, H. H., 1938, A primary periodotite magma: Am. Jour. Sci., v. 35, p. 321–344

—— 1941, Pyroxenes of common mafic magmas: Am. Mineralogist, v. 26, p. 515–535, 573–594

—— 1949, Chemical composition and optical properties of common clinopyroxenes: Am. Mineralogist, v. 34, p. 621–666

—— 1955, Serpentines, orogeny, and epeirogeny, p. 391–407 *in* Poldervaart, Arie, *Editor*, Crust of the earth: Geol. Soc. America Special Paper 62, 762 p.

Hjelmqvist, S., 1949, The titaniferous iron-ore deposit of Taberg, Sweden: Sveriges Geologiska Undersökning, ser. C., no. 12, Årsbok 43, no. 10

Ingerson, E., 1935, Layered peridotite laccoliths of the Trout River area, Newfoundland: Am. Jour. Sci., v. 29, p. 422–440

Kennedy, G. C., 1949, Charts for correlation of optical properties with chemical composition of some common rock-forming minerals: Am. Mineralogist, v. 32, p. 561–572

— 1950, A portion of the system silica-water: Econ. Geology, v. 45, p. 630–654

— 1955, Some aspects of the role of water in rock melts, p. 489–503 *in* Poldervaart, Arie, *Editor*, Crust of the earth: Geol. Soc. America Special Paper 62, 762 p.

Kennedy, G. C., and Walton, M. S., Jr., 1946, Geology and associated mineral deposits of some ultrabasic rock bodies in southeastern Alaska: U. S. Geol. Survey Bull. 947–D, p. 65–84

Larsen, E. S., Jr., 1945, Time required for the crystallization of the great batholith of southern and Lower California: Am. Jour. Sci., v. 243–A, p. 399–416

Little, H. W., 1949, The ultrabasic rocks of the Middle River Range, British Columbia: Am. Jour. Sci., v. 247, p. 802–823

Lombaard, B. V., 1934, On the differentiation and relationships of the rocks of the Bushveld Complex: Geol. Soc. South Africa Trans, v. 37, p. 5–52

Lovering, T. S., 1935, Theory of heat conduction applied to geological problems: Geol. Soc. America Bull., v. 46, p. 69–94

— 1936, Heat conduction in dissimilar rocks, and the use of thermal models: Geol. Soc. America Bull., v. 47, p. 87–100

Mead, W. J., 1925, The geologic role of dilatency: Jour. Geology, v. 33, p. 685–698

Osborn, E. F., and Tait, D. B., 1952, The system diopside-forsterite-anorthite: Am. Jour. Sci., Bowen Volume, p. 413–433

Peoples, J. W., 1936, Gravity stratification as a criterion in the interpretation of the structure of the Stillwater Complex, Montana: 16th Internat. Geol. Cong. 1933, Rept. v. 1, p. 353–360

Ross, C. S., Foster, M. D., and Myers, A. T., 1954, Origin of dunites and olivine-rich inclusions in basaltic rocks: Am. Mineralogist, v. 39, p. 693–737

Thompson, J. B., Jr., 1955, The thermodynamic basis for the mineral facies concept: Am. Jour. Sci., v. 253, p. 65–103

Turner, F. J., 1948, Evolution of the metamorphic rocks: Geol. Soc. America Mem. 30, 342 p.

Turner, F. J., and Verhoogen, J., 1951, Igneous and metamorphic petrology: N. Y., McGraw-Hill Book Co., 602 p.

Wager, L. R., and Deer, W. A., 1939, Geological investigations in East Greenland; Part III, The geology of the Skaergaard intrusion, Kangerdlugssuaq, East Greenland: Medell. om Gronl., v. 105, no. 4, 352 p.

Walker, F., 1940, Differentiation of the Palisades diabase: Geol. Soc. America Bull., v. 51, p. 1059–1106

Walton, M. S., Jr., 1951, The Blashke Island ultrabasic complex, with notes on related areas in Southeastern Alaska: N. Y. Acad. Sci. Trans., v. 13, p. 320–323

Washington, H. S., 1925, The chemical composition of the earth: Am. Jour. Sci., v. 9, p. 351–378

Waters, A. C., 1955, Volcanic rocks and the tectonic cycle, p. 703–722 *in* Poldervaart, Arie, *Editor*, Crust of the earth: Geol. Soc. America Special Paper 62, 762 p.

Yoder, H. S., Jr., 1952, The MgO-Al_2O_3-SiO_2-H_2O system and the related metamorphic facies: Am. Jour. Sci., Bowen Volume, p. 569–627

—— 1955, Role of water in metamorphism, p. 505–524 *in* Poldervaart Arie, *Editor*, Crust of the Earth: Geol. Soc. America Special Paper 62, 762 p.

Zaveritsky, A. N., and Betekhtin, A. G., 1937, The Nizhny Tagil dunite massif· 17th Internat. Geol. Cong. Guidebook, Uralian Excursion, Northern Part, p. 66–77

ORINOCO MINING COMPANY, CIUDAD BOLIVAR, VENEZUELA; CALIFORNIA INSTITUTE OF TECHNOLOGY, PASADENA, CALIFORNIA

MANUSCRIPT RECEIVED BY THE SECRETARY OF THE SOCIETY, MAY 16, 1958

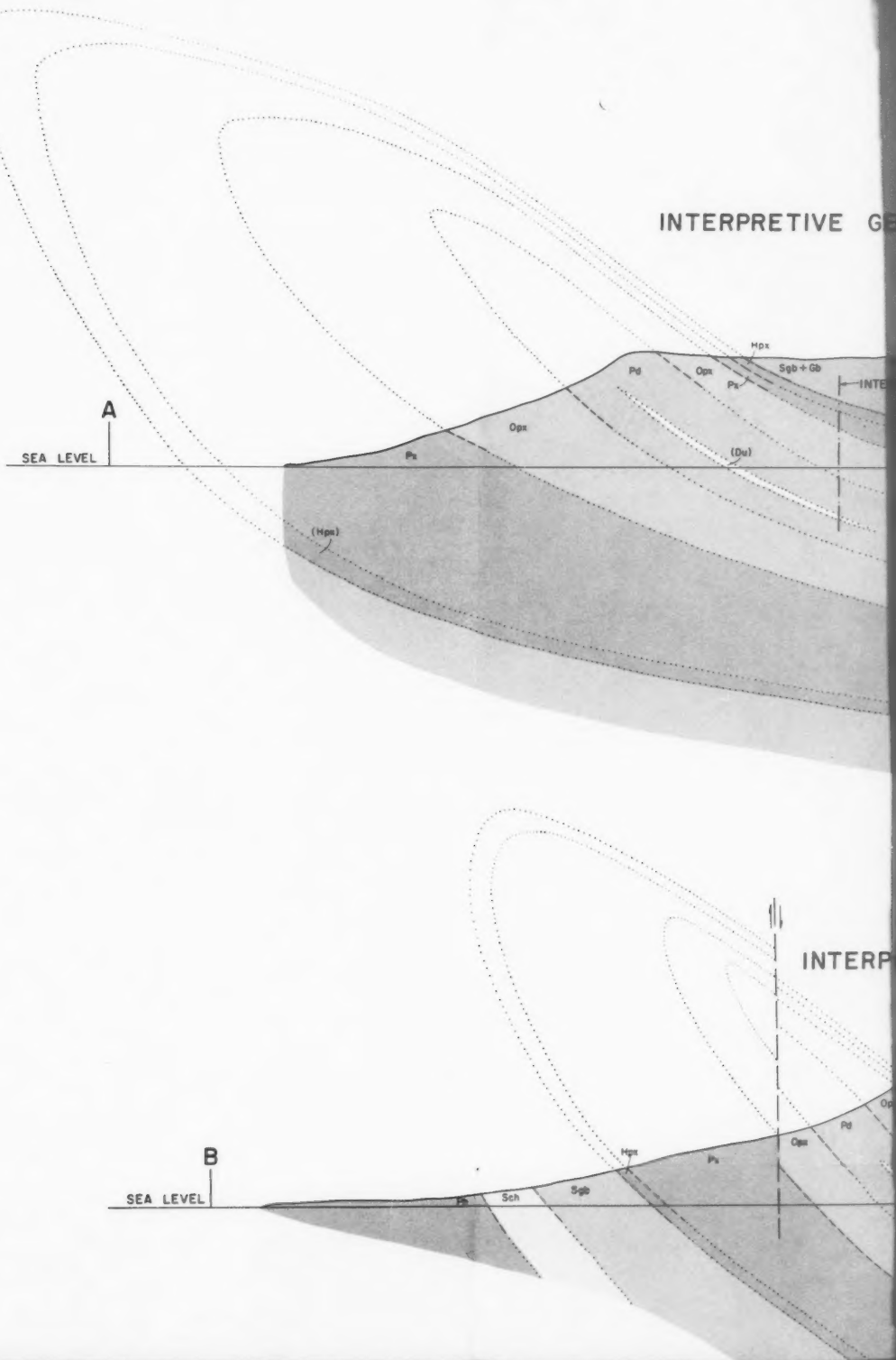
INTERPRETIVE GE
A
SEA LEVEL
Hpx
Pd
Opx
Px
Sgb + Gb
Opx
Px
(Du)
(Hpx)
INTERP
B
SEA LEVEL
Px
Sch
Sgb
Hpx
Px
Opx
Pd

INTERPRETIVE GEOLOGICAL SECTION A–A' (N 80° W)

LOOKING NORTH

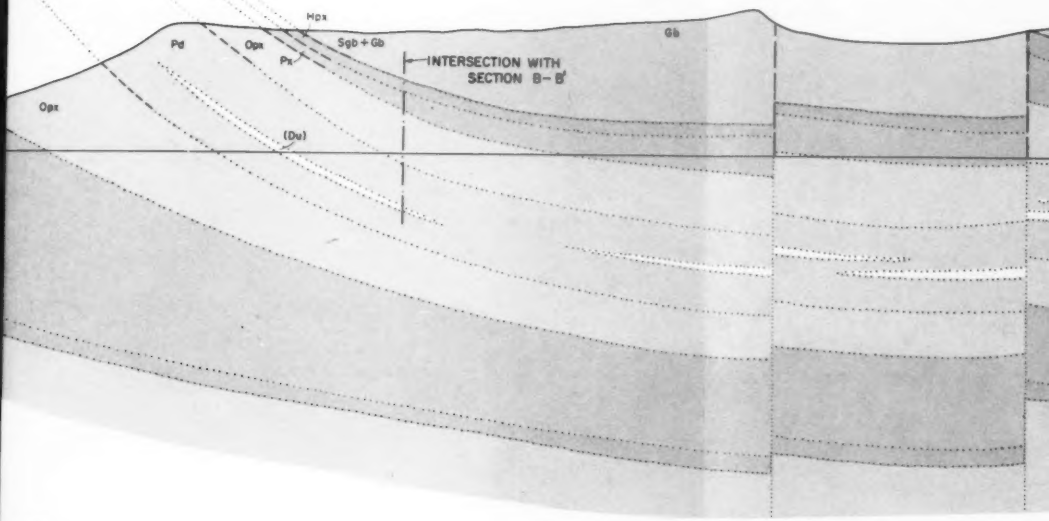

INTERPRETIVE GEOLOGICAL SECTION B–B' (N–S

LOOKING EAST

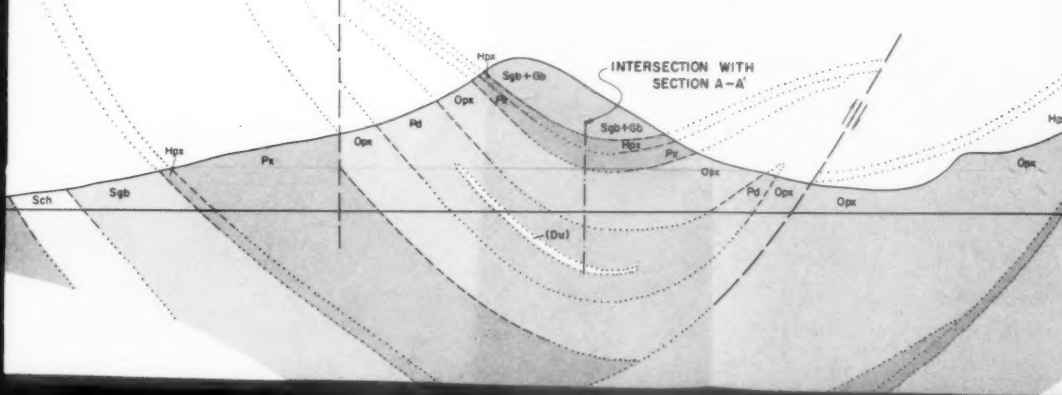

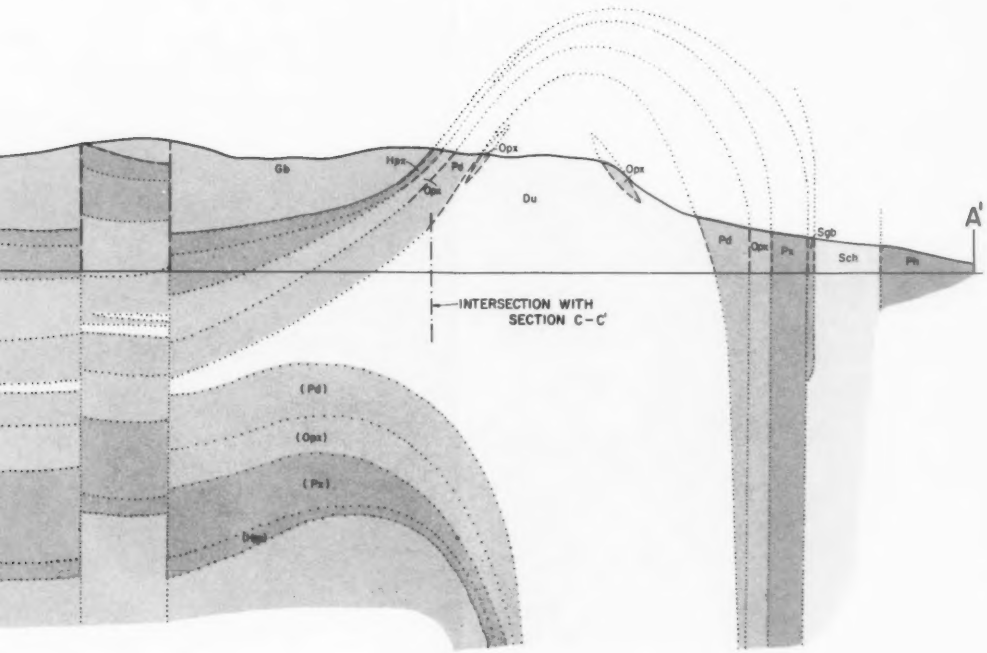
Gb
Hpx
Pd
Opx
Opx
Opx
Du
Pd
Opx
Px
Sgb
Sch
Pm
A'
INTERSECTION WITH
SECTION C-C'
(Pd)
(Opx)
(Px)

-B' (N-S)

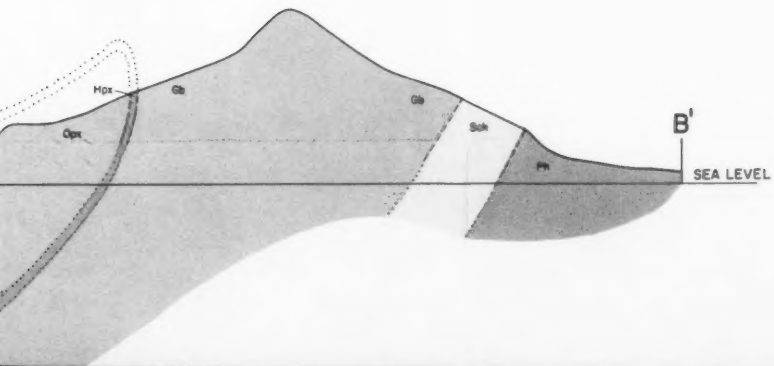
Hpx
Gb
Gb
Opx
Sch
Pm
B'
SEA LEVEL

SEA

SCALE
1320 660 0 1320

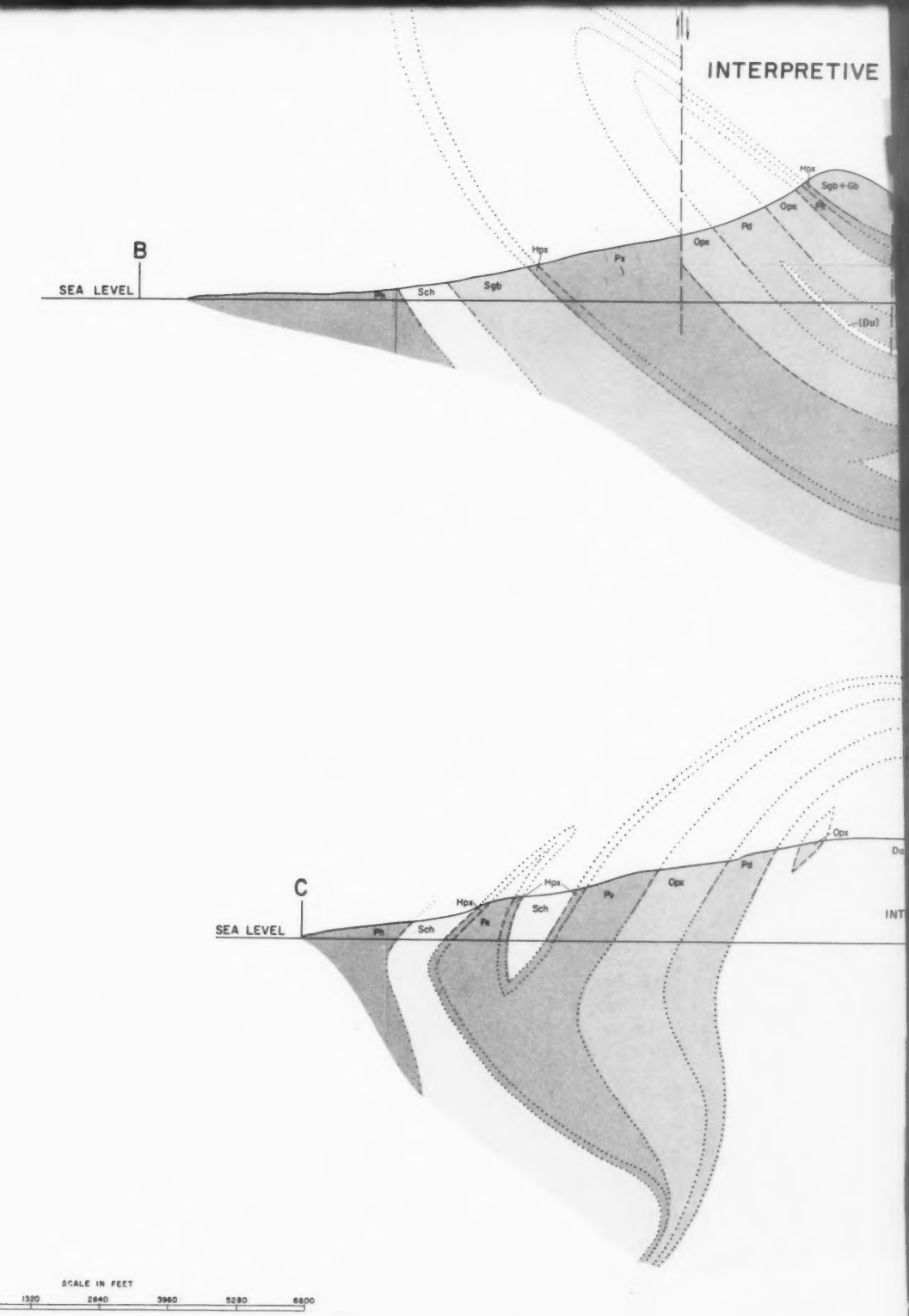

INTERPRETIVE GEOLOGICAL SECTIONS

See Plate

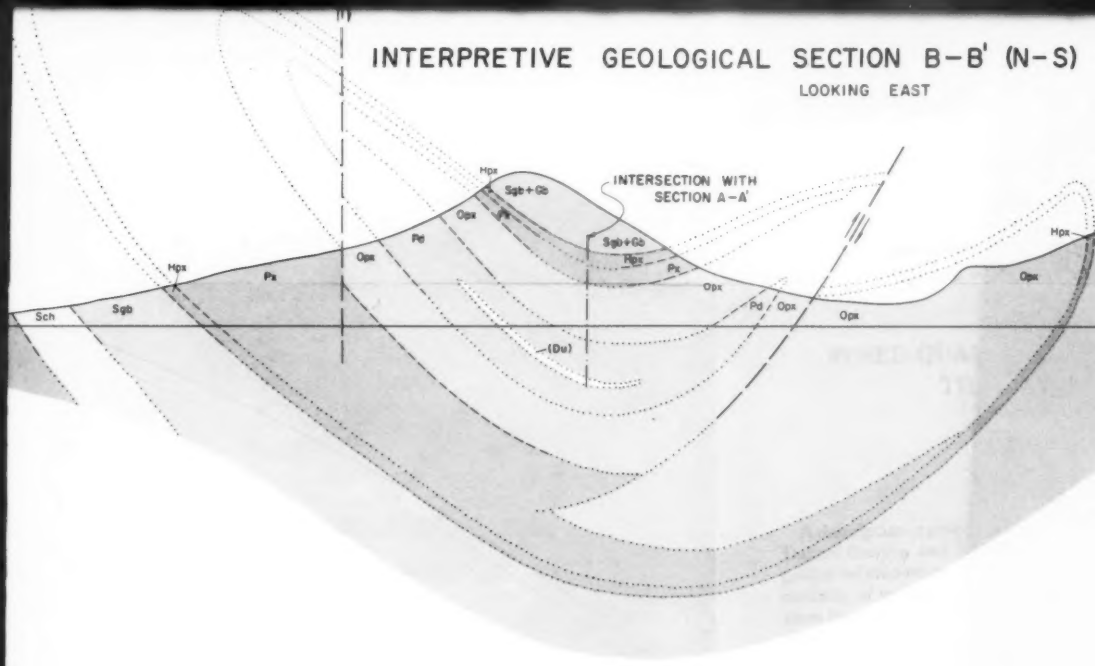

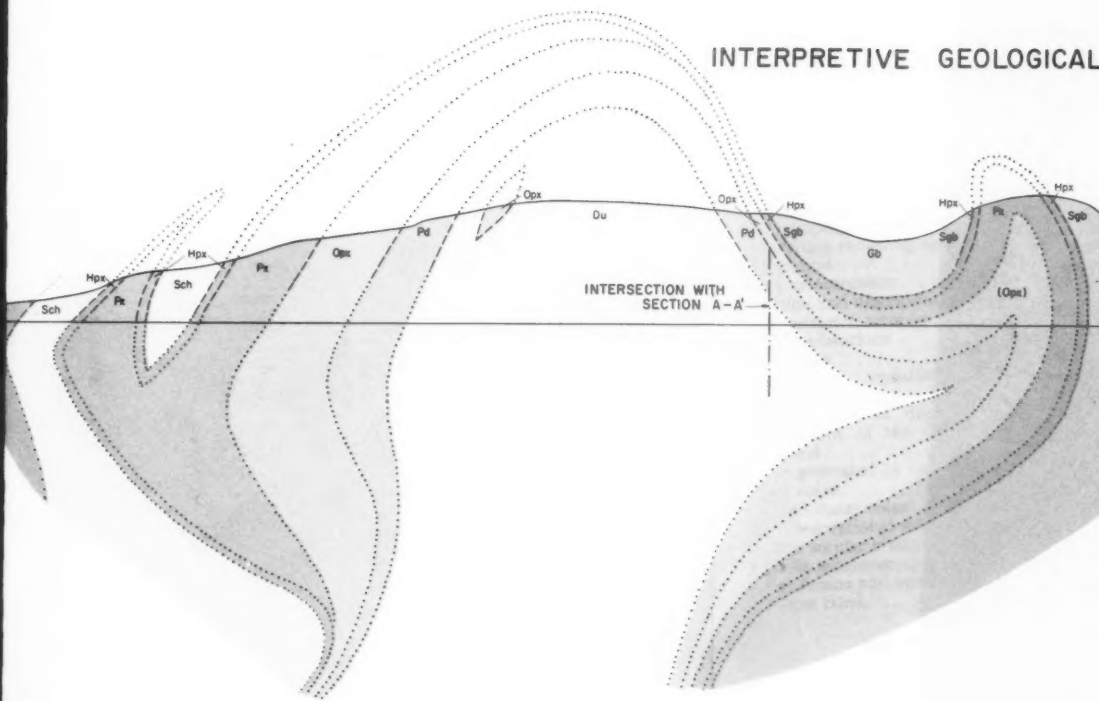

RETIVE GEOLOGICAL SECTIONS OF UNION BAY AREA, SOU

See Plate 1 for location and legend.

(N–S)

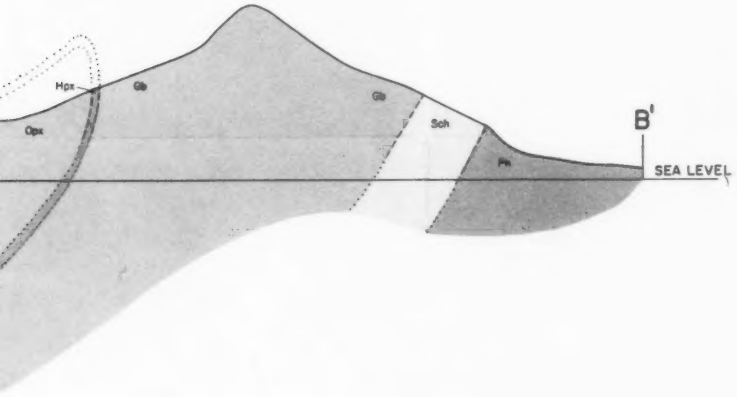

LOGICAL SECTION C-C' (N 7° E)

LOOKING EAST

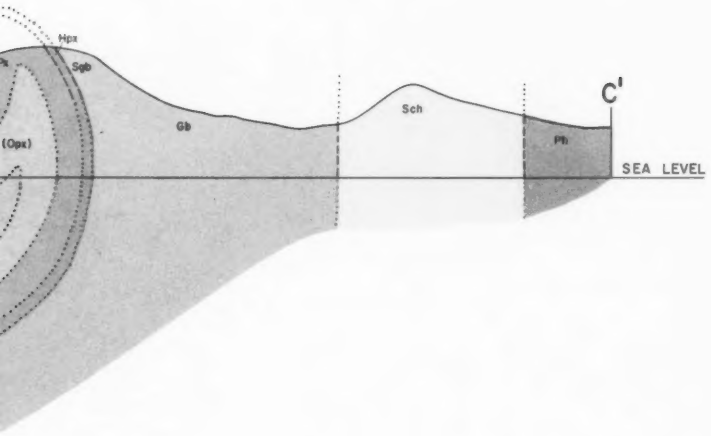

A, SOUTHEASTERN ALASKA

BULLETIN OF THE GEOLOGICAL SOCIETY OF AMERICA
VOL. 70, PP. 1019–1032, 15 FIGS. AUGUST 1959

FUSED-QUARTZ EXTENSOMETER FOR SECULAR, TIDAL, AND SEISMIC STRAINS

BY HUGO BENIOFF

ABSTRACT

A description is given of two fused-quartz extensometers located in mountain tunnels at Dalton Canyon and Isabella in Southern California and designed for observing long-period seismic-wave strains, earth tidal strains, and secular strains. They consist essentially of instruments for measuring and recording variations in the separation of two piers by comparison with a length standard of fused-quartz tubing. The sensitivity for secular strains, defined as the least detectable strain increment, is approximately 10^{-7}. For tidal and seismic-wave strains, the sensitivity is higher—a 1-mm deflection of the recorder represents a strain increment of 5.2×10^{-10}. In both cases the maximum usable sensitivity is limited by ground-strain unrest or noise, generated by wind, barometric-pressure variations, temperature variations of the surface layers of the ground, and variations in ground-water saturation.

CONTENTS

TEXT

	Page
Introduction	1019
Dalton extensometer	1020
Tunnel site and structure of quartz standard	1020
Measuring microscope	1021
Photographic recording system	1021
Ink-writing recording system	1022
Calibration	1024
Isabella extensometer	1025
Location and description of tunnel	1025
Galvanometer recorder for seismic waves	1026
Noise considerations	1026
Definitions	1026
Temperature variations of the quartz standard	1026
Strains induced at depth by temperature variations of the surface layer of the ground	1028
Noise generated by barometric variations	1028
Wind noise	1029
Ground-water noise	1029
Initial observational data	1029
Dalton secular-strain measurements	1029
Isabella secular-strain measurements	1032
Tidal strains and earthquake-wave strains	1032
References cited	1032

ILLUSTRATIONS

Figure	Page
1. Dalton extensometer installation (schematic)	1021
2. Concrete trough and double sling-wire supports of quartz standard	1021
3. Measuring microscope and interferometer calibration assembly (schematic)	1022
4. Double bowstring optical magnifier (schematic)	1022
5. Capacitance-bridge transducer (schematic)	1023
6. Transducer circuit used with tube-driven oscillator	1024
7. Simplified transducer circuit used with transistor-driven oscillator	1024
8. Magnetostriction calibration unit	1025
9. Transducer output circuit showing connection to Esterline-Angus recorder and differentiating circuit for galvanometer recorder G	1026
10. Portion of Isabella seismogram of the great Mongolian earthquake of 1957 December 4 written with galvanometer of 10-minutes period	1027
11. Isabella strain recording for 1957 December 3–4 showing tidal-strain variation and waves from the Mongolian earthquake of December 4	1027
12. Effect of thermal expansion of surface layers of ground on extensometer mounted within a mountain	1029
13. Dalton bowstring tidal recording showing elastic strain discontinuity induced at depth from surface heating of thin layer by morning sunlight	1029
14. Plot of Dalton secular-strain measurements	1030
15. Plot of Isabella secular-strain measurements	1031

INTRODUCTION

The development of an effective linear-strain seismograph (Benioff, 1935) provided, for the first time, an instrument having a response to seismic strains of the ground, instead of ground displacements as given by pendulum instru-

ments. Although in the early years of its development interest in seismology was centered more on the shorter seismic-wave periods, evidence was presented (Benioff, 1935, p. 296) indicating that the strain seismograph has certain inherent advantages over the pendulum for recording of long-period earthquake waves. These include its lack of response to tilt, which is very troublesome in long-period pendulums, and a 6 DB per octave decrease of response with period as compared with the 12 DB per octave decrease of pendulums for wave periods that are long in relation to the period of the instrument.

The original strain seismograph was constructed with a length standard in the form of a steel tube and was mounted in a room having fairly large temperature variations. In order to reduce the very long-period contributions in the response due to temperature variations of the steel tube, the recording galvanometer was operated from an electromagnetic transducer having an output emf proportional to the time derivative of the ground strain. In this form, the period-response characteristic of the strain seismograph is identical with that of the displacement of a pendulum having the same period and damping constant as the galvanometer. Since the galvanometer is concentrically balanced, its stability at very long periods is substantially greater than that of a pendulum which is necessarily excentrically balanced. Thus galvanometers having periods up to 10 minutes have been operated satisfactorily with this instrument, whereas pendulums of such long periods are not practicable. However, at these long periods the inherent noise of the instrument due to temperature variations of the standard and to strains produced by movements of people in the vicinity was sufficiently large to interfere seriously with its effectiveness. For strains of still longer periods, such as secular strains—the sources of earthquake energy—and tidal strains, the local noise level rendered the instrument useless. To reduce the long-period noise, a modified instrument was required which would conform to the following conditions: (1) location of the vault at sufficient depth in rock to reduce the annual temperature variation to 1°C. or less; (2) construction of the length standard with fused quartz or invar in order further to reduce its temperature response; (3) location of the vault away from habitations and vehicular traffic; (4) means for keeping the vault dry. Construction of an experimental installation meeting these conditions was made possible by a grant from The Geological Society of America. Operation of this instrument located at Dalton Canyon, California, and another built later at Isabella, California, has demonstrated that satisfactory recording of tidal and secular strains can be made.

Dalton Extensometer

Tunnel Site and Structure of Quartz Standard

Since the new instrument was intended for recording tidal and secular strains as well as seismic waves, it was desirable to change its name to extensometer. The available funds were insufficient to cover the cost of boring a tunnel, and consequently it was necessary to find one already in existence, located at a suitable site and available for this use. Fortunately one was found in Dalton Canyon about 33 km northwest of Pasadena ($\lambda = 117° 48.55'$ W., $\phi = 34° 10.23'$ N., h = 520 m). This tunnel had been constructed by the Los Angeles County Flood Control District to test the character of the rock at the site of a proposed flood-control dam. It is approximately 100 feet long and quite dry. Through the good offices of R. E. Hedger, Chief Engineer, and Paul Bauman, Assistant Chief Engineer of the Los Angeles Flood Control District, the tunnel was made available to the California Institute of Technology. To reduce temperature fluctuations, the tunnel was sealed with two bulkheads and a concrete recording room at the entrance (Fig. 1). The tunnel segment between the recording room and the instrument portion serves as a thermal insulation barrier. The fixed end of the quartz standard is located at the inner end of the tunnel and is anchored to a pier consisting of a 10-inch galvanized-steel pipe set 6 feet into the rock and cemented in with concrete. A similar pier near the free end of the standard supports the microscope for measuring secular strains. The fused-quartz standard is 24.08 m in length and is made up of 10-foot sections of milky quartz tubing 6.4 cm in outside diameter by 0.6 cm wall thickness. The sections are cemented end to end with Sauereisen low-expansion ceramic cement with the addition of a wrapping of glass tape saturated with the same cement. Tensile tests of the joints indicated strengths of 750-1000 pounds. The standard is housed within a concrete trough (Fig. 2) that is formed in 5-foot sections and has soft fiber spacers between sections in order to reduce effects resulting from differential expansion of the trough relative to the rocks. The trough is covered with ¾-inch resin-bonded waterproof plywood planks. The

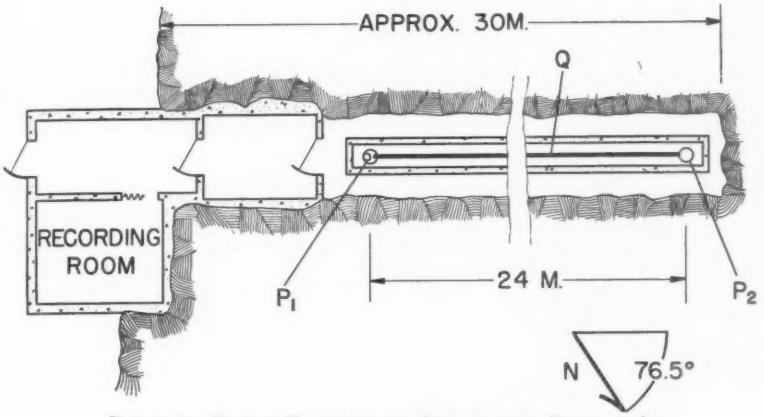

FIGURE 1.—DALTON EXTENSOMETER INSTALLATION (SCHEMATIC)

quartz tube is supported at 5-foot intervals by double slings of stainless-steel wires 0.036 cm in diameter attached to anchor bolts set in the walls of the concrete trough (Fig. 2). The low friction and hysteresis introduced by the wire supports can be demonstrated by freeing the fixed end of the quartz standard. In this condition it oscillates as a pendulum and when started with 1–2 cm amplitude continues to oscillate for several hours. A small constant flow of air for maintaining the relative humidity within the tunnel below the saturation point enters the tunnel at the rear through a 6-inch metal conduit connected to a blower located in the entrance cubicle.

Measuring Microscope

For measurements of secular-strain increments, the position of an accurately ruled glass scale attached to the end of the quartz tube is read in a measuring microscope mounted on a heavy stainless-steel pedestal anchored to the pier (Fig. 3). The glass scale (A) is illuminated from below by a small incandescent lamp (S). The scale is ruled with lines spaced 0.01 mm apart. A cross hair in the microscope eyepiece is used as a fiducial line, and the position of the numbered lines of the scale can be estimated to tenths of their interval or 0.001 mm. Since the length of the quartz standard is 24.08 m, the least detectable strain increment with the microscope is 4.15×10^{-9}.

Photographic Recording System

Originally the Dalton installation was provided with a mechanical-optical magnification

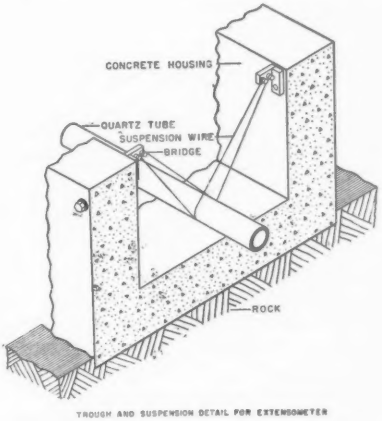

FIGURE 2.—CONCRETE TROUGH AND DOUBLE SLING-WIRE SUPPORTS OF QUARTZ STANDARD

assembly with photographic recording. The magnifier (Fig. 4) used the bifilar bowstring principle. The bowstrings are made of stainless-steel wire 0.0025 cm in diameter and 20 cm long. A small mirror is attached to the two strings at their centers. Movement of the end of the quartz tube relative to the pier tightens one string and loosens the other and thus rotates the mirror. If b is the separation between the end points of either string, a is the vertical depression of the strings at the mirror, and d is their separation, the magnification is given by $V = bL/ad$, where L is the distance from the mirror lens to the recording drum. The remaining constants of the bowstring structure were chosen to produce a magnification V of approxi-

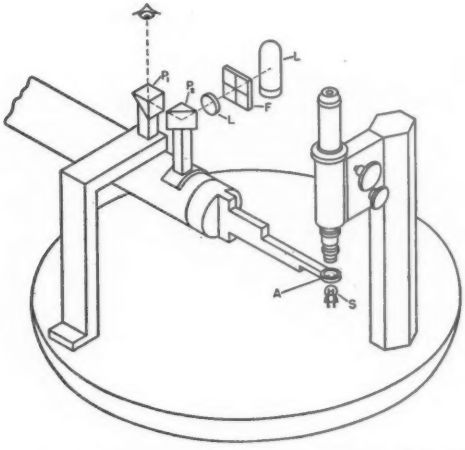

FIGURE 3.—MEASURING MICROSCOPE AND INTERFEROMETER CALIBRATION ASSEMBLY (SCHEMATIC)

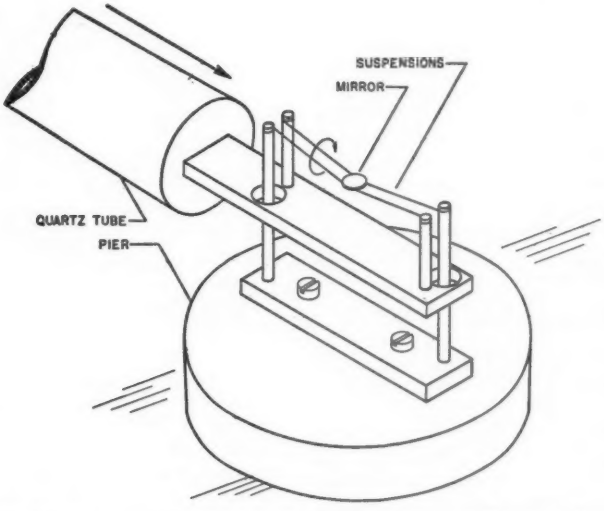

FIGURE 4.—DOUBLE BOWSTRING OPTICAL MAGNIFIER (SCHEMATIC)
The suspension system is damped electromagnetically by immersion in the field of a permanent magnet not shown in the drawing.

mately 10,000. Since the quartz-tube length is 24.08 m, this value of magnification gives a trace amplitude of 1 mm for a strain of 4.15×10^{-9}. The trace-recording speed was 1 cm per hour.

Ink-Writing Recording System

During several years of operation the bowstring recorder operated fairly well. However, rather frequent adjustments were required, and the sensitivity was found insufficient for best recording of tidal strains and seismic waves. Accordingly a new electrical recording system with ink writing was developed. The recorder derives its actuating power from a 5-megacycle/second carrier-current capacitance-bridge transducer, modified from an original assembly designed for pendulum seismographs (Benioff, 1955). The capacitance bridge is formed by two

insulated plates anchored to the adjacent pier or to the trough and a third grounded plate mounted between the fixed plates and attached to the quartz tube near its end. Two forms of attachment of the grounded plate to the quartz tube have been used. In one the attachment is direct (Fig. 5). In the other, the plate is mounted on the end of a cantilever beam which is anchored to the base plate of the transducer to serve as a magnifying lever. A narrow thin-section compliance introduced near the fixed end of the beam serves to concentrate the bending in the compliance. A small spherical member attached to the quartz tube presses against a flat on the beam near the fixed end. Motion of the quartz tube relative to the pier is thus magnified 10 times at the end of the lever where the grounded plate is fastened. In either the direct or the lever type the two capacitances formed between the grounded plate, F (Fig. 6), and the insulated plates, P, P, are shunted by two equal inductances, L_1, to produce two resonant circuits. These are loosely coupled to a 5-mc crystal-controlled oscillator. When the grounded plate is positioned midway between the plates, the two circuits are resonant at a common frequency which differs from the oscillator frequency sufficiently to reduce the currents to approximately 0.8 of their resonant value. When the grounded plate is in the mid-position the currents are equal. Movement of the fixed plates relative to the grounded plate produced by change in the strain of the ground between the two piers varies the two capacitances oppositely and makes one circuit more nearly resonant with the oscillator and the other less so. The resulting unbalance in the magnitude of the currents flowing in the two circuits is proportional to the displacement of the end of the quartz standard relative to the adjacent pier. In the Isabella installation the oscillator is driven by a vacuum tube. The Dalton oscillator is driven by transistors. In the vacuum-tube type, sufficient power circulates in the resonant circuits to operate directly an Esterline-Angus 0–5-milliampere ink-writing recorder, RG, from the rectified current output of two germanium diodes (D) connected to low impedance taps on the inductances (Fig. 6).

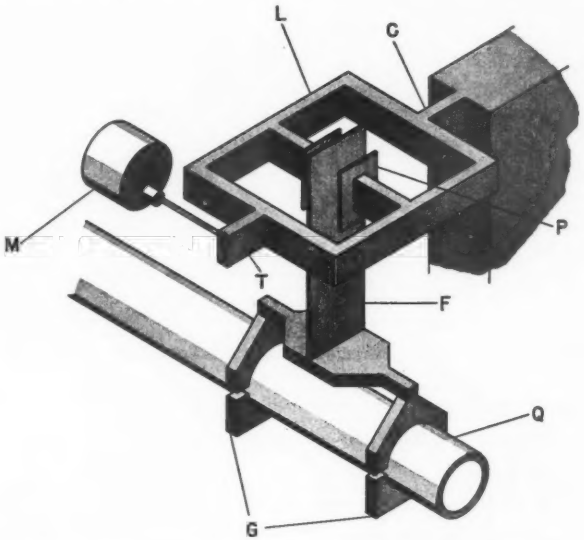

FIGURE 5.—CAPACITANCE-BRIDGE TRANSDUCER (SCHEMATIC)

With a transistor oscillator the circulating power in the resonant circuits is insufficient to provide enough output power from the diodes directly, and a circuit modification (Fig. 7) developed by J. L. Blayney of the Seismological Laboratory staff serves to increase the available output power. In this adaptation the full resonant circuit voltages are applied to the diodes, and their rectified output voltages serve to drive a pair of double push-pull transistor cathode followers which in turn supply sufficient output to drive an Esterline-Angus 0–1 milliampere recorder. The low power consump-

tion of the transistor-operated recorder permits the use of two dry batteries, with voltages 6 and 4 respectively, for the power source. One set lasts more than 3 months on continuous service.

deflection from going off scale. If M is the recorder magnification and L is the length of the quartz standard in millimeters, the strain sensitivity is given by $S = LM$, where S is the

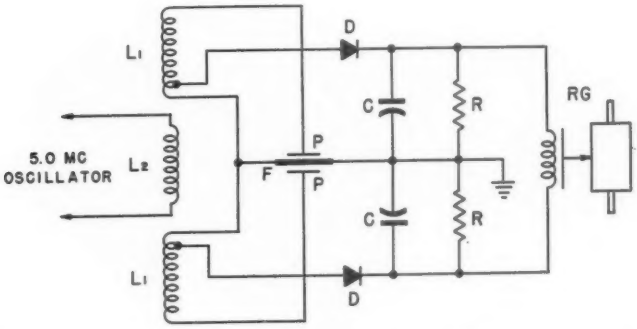

FIGURE 6.—TRANSDUCER CIRCUIT USED WITH TUBE-DRIVEN OSCILLATOR

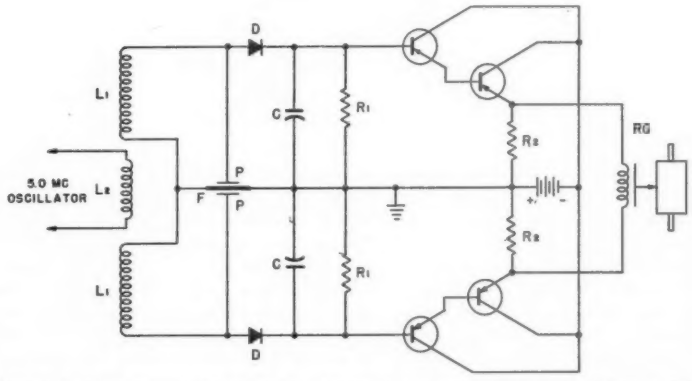

FIGURE 7.—SIMPLIFIED TRANSDUCER CIRCUIT USED WITH TRANSISTOR-DRIVEN OSCILLATOR

The insulated plates of the transducer are individually adjustable for fixing the capacitor air gaps and are arranged for common movement by means of a reversible motor and gear train (Fig. 5, M). The transducer can thus be balanced remotely by operation of push buttons situated near the recorder. The transducer assembly is housed in a hermetic enclosure sealed to the moving member by a ring of silicone grease which also serves to damp transverse vibrations of the quartz tube.

The available magnification of the recording system with either the tube or the transistor oscillator is more than 100,000. In routine operation the magnification is limited to about 80,000 to prevent the maximum tidal-strain

recorder deflection in millimeters for unit ground strain. For the Dalton extensometer the sensitivity is thus

$$S = 8 \times 10^4 \times 2.41 \times 10^4 = 1.93 \times 10^9.$$

A 1-mm deflection on the recorder corresponds to an earth strain of 5.18×10^{-10} or approximately 1 mm in 2000 km or $\frac{1}{16}$ inch in 2000 miles.

Calibration

Calibration of the extensometer is effected by compressing the quartz tube a known amount using two standard helical springs stretched a predetermined distance by a motor-driven cam.

The amount of the compression is calculated by substitution of a pair of stronger springs in the cam mechanism for producing a compression large enough to be read in the secular-strain microscope. The ratio of the force constants of the two sets of springs is determined in the laboratory, so that the compression produced by the weaker springs is easily determined. The recorded deflections thus produced serve as secondary calibration standards as well as time marks.

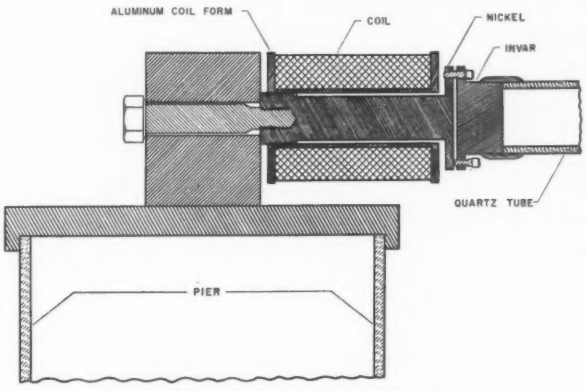

FIGURE 8.—MAGNETOSTRICTION CALIBRATION UNIT

An improved calibration method now being developed uses a 6-inch section of nickel bar interposed between the fixed end of the quartz standard and the adjacent pier (Fig. 8). The nickel bar is surrounded with a coil of wire. Current in the coil produces a shortening of the nickel bar owing to magnetostriction. The corresponding movement of the end of the quartz tube is measured with a Fabry-Perot interferometer. Interference takes place in the space between the two parallel faces of two prisms (P_1 and P_2) attached to the pier and to the quartz tube respectively (Fig. 3). Light from the mercury vapor lamp (L) passes through a filter (F) with an attached reticle which serves as a fiducial line. It then passes through a lens (L) which images the source at infinity. The fringes are observed from above. The construction details of the magnetostriction interferometer calibration assembly were worked out by J. L. Blayney of the Seismological Laboratory staff.

In addition to its use in calibration, the magnetostriction unit serves to provide time marks on the recording line. These are made by clock contacts which close for 1–2 minutes at 6-hour intervals and supply current to the magnetostriction coil from a local dry battery.

ISABELLA EXTENSOMETER

Location and Description of Tunnel

The effectiveness of the Dalton installation established the desirability of building additional units eventually to include a network of such stations over the State of California and over other regions of the earth in which seismic, tectonic, or tidal strains are studied. An excellent tunnel was found in the southern part of the Sierra Nevada in the vicinity of the Isabella dam ($\lambda = 118° 28.39'$ W., $\phi = 35° 39.78'$ N., $h = 835$ m) on land controlled by the U. S. Army Corps of Engineers. It was originally a gold mine but has since been abandoned. Its existence and availability were indicated to the writer by Mr. Harold Cate, resident engineer of the Army Corps of Engineers at Isabella. Negotiations for permission to construct the extensometer were carried out by Mr. C. P. Holridge, also of the Corps of Engineers. The tunnel is 600 feet long and is bored in granite. Because of the greater penetration within the mountain compared with the Dalton tunnel, this site provides a lower noise level.

The installation was completed with funds given by the Donors of the Seismological Laboratory of the California Institute of Technology. The quartz standard is situated about 100 m from the entrance. The recording room is large enough to accommodate a number of experimental pendulum seismographs in addition to the strain recorder.

Galvanometer Recorder for Seismic Waves

The strain produced by plane progressive seismic waves is proportional to the ground-particle vibration velocity. Hence for waves of constant energy the recorded amplitude is the same for all periods. If the waves have constant ground-particle displacements, they are recorded with amplitudes which decrease as $1/T$ where T is the wave period. Observations have shown that in earthquake waves the ground-particle velocity generally decreases with increasing period for periods greater than about 60 seconds. For these longer-period waves, therefore, a recorder in which the pen deflection is proportional to the ground displacement permits the long-period waves to be more clearly distinguished from the background of short-period waves. Accordingly an additional recorder having such characteristics was installed at Isabella. A high-impedance resistance-capacitance differentiating network (Fig. 9) is shunted across the transducer output. The output voltage of the network is thus proportional to the ground-particle acceleration. It is applied to the terminals of a 10-minute-period recording galvanometer, designed by Francis Lehner, in accordance with specifications dictated by the differentiation network. Since a galvanometer is a double integrator for periods shorter than its own period, recordings made with this combination are proportional to ground-particle displacements up to wave periods of 10 minutes, where the amplitude falls to half value. A portion of the recording of the great Mongolian earthquake of December, 4 1957 (45° N., 101.5° E., M = 8+, Δ = 10,700 Km), made at Isabella with this combination is reproduced in Figure 10. The direct-strain recording from the Esterline-Angus recorder of the same instrument is shown in Figure 11. Since the time constant of the differentiating network is only 4 seconds, the response of the network-galvanometer combination to tidal strains is negligibly small. This combination is useful for long-period waves of intermediate range, roughly 30 seconds to 10 minutes. For the ultra long-period waves ranging into hours the unmodified direct tidal-strain recorder is greatly superior.

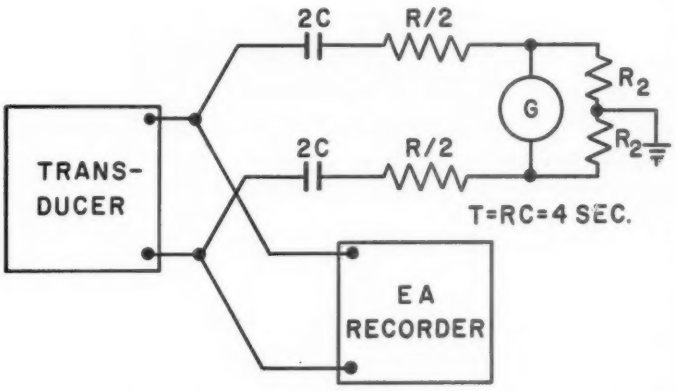

FIGURE 9.—TRANSDUCER OUTPUT CIRCUIT SHOWING CONNECTION TO ESTERLINE-ANGUS RECORDER AND DIFFERENTIATING CIRCUIT FOR GALVANOMETER RECORDER G
R_2, R_2 are high-resistance leaks for draining off electrostatic charges.

NOISE CONSIDERATIONS

Definitions

The recorded unrest not due to seismic waves, tectonic-strain increments, or tidal forces is here termed noise. The limit of useful sensitivity within a given frequency band is determined by the noise level in that band. Since this useful limit appears to be reached in the Dalton and Isabella extensometers, a consideration of the characteristics of the several known sources of noise should provide the clues to the design of instruments of higher sensitivity and greater precision.

Temperature Variations of the Quartz Standard

These include the annual temperature cycle of the tunnel as well as shorter-period fluctu-

FIGURE 10.—PORTION OF ISABELLA SEISMOGRAM OF THE GREAT MONGOLIAN EARTHQUAKE OF 1957 DECEMBER 4 WRITTEN WITH GALVANOMETER OF 10-MINUTES PERIOD

S and SS are the direct and once surface-reflected shear waves. G_1 is the first G wave—a horizontally polarized surface shear wave. R_1 is the first Rayleigh wave arrival.

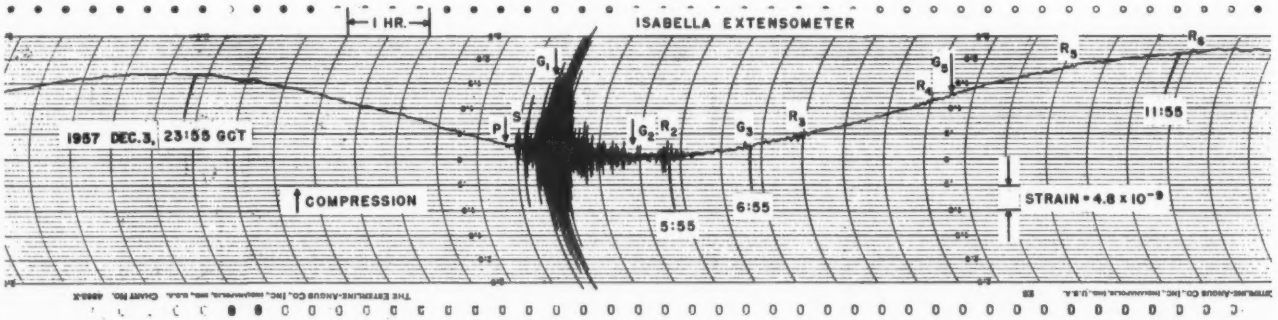

FIGURE 11.—ISABELLA STRAIN RECORDING FOR 1957 DECEMBER 3–4 SHOWING TIDAL-STRAIN VARIATION AND WAVES FROM THE MONGOLIAN EARTHQUAKE OF DECEMBER 4

P and S are the direct longitudinal and transverse body waves. G_1 is the first G wave. G_2 is the first G wave travelling over the long arc to Isabella. R_2 is the first Rayleigh wave travelling over the long arc. G_3 is the G_1 wave after travelling an additional circuit about the earth. The remaining numbered Rayleigh and G waves have travelled two and three times around the earth.

ations arising from variations in the circulating air temperature and presence of operating personnel. The annual cycle can be reduced sufficiently by location of the tunnel at sufficient depth within the ground. The expansion coefficient of fused quartz is approximately 5×10^{-7} per degree centigrade. If the annual cycle is reduced to 0.01°C. amplitude, the corresponding noise level due to this source is 5×10^{-9}. This is already considerably above the operating level of the present instruments. However, since this noise occurs in a very narrow frequency range, far removed from that of seismic waves and tidal strains, its effect in the study of these phenomena can be eliminated satisfactorily with the use of filter-type devices, and in most cases even these are unnecessary owing to the slowness of the temperature cycle. Although it falls within the range of secular tectonic strains its adverse effect in this range also is reduced, owing to the narrowness of its band width (*i.e.*, it is nearly sinusoidal in form). Furthermore, temperature measurements within the tunnel provide corrections to the recorder readings sufficient to reduce this effect by a factor of 10 or more. Thus if limited by the annual temperature cycle of the quartz standard only, tectonic strains of very small magnitude can measured. The quartz tube is wrapped with a layer of glass wool which, together with the trough enclosure, reduces the short-period temperature fluctuations to negligible amplitudes.

Strains Induced at Depth by Temperature Variations of the Surface Layer of the Ground

Even though temperature variations of the rock at the depth of the instrument are negligibly small, relatively large strains can nevertheless be induced there by temperature variations of the surface layers. This may be illustrated by reference to Figure 12 which is a schematic sectional representation of an extensometer installation located in a tunnel within a mountain. We assume that temperature variations of the rock surrounding the extensometer are negligibly small. The outermost 10-cm layer of rock at the surface may exhibit annual variations of 10°C. or more. Letting the solid line represent the surface at some mean temperature, the dashed line represents its position at maximum temperature. The whole triangular section is enlarged by the surface-layer expansion so that a substantial dilatation of the rock is elastically induced in the vicinity of the extensometer. Moreover, the surface layers are subject to relatively large diurnal and shorter-period temperature variations also, and these fall within the period ranges of tidal and seismic strains which are recorded with high sensitivity. Owing to its nearness to the surface, the Dalton extensometer tidal recorder shows the short-period strains induced by insolation at the surface. On cloudy days the tidal-strain recording is regular as one would expect, whereas on clear days a sharp discontinuity occurs in the morning at the time the sun's rays first strike the nearly vertical bare eastern rock wall of the canyon. Figure 13 is a reproduction of the Dalton bowstring record for 1957, December 9 and 10. December 9 was cloudy and December 10 was clear. The sharp discontinuity at 8:08 on the 10th and subsequent distortion represent the induced strain at depth resulting from the surface heating. The abruptness of the discontinuity is evidence for the shallowness of the heated layer. At the Isabella installation where the quartz standard is situated 100 m in from the surface, the effect of surface heating by the sun is not discernible on the tidal records. It may contribute to the noise on the higher magnification seismic-wave recorder. These observations show that in order to effect a maximum reduction of surface-generated noise, the extensometer must be located as far as possible from the surface, and probably the site must be in level country since, if the surface is horizontal, surface-temperature variations produce stress variations at depth but little or no strain increments.

Noise Generated by Barometric Variations

Barometric fluctuations produce changes in the length of the quartz standard and changes in the dimensions of the rock mass. The effects of these changes on the recording system are opposite in sign so that if they are equal in magnitude, no noise is produced. The response of the quartz standard itself is easily computed. Let P be the magnitude of the pressure change in dynes/cm^2 and k be the bulk modulus. Then the strain increment in the standard is $\sigma = P/3k$. The strain increment in the rock depends upon the geometry of the mountain as well as its bulk modulus and is not readily computed. In general, the two responses are unequal, and consequently a barometric noise proportional to their difference appears in the recording. It should be possible to introduce a barometric compensation mechanism into the recording system for reducing the barometric noise, and work is in progress on such a device.

Wind Noise

Another source of noise is wind blowing over the ground surface. At Isabella wind noise is discernible on the strain record whenever the velocity exceeds about 20 miles per hour. Reduction of this type of noise can be effected by locating the vault in smooth level country as far as possible from the surface.

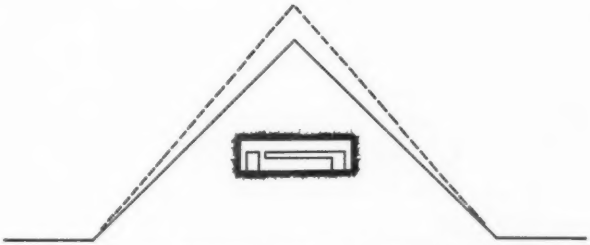

FIGURE 12.—EFFECT OF THERMAL EXPANSION OF SURFACE LAYERS OF GROUND ON EXTENSOMETER MOUNTED WITHIN A MOUNTAIN

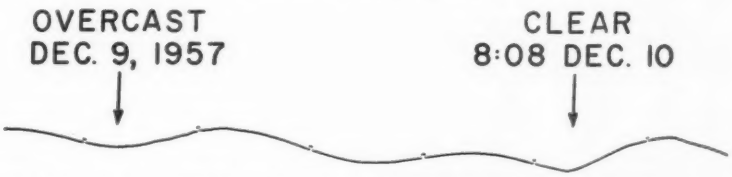

FIGURE 13.—DALTON BOWSTRING TIDAL RECORDING SHOWING ELASTIC STRAIN DISCONTINUITY INDUCED AT DEPTH FROM SURFACE HEATING OF THIN LAYER BY MORNING SUNLIGHT

Ground-Water Noise

Noise produced by changes in the ground-water content of the surface layers also produces strain variations. Thus at the Dalton site a heavy rain following a long dry season is accompanied by a rapid dilatation of the ground. This was at first attributed to the rise in level of water impounded back of the dam. However, when the valves of the dam were opened later and the level of the water fell rapidly, the strain recovery represented only a small portion of the original increment which was therefore caused principally by water held in the interstices of the surface rock and soil. Location of the vault in level country would reduce the noise generated by variations in ground water somewhat, although the reduction would be limited by local variations of porosity.

INITIAL OBSERVATIONAL DATA

Dalton Secular-Strain Measurements

A plot of the Dalton secular-strain measurements to date is shown in Figure 14. The elevation of the water in the reservoir and the average temperature reading of three thermometers situated at the two ends and middle of the trough are also indicated.

Following completion of the installation in November 1953, equilibrium conditions in temperature and strain were not reached for several months until about July 1, 1954. During this interval, the time of minimum of the annual temperature cycle changed from about January 1 in 1954 to about March 1 in 1955. The secular-strain curve is less regular than the temperature curve although the points scatter less. It exhibits a rather rough annual cycle, with the phase of dilatation maximum approximately coinciding in time with the temperature minimum. The temperature range from maximum to minimum is approximately 1.1°C. The corresponding range in strain is about 2.2×10^{-6} or approximately four times the variation produced by the thermal expansion of the quartz standard. This increase must be due to expansion of the rock. Moreover, the phase of the strain does not correspond to the phase of the tunnel temperature. It must, therefore, be induced by a temperature cycle in rock at some distance (presumably shallower) from the quartz standard. The lack of phase correspondence is particularly notable in the first 6 months of operation.

The strain-noise level in an annual period is roughly 1×10^{-6}. This, therefore, represents the precision limit for measurements of secular-

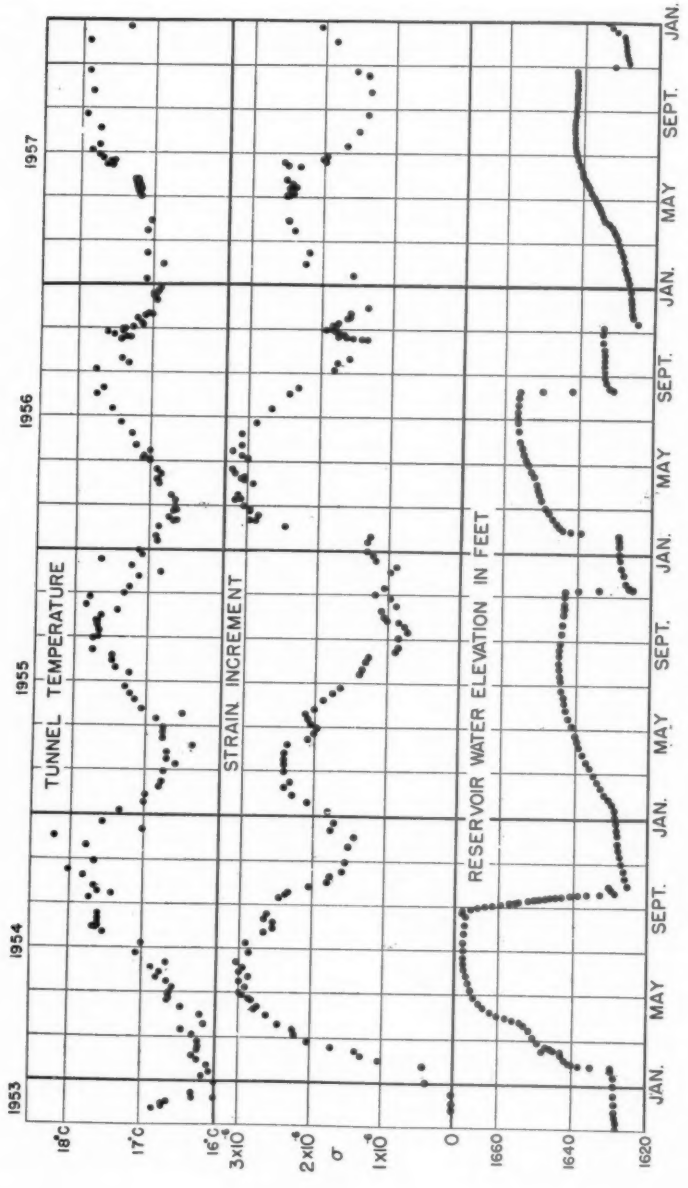

FIGURE 14.—PLOT OF DALTON SECULAR-STRAIN MEASUREMENTS

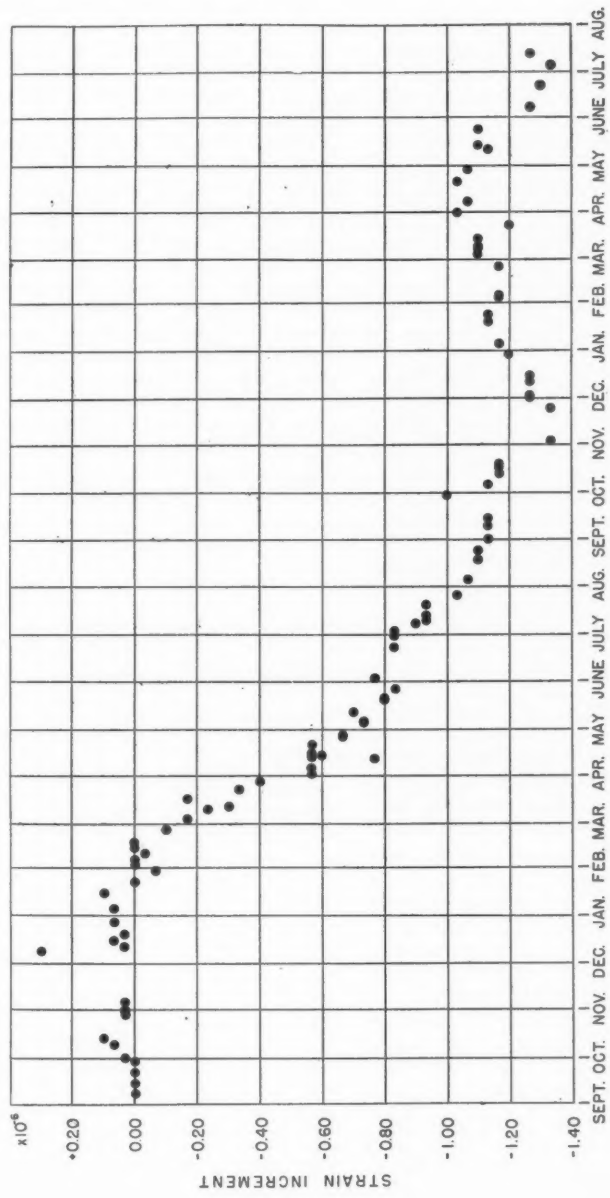

FIGURE 15.—PLOT OF ISABELLA SECULAR-STRAIN MEASUREMENTS

strain increments measured annually. Accumulation of smaller annual increments would be discernible if measured over a number of years. Since a strain increment of 1×10^{-6} represents about 1 per cent of the earthquake-generating strain increment in the vicinity of the source, measurements with this instrument are significant only for sources that are fairly close—about 20–30 km. Installations with lower secular-noise levels are, therefore, highly desirable for secular-strain recording. In this regard, the Isabella extensometer appears to offer a substantial improvement principally because the instrument is located at a much greater distance from the surface.

Isabella Secular-Strain Measurements

A plot of the observed Isabella secular-strain increments in parts per million is shown in Figure 15. The greater regularity and much smaller annual effect of this curve as compared with the Dalton readings demonstrates the advantage of a deep location within the mountain for the quartz standard. The duration of observations at this site is insufficient to allow generalizations concerning the progress of secular strain. The strain variation from January 1957 to January 1958 was very nearly 1 part per million, with no substantial subsequent recovery.

Tidal Strains and Earthquake-Wave Strains

Tidal strains are well recorded at both the Dalton and Isabella sites, although disturbances resulting from surface temperature variations are clearly seen on the Dalton records. The recording reproduced in Figure 11 is typical. As a result of secular-strain variations, the tidal recorded line slowly drifts toward one or the other edge of the chart. It is recentered by means of the push-button control of the adjusting motor and gear train (Fig. 5). Eventually the recentering will be accomplished automatically.

Although the tidal recorder is well adapted to recording seismic waves with very long periods ranging from about 10 minutes to several hours, no earthquake has occurred since the instrument has been in operation in which such waves have been generated. The last earthquake exhibiting these waves was the Kamchatka shock of 1952 November 4. Although it is generally believed that the very long-period waves are produced by great earthquakes only, size is not the sole condition of their generation, since in the years since 1952 several shocks of equal or greater size than the Kamchatka earthquake have occurred without the appearance of the waves. Differences in the earthquake-generating mechanism must also be involved.

References Cited

Benioff, Hugo, 1935, A linear strain seismograph: Seismol. Soc. America Bull., v. 25, p. 283–309

—— 1955, Earthquake seismographs and associated instruments, p. 219–275 *in* Landsberg, H. E., *Editor*, Advances in geophysics, V. 2: N. Y., Academic Press, Inc., 286 p.

Seismological Laboratory, California Institute of Technology, 220 N. San Rafael Ave., Pasadena, Calif.

Manuscript Received by the Secretary of the Society, August 18, 1958

Publication of the Division of Geological Sciences. Contribution No. 898

BULLETIN OF THE GEOLOGICAL SOCIETY OF AMERICA
VOL. 70, PP. 1033–1046, 5 FIGS. AUGUST 1959

HISTORY OF IMURUK LAKE, SEWARD PENINSULA, ALASKA

BY DAVID M. HOPKINS

ABSTRACT

A study of Imuruk Lake, a large, shallow lake in north-central Seward Peninsula, Alaska, illuminates the climatic history of northwestern Alaska and the tectonic history of central Seward Peninsula during Pleistocene and Recent time. Special interest attaches to the older lake sediments, because they contain evidence concerning the climate, fauna, and flora that existed in the vicinity of Bering Strait at a time when the Bering land bridge was open and when animal and plant populations were being exchanged between the eastern and western hemispheres.

The lake is 8 miles long and less than 10 feet deep; bottom sediments consisting of reworked wind-blown silt bury a rolling bedrock topography of much greater relief. Analysis of the hydrologic regime indicates that much of the water draining into the lake is lost by evaporation; smaller quantities are lost by discharge through the outlet, the Kugruk River, and by leakage into the lava flows along the lake shore. Changes in the duration and temperature of the summer ice-free season would result in changes in the amount of water lost by evaporation and thus in appreciable changes in lake level.

Imuruk Lake occupies an initial low area on basaltic lava flows of Quaternary age, but the initial low area has been modified by faulting and now lies in a poorly defined graben. Topographic evidence confirmed by study of lacustrine terraces indicates that until recently Imuruk Lake drained westward into the Noxapaga River instead of eastward into the Kugruk River. A history of repeated warping of the lake basin, on which is superimposed a history of oscillating lake level which is due to changes in climate, is recorded by three systems of abandoned shore-line features found along the shores: a warped shore cliff of probable Illinoian age, a double set of warped terraces of probable Wisconsin age, and a low, horizontal terrace of Recent age. Bones of bison, horse, and mammoth were found in peaty sediments containing many twigs but no large wood; their presence indicates that these mammals, at least, were capable of surviving in a tundra environment during cold stages of the Pleistocene epoch and at a time when the Bering land bridge was in existence nearby.

The sediments filling the deeper parts of the bedrock basin of Imuruk Lake probably contain an uninterrupted pollen record that reflects vegetation changes in central Seward Peninsula beginning in middle Illinoian time and terminating a few thousand years ago. Core drilling and pollen analysis of these sediments would greatly amplify our understanding of late Pleistocene events in the vicinity of the Bering land bridge.

CONTENTS

TEXT

	Page
Introduction	1034
Acknowledgments	1036
Geographic setting	1036
Topography and drainage	1036
Geology	1037
Vegetation and climate	1039
Present-day lake	1039
Topography and sediments	1039
Annual regime	1039
Sedimentation	1040
Effect of evaporation upon lake level	1040
Terraces and raised beaches	1040
General statement	1040
High, tilted wave-cut scarp	1041
Description	1041
Age and significance	1041
Intermediate terraces	1041
Topographic expression	1041
Terrace sediments	1041
Fossils	1042
Age and significance	1043
Low terraces	1044
Description	1044
Age and significance	1044
Summary of the history of Imuruk Lake	1044
Significance for the history of the Bering Strait region	1045
References cited	1045

ILLUSTRATIONS

Figure		Page
1.	Index map of Seward Peninsula	1034
2.	Topography and fault pattern of the drainage basin of Imuruk Lake and of the upper valley of the Noxapaga River	1035
3.	Valley of the Noxapaga River north of Lava Lake	1037
4.	Profiles through shore-line features of Imuruk Lake	1038
5.	Former shore lines of Imuruk Lake	1042

Introduction

Imuruk Lake, a large shallow lake in north-central Seward Peninsula (Fig. 1), lies near the center of the migration route through which Imuruk Lake was used from 1907 until about 1930 to augment the supply available for placer mining at the junction of the Pinnell and Inmachuk rivers. For this purpose the

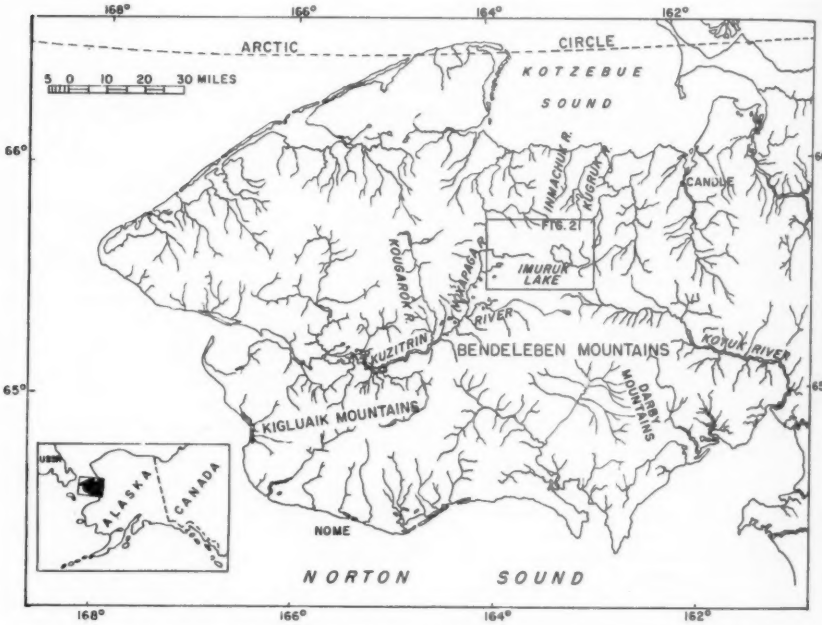

FIGURE 1.—INDEX MAP OF SEWARD PENINSULA SHOWING LOCATION OF FIGURE 2

plant, animal, and human populations have moved between the old and new worlds via the Bering land bridge. The lake is adjoined by a series of terraces that record local tectonic events and regional climatic episodes during late Quaternary time, and some of the terrace sediments accumulated during intervals when sea level was low and the land bridge open (Hopkins, 1959). A description of the lake and its ancient sediments thus forms part of the basis for developing a more general Pleistocene stratigraphy and chronology for areas bordering the site of the Bering land bridge.

Imuruk Lake is an irregularly shaped body of fresh water, about 8 miles across, in north-central Seward Peninsula, 100 miles northeast of Nome and 60 miles south of the Arctic Circle. The area surrounding the lake is uninhabited and can be reached by aircraft equipped to land on the lake or by overland travel on foot from the heads of roads in the Kougarok River and Inmachuk River valleys. Water from discharge of the Kugruk River was intermittently diverted at a dam 1100 feet downstream from Imuruk Lake into the Fairhaven Ditch, through which it was conducted 17 miles to the head of the Pinnell River (Fig. 2).

This report is based primarily on investigations incidental to geologic mapping in the Imuruk Lake area in 1947 and 1948, during which repeated traverses were made around the lake shores. Six boat traverses were made across the lake, and 390 soundings were taken; bottom samples were dredged up with an improvised drag sampler at several points on each transect. Henshaw and Parker (1913) record the results of stream gaging on the Kugruk River and the Fairhaven Ditch in 1909 and provide the basis for rough calculations of the hydrologic balance of Imuruk Lake. Most of the drainage basin of Imuruk Lake is shown on the Bendeleben C-3 quadrangle (U. S. Geol. Survey, 1950, 1:63,360).

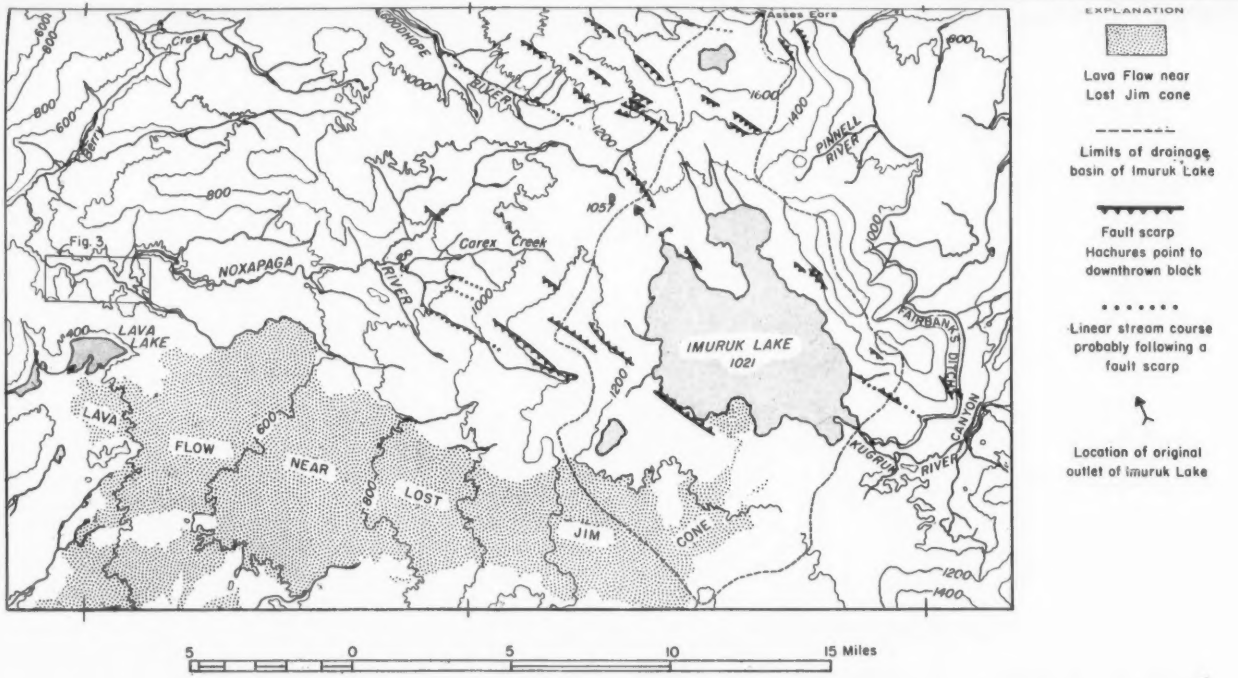

FIGURE 2.—TOPOGRAPHY AND FAULT PATTERN OF THE DRAINAGE BASIN OF IMURUK LAKE AND OF THE UPPER VALLEY OF THE NOXAPAGA RIVER

Contour interval: 100 feet. The lake occupies a primary depression on the lava flows, but the form of the depression has been modified by faulting. Location of Figure 3 shown by box near left margin. (Editor's note: Fairhaven Ditch is incorrectly labeled Fairbanks.)

Acknowledgments

The investigations reported here are a part of the permafrost program of the U. S. Geological Survey; field work was financed in part by the Office of the Chief of Engineers, United States Army. The writer was assisted at Imuruk Lake by E. H. Muller, A. T. Fernald, and J. F. Seitz, geologists; R. F. Sigafoos, botanist; and J. G. Sieh and W. B. Quay, zoologists. The manuscript was critically read by R. P. Goldthwaite, Clyde Wahrhaftig, and A. L. Washburn, who offered many helpful comments.

Geographic Setting

Topography and Drainage

Imuruk Lake receives drainage from an area of about 110 square miles extending from the Asses Ears, 6½ miles north of the north shore, to the northeastern part of the Lost Jim lava flow, about 4 miles south of the south shore (Fig. 2). Drainage divides east and west of the lake lie within 1 or 2 miles of the shore. Freewater surfaces constitute more than a quarter of the drainage basin; Imuruk Lake occupies approximately 27 square miles, and smaller lakes constitute an area of about 2 square miles.

Altitudes in the drainage area range from 1021 feet on the surface of Imuruk Lake to 2055 feet on a hill summit near the Asses Ears. Much of the drainage divide is formed by hill crests standing 200–1000 feet above Imuruk Lake, but long segments of the divide extend along interfluves between swales on otherwise featureless slopes, across swampy valleys, and through small lakes that drain in two directions. A lowland extending 3 miles northwestward from the northwest corner of Imuruk Lake rises about 60 feet above present lake level; Imuruk Lake once drained through this lowland into a tributary of the Noxapaga River.

A study of deformed lake terraces along the northern and western shores of Imuruk Lake strongly suggests that the present outlet through the Kugruk River has developed relatively recently and that throughout most of its history the lake drained westward into the Noxapaga River. The evidence of the terraces is strongly supported by the youthful appearance of the Kugruk River Valley above Kugruk Canyon, and by the underfit appearance of the segment of the Noxapaga River between Carex Creek and Berry Creek (Fig. 3).

The lake is drained at present by the Kugruk River, a swift, narrow stream that has a summer discharge of generally less than 60 cubic feet per second at the outlet. The course of the Kugruk River from Imuruk Lake to Kugruk Canyon, 4½ miles downstream, lies in a wide, irregular valley that appears to represent primary relief on the surface of lava flows, modified only slightly by the work of the river.

Throughout most of this reach, the river is confined between banks 1–3 feet high, and the channel is choked with subangular boulders of basalt up to 10 feet across. About halfway between Imuruk Lake and Kugruk Canyon, the swift, steep course is interrupted by a reach in which the river flows through a lake about 1000 feet in diameter. The stream enters the Kugruk Canyon in a series of precipitous rapids entrenched slightly into the west wall. The canyon appears to have been carved by a smaller tributary entering from the south.

The river lacks a flood plain in most places, and no stream terraces are seen upstream from Kugruk Canyon. The valley is so shallow near Imuruk Lake, however, that the width of the channel would increase to several hundred feet if lake level rose as much as 10 feet. General appearances suggest that the upper Kugruk River has occupied its valley for only a short time and that it has neither deepened nor aggraded its valley appreciably.

The original outlet of Imuruk Lake was through a low swampy area extending 3 miles northwestward from the northwest corner of the lake. The outflow drained through an unnamed northern tributary to Carex Creek and entered the Noxapaga River about 10 miles below the former outlet (Fig. 2).

From the mouth of Carex Creek to the mouth of Berry Creek, 17½ miles farther downstream, the Noxapaga River flows within but does not fill a meandering channel that must have been carved by an ancient stream that had much greater discharge. The Noxapaga River in this segment flows in deep, winding, lakelike reaches, without perceptible current, that are connected by narrow, shallow reaches of swift current (Fig. 3). The lakelike reaches occupy the width of the ancient channel, but the water surface at normal discharge is 10 or 15 feet below the tops of confining banks of flood-plain silt. The swift reaches occupy only part of the width of the ancient channel and have developed incipient secondary meanders that have about half of the radius of the larger meanders of the ancient channel in which the stream is confined. Low terraces extending

ong most of the segment from Carex Creek to Berry Creek appear to have been the flood plain of the Noxapaga River when the ancient channel was fully occupied.

A lava flow of late Wisconsin or Recent age graben involving the basaltic lava flows and older rocks and extending northwestward across the area shown in Figure 2. The graben is bounded on the northeast by a wide swarm of short southward-facing escarpments and linear

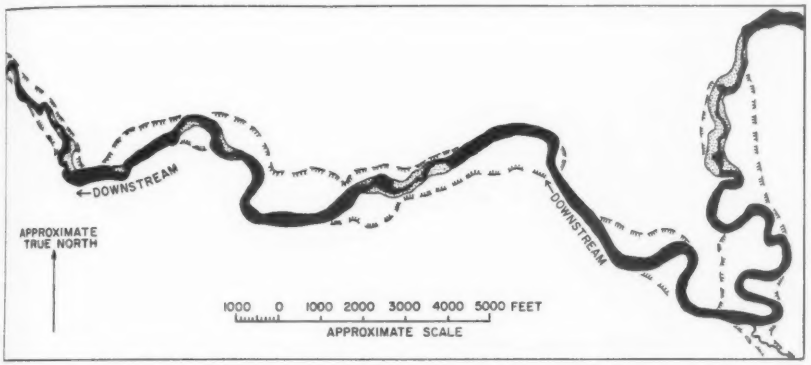

FIGURE 3.—VALLEY OF THE NOXAPAGA RIVER NORTH OF LAVA LAKE

Showing wide lake-like reaches where ancient channel is filled with water and narrow swift reaches where part of ancient channel is now dry (stippled areas). Note the much smaller meanders in the narrow, swift reaches as compared with those in the wide, lake-like reaches. Hachures mark the outer limits of a low terrace that probably was the flood plain when the Noxapaga River carried the outflow from Imuruk Lake and the entire width of the ancient channel was occupied. Muskellunge Creek enters at lower right. Sketched from an aerial photograph. (*See* Fig. 2 for location.)

invaded the Noxapaga Valley at Andesite Creek, about 12 miles below Berry Creek, but does not seem to have played any role in the anomalies of the course between Carex Creek and Berry Creek. Instead, the river seems to be underfit and to be flowing within the channel of a stream that originally carried at least twice the present discharge. The Noxapaga River now drains an area of 145 square miles above the mouth of Berry Creek; 60 square miles of this area is drained by Carex Creek and the Noxapaga River above Carex Creek. If the Noxapaga River received the outflow from Imuruk Lake, its drainage area and presumably its discharge would be nearly doubled above the mouth of Berry Creek and nearly tripled at the mouth of Carex Creek.

Geology

Imuruk Lake occupies a primary depression on the surface of a sequence of basaltic lava flows of middle Pleistocene (probably Illinoian) age (Hopkins, 1955, Ph.D. thesis, Harvard Univ.), but the form and extent of the depression has been modified by faulting during late Pleistocene time. The lake basin now lies in a segment of a complex and vaguely defined topographic features (Fig. 2) that apparently are the traces of faults having displacements of a few tens of feet each. A northward-facing scarp 50–100 feet high defines the southwest boundary of the graben and locally forms the southwest shore of the lake. Deformation of the lake terraces indicates that the part of the graben occupied by the lake has been irregularly warped at least twice in late Pleistocene time.

The basaltic lava flows of middle Pleistocene age form most of the lake shores; a lava flow of Recent age forms the Lost Jim Peninsula (Fig. 4); and a hill underlain by quartz monzonite and metamorphic rocks rises from the northeast shore. All the rocks except the youngest lava flow are mantled by wind-blown silt, commonly about 20 feet thick, derived during glacial intervals from outwash plains to the southwest. Fine-grained lake sediments are present in terraces distributed chiefly along the northern and western shores. The detailed outline of the lake has been modified recently in these areas by collapse resulting from the thawing of the perennially frozen terrace sediments. (*See* Hopkins, Karlstrom, and others, 1955, Pl. 31.)

FIGURE 4.—PROFILES THROUGH SHORE-LINE FEATURES OF IMURUK LAKE

Vegetation and Climate

Imuruk Lake lies west of the western limit of spruce on Seward Peninsula, and the hills surrounding the lake are covered by tundra and shrub vegetation of several types (Hopkins and Sigafoos, 1951, p. 63–66, Fig. 18). Spruce forest has extended farther westward, well beyond Imuruk Lake, at several times in the past (Hopkins and Giddings, 1953, p. 25–28), but not during the periods when the terraces of Imuruk Lake were being formed.

The climate, generally similar to the climate at Candle (U. S. Weather Bureau, 1943), is characterized by cool summers and very cold winters. The mean annual temperature is probably about 20° F. The absolute maximum temperature recorded at Candle before 1943 is 85°; the absolute minimum is −60°. Subfreezing temperatures predominate from early October to mid-May. Winters are cold and rather dry. Clear weather predominates, but intense storms, accompanied by high winds and precipitation, are frequent. Storms are less frequent from April until late July. Periods of drizzle and light showers are interspersed during early summer with periods of clear or partly cloudy weather. In late July, frontal passages again become common, and few days pass without at least a trace of precipitation. The air is seldom calm during summer, and winds having an estimated velocity of more than 30 miles per hour are frequent.

The mean annual precipitation recorded at Candle is 7.43 inches, of which about 25 per cent falls as snow; more than 50 per cent of the recorded precipitation occurs during a well-defined rainy season from July through September. The true precipitation at Candle and other stations in northern Seward Peninsula may be much greater than the measured precipitation and of the order of 15 inches.[1] Henshaw and Parker (1913, p. 231) show that the Kugruk River and Fairhaven Ditch discharged the equivalent of about 7 inches of annual runoff in 1907 and 1908, and that at least an equal quantity was removed by evaporation and leakage.

Present-Day Lake

Topography and Sediments

Imuruk Lake is monotonously shallow and flat-bottomed. A basin 9 or 10 feet deep lies between the Gull Islands and Camp Point (Fig. 4); Salix Bay and smaller embayments are nowhere deeper than 6 feet; elsewhere the lake is about 8 feet deep.

Basaltic rubble forms the lake bottom in several areas lying within a few hundred feet of the shore and in areas within a radius of several hundred feet of the Gull Islands. Elsewhere, Imuruk Lake is floored by reworked wind-blown silt. The total thickness of the silt is unknown, but judging from the character of the surrounding terrain, a rolling bedrock surface that has a relief of at least several tens of feet and possibly several hundreds of feet must be buried beneath the flat lake bottom.

Most of the beaches consist of steep planar slopes 5–50 feet wide extending from the bases of shore-line bluffs into the lake. Ice push plays a major role in the detailed sculpture of the beach; features resulting from ice push, including stone pavements, ice-abraded terrace faces, ice-plowed grooves extending perpendicular to the strand, and beach ramparts composed of large blocks heaped as much as 8 feet high line much of the shore. Shore-line features built primarily by waves are rare except in the beaches of quartz-feldspar sand along the northwest shore.

The beaches are composed in most places of discoidal or elliptical pebbles of basalt from half an inch to 3 inches in diameter that form a thin shingle or pavement over bimodal mixtures of rocks and silt. Much of the basaltic gravel is derived from relatively distant shores and has reached its present position by ice rafting. Blocks of basaltic lava 1–6 feet in diameter line much of the south shore, and well-sorted quartz-feldspar sand predominates in beaches along the northwest shore adjoining hills of granite and schist. The heads of sheltered coves and bays are lined by windrows of finely comminuted organic material composed of fresh plant remains and fragments of reworked peat eroded from terrace faces nearby.

Annual Regime

Imuruk Lake is covered with ice more than two-thirds of the year. Ice forms in early October and covers the lake until mid-June; the thickness of ice formed is unknown, but freshwater lakes in this latitude in central Alaska acquire an ice cover about 4 feet thick during a normal winter (Max Brewer, 1956, oral communication).

Most of the winter precipitation remains on the ground in the form of snow until late May;

[1] The difficulties of measuring true precipitation in windy, treeless regions such as Seward Peninsula are discussed by Black (1954).

the snow melt then drains to the lake, raising its level, and frees the ice cover from the shores. Summer precipitation seems to reach the lake with little delay, for lake level responds with considerable sensitivity to periods of rain. During the relatively dry summer of 1947, lake level fell several inches between July 1 and August 8; 3 days of continuous rain from August 9 through August 11 then brought lake level well above the highest previously noted position. During the dry weather, only a few clear streams entered the lake, but after the 3 days of continuous light rain, small, turbid streams entered the lake through every ice-wedge-polygon furrow.

Sedimentation

Nearly all the sediment introduced into the lake consists of silt; the silty sediments are introduced into the lake basin during rainstorms in late summer and perhaps during the period of heavy snow-melt runoff in late May and early June. Alluvial fans of silt are built across gravel or rubble beaches during each summer storm by ephemeral streams draining through ice-wedge-polygon trenches. Waves then move most of the silt into the lake, where it settles when the wind subsides.

Sustained winds of about 30 miles per hour generate waves that stir the bottom of the lake; enough bottom sediments are stirred into suspension to make the surface of the lake a dull red-gray within a few hours after the winds begin. Much of the sediment brought in suspension by the waves probably is carried out of the lake and down the Kugruk River. The frequent redistribution of bottom sediments by waves generated by summer winds probably is the chief factor responsible for the monotonously flat topography of the lake bottom.

Effect of Evaporation upon Lake Level

The intermediate and low terraces at Imuruk Lake apparently record increases in lake level related to climatic changes that are superimposed upon changes in lake level resulting from tilting of the lake basin. An evaluation of climatic and hydrologic factors affecting lake level is important in interpreting the significance of the terraces.

The level of Imuruk Lake is controlled at present by precipitation in and runoff from the drainage basin, outflow through the Kugruk River and Fairhaven Ditch, leakage into lava flows along the shores, and evaporation from free-water surfaces. Not enough data are available to permit a rigorous evaluation of all these factors, but data collected by Henshaw and Parker (1913, p. 231–235) demonstrate that leakage and evaporation are major factors affecting the level of the lake. In three places water from the lake can be seen draining with perceptible current into the basalt rubble lining the shore; the three visible subterranean outlets have a combined discharge of about 2 cubic feet per second.

Henshaw and Parker report that lake level was lowered by 0.85 foot during a 2-month period in 1909. Outflow through the Kugruk River and the Fairhaven Ditch accounted for the removal of 0.31 foot of water, and the remaining 0.54 foot was removed by leakage and evaporation. The three known subterranean outlets would have removed about 0.01–0.02 foot of water at the rate of outflow observed by the writer. The unobserved leakage may have been much greater, but even if it were 10 times as great only 0.1–0.2 foot of water would have been removed by leakage during a 2-month period, and roughly 0.4 foot of water, or nearly half of the total observed reduction in lake level, would remain to be accounted for by evaporation. The total evaporation loss may have been even greater, for Henshaw and Parker neglect the additional water that was contributed to the lake by direct precipitation and by inflow from tributaries during the gaging period. The precipitation was not recorded at Imuruk Lake, but Candle received 2.28 inches or 0.19 foot of precipitation during the gaging period (Henshaw and Parker, 1913, p. 25–26).[5]

Increases or decreases in summer temperatures and in the length of the ice-free season would have profound effects upon annual evaporation losses. Longer or warmer summers should result in a lowering of lake level, and shorter or cooler summers should produce higher lake levels.

Terraces and Raised Beaches

General Statement

Three systems of abandoned shore-line features are found along the shores of Imuruk Lake (Fig. 4). The highest is a wave-cut scarp

[5] The indicated summer evaporation rate of 0.2–0.3 foot per month at Imuruk Lake appears to be reasonable by comparison with the evaporation rates reported for the coldest months at Lake Mead, Nevada: 0.2 to 0.5 foot is lost per month at Lake Mead when mean monthly temperatures are between 45° and 50°F. (Harbeck, Kohler, Koberg, and others, 1958, Tables 18, 19).

without associated sediments. The intermediate and lower systems consist of terraces composed mostly of lacustrine silt and peat. The high, wave-cut scarp has been strongly warped, and the intermediate terraces less intensely warped, evidently as a result of deformation of the floor of the graben in which the lake lies (Fig. 2); the lowest terrace is essentially horizontal.

High, Tilted Wave-Cut Scarp

Description.—The highest set of shore-line features at Imuruk Lake consists of a sinuous wave-cut escarpment extending discontinuously along the north shore from the base of Kettle Dome to the west side of the entrance to Salix Bay (Fig. 4, hachures). The old shore line is cut in lava flows of middle Pleistocene age and in granite and schist. It is expressed in most places by concentrations of rubble along minor nicks in hill slopes elsewhere deeply mantled with wind-blown silt. Solid rock is exposed in escarpments 5–15 feet high in a few places. No associated water-laid sediments were seen, but the scarp's sinuous trace indicates that it is not a fault scarp.

The old shore line stands only 3 or 4 feet above present lake level along the base of Kettle Dome (Fig. 4 *B*). It rises steeply northwestward, however, to a height of 30 feet above present lake level east of the center of Granite Bay (Fig. 4 *A*). It stands between 30 and 40 feet above present lake level wherever it can be identified farther west.

Age and significance.—The high, tilted wave-cut scarp is believed to have represented the margin of Imuruk Lake until, and perhaps beyond, the end of the time of the Nome River glaciation (Illinoian)[3]. The lake evidently originated during the Nome River glaciation, for it is confined by lava flows that are contemporaneous with part of the Nome River glaciation (Hopkins, 1955, Ph.D. thesis, Harvard Univ.). The high tilted wave-cut scarp is the oldest recognized shore-line feature, and it is evidently contemporaneous with or younger than the principal period during which wind-blown silt accumulated, for rubble along the old shore line lacks a thick mantle of silt, though bedrock on adjoining slopes is deeply buried.

The height of the old shore line on Salix Peninsula indicates that Imuruk Lake probably drained to the Noxapaga River through the low pass at the northwest corner of the lake during the period when the high wave-cut scarp was being carved. The high shore line evidently was abandoned as a consequence of uplift of the northern part of the lake basin, which reached maximum intensity in the vicinity of Salix Peninsula and Salix Bay (Fig. 5).

Intermediate Terraces

Topographic expression.—Terraces representing two intermediate systems of shore-line features are found discontinuously along the west, north, and northeast shores of Imuruk Lake from 1½ miles south of Camp Point to 1 mile southeast of Granite Bay; a comparable terrace is found on the largest of the Gull Islands. The terraces stand 5–20 feet above present lake level and reach maximum height along the east shore of Salix Bay. In most places the terraces are less than 100 feet wide normal to the lake shore; their surfaces commonly slope lakeward at angles of 1°–5°. Wider horizontal terraces underlie areas of about 1 square mile southwest of Camp Point and northwest of Granite Bay. The easternmost and largest of the Gull Islands is surmounted by a terrace remnant about 600 feet long and 100 feet wide; the surface slopes uniformly from an elevation of 9 feet at the northwest end to 6 feet at the southeast end.

The gently sloping surface extending 3 miles northwestward from the northwest corner of the lake to the headwaters of the Noxapaga River and reaching a height of about 60 feet above present lake level is thought to represent the bottom of a former shallow bay occupied by the lake when the intermediate terraces were being formed (Fig. 5).

The only erosional feature clearly associated with the intermediate terraces is a platform 8 feet above present lake level beveled across the frost-rived rubble of a lava flow and adjoined at its inner edge by an escarpment 6 feet high (Fig. 4 *C*). The platform is surmounted by a ridge, possibly an ancient ice rampart, of beach gravel 2 feet high.

The two groups of intermediate terraces can be distinguished from one another with certainty only in the vicinity of Granite Bay and along the southeast shore of Salix Bay, where they are separated by a vertical interval of about 10 feet, but both groups are probably represented elsewhere around the perimeter of the lake.

Terrace sediments.—The terrace deposits are composed of inorganic sediments as much as 9 feet thick overlain by 2–16 feet of detrital peat. The higher of the two groups of intermediate

[3] The glacial chronology of Seward Peninsula is summarized by Péwé and others (1953, p. 10–11).

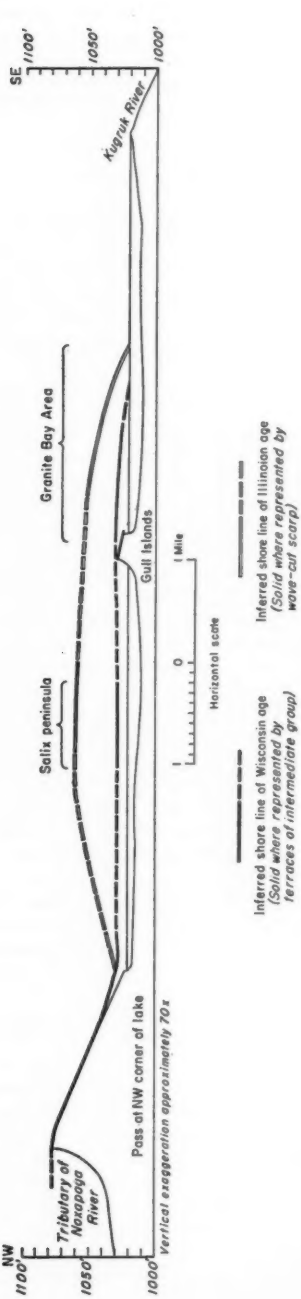

FIGURE 5.—FORMER SHORE LINES OF IMURUK LAKE

Projected to a northwest-southeast cross section from the former outlet to the Noxapaga River to the present outlet to the Kugruk River (Fig. 4).

terraces is generally capped by a layer of volcanic ash half a foot to 2 feet thick. The surfaces of both sets of intermediate terraces are formed by half a foot to 3 feet of peat that developed in place.

The basal inorganic sediments commonly consist of frost-rived basaltic rubble, mixtures of wind-blown silt and rubble, or massive blue-gray wind-blown silt. Locally, however, the basal part of the terrace deposits consist of beach sand, beach gravel, or stratified organic silt.

The detrital peat is similar to wave-deposited peat accumulating along the present shores of sheltered coves. The detrital peat generally overlies the inorganic substratum with a sharp contact. It consists of thin layers of short, broken twigs, sedge stems, and moss fibers, alternating with layers that consist predominantly of moss fibers and layers in which sedge stems constitute as much as 95 per cent of the total volume. The woody twigs range from $\frac{1}{16}$ to $\frac{1}{2}$ inch in diameter and seldom exceed 3 inches in length. Twigs in a single layer are generally of uniform size. None had attached roots. The twigs and sedge stems commonly are oriented parallel to one another; their long axes plunge 50°–60° toward the lake shore. A similar imbrication can be seen in the masses of organic debris accumulating at the present-day shores of protected bays.

Rocks up to 2 feet in diameter—probably ice-rafted—are scattered sparsely through the detrital peat in many exposures. Sand is disseminated in some peat layers in the vicinity of Granite Bay. Lenses a few inches thick of subangular pebbles in a matrix of silt are present locally. Detrital peat in the narrow point 1 mile south of Camp Point is interrupted by a series of wedges 4 feet wide and 8 feet deep composed of basalt pebbles in silt. The form of the wedges suggests that they are casts of ice wedges.

Brown, silt-sized volcanic ash half a foot to 2 feet thick overlies the detrital peat and is overlain in turn by half a foot to 3 feet of autochthonous peat in the higher group of intermediate terraces; similar ash is found in a comparable stratigraphic position in bogs and lake terraces elsewhere in the area. The ash generally shows no stratification, but layers of dark-gray stratified organic silt are intercalated in some exposures.

Fossils.—Megascopic plant remains are abundant in the terrace sediments, but they have not been studied in detail. Leaves of willow

and dwarf birch were recognized in the field. The wood consists entirely of twigs less than half an inch in diameter. No poplar or coniferous wood was seen in specimens examined by R. S. Sigafoos (Oral communication, 1953). Tundra vegetation similar to the present vegetation and a climate having summers no warmer than present summers are strongly suggested.

Abundant remains of extinct mammals were found in positions indicating almost certain derivation from sediments of the intermediate terraces. A definitive find consisted of several mammoth bones encased in stratified sediments freshly slumped from the thawing bank of a terrace of the lower group, about halfway between Granite Bay and Salix Bay. An additional 20 bones and bone fragments and 3 well-preserved teeth of mammoth lay strewn along 100 feet of beach adjoining the terrace. Another find in place seems to be represented by Quackenbush's report (1909, p. 123) of a mammoth tusk "projecting from the surface of the ground near Imuruk Lake." Bones, tusks, and teeth of mammoth, bison, and horse, identified by Otto Geist, collector for American Museum of Natural History (Written communication, 1948), were found by the writer in several other places on beaches adjoining lake terraces of the intermediate system.

Age and significance.—The sediments underlying the intermediate terraces probably were deposited during the Salmon Lake glaciation (Wisconsin). The two groups of intermediate terraces seem to record two periods of rising lake level that probably coincided with glacial advances and that were separated by a period of falling lake level that possibly coincided with a glacial recession. The lake basin was warped again after the formation of the intermediate terraces, and the present outlet to the Kugruk River probably originated as a consequence of the warping.

The sediments of the intermediate terraces lie in positions that were covered with 10–20 feet of water when the high wave-cut scarp represented the lake shore and are therefore younger than the Nome River glaciation (Illinoian). The bones of horse, bison, and mammoth indicate an age greater than 10,000 years, however, for bones of these mammals are lacking in sediments of north-central Seward Peninsula that are shown by radiocarbon dating to be less than 10,000 years old (Kulp, *et al.*, 1952, p. 412, sample L117C; Broecker, Kulp, and Tucek, 1956, p. 156–157, samples L117E, L137N, L137G).

Strand-line sediments extend from present lake level to a maximum height of nearly 20 feet in some of the older intermediate terraces, and from below present lake level to a height of about 10 feet in the younger intermediate terraces; this indicates that lake level was rising while the terrace sediments accumulated. Because lake level is controlled to a considerable extent by evaporation from the free-water surface during the ice-free season, the terrace sediments must have accumulated during intervals when summers were shorter and cooler than at present. Periods of short, cool summers can be equated on Seward Peninsula with glacial advances, retreats eastward of the forest boundary, and periods of intense frost riving of exposed bedrock; periods of longer, warmer summers can be equated with glacial recessions, extensions of the forest boundary to positions west of Imuruk Lake, and cessation of intense frost riving (Hopkins, in press; Hopkins, 1955, Ph.D. thesis, Harvard Univ.). The two periods of rising lake level probably coincide with glacial advances during the Salmon Lake glaciation; the intervening period of falling lake level may record a glacial retreat within the time of the Salmon Lake glaciation. The tundra plant assemblage represented by the plant remains in the terrace sediments supports this hypothesis and eliminates the possibility that the periods of rising lake level could have taken place while summers were appreciably warmer than at present. The interpretation of the significance of the intervening period of falling lake level is less certain, for tilting of the lake basin may have been a contributing factor.

The presence of remains of mammoth, bison, and horse in the sediments of the intermediate terraces indicates that these herbivores were able to support themselves in a region of tundra vegetation, and it places these three genera in the vicinity of Bering Strait at a point in time when the Bering land bridge was in existence (Hopkins, 1959).

The widespread brown ash layer near the top of the older intermediate-terrace deposits represents an ash fall that took place just before or just after lake level fell from the highest position recorded in the older intermediate terraces and before the sediments in the younger intermediate terraces began to accumulate.

Several lines of evidence indicate that the basin of Imuruk Lake was again warped southward or southeastward after the deposition of the sediments of the intermediate terraces. Terraces assignable to the older intermediate

group on the basis of the presence of the ash layer range from 5 to 20 feet in height above present lake level; however, the terrace deposits are composed primarily of detrital peat that evidently accumulated at a strand line, and the terrace surfaces must originally have been a nearly horizontal plane. The present differences in elevation imply warping. Intermediate terraces are lacking along the east and south shores in terrain where they would be expected if there had been no tilting; correlative sediments there must have been submerged below present lake level. The clearest evidence of tilting, however, is found on east Gull Island, where a terrace formed by detrital peat capped by the ash layer slopes southeastward at a gradient of 3 feet in 600.

If Imuruk Lake had any outlet during this period, it probably continued to drain westward to the Noxapaga River until after the tilting of the intermediate terraces. The present outlet valley contains neither terraces nor filled channels that could reflect fluctuations in the level of Imuruk Lake and appears to have been occupied by the Kugruk River for only a short time. The valley is so shallow that the river's discharge would be multiplied many times if lake level were raised 10–20 feet. The present outlet apparently developed as a consequence of irregular warping of the lake basin that reached maximum intensity in the pass to Noxapaga River drainage at the northwest corner of the lake (Fig. 5).

Low Terraces

Description.—A single set of low terraces occupies discontinuous small areas on all sides of Imuruk Lake. Low terraces underlain chiefly by peat stand 3–5 feet above present lake level, but ancient storm beaches composed of sand or gravel reach heights of 7 feet at Granite Bay (Fig. 4 *D*) and on the west shore of Salix Bay.

Detrital peat predominates in terraces at the heads of protected bays. Elsewhere, the terrace deposits generally consist of autochthonous sedge or grass peat containing lenses of stratified organic silt and commonly extending 3 feet or more below lake level. Low terraces at Granite Bay and on the east shore of Salix Bay are formed by beach sand, and an elevated spit (perhaps an ancient ice rampart) on the west shore of Salix Bay is composed of pebble gravel.

Plant remains in the sediments of the low terraces are similar to those in the sediments of the intermediate terraces; they suggest tundra vegetation and a climate having summers similar to or colder than present summers. Fragmentary bones and antlers of caribou and moose were found in detrital peat overlying beach sand in a low terrace at the east end of Imuruk Lake. The bones were rotted but were considerably lighter in color than the thoroughly patinated bones associated with terraces of the intermediate system.

Age and significance.—The lack of bones of extinct mammals suggests that the low terraces are less than 10,000 years old. An oscillation of lake level from 3 feet lower than at present to about 5 feet higher than at present seems to be indicated. Oscillations resulting from manipulation of the diversion dam at the head of the Fairhaven Ditch have been of the order of only 2 feet (Henshaw and Parker, 1913 p. 230–231) and thus cannot be related to the development of the low terraces; instead, the low terraces probably reflect low lake level during a period when summers were longer and warmer than at present, followed by high lake level during a period when summers were shorter and cooler. Periods of warmer summers about 8500 years ago and about 3600 years ago are recorded in north-central Seward Peninsula (Hopkins and Giddings, 1953, p. 25–28). The rise in lake level during which the low terraces were formed probably followed one of these two periods.

The low terraces are scattered around the perimeter of Imuruk Lake and do not appear to have been deformed. The minor differences in elevations of their surfaces above present lake level are adequately explained by differences in the processes by which different deposits were formed.

Summary of the History of Imuruk Lake

Imuruk Lake originated during the Nome River glaciation (Illinoian) when water began to accumulate in a large depression on the rolling surfaces of some recently extruded basaltic lava flows. The lava flows were undoubtedly highly permeable, and at first the lake probably discharged the excess of inflow over evaporation entirely by leakage into the volcanic rocks. However, the lake originated during a period of intense deposition of wind-blown silt imported from glacial outwash plains to the southwest. Silt deposited directly in the lake and washed in from adjoining slopes soon sealed off much of the lake bottom from the underlying permeable rocks, and

water accumulated to a depth of at least 40 feet. The lake then spilled over a low divide to the west and drained to the Noxapaga River and ultimately to Bering Sea. The fact that enough water accumulated to initiate external drainage indicates that evaporation rates did not exceed present evaporation rates and thus that summers were no warmer than at present during Nome River (Illinoian) time.[4]

Lake level fell during the Nome River-Salmon Lake interglacial interval, presumably as a result of an increase in water loss which was due to increased evaporation during a period when summers were considerably warmer. The lake basin was sharply warped at about this time, probably by deformation associated with the development of the northwestward-trending graben enclosing the lake basin.

The intermediate terraces record two episodes of rising lake level during the Salmon Lake glaciation. The increases in the level of the lake were a consequence of reduced evaporation during periods when summers were at least as cool as at present. The two periods of rising lake level may have been separated by a period of falling lake level, reflecting a brief interval of warm summers, or they may have been separated by renewed warping of the lake basin.

Late in the time of Salmon Lake glaciation, the lake basin was warped again, and uplift centered near the former outlet to the Noxapaga River; a new outlet developed draining into the Kugruk River and ultimately to Kotzebue Sound. A subsequent period of low lake level during an interval of warm summers, followed by an interval of shorter, cooler summers, is reflected by low terraces containing detrital peat extending from 3 feet below to 5 feet above present lake level.

Significance for the History of the Bering Strait Region

Central Seward Peninsula had a severe climate characterized by cold summers, heightened frost action, and reduced evaporation from free-water surfaces during the last two major glacial intervals. The forest boundary lay far to the east during the last (Wisconsin) glacial age as well as in the previous (Illinoian) glacial age. I have shown elsewhere (Hopkins, 1959) that the entire Bering land bridge probably supported only tundra vegetation. Animals and plants migrating between the continents must have been adapted to life in a tundra environment. Three well-established migrants evidently were adapted to tundra life, for the intermediate terraces at Imuruk Lake contain remains of bison, horse, and mammoth.

Because of their geographic position and probable stratigraphic significance, the terraces and bottom sediments of Imuruk Lake offer a fruitful field for further paleontological and paleobotanical investigations. A systematic study of the terrace sediments should yield a much richer vertebrate assemblage than is recorded in this report. The abundant plant remains in the terraces will facilitate paleoecological interpretations and also offer an opportunity to test by radiocarbon dating the correlations proposed here. Beneath the floor of the lake is a thick fill of silty sediments that should contain an uninterrupted pollen record extending from Illinoian through Sangamon, Wisconsin, and well into Recent time. This long record of uninterrupted sedimentation would seem well worth exploring by means of core drilling and pollen analysis.

[4] Precipitation may have been higher on Seward Peninsula than at present during the Nome River (Illinoian) glacial interval, but I have shown elsewhere (Hopkins, in press) that precipitation was not higher than at present during the Salmon Lake (Wisconsin) glacial interval.

References Cited

Black, R. F., 1954, Precipitation at Barrow, Alaska, greater than recorded: Am. Geophys. Union Trans., v. 35, p. 203–206

Broecker, W. S., Kulp, J. L., and Tucek, C. S., 1956, Lamont natural radiocarbon measurements III: Science, v. 124, no. 3213, p. 154–165

Harbeck, G. E., Kohler, M. A., Koberg, G. E., and others, 1958, Water-loss investigations: Lake Mead studies: U. S. Geol. Survey Prof. Paper 298, 100 p.

Henshaw, F. F., and Parker, G. L., 1913, Surface water supply of Seward Peninsula, Alaska: U. S. Geol. Survey Water-Supply Paper 314, 317 p.

Hopkins, D. M., 1959, Cenozoic history of the Bering land bridge: Science, v. 129, p. 1519–1528

—— in press, Pleistocene climates and the Bering Sea land bridge: 20th Internat. Geol. Cong., Comptes Rendus

Hopkins, D. M., and Giddings, J. L., Jr., 1953, Geological background of Iyatayet archaeological site, Cape Denbigh, Alaska: Smithsonian Inst. Misc. Coll., v. 121, no. 11, 33 p.

Hopkins, D. M., and Sigafoos, R. S., 1951, Frost action and vegetation patterns on Seward Peninsula, Alaska: U. S. Geol. Survey Bull. 974, p. 51–101

Hopkins, D. M., Karlstrom, T. N. V., and others, 1955, Permafrost and ground water in Alaska: U. S. Geol. Survey Prof. Paper 264-F, p. 113–146

Kulp, J. L., Tryon, L. E., Schleman, W. R., and Snell, W. A., 1952, Lamont natural radiocarbon measurements II: Science, v. 116, no. 3016, p. 409–414

Péwé, T. L., and others, 1953, Multiple glaciation in Alaska, a progress report: U. S. Geol. Survey Circ. 289, 13 p.

Quackenbush, L. S., 1909, Notes on Alaskan mammoth expeditions of 1907 and 1908: Am. Mus. Nat. History Bull., v. 26, p. 87–130

U. S. Weather Bureau, 1943, Climatic atlas for Alaska: Army Air Forces Weather Inf. Bur. Rept. 444, 229 p.; supp., 72 p.

U. S. Geological Survey, Menlo Park, Calif.

Manuscript Received by the Secretary of the Society, June 23, 1958

Publication Authorized by the Director, U. S. Geological Survey

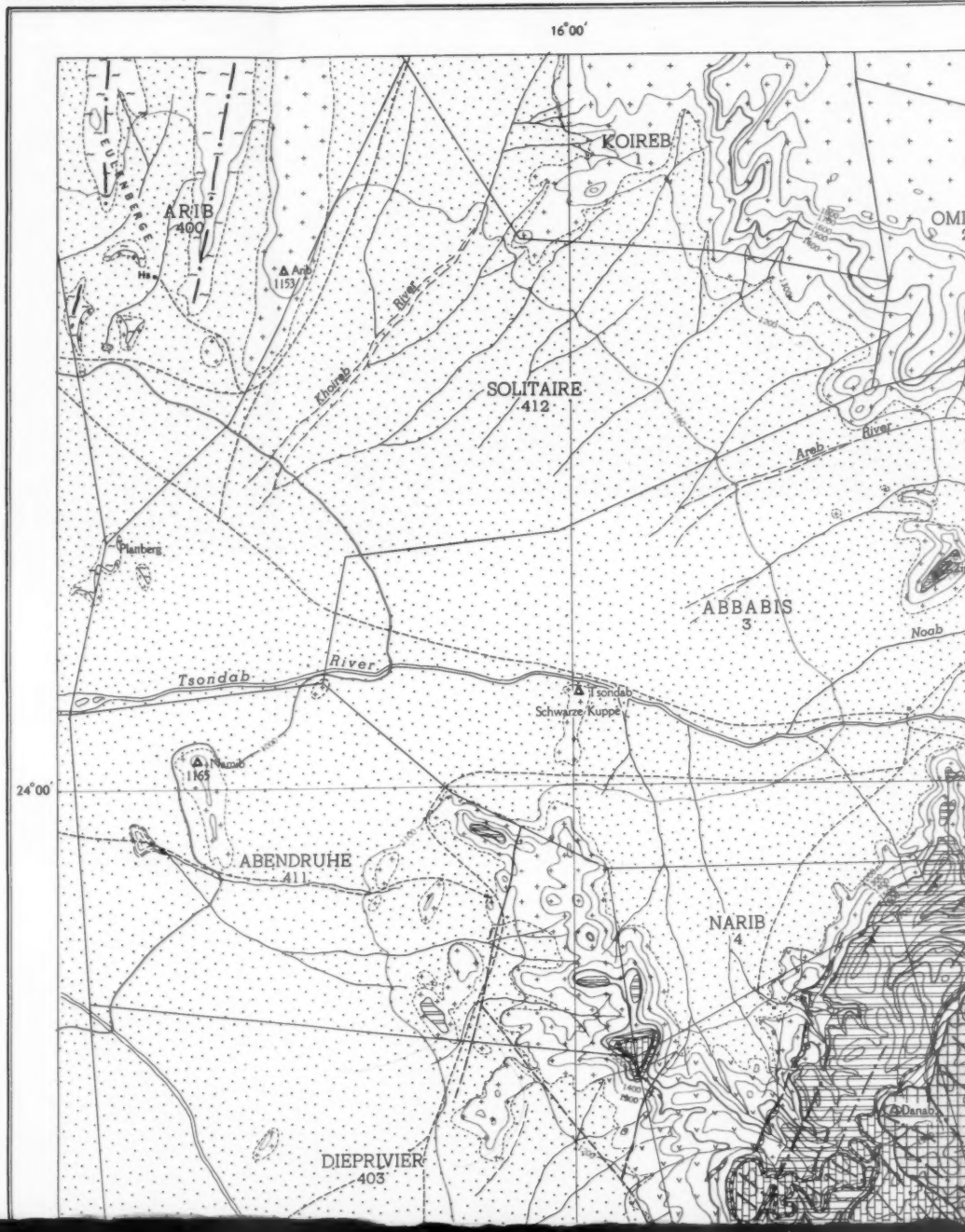
16°00'
24°00'
KOIREB
ARIB
400
EUKUNDBERGE
Ha
Arib
1153
Khumib
River
SOLITAIRE
412
Areb
River
Planberg
ABBABIS
3
Noab
Tsondab
River
Tsondab
Schwarze Kuppe
Namib
1165
ABENDRUHE
411
NARIB
4
Danab
DIEPRIVIER
403

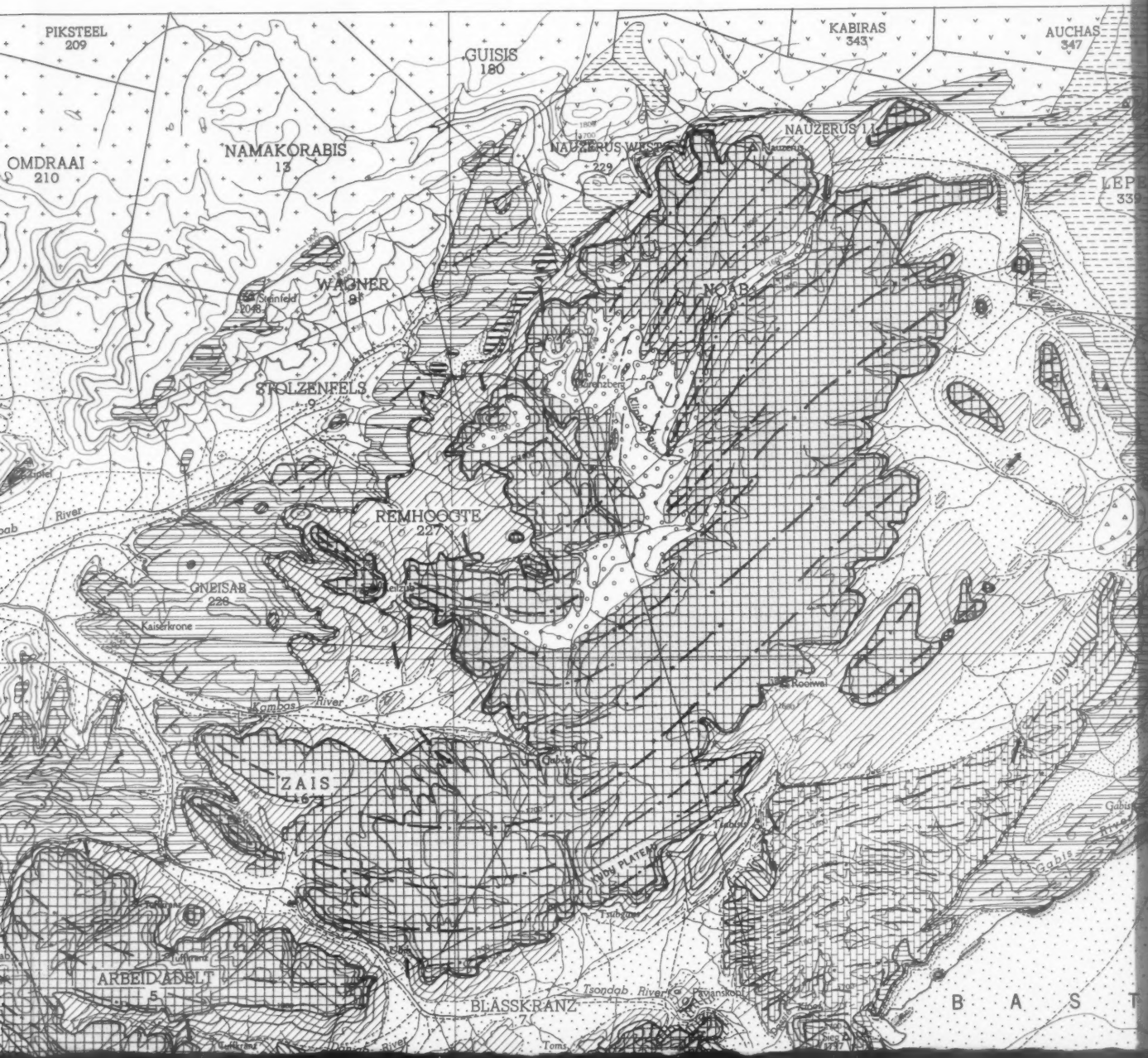
16°15'
PIKSTEEL
209
GUISIS
180
KABIRAS
343
AUCHAS
347
NAMAKORABIS
13
NAUZERUS WEST
229
NAUZERUS
OMDRAAI
210
WAGNER
91
NOAB
STOLZENFELS
9
REMHOOGTE
227
ONDISAB
228
Kaiserkrone
Kombos River
ZAIS
116
ARBEIDADELT
5
BLÄSSKRANZ
7
Tsondab River
B A S T

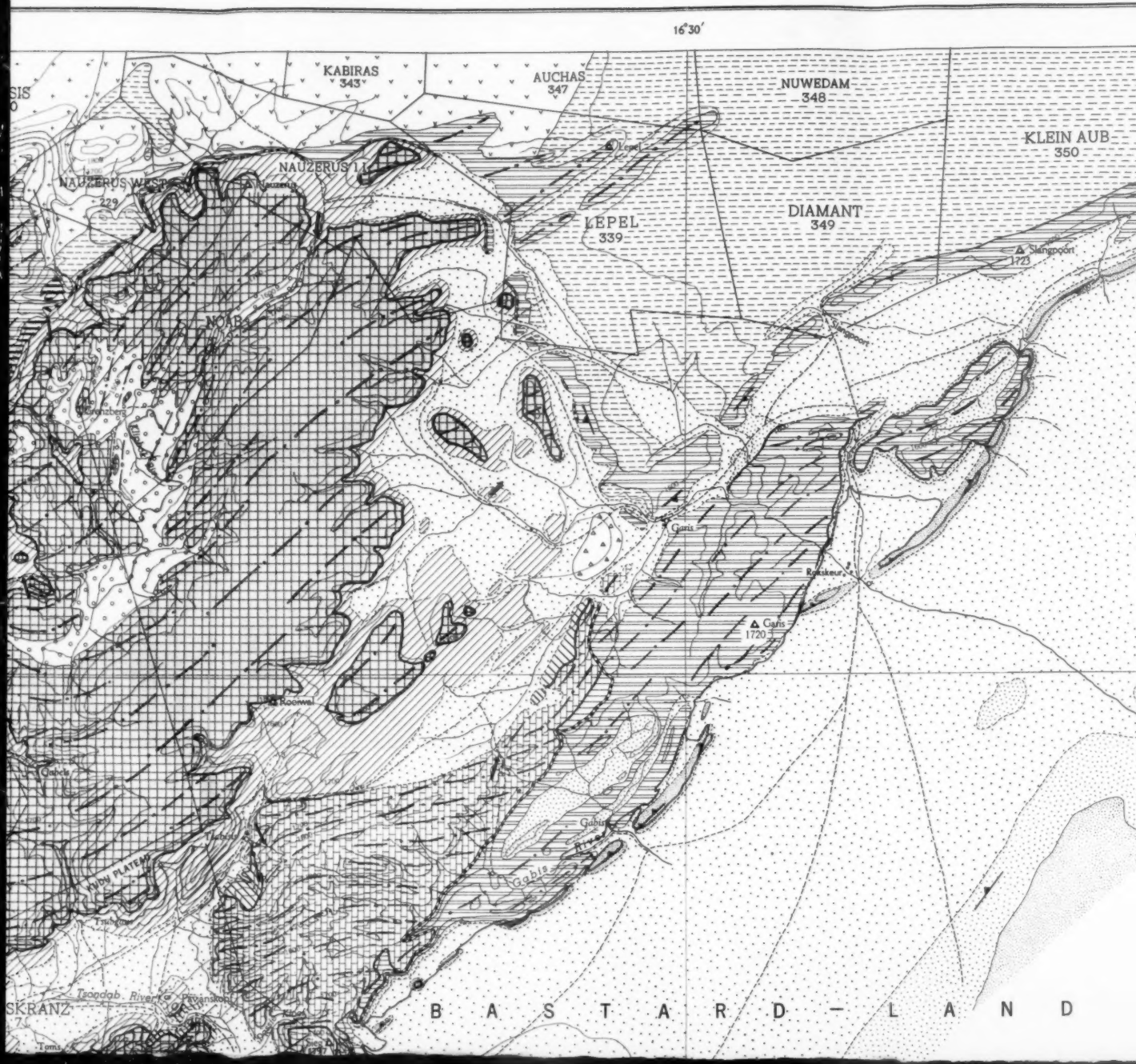
16°30'
KABIRAS
343
AUCHAS
347
NUWEDAM
348
KLEIN AUB
350
NAUZERUS 1
NAUZERUS WEST
229
LEPEL
339
DIAMANT
349
Lepel
Slangpoort
1723
NOAB
Garis
Rooiwal
Gabis
Gabis
Tsondab River
Tsondab
Tsondab
Toms
SKRANZ
B A S T A R D – L A N D

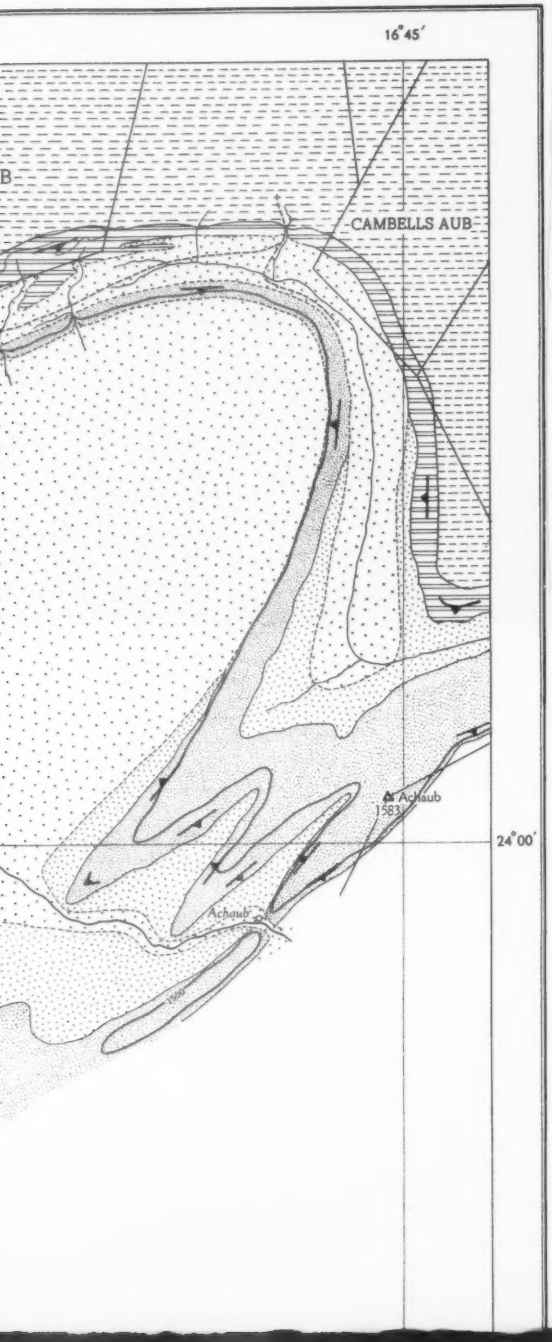
16°45′
CAMBELLS AUB
Achaub
1583
24°00′
Achaub

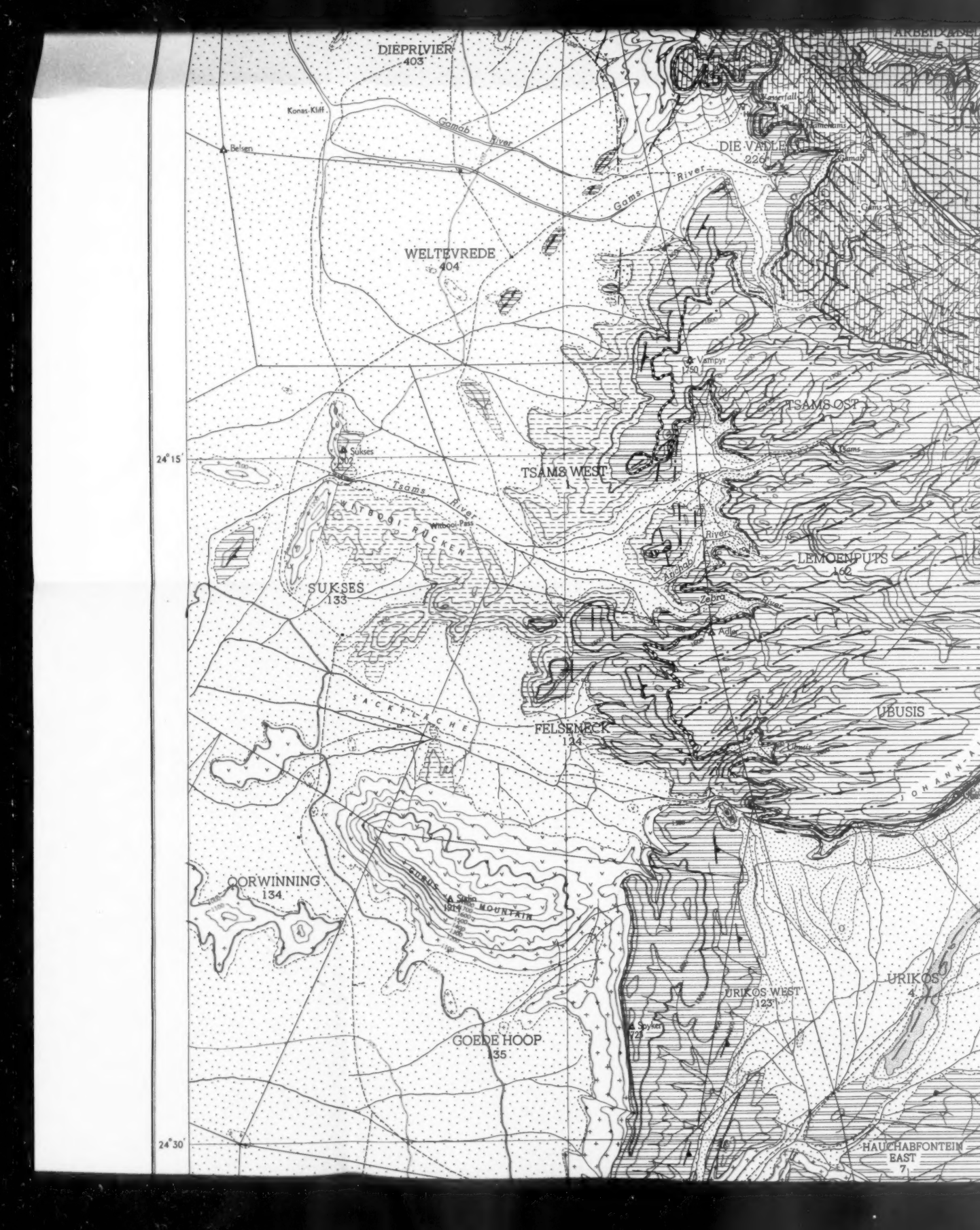
DIEPRIVIER
403
Konas-Kliff
Belsen
Gamab River
Gams River
DIE VALLEI
226
WELTEVREDE
404
Vampyr
750
TSAMS OST
TSAMS WEST
Sukses
902
24°15'
Tsams River
WITBOOI RACKEN
Witbooi Pass
SUKSES
133
Anchas River
LEMOENPUTS
460
Zebra River
Adler
SACKFLACHE
FELSENECK
124
UBUSIS
Ubusis
JOHANNA
OORWINNING
134
CIRQUE
Stein
1914
MOUNTAIN
URIKOS
4
URIKOS WEST
123
Spyker
GOEDE HOOP
135
24°30'
HAUCHABFONTEIN
EAST
7

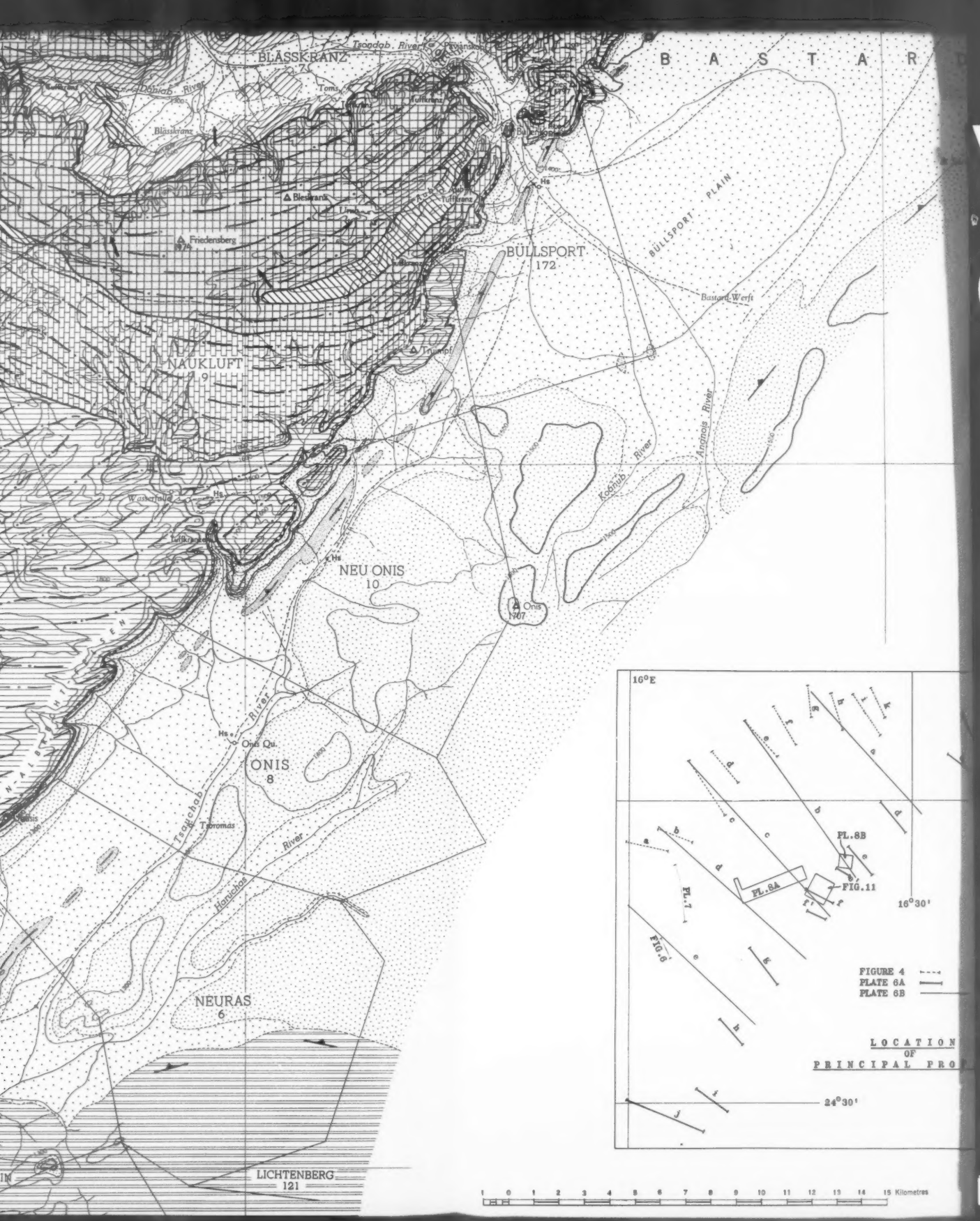
BLÄSSKRANZ
Tsoadab River
Tsoamanabes
B A S T A R D
Tsaobis
Blässkranz
Tuffkranz
Blesskranz
Friedensberg
976
BÜLLSPORT
172
BÜLLSPORT PLAIN
Bastard Werft
Trumpf
NAUKLUFT
9
Wasserfall
NEU ONIS
10
Onis
1707
Kodnub River
Anonais River
Onis Qu.
ONIS
8
Tsachab River
Tsaromas
Hanichas River
NEURAS
6
LICHTENBERG
121
16°E
16°30'
24°30'
FL.8B
FL.8A
FIG.11
FIG.6
FIGURE 4
PLATE 6A
PLATE 6B
LOCATION
OF
PRINCIPAL PRO
1 0 1 2 3 4 5 6 7 8 9 10 11 12 13 14 15 Kilometres

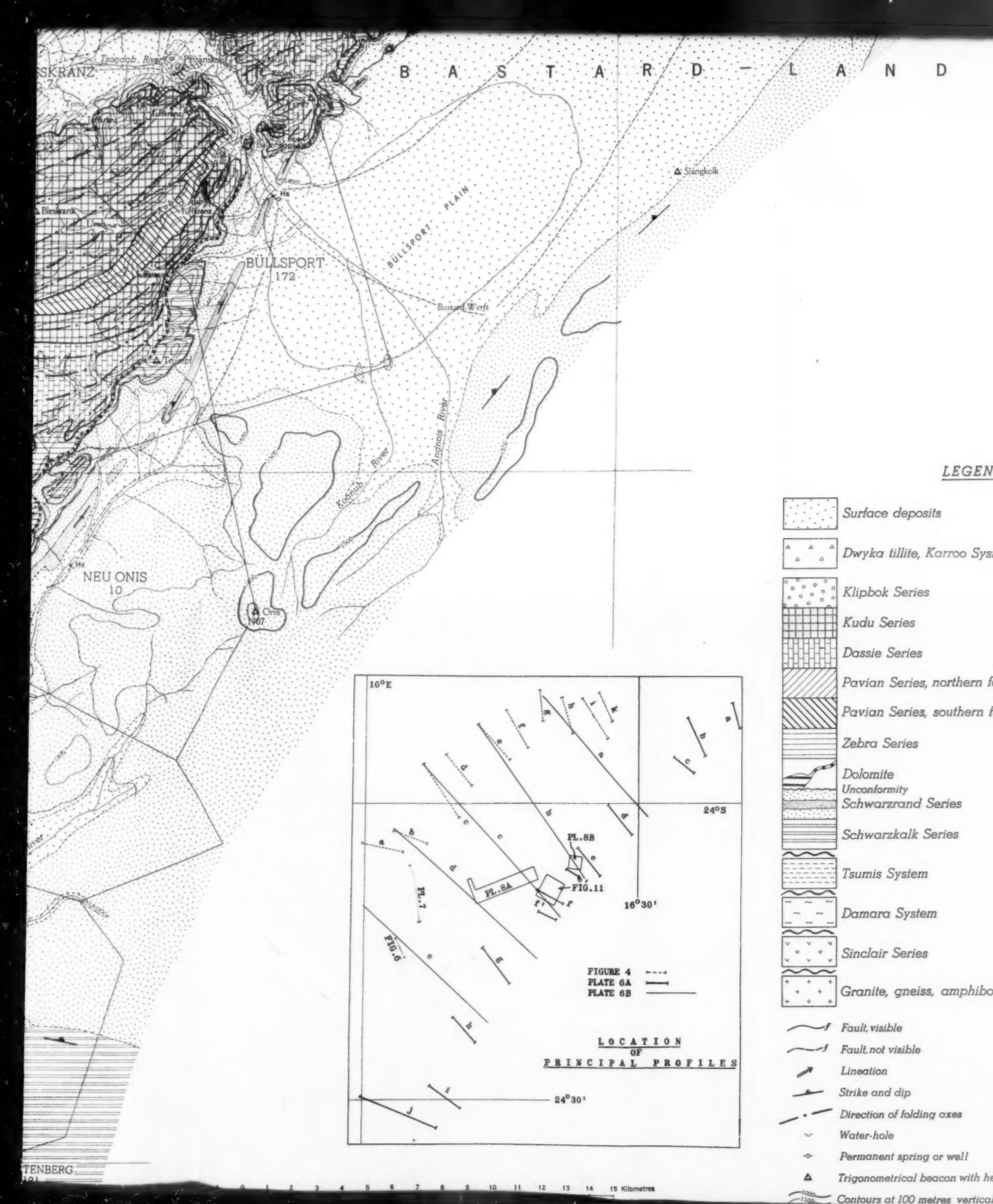
B A S T A R D – L A N D
SKRANZ
Tsondab River
Tsaobis
Tsams
Kuiseb
Bleskrank
Kuiseb River
Trumpf
BÜLLSPORT
172
BÜLLSPORT PLAIN
Bastard Werft
Stängkolk
Khan River
Anghois River
NEU ONIS
10
Onis
1707
16°E
24°S
16°30'
24°30'
PL.8B
PL.8A
PL.7
FIG.11
FIG.6
FIGURE 4
PLATE 6A
PLATE 6B
LOCATION
OF
PRINCIPAL PROFILES
TENBERG
0 1 2 3 4 5 6 7 8 9 10 11 12 13 14 15 Kilometres
LEGEN
Surface deposits
Dwyka tillite, Karroo Sys
Klipbok Series
Kudu Series
Dassie Series
Pavian Series, northern f
Pavian Series, southern f
Zebra Series
Dolomite
Unconformity
Schwarzrand Series
Schwarzkalk Series
Tsumis System
Damara System
Sinclair Series
Granite, gneiss, amphibo
Fault, visible
Fault, not visible
Lineation
Strike and dip
Direction of folding axes
Water-hole
Permanent spring or well
Trigonometrical beacon with he
Contours at 100 metres vertical

GEND

o System

ern facies

ern facies } Nama System

ohibolite & migmatite

ll

with height shown in metres

ertical intervals

24°15′

24°30′

UI

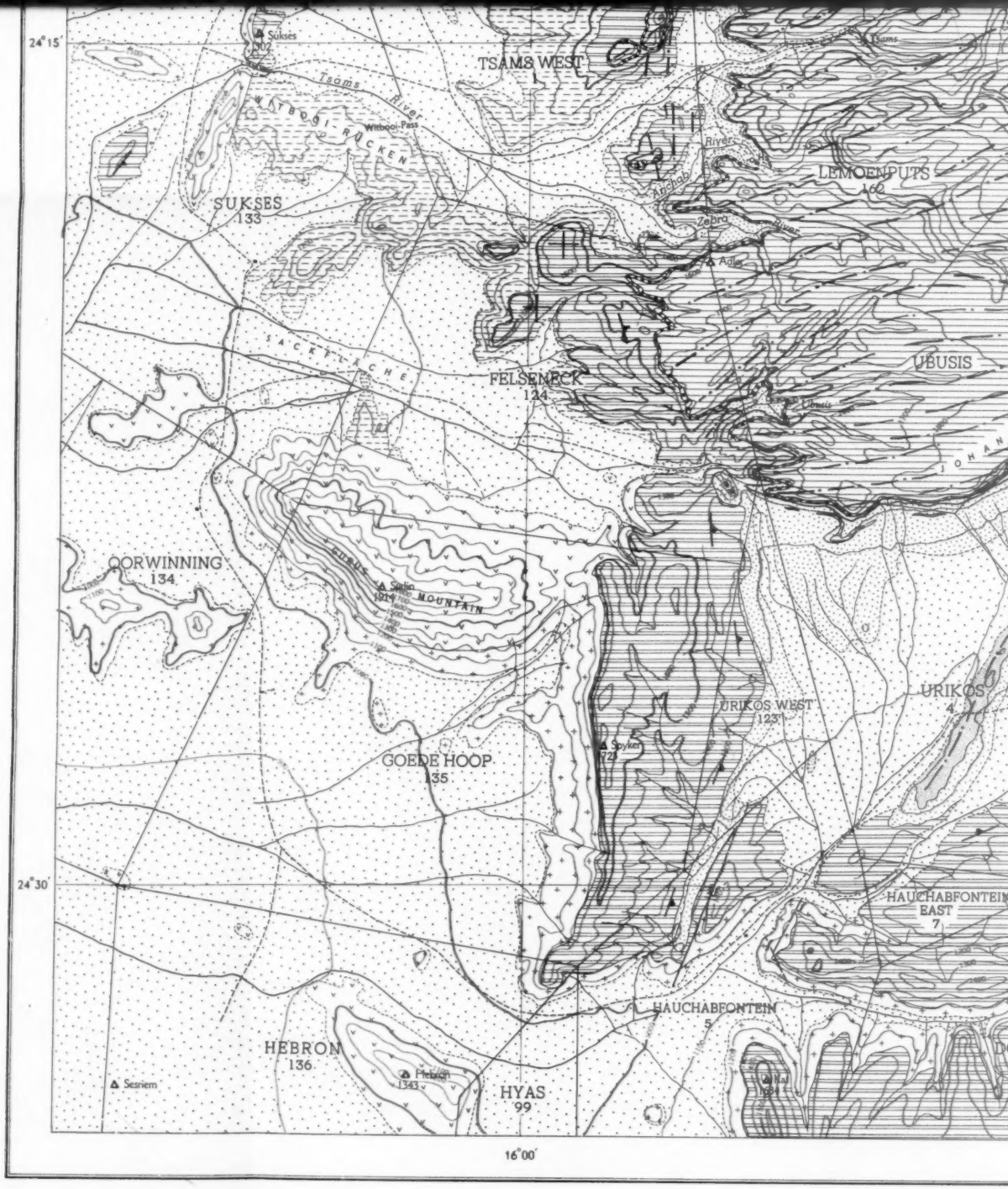
24°15'
TSAMS WEST
Tsams
Tsams River
WITBOOI RÜCKEN
Witbooi-Pass
SUKSES
133
Sukses
LEMOENPUTS
160
Aichab
Zebra River
Adler
UBUSIS
Ubusis
FELSENECK
124
SACKTLÄCHE
JOHAN
OORWINNING
134
Spitz
1814
MOUNTAIN
URIKOS
4
URIKOS WEST
123
Spyker
GOEDE HOOP
135
24°30'
HAUCHABFONTEIN
EAST
7
HAUCHABFONTEIN
5
HEBRON
136
Hebron
1343
Sesriem
HYAS
99
16°00'

GEOLOGI

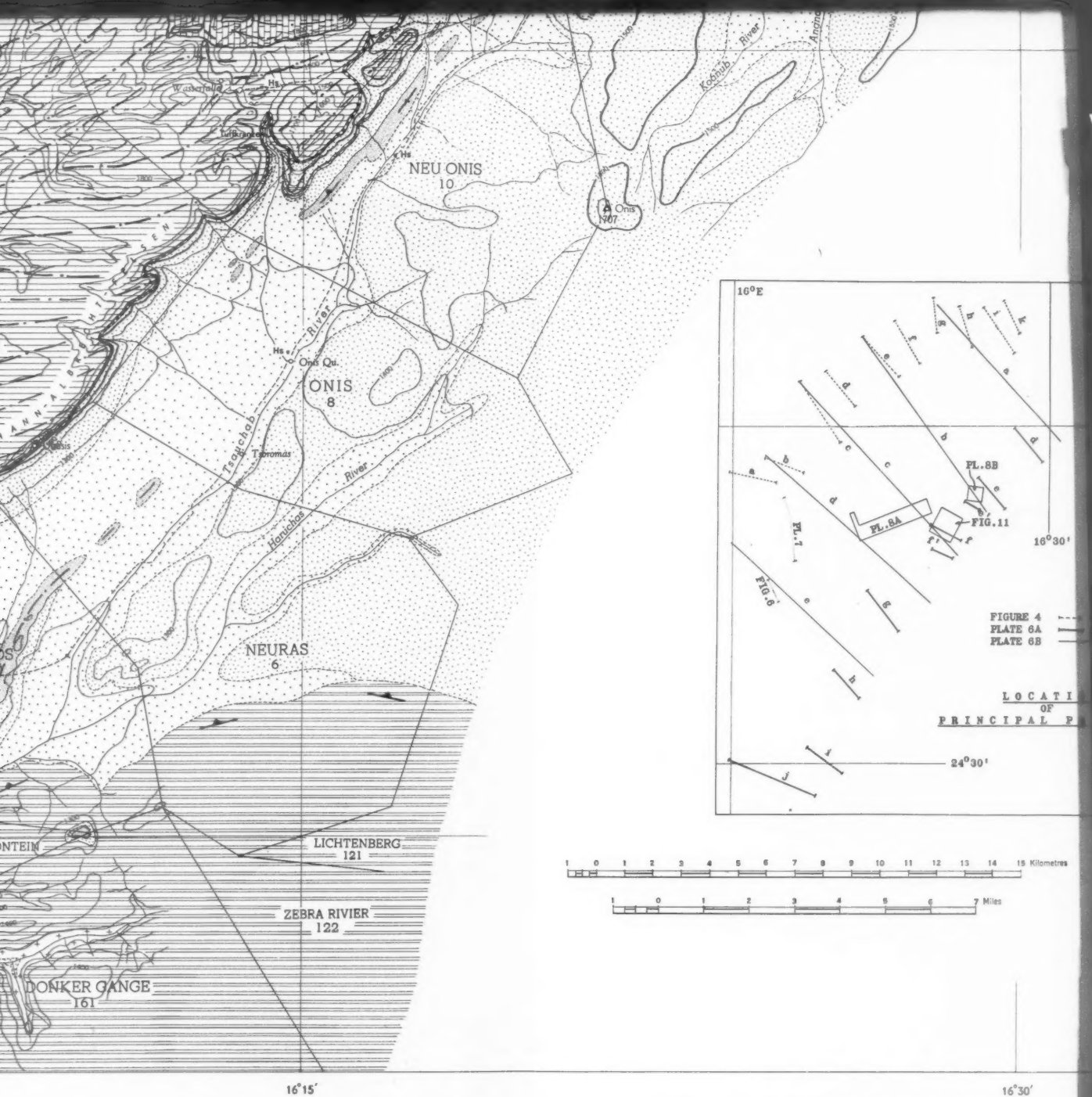

OGIC MAP OF THE NAUKLUFT MOUNTAINS AREA, SOUTH WEST AFRICA

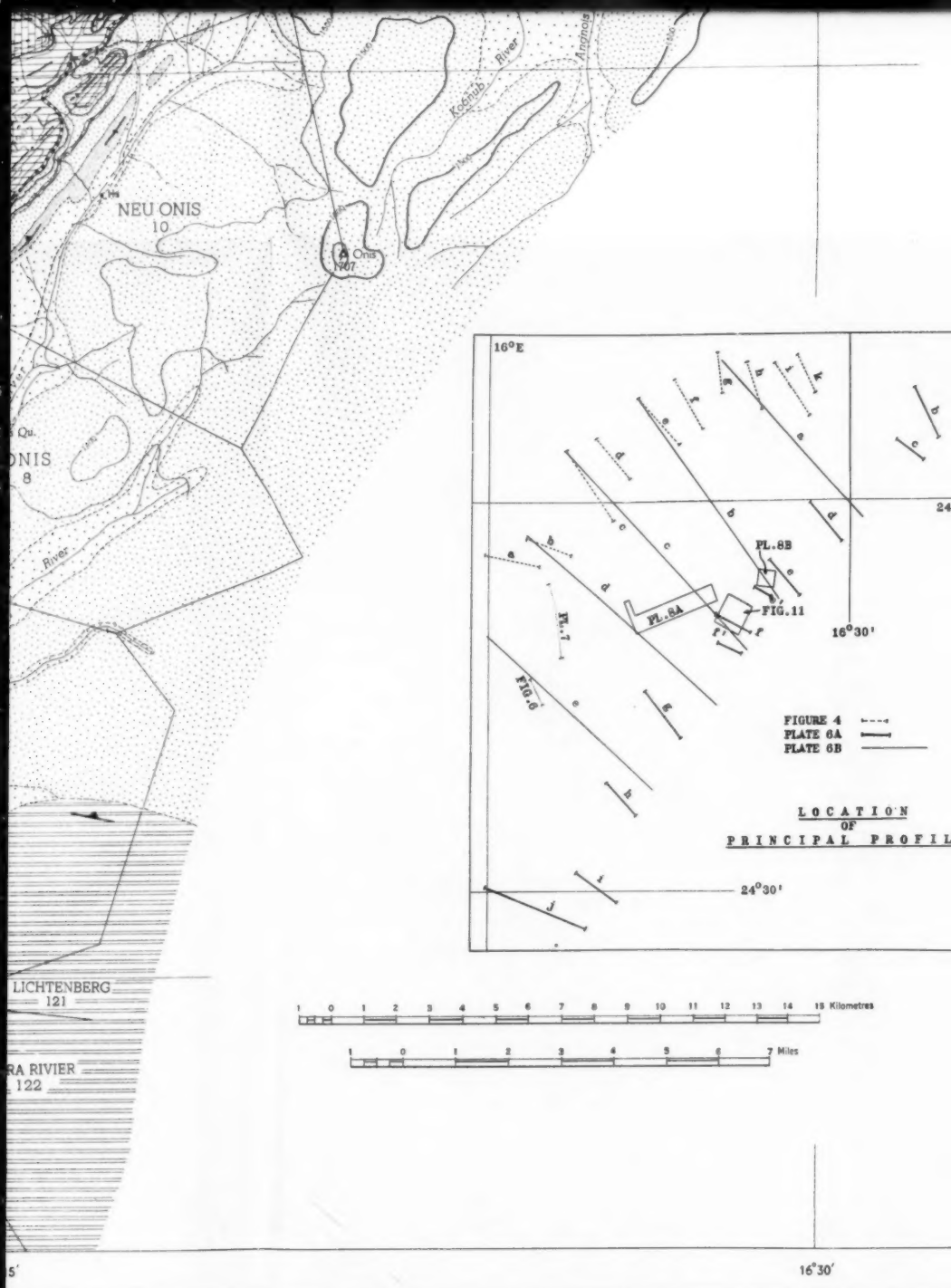

AUKLUFT MOUNTAINS AREA, SOUTH WEST AFRICA

LEGEND

- Surface deposits
- Dwyka tillite, Karroo System
- Klipbok Series
- Kudu Series
- Dassie Series
- Pavian Series, northern facies
- Pavian Series, southern facies
- Zebra Series
- Dolomite
- Unconformity
- Schwarzrand Series
- Schwarzkalk Series

} Nama System

- Tsumis System
- Damara System
- Sinclair Series
- Granite, gneiss, amphibolite & migmatite

- Fault, visible
- Fault, not visible
- Lineation
- Strike and dip
- Direction of folding axes
- Water-hole
- Permanent spring or well
- Trigonometrical beacon with height shown in metres
- 1000 / 1100 Contours at 100 metres vertical intervals
- Road
- •HS House

24°15′

24°30′

16°45′

24°S

FILES

Drawn in the Geological Survey Office, Pretoria, 1957.

Introd
Atkin
Physi
Geolo
Strati
Pre
Na
Na
Suc
Ag
Pe
Su
Tecto
Di
Te
Fo
"D
Te
Te
Te
Te
Te

BULLETIN OF THE GEOLOGICAL SOCIETY OF AMERICA
VOL. 70, PP. 1047–1078, 18 FIGS., 8 PLS. AUGUST 1959

GRAVITY TECTONICS IN THE NAUKLUFT MOUNTAINS OF SOUTH WEST AFRICA

BY HERMANN KORN[1] AND HENNO MARTIN

(TRANSLATED BY JOHN G. DENNIS)

ABSTRACT

The late Precambrian Nama beds of the Naukluft Mountains in South West Africa show intense Alpine-type deformation.

The crystalline basement underlying these rocks is little disturbed. Its upper surface is basin-shaped. The intensity of deformation in the overlying Nama beds increases upward to a practically undedormed unconformity which separates the Nama into two folded units. The unconformity is overlain by a strikingly uniform and little disturbed dolomite bed. Above this dolomite the intensity of deformation once more increases; it reaches its maximum in this upper deformed unit. The folds delineate a cascading movement from the topographically higher northern hinterland and form a great arc in front of the steepest slope of the basin, overriding the undeformed Nama beds of the southern foreland in a number of thrust sheets and nappes.

These observations, based on detailed mapping from exceptionally favorable exposures, bring out a movement pattern which is plainly controlled by the shape of the basin. Such a pattern is best interpreted as due to plastic flow under the influence of gravity.

CONTENTS

TEXT

	Page
Introduction	1048
Acknowledgments	1048
Physiography	1048
Geological setting	1050
Stratigraphy	1050
Pre-Nama basement	1050
Nama system, foreland facies	1051
Stratigraphic relationships	1051
Basal beds	1051
Schwarzkalk series	1051
Schwarzrand series	1052
Fish River series	1052
Nama system, Naukluft facies	1053
Stratigraphic relationships	1053
Basal and Schwarzkalk series	1053
Schwarzrand series	1054
Schwarzrand-Zebra unconformity	1056
Succession above Unconformity dolomite	1058
Age of the Nama system	1060
Post-Nama deposits	1061
Summary of stratigraphic results	1061
Tectonics	1061
Distinctive features of tectonic style	1061
Tectonics of the basement	1062
Folding in Schwarzkalk and lower Schwarzrand beds	1062
"Double unconformity"	1063
Tectonics of Zebra series	1064
Tectonics of Pavian series	1064
Northern-facies area	1064
Southern-facies area	1065
Tectonics of Dassie series	1067
Tectonics of Kudu series	1070
Tectonics of Klipbok series	1070
Structure of southeastern mountain border	1071
Movement pattern	1072
Internal structures and rock deformation	1073
Summary	1076
References cited	1077

[1] Deceased.

ILLUSTRATIONS

Figure		Page
1.	Map showing location of Naukluft area	1049
2.	Wedges of basal beds infolded in basement granite (farm Stolzenfels)	1052
3.	Detail of infolded basal quartzite	1054
4.	Profiles *a-k* through boundary region between Naukluft Mountains and Nauchas Highland	1055
5.	Zipfelberg: transgression of basal beds on northern slope of Tsondab trough	1056
6.	View of mountain face on farm Tsams	1057
7.	Unconformity above folded black limestone	1058
8.	Stratigraphy of Zebra, Pavian, Dassie, and Kudu series and probable correlations	1059
9.	Schwarzkalk series wedged into basal granite at entrance to Gams Valley on farm "Die Valle"	1063
10.	Folding of Pavian series under Kudu nappe	1065
11.	Profiles through front range, Farm Büllsport, southwest of Tsondab River	1066
12.	Diagrammatic interpretation of Naukluft folding	1068
13.	Block diagram of front range northeast of Büllsport	1069
14.	Dolomite bands of Kudu series showing boudinage structure	1071
15.	Diagram showing tectonic relationship of Pavian, Kudu, and Klipbok series	1071

Figure — Page
16. Deformed dolomite block in small anticlinal flexure ... 1074
17. Shale band fractured in plastically deformed limestone ... 1074
18. Structure of Kudu nappe ... 1075

Plate — Facing page
1. Geologic map of the Naukluft Mountains area, South West Africa ... 1047

Following page
2. Physiography of the Naukluft area
3. Deformation in the Naukluft area ... 1060
4. Folding in the Naukluft area
5. Structure details

Facing page
6. Composite sections through Naukluft Mountains ... 1064
7. Panoramic view of western mountain face on farm "Die Valle" showing imbricated folding of Dassie series above Unconformity dolomite ... 1070
8. Profiles, farms Blässkranz and Büllsport ... 1078

TABLES

Table — Page
1. Tentative stratigraphic column of South West Africa ... 1051

Introduction

The work on which the present paper is based was suggested by the late H. Lotz.

Geological maps of the western part of the Rehoboth area by Rimann (1915) and de Kock (1934) include the northern part of the Naukluft Mountains. Both surveys were primarily concerned with the basement complex and did not deal with the complicated stratigraphy and deformation of the Nama beds.

The field work was done in 1935–1936 with several shorter visits later on. No serviceable topographic maps were available except for that of the Abbabis area by Maak (1924); hence the authors had to map topography and geology simultaneously. Owing to the extraordinarily complicated stratigraphic and structural relationships, a key area including farms Büllsport, Blässkranz, and Tsawisis was first mapped on a large scale (1:10,000). This map is not reproduced here because detailed sections (Fig. 11; Pl. 8) give a clearer picture of the structure. The survey was then extended to the whole area at 1:50,000 (Pl. 1). The accuracy of Plate 1 is not uniform. There may be appreciable errors in the position of the valleys of the Meilenrücken Plateau and the eastern parts of farms Ubusis, Tsams Ost, and Lemoenput.

The geology is well exposed. Only the bottoms of the greater valleys are alluviated. The valley sides are practically fully exposed. Hence the profiles in this paper could be copied directly from nature, with correct rendering of the finest structural details.

South African stratigraphic terminology is adhered to in this paper. In particular, "series" and "system" do not necessarily denote time-rock sequences.

Acknowledgments

The work was greatly facilitated by the interest and help of the Administration of South West Africa. From 1937 to 1940 the authors were allowed to use the Department of Mines laboratory as their headquarters in Windhoek. In 1951 the Administration allowed Martin to spend 6 months on the compilation of scientific papers, including the present one, and also appointed Charlotte Korn to assist in this work.

Thanks are also due to members of the Geological Survey of South Africa drawing office for redrawing the map; to Charlotte Korn for help with the preparation of the map; and to John G. Dennis for translation of the manuscript and other help in editing the paper.

Ernst Cloos read the manuscript and made valuable suggestions.

Two compasses and two small level-glasses lent by the Deutsche Forschungs-Gemeinschaft were used for the mapping.

Many helpful discussions took place between the authors and Hans Cloos when the latter visited the area in 1936.

It is a pleasure to recall the kindness, helpfulness, and hospitality of all the farmers of the Naukluft region. Their help and friendship greatly facilitated the strenuous work in a difficult and often not easily accessible terrain.

Physiography

The Naukluft Mountains form one of the corner buttresses of Africa's Great Escarpment. Their elongation, however, does not follow that of the escarpment (north-northwest) but points into the interior in a northeasterly direction (Fig. 1). The Naukluft range is the southernmost unit with the characteristic northeast trend of central South West Africa (Fig. 1).

The Naukluft Mountain area is about 70 miles long and 30 miles wide (Pl. 1). It is truncated by a great peneplain. Therefore the highest mountains are flat-topped, and some are true plateaus. The peneplain is inclined, rising from east to west to a height of nearly

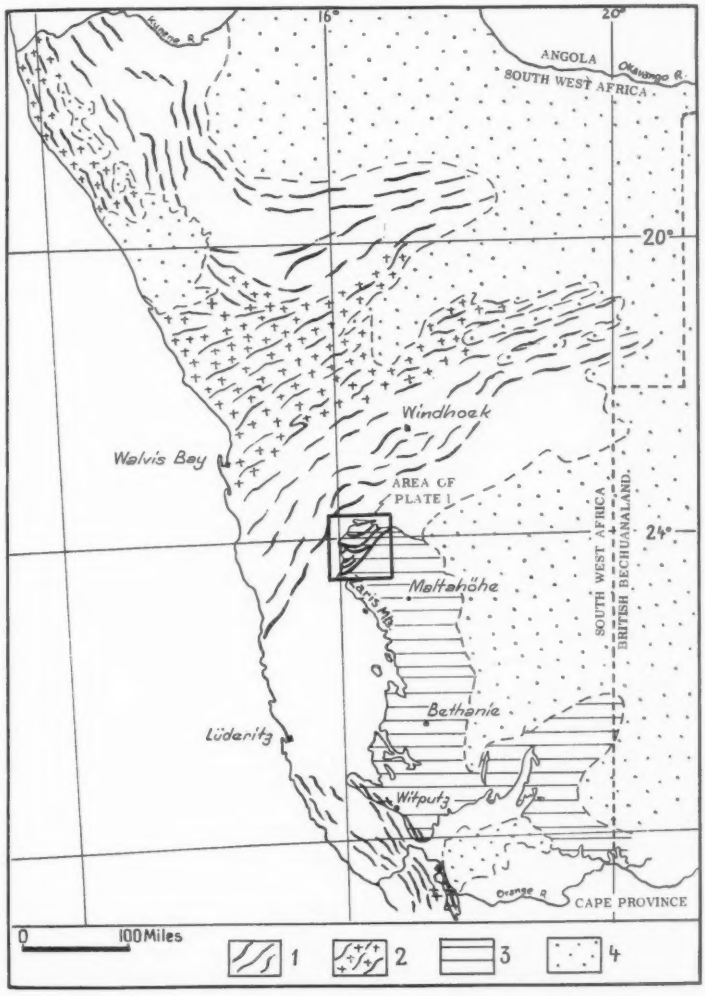

FIGURE 1.—MAP SHOWING LOCATION OF NAUKLUFT AREA
1, Directions of late Precambrian folds; 2, late Precambrian granites; 3, undeformed Nama beds; 4, post-Nama rocks

2000 m at the Friedensberg Plateau. To the west the plateau is cut by precipitous gorges and breaks off abruptly toward the wide Namib Plains, 600–800 m below. To the southeast a steep, almost straight scarp divides the Büllsport Plain and the broad basin of the Tsauchab Valley on farms Onis and Urikos. This imposing cliff is pierced by the Tsondab River on farm Büllsport. The river originates in low hills south of the Büllsport Plain and, flowing straight into the high Naukluft Mountains, cuts the high, lands in a magnificient valley flanked by precipitous dolomite cliffs. On farm Abbabis the valley emerges into the wide Namib Plains. To the north the deep Noab Valley, extending from Nauzerus to Abbabis, divides the Naukluft Mountains from the granite hills of the Nauchas Highlands.

By far the greater part of the Naukluft Mountains is drained to the west, into the

Namib Desert. The calcareous waters of the springs which run through the great gorges cut in the limestone plateau have commonly deposited enormous promontaries of tufa which jut out into the valleys and attain heights of up to 400 feet. One of the biggest of these (Pl. 2, fig. 1) has given its name to farm Blässkranz. The Naukluft valleys provide some of the prettiest landscapes of South West Africa.

None of the valleys trending westward into the Namib Desert now reach the sea. They all end in great clay pans in front of or among the enormous red dunes of the central Namib Desert.

Only the northeast corner of the range drains into the Fish River. Here broad, mature valleys dissect a low plateau, leaving only a few low but steep-sided ridges. These too terminate east of Slangpoort.

The high peneplain and the broad eastward-draining valleys are both pre-Karroo, as evidenced by Dwyka tillite found in the broad raised valley east of Garis. The tillite there rests 200 m below the pre-Karroo peneplain. It is not bounded by faults and therefore appears to be a remnant of Dwyka beds which once filled the valley. Probably all the broad, mature U-shaped valleys were shaped by Dwyka ice. The difference in resistance to erosion between the Nama limestones and dolomites and the easily eroded Dwyka boulder shales facilitated renewed excavation of the original valleys. The extraordinary "poort" (gateway) of the Tsondab Valley at Büllsport must also be a pre-Dwyka feature, for there is a remnant of glacial till on a terrace in the poort.

Geological Setting

The Naukluft Mountains are entirely made up of rocks of the Nama system (Fig. 8). Beds of the same age (late Precambrian?) cover a considerable area to the south, where they are only slightly affected by folding or faulting; they are undeformed even where they come up against the steep southeastern edge of the Naukluft Mountains (Pl. 2, figs. 2, 3). In contrast to this southern foreland, the mountains exhibit extreme folding of Alpine type. The folds, imbricate structures, and thrust sheets face south and southeast and terminate abruptly at the almost rectilinear southeastern scarp.

The upper Nama beds in the folded area differ markedly from those in the foreland. The normal succession consists of sandstones, quartzites, and shales. The deformed succession is one of limestones, dolomites, shales and conglomeratic shales, and limestones. The lower Nama beds in the mountains and in the foreland are identical.

The deformed rocks fill a basin formed by older basement rocks and elongated in a northeasterly direction. The basement rises abruptly to great heights, especially in the north. Thus the nature and extent of disturbances in the basement which accompanied deposition and folding of the Nama beds can be observed in the northern and western valleys and mountain sides. Here it is plainly evident that basement deformation is surprisingly slight compared with the intense folding of the higher levels.

Stratigraphy

Pre-Nama Basement

The basement complex is made up of several systems of widely different ages, separated from one another by great unconformities (Table 1).

De Kock (1934) described the Marienhof series in the area north of the Naukluft Mountains. The western and northern boundaries of the Naukluft Basin seem to be roughly outlined by the strike of Archean crystalline rocks, which probably represent the Marienhof series in this area.

Numerous north-northeast-striking diabase dikes traverse the gneisses and granites. They have not been observed in any of the succeeding formations.

The Sinclair series consists of a great thickness of acidic extrusive rocks with andesitic lavas and sedimentary rocks present locally. The quartz porphyry hills on farm Nauzerus belong to this series, which also constitutes the high red ridge of Gurus Mountain to the west.

The Sinclair series is overlain with marked unconformity by the Tsumis system, a thick succession of sandstones, arkoses, quartzites, conglomerates, and shales. A detrital breccia is commonly found at its base.

This succession may be up to 30,000 feet thick. Rimann (1915) and de Kock (1934) have included it in the basal beds of the Nama system, on the basis of observations east of Garis. There the Nama system overlies older sedimentary rocks more or less conformably over great distances. Nevertheless, the transgressive nature of the contact can be recognized. The numerous quartz veins which traverse the Tsumis series are cut off at the base of the Nama system. Not one penetrates the basal

conglomerate. In the neighborhood of Nauzerus the unconformity is clearly recognizable. The base of the Nama beds transgresses from the Tsumis rocks over the porphyries of the Sinclair series and finally overlies the older granites.

Fish River series	Upper Nama
Schwarzrand series	
Schwarzkalk series	
Kuibis series	Lower Nama
basal beds	

TABLE 1.—TENTATIVE STRATIGRAPHIC COLUMN OF SOUTH WEST AFRICA

Age		Representatives in Naukluft area
Recent and Pleistocene		River deposits Terraces
	—unconformity—	
Tertiary		Gravels Desert deposits
	—unconformity—	
Lower Jurassic to Pennsylvanian	(Karroo system)	Stormberg volcanic rocks and sedimentary rocks *—unconformity—* Dwyka series (marine and continental)
	—unconformity—	
Late Precambrian?	(Nama system)	upper Nama lower Nama
	—unconformity—	
Precambrian	Damara system *—unconformity—* Tsumis system *—unconformity—* Sinclair formation *—unconformity—* Marienhof series?	

A distinction had to be made between the two series. The pre-Nama series was named the "Tsumis system", after farm Tsumis 80 miles south of Windhoek (Fig. 1). The Tsumis rocks deserve the status of a system (South African terminology) because of their great thickness and wide distribution. They can be followed from Nauzerus, past Tsumis and Gobabis, and far into Bechuanaland.

West of the Naukluft Mountains, the Tsumis system reappears under the Nama beds on farms Die Valle, Tsams, Sukses, and Felseneck. In this area the angular unconformity is very marked.

The late Proterozoic Damara system is represented by a series of highly folded dolomitic marbles and phyllitic shales in the northwestern corner of Plate 1. Its relationship to the Tsumis system is not yet clear, but the Damara system is probably the younger.

Nama System, Foreland Facies

Stratigraphic relationships.—Range (1912) subdivided the Nama formation as follows:

This subdivision is based mainly on the development of the Nama series in the Bethanie district. The Kuibis quartzite thins to disappearance toward the north, so that the Schwarzkalk series directly overlies the basal beds in the Naukluft area (Haughton and Martin, 1956).

Basal beds.—Few of the basal beds exceed 10 m in thickness, and many are even less than 1–2 m. Commonly a psephitic quartzite, 1–2 m (3–6 feet) thick rests on the basement. This basal conglomerate is overlain in places by alternating marly, dark-gray shales and thin layers of quartzite with an occasional thin, yellowish-brown dolomite band, and passes upward into the Schwarzkalk series.

Schwarzkalk series.—The limestones forming this series are distinctly bedded and are dark gray to bluish black owing to finely divided disseminated carbonaceous matter. Many of the black limestones are *stinkkalke*.

The series varies considerably in thickness. In the Zaris Mountains, south of Hauchabfontein, it attains a thickness of about 300 m (1000 feet). It thins toward the east and ex-

tends beyond the map area near Cambells Aub with a thickness of about 270 feet. It is here at least partly replaced by a shale-dolomite facies. The Schwarzkalk series where fully developed shows three great cycles of sedimentation (Pl. 2, figs. 2, 3). Each cycle is represented by about 330 feet of rocks, beginning with shales and thinly bedded limestones and ending with thicker beds. The incompetent shales representing the beginning of each cycle have guided the subsequent folding. In the neighborhood of Hauchabfontein, and east of Slangpoort, reef dolomites with stromatoporid structures occur in the upper Schwarzkalk beds. These shallow-water deposits seem to indicate a northeasterly ridge in the Nama basin which may have confined the later folding on its southeastern boundary.

Schwarzrand series.—On farm Urikos the lower part of the Schwarzrand series is well exposed at the foot of the Zaris Mountains.

Above the Schwarzkalk is 100–120 m (330–400 feet) of soft gray and greenish shales. They are overlain by dark-gray limestone, yellow dolomite, and brown-weathering quartzite beds. About 5 km farther north, between Urikos farmhouse and the southeast scarp of the Naukluft Mountains, this unit has been involved in the folding. It forms a line of northeast-trending hogback hills which follows the main Naukluft escarpment along its whole length (Pl. 6, *A*). In this horizon, as in the underlying Schwarzkalk beds, the facies changes toward the northeast. Between farms Urikos and Onis, limestone and dolomite beds grade into quartzites, so that northeast of Onis the whole zone consists of brown-weathering quartzites with brown shaly intercalations. The facies transition takes place in each bed. This quartzite horizon (Pl. 6, *A*, stippled layer in Schwarzrand series) has resisted erosion and is mainly responsible for the straight outline of the southeastern mountain face.

In the northeast corner of the map the quartzite swings away toward the south, forming the steep anticline of Achaub.

The quartzites are succeeded by brown shales. De Kock (1934) designates the shales below the quartzites as the Lower Shales and the higher shales as the Upper Shales of the Schwarzrand series.

Fish River series.—The red to reddish-brown and purple sandstones, quartzites, and shales of the Fish River series do not occur within the boundaries of Plate 1.

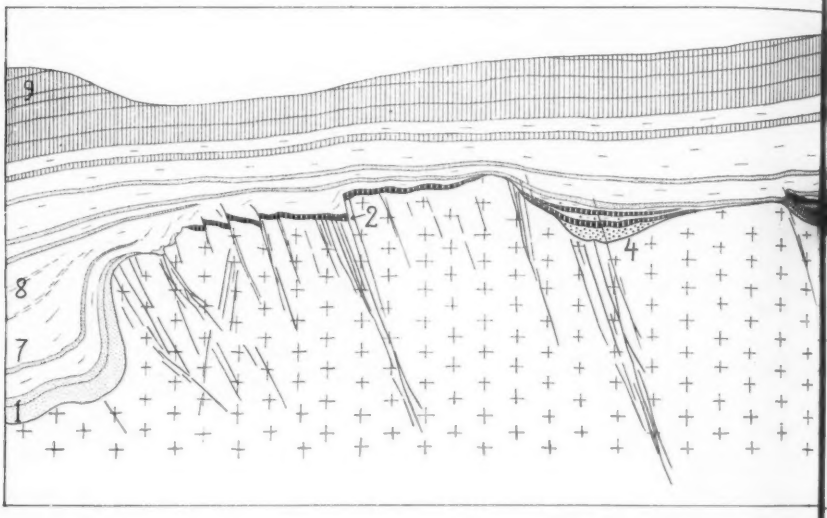

FIGURE 2.—WEDGES OF BASAL BEDS IN

Horizontal and vertical scales are equal. Dolomite and limestone of ridges (heavy black stripes unconformities within the wedges and deformation increasing from highest to lowest bed show th with dolomite matrix; 4, coarse psephitic quartzite; 5, dolomite; 6, dark-gray limestones alternati

Nama System, Naukluft Facies

Stratigraphic relationships.—In the mountains, the Nama system displays a great variety of formations. Deciphering of the succession is very difficult because of (1) intensive folding coupled with large-scale horizontal displacement of entire series and (2) absence of fossils. Therefore, in spite of excellent exposures, the relationship between the various series remains to some extent uncertain.

The Schwarzkalk and the lower part of the Schwarzrand series have the same development in the mountains as in the foreland, so that there can be little doubt that the whole sequence belongs to the Nama system (Pl. 1). The Schwarzkalk beds can be followed around the folded central part of the mountains. All the higher units have an entirely different facies in the mountains, characterized by a great variety of dolomites and limestones. The series which can be distinguished above the Schwarzrand are here named the Zebra, Pavian, Dassie, Kudu, and Klipbok series.

Basal and Schwarzkalk series.—The basal and Schwarzkalk beds link the foreland and the mountains. All along the western and northern flanks they form the base of the higher series. Their development remains the same everywhere.

The mountains, compared with the foreland, display a greater irregularity of basement topography. In the foreland, along the Zaris Mountains, the base of the Nama is an almost flat plain. Farther south, in the districts of Bethanie and Warmbad, the relief includes buried hills rising like monadnocks far above base level. In the folded area, by contrast, it shows depressions and gullies of varying dimensions. Some of the depressions existed before sedimentation began. They are filled with coarse local debris. Rimann (1915) and de Kock (1934) have described this feature from farm Nauzerus. Other depressions formed and deepened while the basal beds were being laid down, and some of these depressions were finally compressed into deep wedges.

The mutual reaction between sedimentation and deformation has led to some interesting phenomena. They can be observed particularly well on farms Abbabis and Stolzenfels. In Figure 2 the greater thickness of beds in the disturbed zone is immediately obvious. Both the number and thickness of strata increase. Movement was continuous, for the degree of deformation decreases upward. Each higher

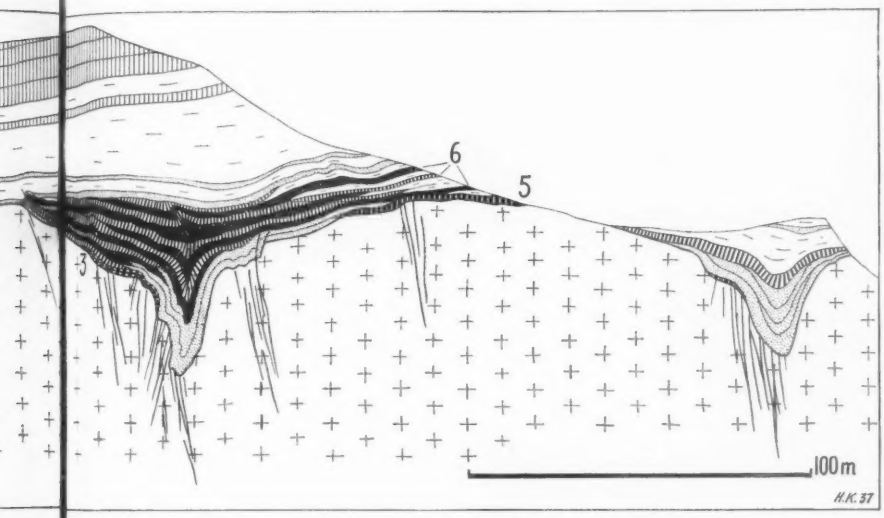

ASEMENT GRANITE (FARM STOLZENFELS)
to a quartzitic facies in the depressions; note the deepest depression to the southeast. Several small on, subsidence, and sedimentation were contemporaneous. 1, Quartzite; 2, dolomite; 3, conglomerate and dolomitic limestones; 7, thin quartzite; 8, gray shale; 9, black limestone of Schwarzkalk series.

bed is less intensely folded than its predecessor. In the central infolded wedge the basal bed is shortened by about 40 per cent; in the upper beds, shortening amounts to only about 5 per cent.

of the mountains. (In Figure 4, profile *c*, the base of the Schwarzkalk is at a lower elevation than in the other profiles.) This depression, too, existed at the start of sedimentation. The basal quartzite, normally only 3–12 feet thick, here

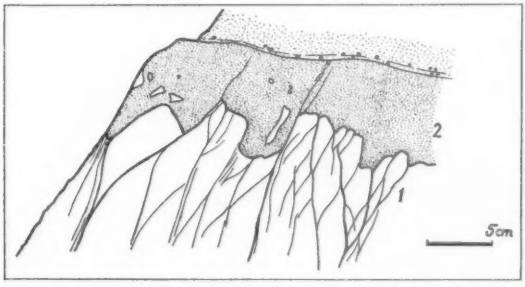

FIGURE 3.—DETAIL OF INFOLDED BASAL QUARTZITE

1, Granite; 2, quartzite. Small granite wedges bounded by two sets of chloritized shear planes have been forced into the apparently still unconsolidated sand. The overlying quartzite layer with a few small pebbles at its base has remained unaffected by these earliest movements.

Although only small areas are affected, movements and relief differences have influenced facies. On the ridges a dolomite band (bed 5 of Figure 2) comes to lie directly on granite, a phenomenon which has been observed nowhere else in the area. Furthermore, the dolomite facies of the ridges grades into quartzite in the depressions. Similar phenomena are well known in the case of the great ridges in geosynclines. But it is surprising to find them on such a small scale, where differences in level amount to only a few feet. This example shows that sedimentation can reflect small movements with great accuracy.

The different granite blocks are separated by steep, chloritized zones of movement, and these commonly caused infolding of wedges. Figure 3 gives a small detail from the edge of one of the deeper infolded wedges on farm Abbabis. It shows that during movement small granite wedges were dragged up until they became detached.

These profiles reveal an embryonic folding phase, a kind of orogenic unrest during the first subsidence, before deposition of the Schwarzkalk beds. Thus the contrast between deformed zone and foreland manifests itself early in the sedimentary record of the area.

The base of the mountains contains depressions of vastly greater dimensions. The present Tsondab Valley follows such a depression from farm Zais to the west. Here the base of the Nama is at its lowest point in the northern part attains 60–70 feet. At the Zipfelberg, north-northeast of farmhouse Abbabis, transgression of psephitic basal beds is clearly visible (Fig. 5).

In this Abbabis trough the Schwarzkalk series is largely undeformed. The reason for this will be discussed later. South and east of Abbabis, however, the Schwarzkalk is only incompletely preserved, owing to folding and unconformities.

The transition from Schwarzkalk to overlying Schwarzrand is by an alternation of thinly laminated limestones and shales, as in the foreland.

Schwarzrand series.—The Schwarzrand series has been affected by folding along the entire southeastern border of the mountains. The quartzite horizon is nearly everywhere overturned toward the southeast. The profiles of Plate 6, *A* through the southeast scarp of the mountains reveal that the Schwarzkalk overlaps the Schwarzrand series over wide areas as a thrust sheet or nappe. Profiles *b* and *f* show how the vertically hachured Schwarzkalk series overrides and planes off the stippled quartzite unit. Above this thrust sheet and interfolded with it, remnants of the Schwarzrand series occur in a facies somewhat different from that of the foreland. North of Gabis Spring a white dolomite, overlain in turn by a dark-brown sandy conglomerate, overlies the Schwarzkalk beds. The pebbles of the conglomerate are black limestone and gray dolomite exclusively. This conglomerate is probably connected with folding and emergence culminating in the un-

FIGURE 4.—PROFILES *a–k* THROUGH BOUNDARY REGION BETWEEN NAUKLUFT MOUNTAINS AND NAUCHAS HIGHLAND
1–3, Pre-Nama basement (1, granite; 2, Sinclair series; 3, Tsumis system); 4–8, Nama system (4, Schwarzkalk series; 5, Unconformity dolomite; 6, Pavian series, northern facies; 7, Kudu series; 8, Klipbok series). Datum of profiles, 600m.

conformity not more than a few hundred feet above. The conglomerate layers alternate with brown-weathering quartzites and are overlain by greenish shales of typical Schwarzrand facies. A similar succession, but without conglomerates, overlies the Schwarzkalk series northeast of Rokskeur (Pl. 6, *A*, middle of profile *b* on thrust sheet overriding stippled Schwarzrand quartzite).

This seems to be an early more or less local beginning of dolomite development which is so characteristic of all the succeeding series.

At the north and west end of the mountains no dolomites were observed, and Schwarzrand shales are preserved only locally above the Schwarzkalk series and underneath the unconformity.

Schwarzrand-Zebra unconformity.—This unconformity can be followed around the mountains (Pl. 1). Dipping inward at low angles, it forms a great shallow basin; it is everywhere overlain by a yellow-weathering dolomite. The dolomite is generally a little sandy and commonly contains small quartzite pebbles, normally less than 1 cm in diameter. Coarse dolomite crystals, possibly clastic, give a very characteristic appearance to this formation over wide areas. The thickness of this "Unconformity dolomite" ranges from 6 to 170 feet but is generally within a range of 15 to 30 feet. It normally overlies and truncates intensely folded Schwarzkalk beds or Schwarzrand shales folded into Schwarzkalk beds. Between Nauzerus and Stolzenfels it even transgresses from Schwarzkalk onto pre-Nama formations (Fig. 4, profile *f*). In this profile the Unconformity dolomite, represented as a thin black and white checkered band, transgresses from the southeast over Schwarzkalk beds onto a basement wedge capped by Tsumis quartzites and again onto Schwarzkalk beds without being disturbed. Only on the basement slope at the northwest end of the profile has it been affected by folding.

The Schwarzkalk series is commonly altered to a yellow rock and dolomitized below the unconformity. This alteration may in certain zones extend down into the Schwarzkalk to a depth of 20 m (60 feet).

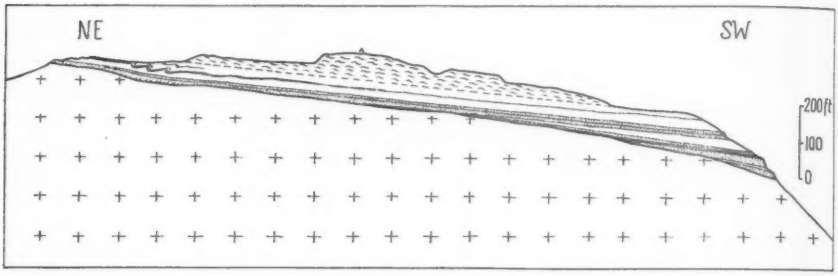

FIGURE 5.—ZIPFELBERG: TRANSGRESSION OF BASAL BEDS ON NORTHERN SLOPE OF TSONDAB TROUGH
From southwest to northeast the stippled basal quartzites progressively transgress the sloping granite surface

Northwest of Gabis a green silicified rock with asbestos nests was observed under the unconformity. This occurrence is very small and it has not been possible to determine whether it is an inclusion in the Schwarzkalk series or a basement wedge.

The relationship of the Unconformity dolomite to the overlying series is unusual and perhaps unique in two respects. First, the dolomite has no part in the intense folding and thrust tectonics of the higher units (Fig. 6). Wherever it is observed, with rare exceptions, it is found undeformed between intensely folded Schwarzkalk beds below and intensely folded piles of nappes which are sheared off immediately above the dolomite. In addition, surprisingly, different units overlie the Unconformity dolomite in different parts of the mountains. On farms Naukluft, Ubusis, Tsams Ost, and in the western part of Die Valle, the Zebra series succeeds the Unconformity dolomite. In the eastern part of Die Valle and along the edge of the mountains between Naukluft and Büllsport and thence to the northeast, the Dassie series overlies the dolomite. On farms Zais, Abbabis, Stolzenfels, and Nauzerus the northern facies of the Pavian series succeeds it; underneath the Tsondab Valley on farm Büllsport, the southern facies probably directly overlies the dolomite. Thus, no less than four different series are in contact with Unconformity dolomite (Pl. 6, *B*).

FIGURE 6.—VIEW OF MOUNTAIN FACE ON FARM TSAMS
Undisturbed Unconformity dolomite (checkered) overlies and truncates folded Schwarzrand shales and is in turn overlain by the highly folded Zebra series, consisting of shales (white), a quartzite band (stippled), and dolomite (vertical hachuring).

These circumstances are so unusual that conceivably the unconformity in each place is not the same one; possibly this may not be an unconformity at all. In fact, while mapping was in progress, the unconformity was for a long time regarded as a thrust plane, but eventually this view became untenable. Fortunately exposures are so good that the main inferences are no longer in doubt.

On farms Tsams Ost and Die Valle the unconformity is well exposed over great distances. For many miles the Unconformity dolomite may be observed as a straight yellow band in the mountain flank. It is everywhere overlain and underlain by intensely folded formations. (*See* Plate 7, in which the Unconformity dolomite is represented by the checkered line, and Plate 3, figure 1, which is a photograph of part of the southeastern end of Plate 7. Note how evenly the Unconformity dolomite underlies the imbricated higher dolomite anticlines.) The sedimentary nature of the lower contact is best seen where it transgresses Schwarzkalk beds; there it is completely undisturbed and not even jointed over wide areas. Figure 7 shows conditions at a hill 1.4 miles northwest of the farmhouse of Lemoenput. As the hill is immediately west of the road, the unconformity is easily accessible. The wholly undisturbed dolomite overlies the somewhat irregular erosion surface, filling pockets between truncated Schwarzkalk beds. It also contains small fragments of Schwarzkalk near its base. The sedimentary nature of the contact is unmistakable.

The best examples of different series overlying this dolomite occur on farm Die Valle. In the Gams River Valley the dolomite extends from the base of the Zebra series under the Dassie series without being folded or faulted. Moreover, the folds of the Zebra and Dassie series have quite different axial trends, and the two series show no stratigraphic resemblances. Where they meet, above the dolomite, their fold axes form a complicated interference pattern. The Dassie series appears to intrude the Zebra series tectonically and to "underthrust" it. Away from this contact zone no fragment of the Dassie series exists underneath the Zebra series, and vice-versa. Here also, the Unconformity dolomite rests smoothly underneath the two series.

Along the eastern cliffs of the Gams Valley the Unconformity dolomite rests perfectly smoothly (although it is somewhat crushed) underneath the steeply imbricated Dassie series (Pl. 3, fig. 1; Pl. 7). From there it can be followed northward continuously around the corner of the mountains to below Trig Point Danab, where the Pavian series takes the place of the Dassie. There the Pavian is pressed against the Dassie, and in both the folding trend is the same. There, too, the Unconformity

dolomite remains unaffected underneath the contact zone and extends to form the base of the Pavian series everywhere on farms Zais, Stolzenfels, and Nauzerus. In this area not even the smallest remnant of the easily recognizable Dassie series has been found (Fig. 8).

sufficient to explain the position of the Dassie series.

The Dassie series in no way resembles the other three. Coloration differences are especially conspicuous. In contrast to the greens and blues of the other three series, the Dassie rocks are

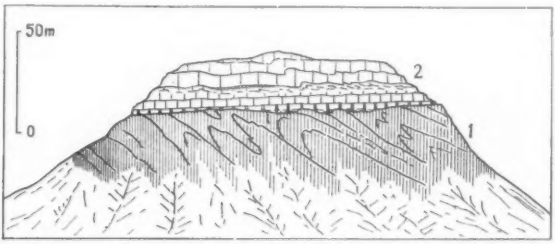

FIGURE 7.—UNCONFORMITY ABOVE FOLDED BLACK LIMESTONE
1. Black limestone of Schwarzrand series; 2, Unconformity dolomite

In the southern part of the mountains the contact between the Dassie and the Zebra series is well exposed on farm Naukluft. In the contact zone the two series are intensely sheared, interfolded, and brecciated, but the Unconformity dolomite underneath the contact zone is completely unaffected.

There can thus be no doubt that the unconformity is directly overlain by several very different formations. What can be their relationship—especially their age relationship? They meet only at narrow tectonic contact zones which allow no unequivocal interpretation. Hence the nature of their contacts with the Unconformity dolomite is of great importance. Conditions are clearest in the case of the Zebra series. Against it the Unconformity dolomite has no sharp upper contact.

It grades in a normal sedimentary sequence of alternating dolomite, quartzite and gray limestone bands into the lowest portion of the Zebra series. No doubt the Zebra series immediately and without a break overlies the Unconformity dolomite. Conditions are not quite so clear in the case of the Pavian series. But the close resemblance of the Zebra to the southern facies of the Pavian series (Fig. 8) makes it likely that the two might correlate, representing contemporaneous facies deposited in different parts of the Naukluft Basin. The absence of facies transitions is probably due to structure. These assumptions might explain superposition of the Zebra series and of the southern and northern facies of the Pavian series on the same unconformity. They are not red and purple. Such differences would seem to preclude facies substitution. Since at least the Zebra series succeeds the Unconformity dolomite normally, the Dassie must be younger than the Zebra. The nature of the contact of the Dassie with the Unconformity dolomite does not contradict this assumption. The purple slates which form the base of the Dassie are in all places intensely sheared directly above the Unconformity dolomite. Hence the contact may very well be tectonic. This reasoning leads to the conclusion that the Pavian or the Zebra series has been pushed away wherever the Dassie series rests on the unconformity (Pl. 6, *B*).

No unconformity could be discovered in the equivalent foreland succession. But, as mentioned, a portion of the Schwarzrand series is still preserved below the unconformity, at the edge of the mountains. Hence the unconformity must lie within or above the Schwarzrand series.

It is worth mentioning that south of Maltahöhe, layers and lenses of psephitic sandstones are intercalated in the upper divisions of the Schwarzrand series. It thus seems reasonable to assume that the unconformity correlates with rocks or with a diastem in the upper part of the Schwarzrand series.

Succession Above Unconformity Dolomite

Figure 8 shows stratigraphy and assumed correlations between the Zebra and northern and southern Pavian series.

The northern and southern facies of the

Pavian series meet at the Pavianskopf, on farm Blässkranz. There the northern facies is pressed against the southern facies in steep folds and wedges. No transitional facies is preserved, but series has been deformed to such an extent that there can be no hope of finding striations or facets on the blocks. However, the psephitic slates and the conglomeratic limestone resemble

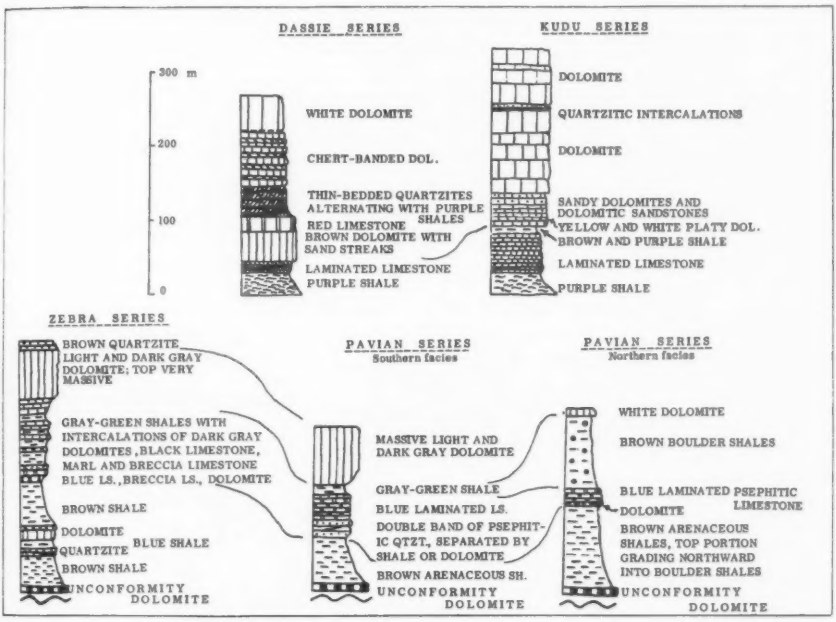

FIGURE 8.—STRATIGRAPHY OF ZEBRA, PAVIAN, DASSIE, AND KUDU SERIES, AND PROBABLE CORRELATIONS
Thicknesses approximate

both are overlain by the Kudu series, right across the contact. The main difference between the two facies is that the northern facies is much thicker and more clastic. Within the boulder shales of the northern facies the proportion of basement constituents increases from south to north.

Many of the conglomerates of the northern facies have the appearance of tillites. The components, neither rounded (with exception of basement constituents) nor sorted, are embedded in a silty or shaly matrix. On farm Blässkranz more than 99 per cent of the components are Schwarzkalk and dolomite fragments. All sizes occur, from small splinters to sharp-edged plates and blocks measuring several meters.

In the Little Karas Mountains, Schwellnus (1941) found a tillite in the Schwarzkalk series. Hence tillites might be expected elsewhere in the Nama beds. Unfortunately the Pavian certain Alpine sedimentary breccias and Alpine wildflysch much more than they do glacial deposits. These Alpine sediments have been correlated with orogenic movements, and the same correlation appears possible and probable in the Naukluft Mountains.

The breccia limestones of the Zebra series, too, are probably an indication of submarine slumping during sedimentation. On the whole the sediments seem to reflect tectonic unrest and quickly changing conditions.

The Dassie and Kudu rocks are easily distinguished by their red and purple coloration. They resemble one another to such an extent (Fig. 8) that they may well be contemporaneous.

In this case, the Dassie would represent a southern facies, and the Kudu a northern facies. On the other hand, the Kudu may be younger, and the resemblance may be due to cyclic sedimentation recurring in each series. The

absence of fossils makes it impossible to determine which of the two alternatives is correct.

The Klipbok series occurs only on farms Noab and Remhoogte. On farm Noab, Kudu dolomite is overlain by brown arenaceous slates, which in places begin with a coarse sedimentary breccia of dolomite blocks, derived from underlying Kudu dolomite. It will be shown that deposition of this rock was related to tectonic movements.

The brown slates in turn are overlain by a breccia limestone. It consists of more or less closely packed dolomite blocks and fragments in a blue-limestone matrix. The resemblance to the breccia limestone of the Pavian series is striking. In the Klipbok breccia several pieces of the characteristic sandy Kudu dolomites were found, proving the younger age of the Klipbok with respect to the Pavian which underlies the Kudu, and in which no sandy dolomite fragments have been observed.

As the Naukluft Mountains have been intensively eroded since the folding, it appears probable that the Klipbok series, as preserved on farm Noab, is only a remnant of a much thicker succession.

Age of the Nama System

The age of the Nama system is still uncertain. A number of fossils have been found (Gürich, 1930; Haughton, 1929; Richter, 1955). None of these fossils is representative of a definite age, but because of the fossils most writers have assigned a Cambrian age to the Nama system. If this is correct, it is astonishing that no diagnostic fossil has yet been found in hundreds of square miles of excellently exposed marine sediments well suited for the preservation of fossils. A late Precambrian age therefore does not seem impossible.

An upper age limit has been established in Cape Province, where the Nama system is found to be older than the Lower Devonian or Upper Silurian Table Mountain sandstone. A lower limit can be recognized in the Witpütz area, where the Nama system overlies the highest members of the Kaigas system. The Kaigas, in turn, is probably the equivalent of the Damara-Otavi system. The Damara and Otavi systems were formerly considered to be of different ages, but it has now been established that they are of the same age and that the Damara is the orthogeosynclinal equivalent of the Otavi, a shelf facies. The Damara-Otavi system is lithologically very similar to the Roan series of the Katanga system, and age determinations based on radioactivity strongly support their equivalence. Mineralization and orogenesis of the Katanga system are dated at $\pm 630 \times 10^6$ years, whereas late syntectonic pegmatites of the Damara system have given age determinations ranging from 600 to 670×10^6 years (Holmes and Cahen, 1955); hence an age of about 630×10^6 years for the final folding phase of the Damara-Otavi system seems highly probable.

In the Witpütz area the Nama beds are conformably folded together with Kaigas rocks but toward the east and the north transgress for hundreds of miles over older basement rocks, where they are entirely undeformed. The same relationship exists in the Katanga system of the Belgian Congo between the Roan series and the overlying Kundelungu series (Cahen, 1954), and, as the Nama system is lithologically very similar to the Kundelungu series (which has also been regarded as Paleozoic), it seems not at all

---

PLATE 2.—PHYSIOGRAPHY OF THE NAUKLUFT AREA

FIGURE 1.—The great Blässkranz Tertiary spring deposit of calcareous tufa (400 feet high).

FIGURE 2.—Undeformed Scharzkalk series, Zaris Mountains. The three cycles of sedimentation form structural benches along the mountain sides.

FIGURE 3.—View from Zaris toward the Naukluft Mountains. Foreground: undeformed Schwarzkalk formation. Background: southeast scarp of Naukluft Plateau.

PLATE 3.—DEFORMATION IN THE NAUKLUFT AREA

FIGURE 1.—Imbricated Dassie series on undisturbed Unconformity dolomite. This photograph shows a part of Plate 7. Unconformity dolomite visible between the two white X's.

FIGURE 2.—Pavian series on farm Blässkranz. Dolomite and black limestone (L) fragments in shaly matrix oriented and elongated (parallel to knife) at right angles to fold axes (black arrow at right). Below the knife a dolomite fragment (X) has been broken by stretching. Tension fractures are filled with white calcite. Note symmetrical conjugate-joint system. Photograph taken in neighborhood of Figure 3 of this plate, which shows accompanying folding.

FIGURE 3.—One of the southern gorges on farm Blässkranz. Pavian series piled up in folds underneath Kudu nappe, (detail of structures shown in Plate 8, *A*).

FIGURE 1

FIGURE 2

FIGURE 3

FIGURE 1

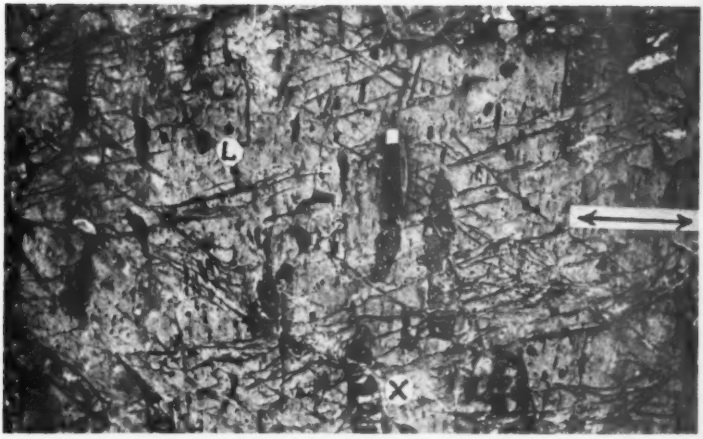

FIGURE 2

FIGURE 3

DEFORMATION IN THE NAUKLUFT AREA

FIGURE 1

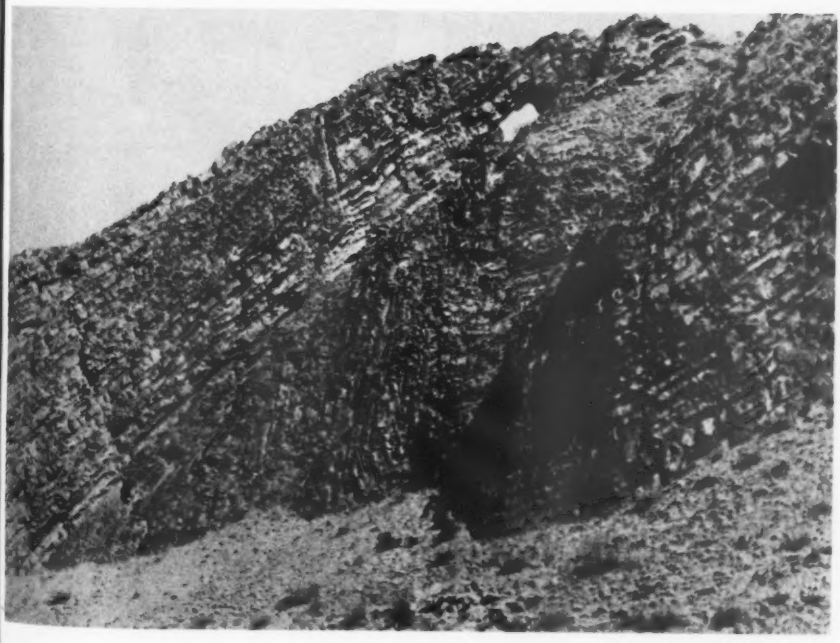

FIGURE 2

FOLDING IN THE NAUKLUFT AREA

FIGURE 3

FIGURE 1

FIGURE 2

impossible that the Nama might be the equivalent of the Kundelungu with an age of approximately 630 × 10^6 years, and that it might, in the Naukluft area, be involved in the latest phase of Damara orogeny. Unfortunately no age determination for the folding of the Kaigas system is yet available.

Figure 1 shows the folding trends of late Precambrian orogeny; it also shows how snugly the Naukluft folding trends fit into one of its major arcs.

Post-Nama Deposits

The Karroo system is represented by a few remnants of Dwyka tillite, as was mentioned.

The Tertiary comprises fossilized dunes which are covered by recent dunes of the Namib Desert. The former are brownish-red, little consolidated sandstones showing dune structures. Their extent coincides essentially with that of the recent dunes.

The thick, calcified conglomerates, screes, and sands which fill all the valleys of the Namib Desert and cover large parts of the plains are younger than the fossilized dunes. They attain thicknesses of several hundred feet in places.

The great tufa promontaries (Pl. 2, fig. 1) may be contemporaneous with these fanglomerates. The tufa deposits were built up mainly by algae. The flow of the springs must have been far greater at the time of tufa formation than it is at present. Tufa formation on a small scale may be observed at the springs to this day. But big tufa deposits are being destroyed today, and in some cases only a few remnants still adhere to the cliff faces.

Summary of Stratigraphic Results

Facies of folded Nama beds in the Naukluft Mountains are very different from their equivalent foreland types. Only the Schwarzkalk and the lower portion of the Schwarzrand series show the same development in both areas. In the folded area they are truncated by an unconformity which is not present in the foreland; above this unconformity the folded area shows a rich variety of shales, limestones, breccia limestones, quartzites, and dolomites, whereas the foreland is characterized by the monotonous clastic rocks of the upper Schwarzrand and Fish River series. The sedimentary sequence in the folded area reveals several cycles of sedimentation. Each cycle (series) seems to have begun with subsidence, followed by deposition of shales leading to an alternation of shales, quartzites (or conglomerates), distinctly bedded limestone, and dolomite, and ended with formation of a massive dolomite. This sequence is typical for basin filling. Each series has at its base a natural gliding horizon, the shales. These are overlain by beds of widely differing competence, which the deforming stresses have affected in a different way in each series. These cricumstances are of considerable importance to the subsequent tectonic history of the rocks.

The succession as a whole with its rapid alternation of clastic rocks, limestones, and reef dolomites recalls the succession of some of the Alpine nappes, especially the Upper East Alpine nappe. This resemblance is increased by intraformational breccias, conglomerates, and wildflyschlike rocks. In contrast to "normal" geosynclinal successions, however, the Naukluft succession is much thinner. The following paragraphs will show that deformation too, notwithstanding its intensity, differs in many respects from that of the great folded belts of the earth. In more ways than one the Naukluft Mountains reveal a miniature orogeny.

TECTONICS

Distinctive Features of Tectonic Style

The tectonic style of the Naukluft Mountains has certain unusual features not known elsewhere.

PLATE 4.—FOLDING IN THE NAUKLUFT AREA

FIGURE 1.—Detail from Figure 10.

FIGURE 2.—Gams Valley on farm Die Valle. Folding and thrusting of chert-banded dolomite, Dassie series.

PLATE 5.—STRUCTURE DETAILS

FIGURE 1.—Purple shales with thin limestone bands of Kudu series showing folding and intense cleavage. Photograph taken in gorge shown on Figure 3 of Plate 3.

FIGURE 2.—Calcite-filled symmetrical joint system. Developed in thin shale band between two deformed limestone bands. Dassie series on farm Büllsport.

FIGURE 3.—Boudinage structure. Formed by brecciated shales between thin layers of deformed limestone. Dassie series, Aub Valley, farm Büllsport.

Deformation is very great. In the frontal zone the beds are piled up in isoclinal folds and imbricated structures; in the central area they are torn, dragged, and rolled out; at the northern edge they cascade into the basin in true cataracts of folds. The movement is oriented toward the south and southeast. Recumbent folds and even down-facing folds (*plis retournés*) abound. The folding is as unidirectional as in the Alps.

In spite of its great intensity, the folding exhibits great freedom from confinement. This freedom is expressed in all structural features, large and small. There is not the high degree of parallelism which is a feature of intense folding in the Alps, and each series has a different deformation style. The nappe front forms a wide arc, and the fold axes are relatively freely oriented. Transverse or diagonal faults are absent.

In addition, the fold axes are differently oriented at different tectonic levels ("axial unconformities"). No confining frame or load can have contained or controlled these divergent movements.

The intensity of metamorphism is low. The shales are changed to slates or phyllitic shales at most. The limestones are only slightly recrystallized, and all the thicker dolomites are brecciated.

The thrusting movement is unusual. In spite of great displacement, older rocks are thrust over younger ones for great distances only exceptionally. The nappes are merely sheared-off sediment packs which remain, more or less, in their true stratigraphic sequence. Real overthrusts are entirely confined to the frontal region.

Tectonics of the Basement

The basement is well exposed all along the northern and western edges of the Naukluft range. As already shown, movement began early in the sedimentary history of the basin. Initial subsidence is connected with these early movements which also affected deposition of the basal beds. Figure 2 shows steep chloritized shear zones striking northeast to north-northeast which are related to this movement. The northward- and southward-dipping faults seem to be conjugate shear planes. Vertical movement of wedge-shaped basement blocks along these shear planes resulted in some horizontal shortening, but the vertical component (subsidence of the basin) was dominant.

Observable zones of movement within the basement are common only at the northern and northwestern edge of the basin, where the basement surface rises abruptly: this is another indication that these comparatively small movements are subsidiary to basin subsidence (Fig. 4).

Undisturbed Schwarzkalk beds overlap many of these movement zones. Hence no appreciable movement appears to have taken place during Schwarzkalk deposition.

Folding in Schwarzkalk and Lower Schwarzrand Beds

Deposition of these sediments was followed by a second, intensified folding phase. During this phase basement movements were a more violent repetition of the movements described in the last few paragraphs. They took place only along zones which had undergone movement in the first phase. Cases of appreciable downfolding into the basement again appear to be restricted to the north and northwest edge of the basin. The most important downfold roughly follows the contact between the Sinclair series and the Tsumis system. It can be followed from the southern end of farm Abbabis southwest as far as farm Sukses, a distance of about 20 miles. The greatest extent of this downfolding is attained by a wedge of Schwarzkalk rocks which extends 600 to 1000 feet into the basement.

Profiles in Figure 4 show the style of this downfolding. Lateral compression has resulted in predominantly vertical movements of the basement (Fig. 9). It is interesting to note how closely these small granite wedges, bounded by steep, slightly curved thrust planes, resemble the great granite wedges which in the Alps form the northern slope of the Aar massif against the basin filled with Helvetic nappes. But as seen in Figure 9, the strike of the granite wedges and zones of downfolding is nearly at right angles to the axial trends in the higher units.

Above the zone of downfolding the folding style of the Schwarzkalk series is entirely different. The intensity of folding is variable, but the folds are in all cases overturned toward the southeast, and in each profile the intensity of movement increases toward the top. The base is undisturbed over wide areas, whereas the upper beds are compressed into tight, commonly isoclinal folds. Even where the Schwarzkalk series is apparently undisturbed, as along the Tsondab Valley between Zais and Abbabis (Fig. 4, profile *c*), closer observation shows that plicated horizons occur between the unde-

formed beds. The undeformed portions have undergone relative movement along bedding planes. Each higher unit has transgressed the unit immediately below it and each has probably drag folding along the zone of movement. The planes of detachment are generally along beds of thin flagstone which form the intercyclic boundaries. The principal displacement, however, took place along the shales at the base of the rocks representing the lowest cycle. Figure 4 shows particularly striking profiles along the slopes of the Steinfeld Range between Stolzenfels and Nauzerus. The main slope between the granite highlands and the basin, together with its sedimentary cover, is still preserved in profile *f*. The Schwarzkalk (4) with its overturned folds looks like a petrified cataract. The Unconformity dolomite (5) transgresses folded Schwarzkalk rocks onto a basement wedge. Toward the northwest, higher up the slope, the unconformity has been locally involved in the folding, whereas the Kudu nappe (heavy black stripes) shows, on the southeast, down-facing folding on a grand scale. Wildflyschlike boulder shales of the Pavian series (6) separate the Kudu nappe from the scarcely disturbed unconformity. In the upper profiles the main slope, which must have been to the northwest of the profiles, has been destroyed by erosion. On profiles *d* and *e* the main slope can still be inferred from remnants of intensely plicated Schwarzkalk beds. The folded Schwarzkalk has been considerably eroded underneath the Unconformity dolomite in profiles *e* to *i*, but it is intact and practically undeformed in profile *c* in the predepositional depression underlying the present Tsondab Valley. In profiles *a* and *b* the basement rises again, and on the northwest side of profile *a* only a thin remnant of Schwarzkalk remains underneath the checkered Unconformity dolomite as in *e* to *i*. A younger fault, related to the formation of the present African Escarpment has probably lifted the southeast half of profile *a* relative to the northwest half. The Schwarzkalk series appears to tumble into the basin in cataracts of folds; around the foot of the Steinfeld Range the fold axes have arranged themselves in an arc, a feature which the higher series repeats on a grander scale.

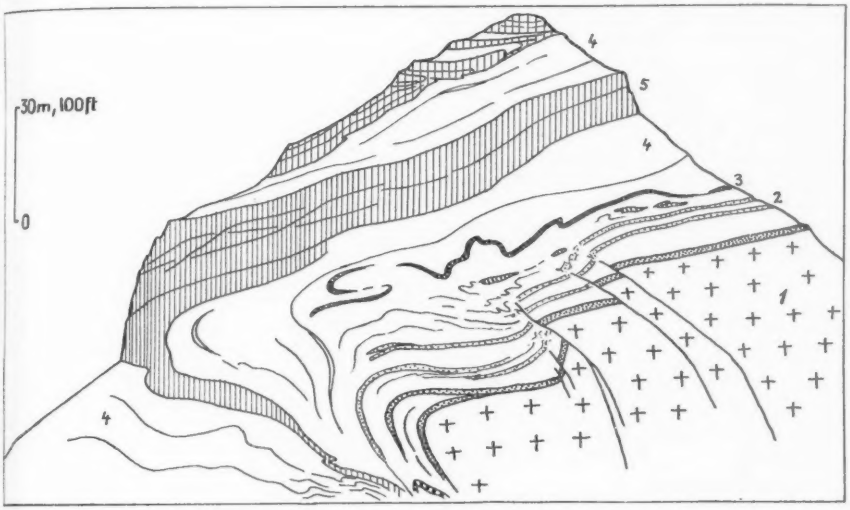

FIGURE 9.—SCHWARZKALK SERIES WEDGED INTO BASAL GRANITE AT ENTRANCE TO GAMS VALLEY ON FARM "DIE VALLE"

1, Granite; 2, shales and quartzite; 3, dolomite; 4, thinly bedded black limestone; 5, massive black limestone

Folding was followed by a slight emergence leading to truncation of the folded beds.

"Double Unconformity"

The unconformity is probably the most unusual structure in this area, which is rich in extraordinary structures (Fig. 6; Pls. 1, 7).

On farms Tsams and Die Valle the unconformity is visible from afar. Identifiable by the

yellow dolomite band (represented in all profiles by a black and white checkered line) it runs in a straight line between blue-black folded Schwarzkalk beds and the folded brown shales and gray dolomites of the Zebra series or the purple shales and yellowish-brown dolomites of the Dassie series. This unconformity between two independently folded piles of sedimentary rocks remains completely unfolded for many miles. Between farms Die Valle and Tsams the unconformity is a smooth plane, dipping about 2° southeast, and for a distance of 10 miles shows no trace of folding or serious disturbance of any kind. In most places where the Unconformity dolomite rests on black limestone, its lowest bands are sparsely jointed. Where it overlies shales, it is commonly somewhat crushed and brecciated but not folded. The upper layers of the Unconformity dolomite, however, are sheared and slightly folded. The intensity of folding increases progressively upward, so that the rocks of the Zebra or Dassie series, respectively, are strongly overfolded and imbricated. The unaffected dolomite between an upper and a lower folded series represents a "double unconformity".

The fold axes above and below the unconformity diverge over wide areas. Folding of the Unconformity dolomite has been observed only at the northern edge of the mountains, between farms Stolzenfels and Nauzerus. These folds represent comparatively unimportant movements, caused by high-angle thrusting at the northern slope of the basin (Fig. 4, profile *f*). Apart from this zone the dolomite appears to have remained unaffected by the intense folding of the overlying formations. On the other hand it transgresses, without disturbance, up to the deep wedges of Schwarzkalk rocks between farms Narib and Die Valle.

Thus the folding of all the different higher series implies complete shearing off (*décollement*) above the Unconformity dolomite.

Tectonics of Zebra Series

Compared with the other units, the Zebra series shows an extraordinarily loose, irregular style of folding (Fig. 6); axial alignment, too, differs from that of the Kudu and Dassie series in the whole western part of the area. The Zebra series must therefore have been folded independently of the other series.

The time of folding cannot be determined exactly. Contact phenomena at the Dassie nappe contact make it appear probable that folding of the Zebra series had ceased before the arrival of the nappes. The time lag cannot be determined. The Zebra series may have been folded immediately following its deposition or more or less contemporaneously with the higher units.

The southernmost exposure of the Zebra series is at the mountain border between Urikos and Onis. There its structure is somewhat different from that farther north. Instead of loose overturned folds, there are low-angle imbricated structures (Pl. 6, *A*, profiles *g* and *h*). This may be explained mechanically by friction along the plane of detachment: the structure originated as friction impeded movement.

Tectonics of Pavian Series

Northern facies area.—Between Zais, Nauzerus, and Garis the Pavian series rests on the unconformity. It begins with a great thickness of brown and green phyllitic boulder shales containing variable proportions of granite and porphyry pebbles and boulders. The tectonic style of these beds is very different from that of the Zebra series.

The rocks show intense cleavage and commonly puckerings, but actual folding is rare in the northern area. Superficial observation, therefore, may give the impression that the series is hardly disturbed. Examination of the conglomerate pebbles, however, shows that the limestone and dolomite inclusions are intensely sheared and elongated, granite blocks have been moulded into droplike or lenslike shapes, and that all these deformed elements are parallel within the schists (Pl. 3, fig. 2), elongated at right angles to the fold axes.

As a result of movement, the conglomeratic blue limestone has been eliminated over wide areas. Where it is flat it is thinned out to such an extent that its dolomite pebbles are nothing but smeared stripes, and the rock itself has been changed into a fine-grained, laminated bluish marble, whose original texture is preserved only in apices of folds. In the northern part of the mountains the white dolomite at the top of the series is preserved only in small remnants. On the other hand, it is accumulated in accordion folds in the frontal zone on farm Blässkranz (Fig. 10; Pl. 8, *A*). These are all indications of intensive deformation under load, such as might be produced by a *traineau écraseur*. This function was probably fulfilled by the thick dolomite slab of the Kudu series which caps all the plateaus and ridges.

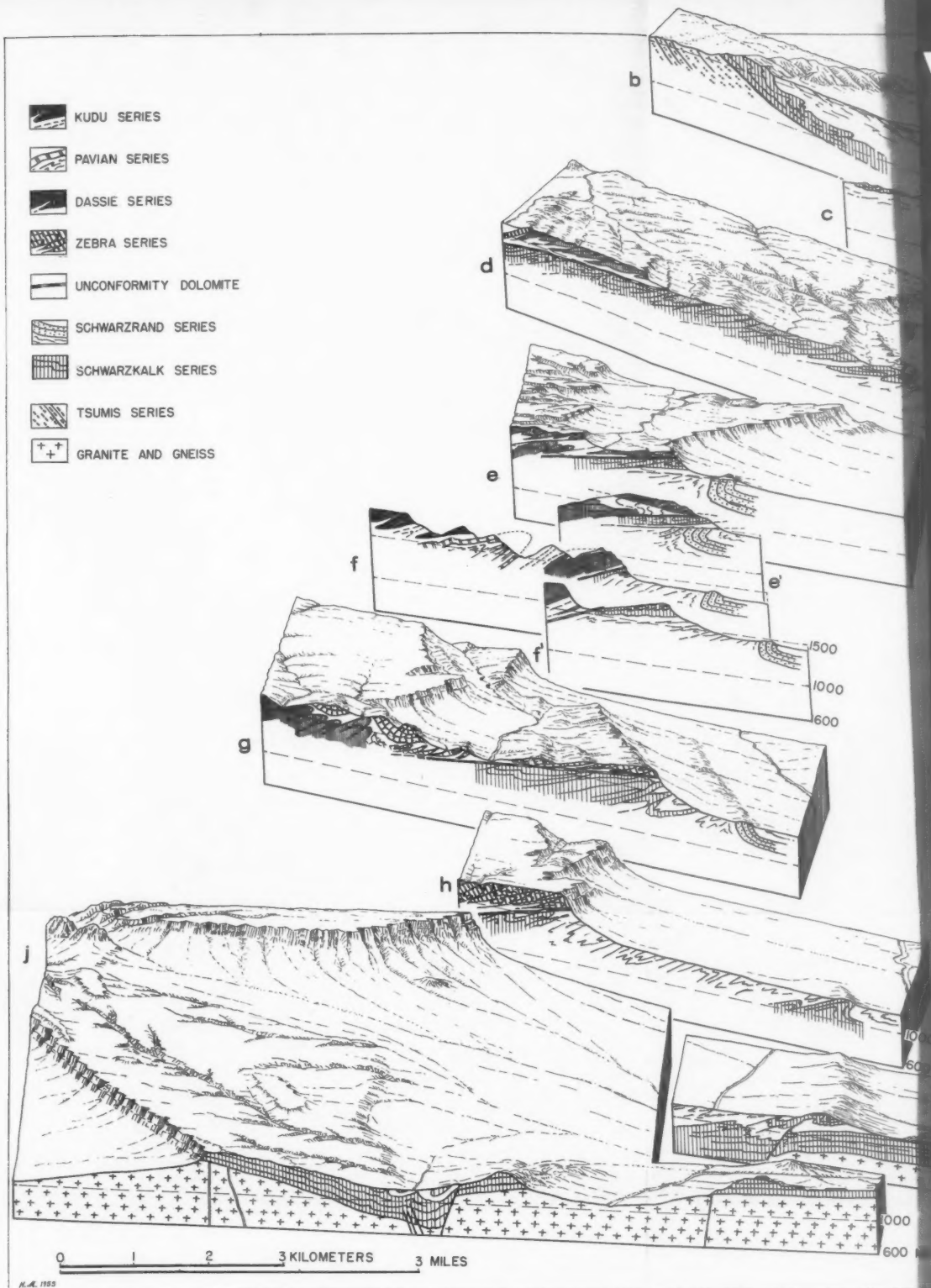

A. SECTIONS THROUGH SOUTHEASTERN FRONT OF NAU

The profiles show the boundary between undeformed foreland and mountains. In the foreground are basement faults which may have deter-

Schwarzrand beds of the fo truncates the folds in the Se

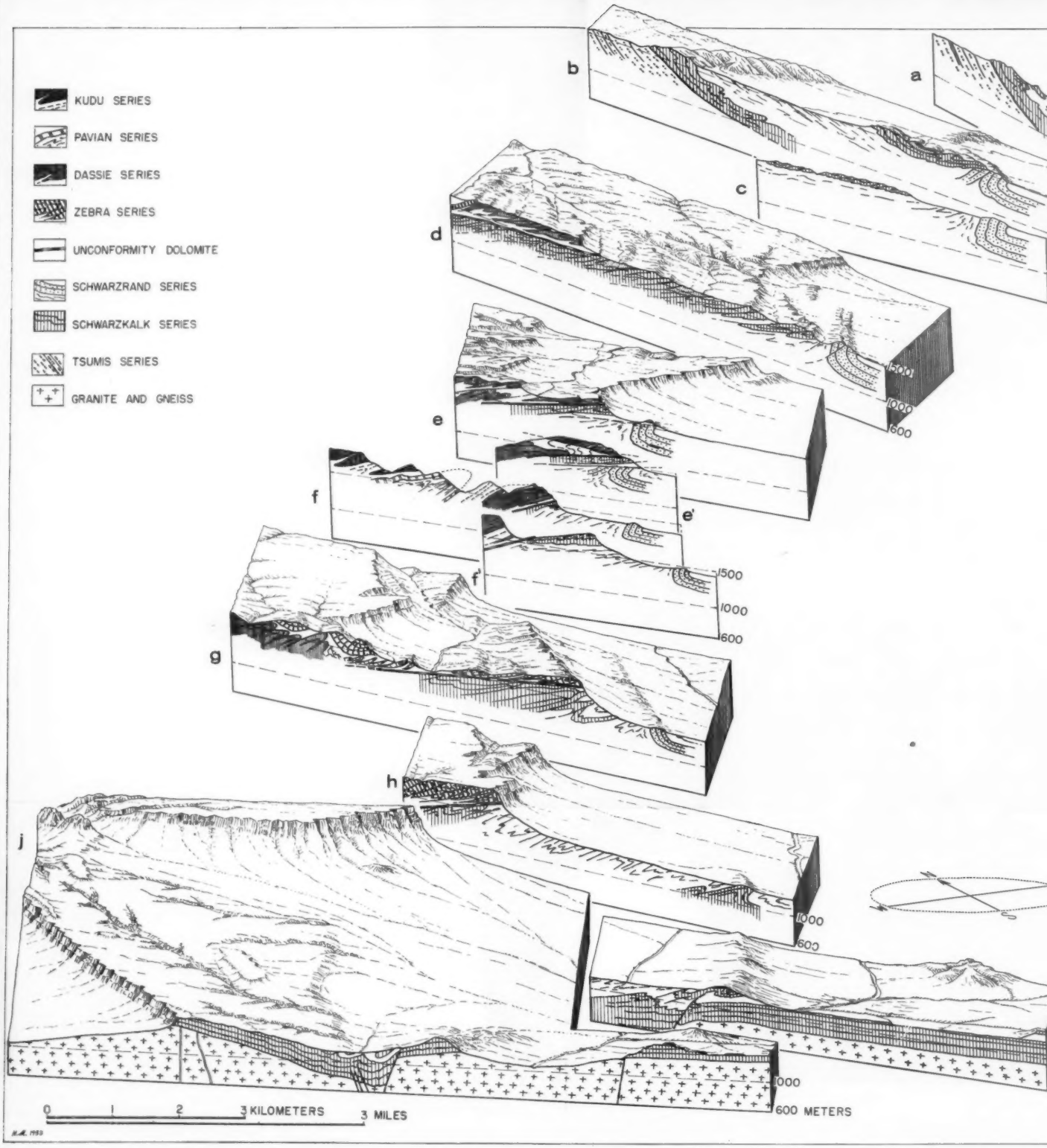

A. SECTIONS THROUGH SOUTHEASTERN FRONT OF NAUKLUFT MOUNTAIN

The profiles show the boundary between undeformed foreland and mountains. In the foreground are basement faults which may have determined the position of this boundary. In profiles *b*, *f*, and *g*, the Schwarzkalk Schwarzrand beds of the foreland. Unconformity dolomite (ch truncates the folds in the Schwarzkalk thrusts. In profiles *g* a overlain by the Zebra series, in the adjacent profiles by the Dassie

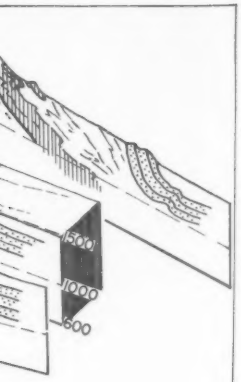

AINS

e (checkered)
s *g* and *h* it is
assie nappe.

V70
1959
UM

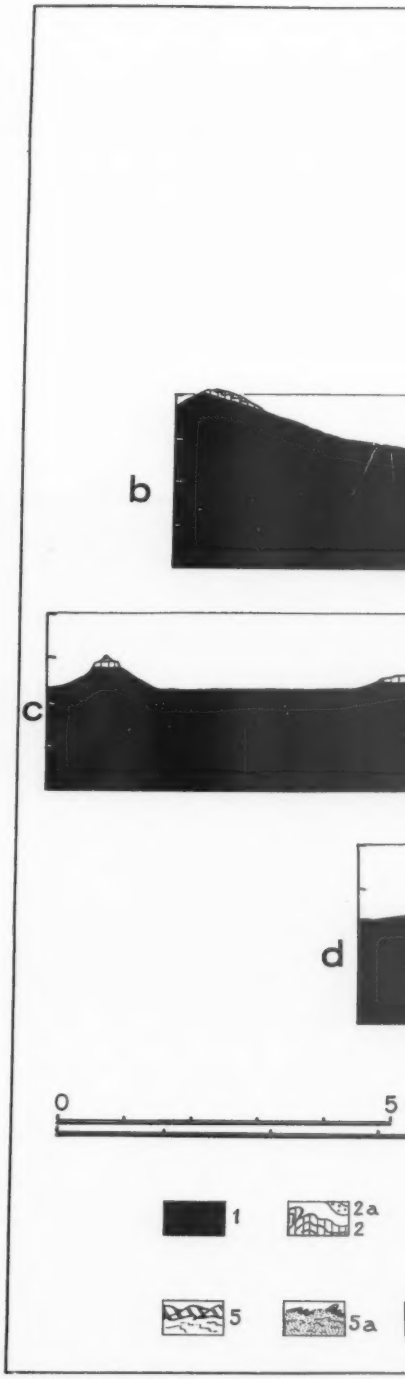
b
c
d
0
5
1
2a
2
5
5a

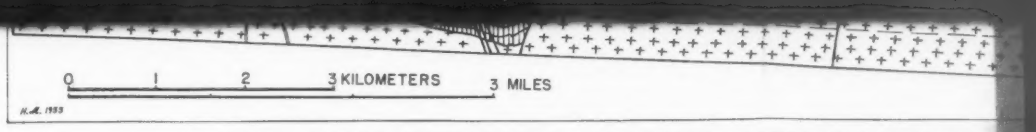

A. SECTIONS THROUGH SOUTHEASTERN FRONT O

The profiles show the boundary between undeformed foreland and mountains. In the foreground are basement faults which may have determined the position of this boundary. In profiles *b*, *f*, and *g*, the Schwarzkalk beds of the mountains override, as a thrust sheet, the overturned younger Schwarzrand beds o truncates the fold overlain by the Zeb

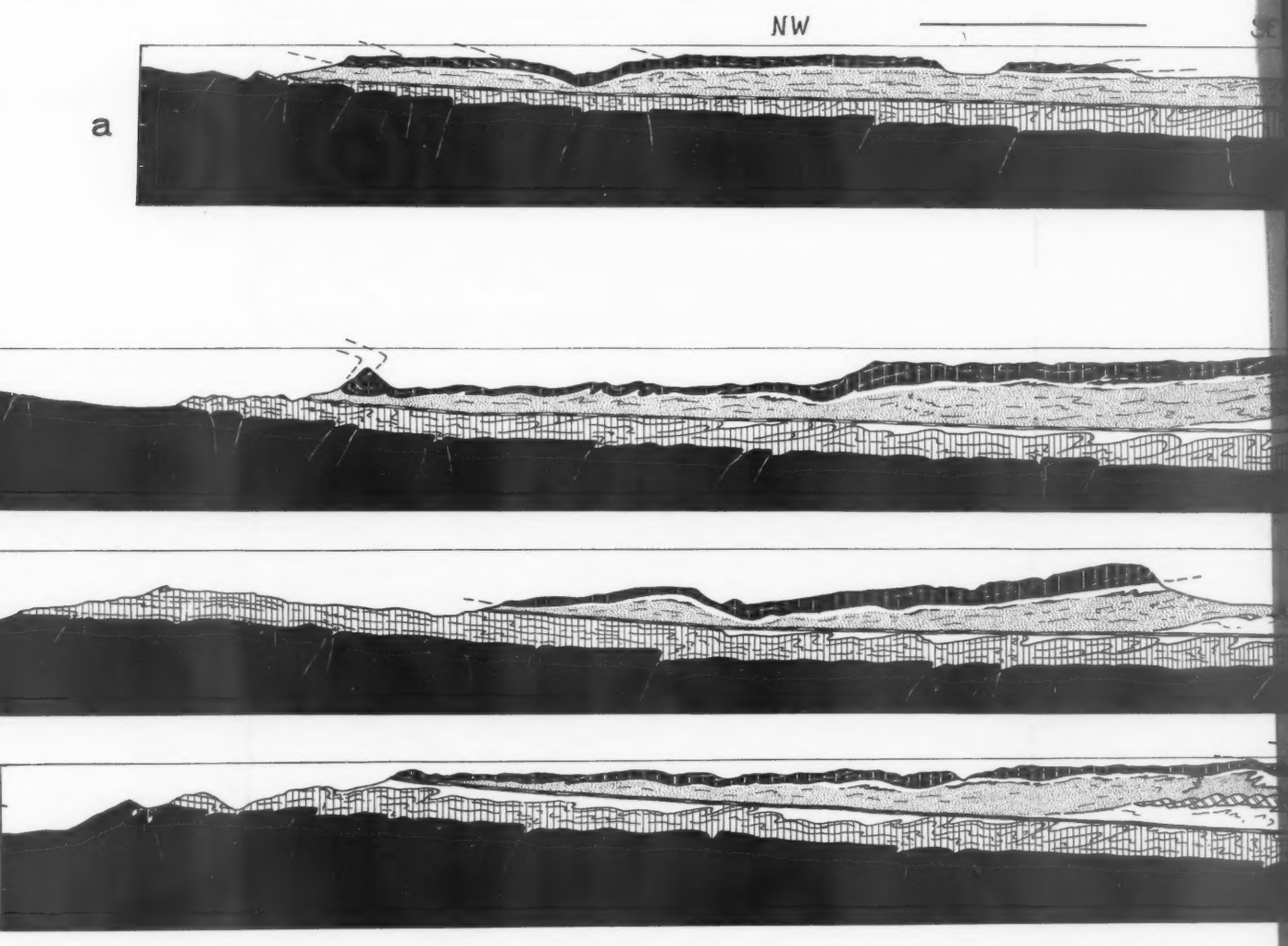

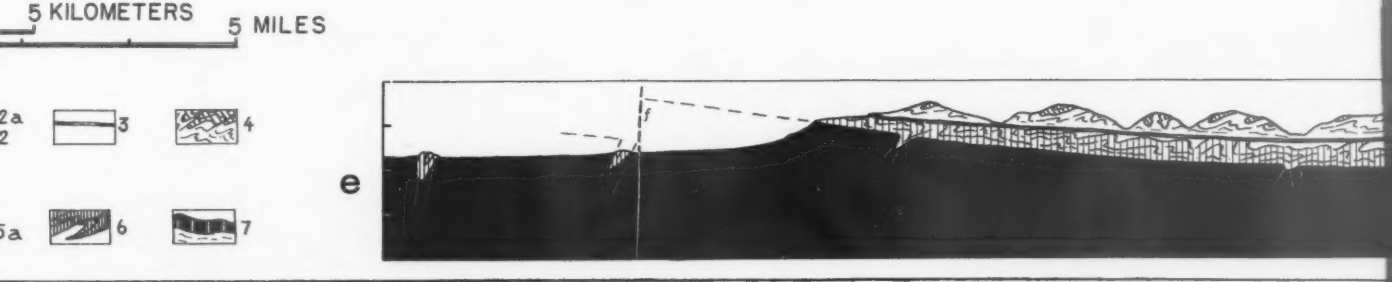

B. NORTHWEST-SOUTHEAST SECTIONS THROUGH N

1, Pre-Nama basement; 2, Schwarzkalk series, 2a, Schwarzrand series (shales and quartzite); 3, Unconformity dolomite; 4, Zebra series; 5, Pavian series Kudu series. The folded sedimentary rocks fill a basin formed ment. Basement rocks have been little disturbed in comparis

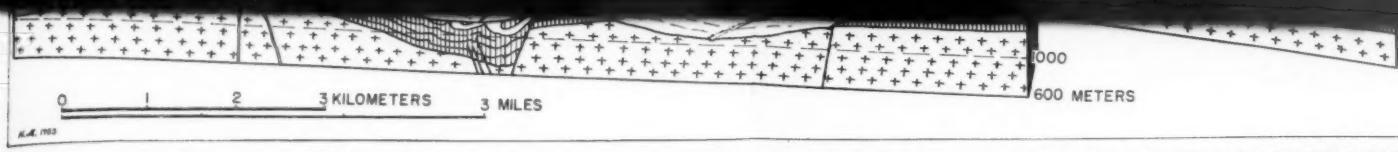

A. SECTIONS THROUGH SOUTHEASTERN FRONT OF NAUKLUFT MOUNTAIN

The profiles show the boundary between undeformed foreland and mountains. In the foreground are basement faults which may have determined the position of this boundary. In profiles *b*, *f*, and *g*, the Schwarzkalk beds of the mountains override, as a thrust sheet, the overturned younger Schwarzrand beds of the foreland. Unconformity dolomite (ch truncates the folds in the Schwarzkalk thrusts. In profiles *g* a overlain by the Zebra series, in the adjacent profiles by the Dassie

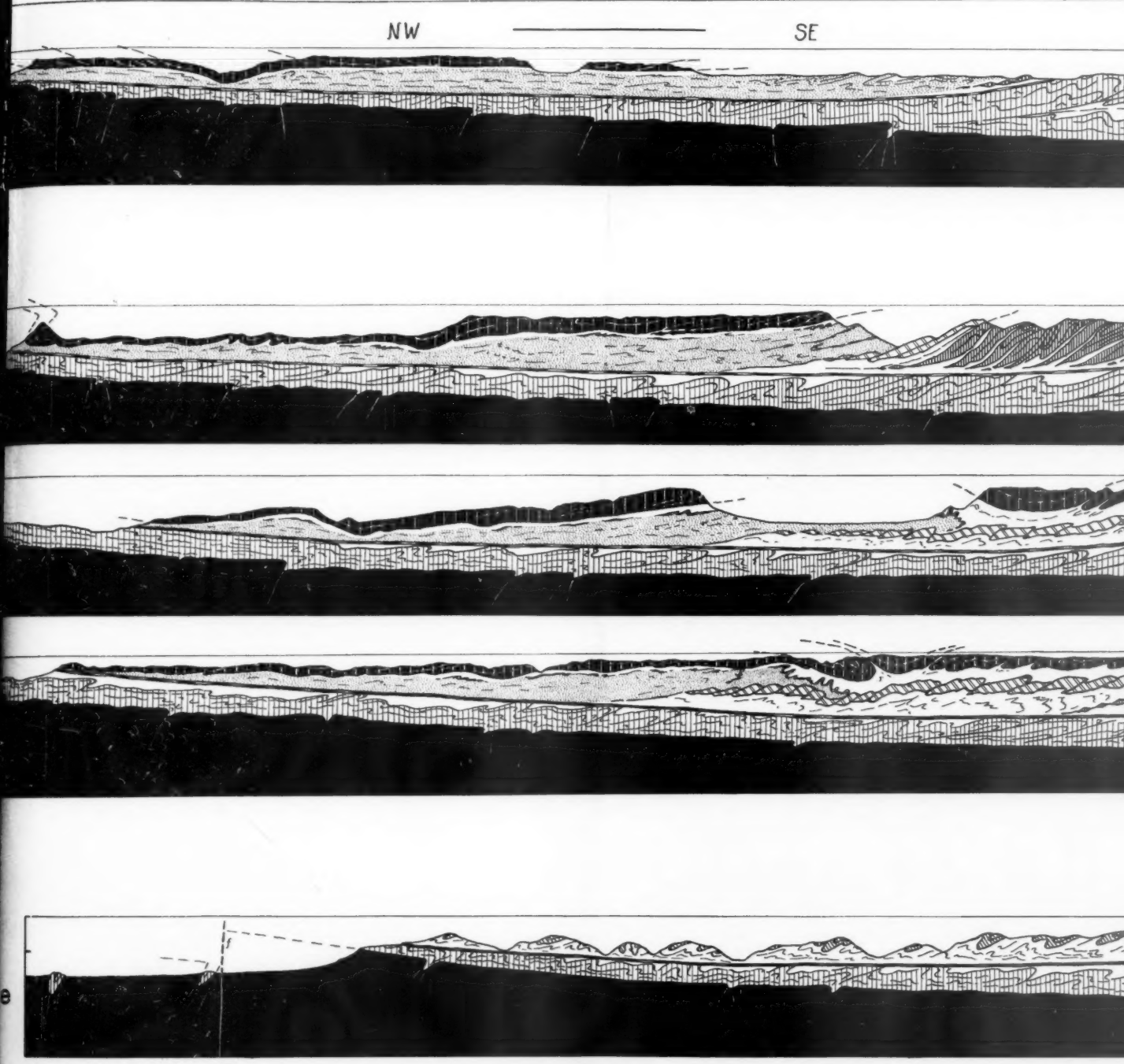

B. NORTHWEST-SOUTHEAST SECTIONS THROUGH NAUKLUFT MOUNTAINS

fill a basin formed by the base- rates an older and younger

AINS

te (checkered)
s *g* and *h* it is
assie nappe.

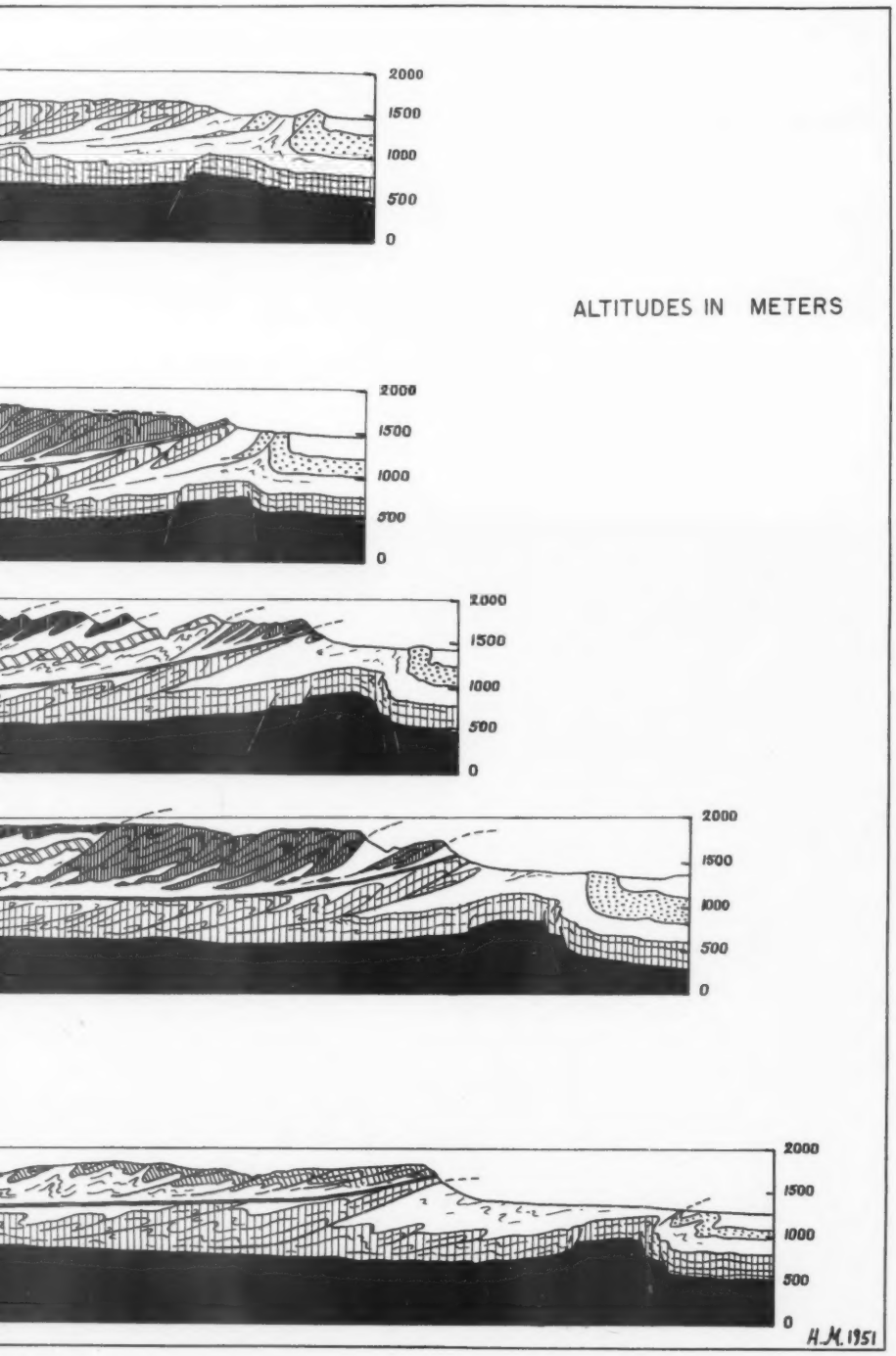

S

ger phase of folding without being itself deformed.

V70
1959
UMI

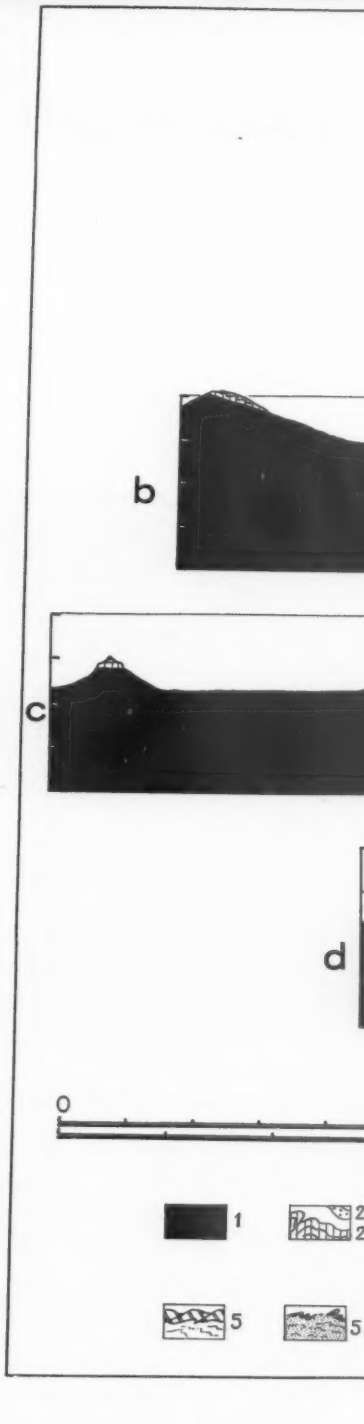
b
c
d
0
1
5
5

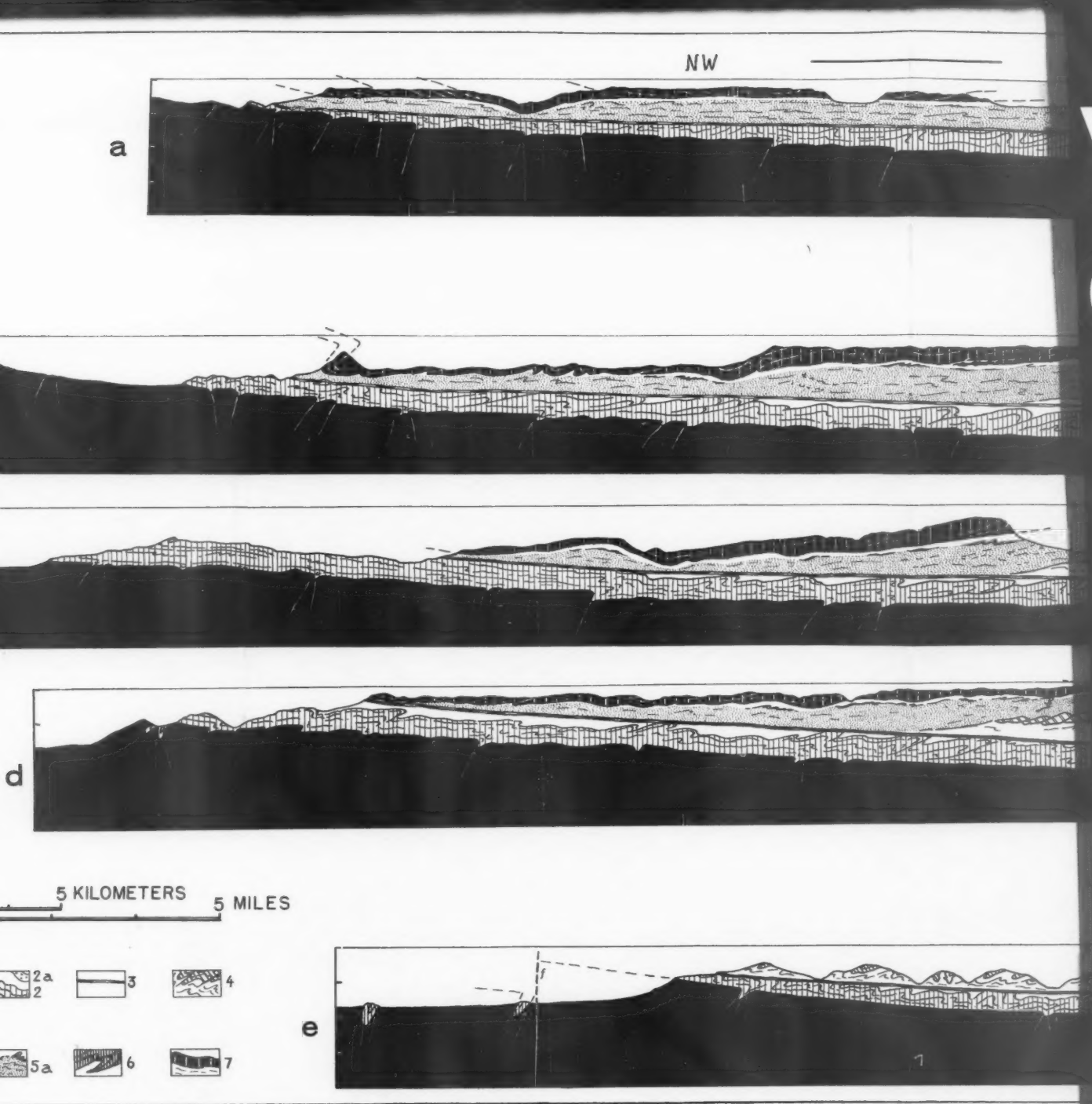

B. NORTHWEST-SOUTHEAST SECTIONS THROUG

1, Pre-Nama basement; 2, Schwarzkalk series, 2a, Schwarzrand series (shales and quartzite); 3, Unconformity dolomite; 4, Zebra series; 5, Pavian series (southern facies); 5a, Pavian series (northern facies); 6, Dassie series; 7, Kudu series. The folded sedimentary rocks fill a basin fo ment. Basement rocks have been little disturbed in co intensely folded sedimentary rocks. The Unconformity

COMPOSITE SECTIONS

V70
1959
U

mined the position of this boundary. In profiles *b*, *f*, and *g*, the Schwarzkalk
beds of the mountains override, as a thrust sheet, the overturned younger

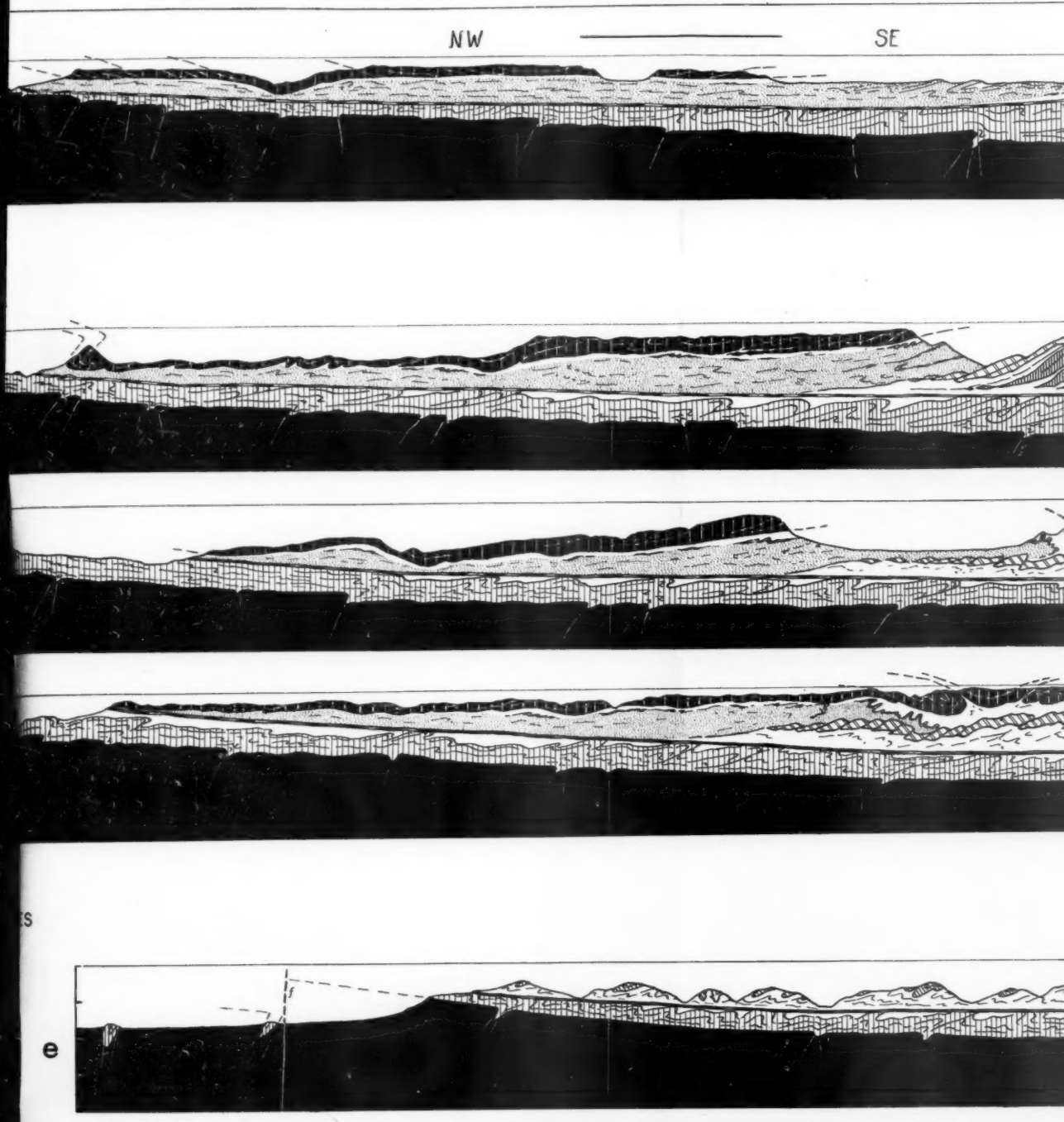

B. NORTHWEST-SOUTHEAST SECTIONS THROUGH NAUKLUFT M

2, Schwarzkalk series, 2a, Schwarzrand series (shales
formity dolomite; 4, Zebra series; 5, Pavian series
avian series (northern facies); 6, Dassie series; 7,

Kudu series. The folded sedimentary rocks fill a basin formed by the base-
ment. Basement rocks have been little disturbed in comparison with the
intensely folded sedimentary rocks. The Unconformity dolomite (3) sepa-

rates
This
ation

COMPOSITE SECTIONS

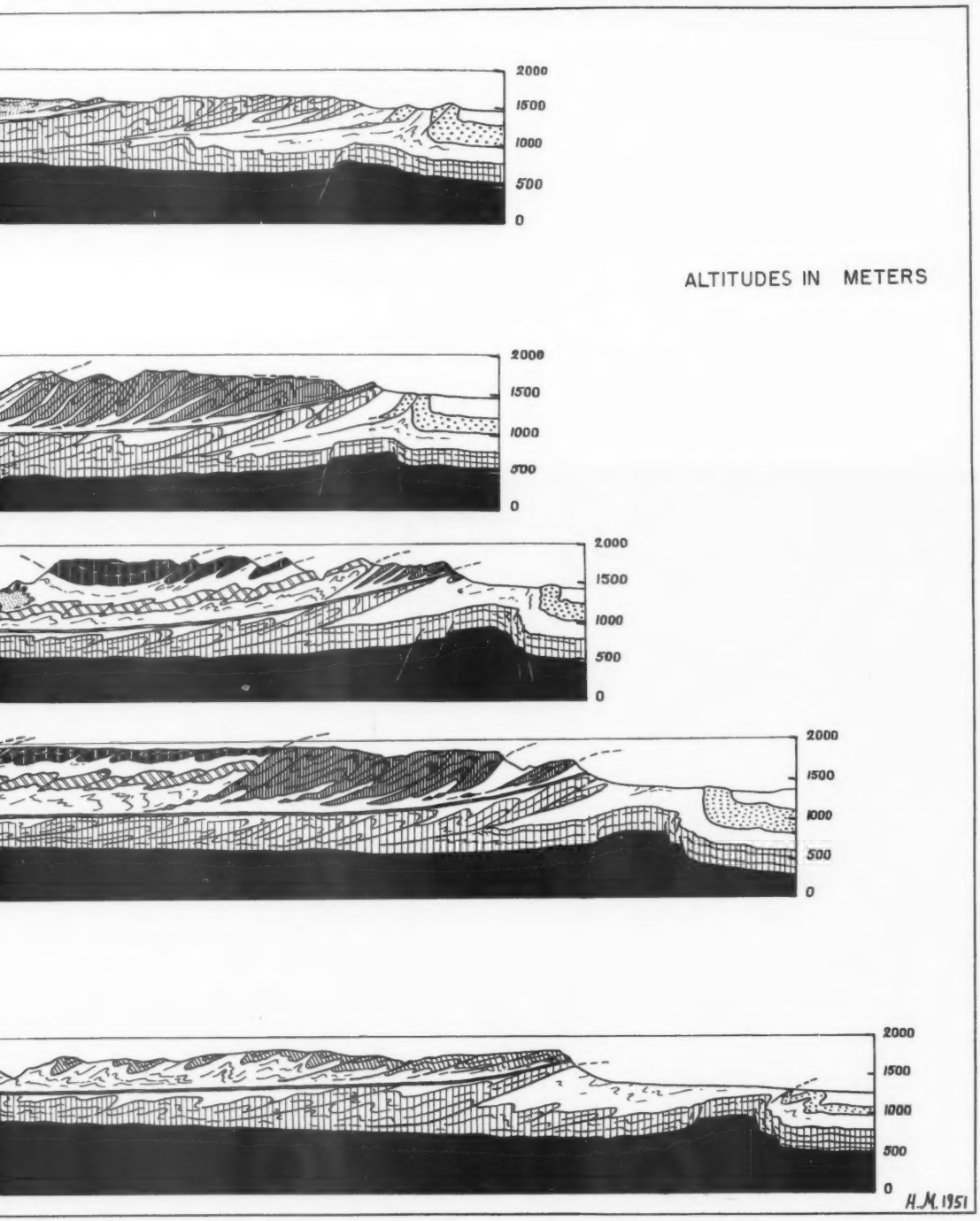

T MOUNTAINS

rates an older and younger phase of folding without being itself deformed. This dolomite is, in different areas, overlain by not fewer than four formations (4, 5, 5a, and 6).

The northern facies of the Pavian series has its front in the southern slopes of the great valley of farm Blässkranz. The valley itself owes its existence to the great thickness of easily eroded argillaceous sediments which are it is the result of flowage in the course of which the higher units have overridden the lower ones. The fluidity of movement is well expressed in profile *g* of Plate 8, *A*. The upper units of the dolomite nappe have moved in downward-

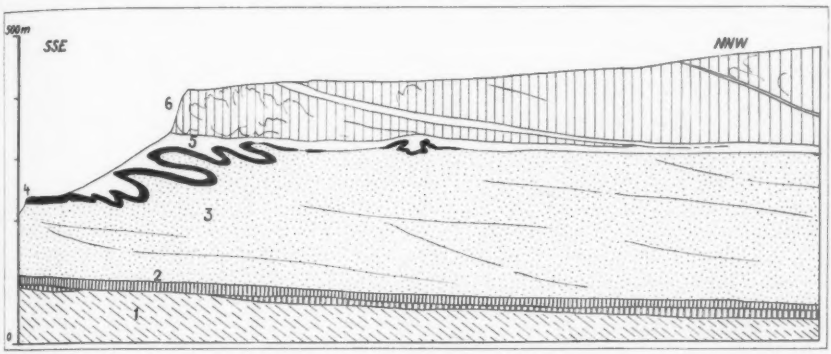

FIGURE 10.—FOLDING OF PAVIAN SERIES UNDER KUDU NAPPE

Mountain slope west of farmhouse Tsawisis. 1–4, Pavian series (1, brown arenaceous slates; 2, blue limestone and breccia limestone; 3, psephitic slates; 4, white dolomite); 5, 6, Kudu series (5, purple slate and banded limestone; 6, dolomite). The advancing dolomite plate of the Kudu nappe (6) has torn off the top dolomite of the Pavian series (4) and piled it up in accordion folds. The nappe itself is imbricated owing to friction along its base.

piled up in the frontal zone. The series of profiles in Plate 8, *A* impressively shows the mechanics of the accumulation. The northern facies of the Pavian series with its white top dolomite (5)—shown in black—forms a bulge of tight accordion folds (*see also* Pl. 3, fig. 3). The Kudu nappe (7) moving over the purple slates (6) has transgressed this bulge in recumbent and downturned folds. In the westernmost profile the top dolomite of the southern Pavian series (1) forms a bulge of imbricated thrusts over which the northern Pavian series has been squeezed forward and partly torn away by the advance of the Kudu nappe. The great profile of the southeast face further shows that the series is not uniformly folded. The movement increases in intensity toward the top. The effect of the Kudu nappe on the underlying beds is clearly revealed by the behavior of the white dolomite band. It is torn off at the right-hand side of the profile, and the torn-off portion reappears in the frontal zone, compressed into accordion folds. Figure 10 shows the same phenomena in the mountain side west of farm house Tsawisis. The ploughing action of the nappe and the breaking effect of the substratum are evident. This phenomenon, on both large and small scale, is repeated throughout the mountain area; facing rolling folds over the fold pile of the Pavian series, into the frontal part of the basin.

With this cascading fold zone, the Kudu series transgresses into the southern-facies area of the Pavian series.

Southern-facies area.—The transition from northern to southern facies of the Pavian series is not exposed. The transition zone has probably been overrun and buried by the northern Pavian series.

The southern Pavian series is less intensely deformed than its northern counterpart. The main reason for this is probably the thick competent top dolomite (Fig. 11). The disparity between the massive competent dolomite (Fig. 11, No. 14) which allowed only very wide folds, with intensive brecciation, and the well-bedded lower horizons (Nos. 9–13) led to extreme disharmony of folding. In Figure 11 the southern end of the Pavian series forms an anticline enveloped in the purple slates of the Kudu series (profiles *a* and *b*). This unit has been thrust against and over the imbricated Dassie series. Profile *b* shows that the Dassie has been considerably attenuated underneath this thrust. Between the isolated hill of laminated Kudu limestone (16) and the thin band of Unconformity dolomite (3) the Dassie is represented

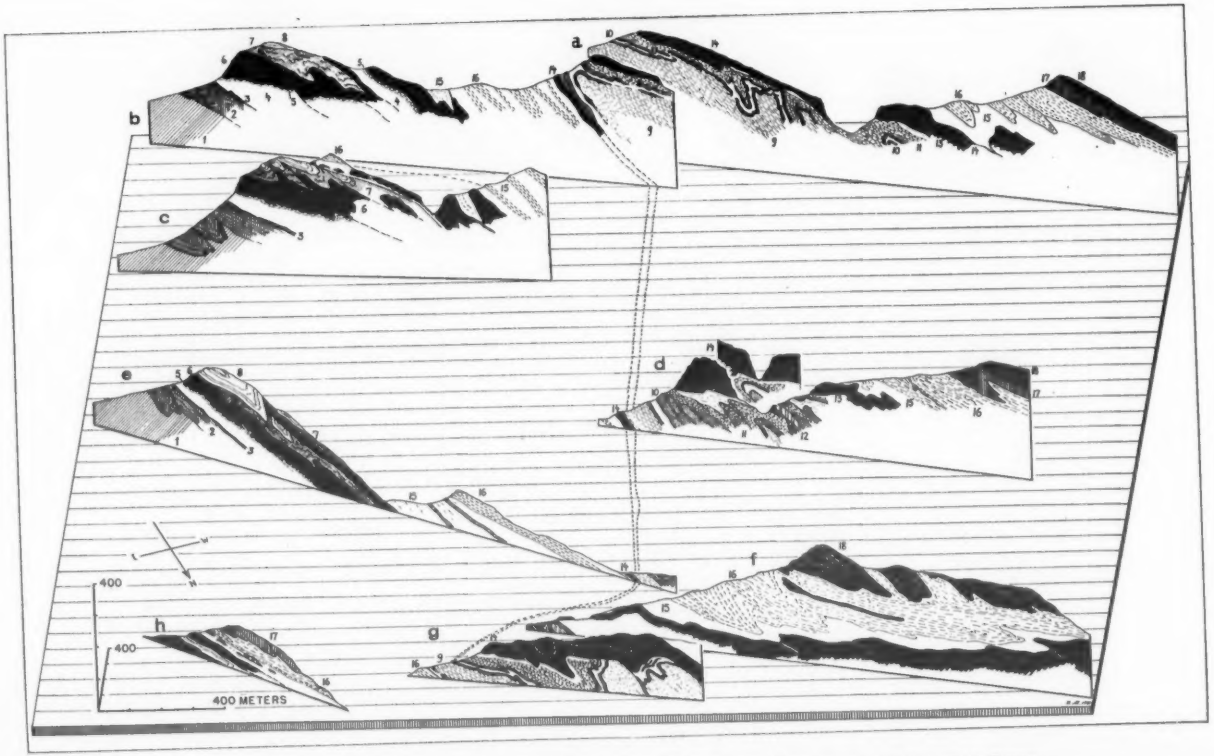

FIGURE 11.—PROFILES THROUGH FRONT RANGE, FARM BÜLLSPORT, SOUTHWEST OF TSONDAB RIVER

1, Schwarzrand shales; 2, Schwarzkalk series; 3, Unconformity dolomite; 4–8, Dassie series (4, purple slates; 5, laminated limestone; 6, massive dolomite and red limestone; 7, thin-bedded quartzites and purple slates; 8, banded dolomite chert); 9–14, Pavian series in southern facies (9, brown, arenaceous slates; 10, psephitic quartzite; 11, blue limestone; 12, yellow dolomite; 13, green slates; 14, massive gray dolomite); 15–18, [illegible] 12, laminated limestone; 17, platy and sandy dolomites and dolomitic sandstones; 18, massive dolomite)

only by
intensely
the lowe
series. In
the Pavi
disharmo
ference i
dolomite
the con
quartzite
datum p
the Pavi

The
of the
may rep
series.
Kudu r
frontal
tongue
ing is a
seen on
farm D
tightly
above t
south-f
dolomi
shallow
dolomi
Dassie
flattene
the int
of the
formity
In t
bottom
appear
over t
indica
even g
is app
the di
Schwa
Schwa
Schwa
north
north
thus a
the a
units.
great
in-lin
move
indep
(Fig.

only by a comparatively thin thrust sheet of intensely imbricated folds formed mostly by the lower dolomite and limestone (6) of the series. In these profiles (especially *a*, *g* and *h*) the Pavian series exhibits an extreme degree of disharmonic folding caused by the great difference in competence between the massive top dolomite and the well-stratified lower beds with the conspicuous double band of psephitic quartzite (10). The stippled lines along the datum plane connect the southernmost unit of the Pavian series in the different profiles.

1, Schwarzrand shales; 2, Schwarzkalk series; 3, Unconformity dolomite; 4–8, Dassie series (4, purple slates; 5, laminated limestone; 6, massive dolomite and red limestone; 7, thin-bedded quartzites and purple slates; 8, banded dolomite chert); 9–14, Pavian series in southern facies (9, brown, arenaceous slates; 10, psephitic quartzite; 11, blue limestone; 12, yellow dolomite; 13, green slates; 14, massive gray dolomite); 15–18, Pavian series in northern facies (15, purple slates; 16, laminated limestone; 17, flinty and sandy dolomites and dolomitic sandstones; 18, massive dolomite)

Tectonics of Dassie Series

The Dassie series forms the frontal portion of the higher units. As mentioned, this series may represent a southern facies of the Kudu series. It surrounds the broad tongue of the Kudu nappe in tight folds and thrusts. The frontal arc of the nappe resembles a glacier tongue advancing into a moraine. Here shortening is at a maximum. The best profile may be seen on the western side of the mountains on farm Die Valle (Fig. 5; Pl. 3, fig. 1). The great tightly wedged dolomite folds crown the cliffs above the broad valley. The movement of these south-facing anticlines over the Unconformity dolomite may be likened to surf overriding a shallow beach. The glide horizon under the dolomite is formed by the basal shales of the Dassie series. The laminated limestone has been flattened into a mylonitic marble. In view of the intensity of the folding and the magnitude of the load it is astonishing that the Unconformity dolomite has remained in position.

In this profile the contrast between top and bottom is striking. The imbricated digitations appear to have been "frozen" while moving out over the static substratum; the dragging tails indicate prolonged transport.

But the contrast between top and bottom is even greater than is apparent at first sight. It is apparent not only in the extent but also in the direction of the movement. The wedges of Schwarzkalk rocks in the basement strike north-northeast, whereas the fold axes of the higher Schwarzkalk zones and of the nappe strike west-northwest. The axial direction of the nappe is thus at right angles to that of its base, revealing the astonishing independence of the higher units. This independence is an expression of the great freedom which distinguishes the Naukluft folding from that of other folded belts. The movement of the higher nappes is entirely independent of the structure of the lower levels (Fig. 12).

The Zebra series, which should overlie the unconformity, must have been entirely planed off by the Dassie nappe. Where the two series meet at the southern boundary of farm Die Valle, the front of the Dassie nappe has abruptly bent and twisted the northeast-striking folds of the older series. The lowest slices of the nappe have even intruded the Zebra series. This phenomenon occurs wherever the front of the nappe is preserved.

The best example may be seen in the gorge which cuts into the mountains, east of the farm boundary of Büllsport (Fig. 13; Pl. 4, fig. 1). The lowest nappe of the Dassie series has pushed the Zebra series away from its original resting place on the Unconformity dolomite, represented by the checkered line. The nappe front seems to have acted like the blade of a bulldozer, and the Zebra series (unshaded) has flowed backward over this front in a backfold (*plis en retour*). This whole complicated structure is overridden by a higher unit of the Dassie series, which has lost the troughs of its tightly packed synclines by attrition on the plane of movement. The profile clearly expresses intense movement, checked by frontal resistance. Once again the axial directions of the two units diverge considerably. Thus within one and the same folding phase the actual direction of movement was different at different levels.

These "axial unconformities", indicating that even small units were able to move independently of one another, constitute the best evidence that folding here is not due to an eroded *traineau écraseur*. The movement pattern clearly suggests flowage under the influence of gravity.

The Dassie series probably owes its arcuate trend to the great advance of the Kudu nappe. But both series reached their present position in one flowing movement. There was no faulting, not even on the northern side of the Tsondab Valley, on farm Büllsport, where the axes of the Dassie series plunge away steeply.

The mechanics of folding can be studied to advantage in the northern side gorges of the Tsondab Valley (Pl. 8, *B*). Differential movement within each unit is brought out by involution and multiplication of digitations along curved thrust planes. Similar folded thrust planes are conspicuous in the Ruhr coal field. Kienow (1955) has investigated these features mathematically and has shown that they are due to friction at a basal shearing plane and not, as previously believed, to a second phase of folding. The profiles of Plate 8, *B* suggest in

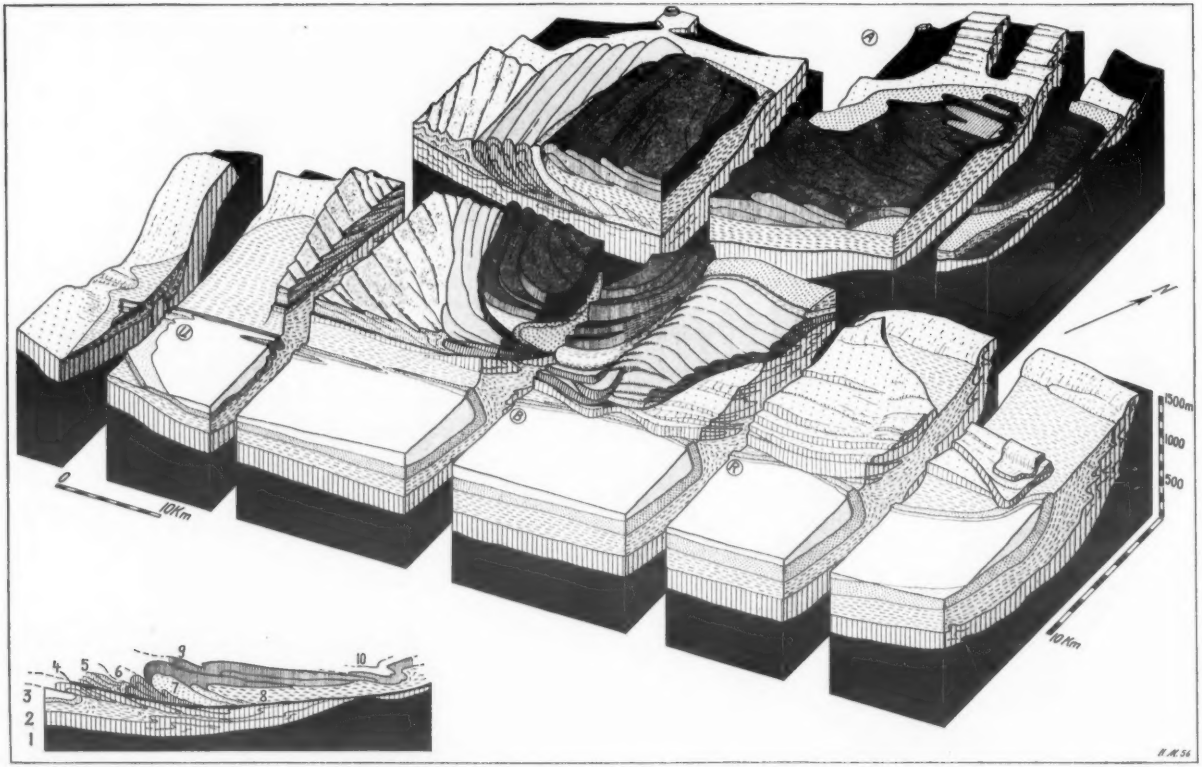

FIGURE 12.—DIAGRAMMATIC INTERPRETATION OF NAUKLUFT FOLDING

A = Abbabis, B = Büllsport, R = Rokskeur, U = Urikos. 1, Pre-Nama basement; 2, Schwarzkalk series; 3, Schwarzrand series; 4, Unconformity dolomite; 5, Zebra series; 6, Dassie series; 7, Pavian series (southern facies); 8, Pavian series (northern facies); 9, Kudu series; 10, Klipbok series. Undeformed foreland beds are in the foreground. Along the northeast-trending mountain edge they are overturned and overridden by several thrust sheets of Schwarzkalk (?).

A = Abbabis, B = Büllsport, R = Rokskeur, U = Urikos. 1, Pre-Nama basement; 2, Schwarzkalk series; 3, Schwarzrand series; 4, Unconformity dolomite; 5, Zebra series; 6, Dassie series; 7, Pavian series (southern facies); 8, Pavian series (northern facies); 9, Kudu series; 10, Klipbok series. Undeformed foreland beds are in the foreground. Along the northeast-trending mountain edge they are overturned and overridden by several thrust sheets of Schwarzkalk (2).

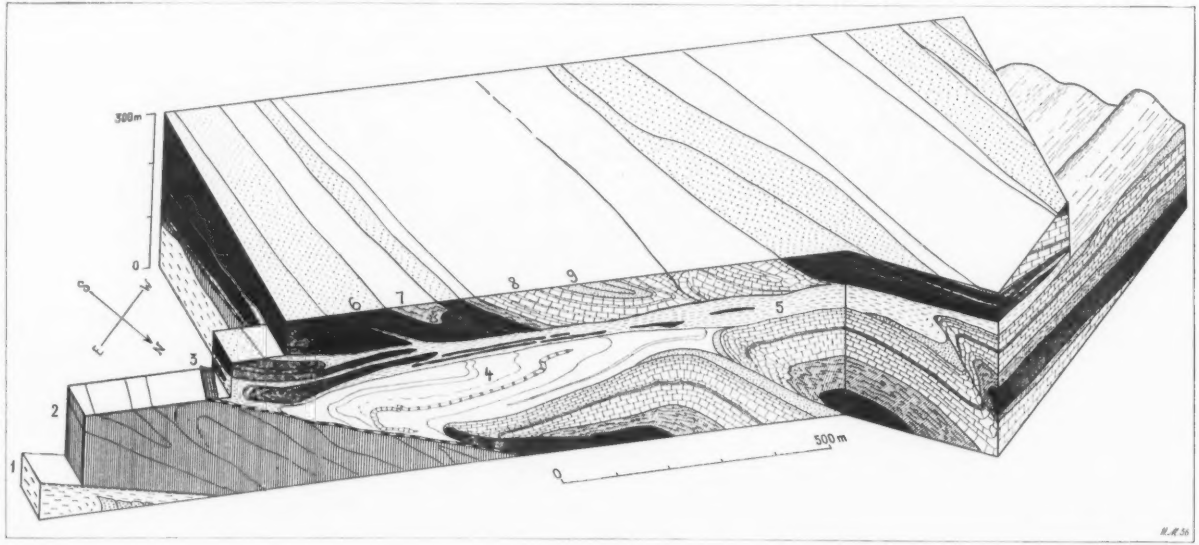

FIGURE 13.—BLOCK DIAGRAM OF FRONT RANGE NORTHEAST OF BÜLLSPORT

1, Schwarzrand shales and quartzites; 2, black limestone of Schwarzkalk series; 3, Unconformity dolomite; 4, Zebra series ? (platy, dark-gray limestones, dolomite, sandy dolomite, and quartzite bands), 5–9, Dassie series (5, purple slates and laminated limestone; 6, lower, massive dolomite and red limestone; 7, thin-bedded quartzites and purple slates; 8, chert-banded dolomite; 9, white dolomite)

every detail a checking of movement at the base of the nappe and at its front; the northern portion kept moving forward until internal friction choked differential movement. Various phases of the dying movement are, as it were, photographed in the multiplied anticlinal crests. The two curved dotted lines on the datum plane, connecting two particular anticlines in the different profiles, show how abruptly even individual fold elements may change their trend.

The axes of the folds shown in Plate 8, *B* rise toward the east. This brings up a broad belt of the lower purplish slates in the raised valley of Gabis; it becomes evident that, as on farm Die Valle (Pl. 7), the imbricate nappe here floats on this zone of slates and laminated limestones. This zone in turn rests directly on the Unconformity dolomite.

Within the Dassie nappe, too, the larger slices are separated from one another by bands of purple slates and laminated limestones. Subsidiary nappes, such as the one represented on Figure 13, also have corresponding glide horizons at their base. The laminated limestone is commonly well plicated. Further movement has intensely compressed the plications into flame-shaped figures. The final stage of this rolling out is commonly represented by fine-grained striped mylonitic marbles in which the original sedimentary structures have been obliterated.

Tectonics of Kudu Series

As in the Dassie series, the main movement horizon is formed by purple slates and laminated limestone. In the frontal area, where the horizontal component of the movement spent itself, these beds are folded more or less conformably together with the higher dolomites, forming several great synclines, overturned to the south (18 on Fig. 11). Further to the north the dolomites grade into an imbricate, independently folded nappe, floating on more plastic rocks (Fig 10; Pl. 8, *A*). Plate 1 shows impressively that the thick dolomite nappe advanced from the north into the Naukluft Basin like a huge glacier tongue. Its effect on the overridden Pavian series has already been discussed. Its own movement is best expressed in the series of profiles of Plate 8, *A*. The downward-facing digitations (*e.g.* Pl. 8, *A*, profile *g*) with which the nappe (vertical ruling) overcomes the bulge in the Pavian series leave no doubt as to the independence of its movement. The profiles also show that the nappe itself is not a uniform mass. It consists of several displaced units, each higher unit overriding the one beneath it.

The northern area has had to carry the main weight of the thrust. There shales and laminated limestone have been preserved only rarely. They have been ploughed forward and piled up in the frontal zone, like the upper beds of the Pavian series. Movement of higher units has also strongly affected the lowest dolomite beds of the nappe. Even where they are practically horizontal they are commonly intensely sheared and drawn out into large-scale boudinage structures (Fig. 14). On farm Nauzerus all the lower beds have been removed from a raised basement wedge, so that imbricate Kudu dolomite is superimposed directly on the Tsumis series (Fig. 4, middle of profile *i*). Here the nappe consists of narrow slices. These are probably derived from folds which faced down and toward the south and lost their apices through friction along the movement plane (Fig. 18, *A* and *B*).

Tectonics of Klipbok Series

The sedimentation of the Klipbok series shows an intimate relationship to the deformation of the Kudu nappe. Actual proof seems to exist that folding was initiated together with a new cycle of sedimentation. Some of the anticlinal crests formed by the Kudu dolomite are surrounded by and dissolved into huge boulder conglomerates and breccias which consist entirely of dolomite blocks in a sparse matrix of brown shales with which the new cycle begins (Fig. 15). The boulders are angular or subangular and are all derived from the dolomite forming the anticlines. As these boulder conglomerates are confined to the neighborhood of the anticlines, and since no major unconformity exists between the dolomite and the overlying shales, the anticlines must have formed during deposition of the shales. As the folding progressed, the shales in their turn were involved. The subsidence of the basin which led to the deposition of the shales must have initiated the folding.

The best exposures of such an anticlinal boulder pack are found in a ravine 1.8 miles southwest of the homestead of farm Noab about a hundred yards from the road.

Deformation of the rocks of the Klipbok series, as shown by the elongation of pebbles, differs radically from the deformation found below the Kudu nappe (Fig. 15). The signifi-

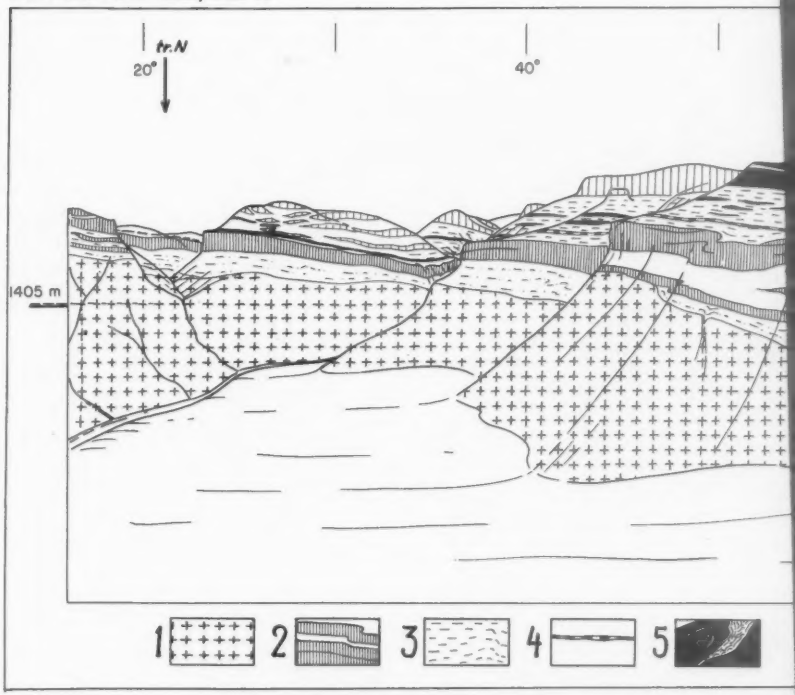

PANORAMIC VIEW OF WESTERN

1, Granite; 2, thick black limestone ba
mite; 5, Dassie series (lower dolomites
dolomite (black and white checkered

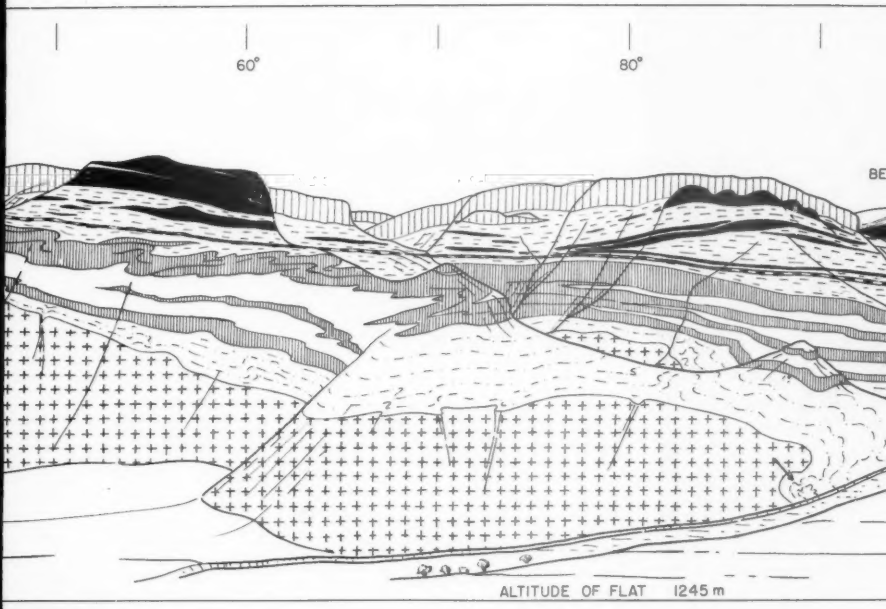

STERN MOUNTAIN FACE ON FARM "DIE VALLE" SHO

k limestone bands; 3, slates; 4, Unconformity dolo-
ower dolomites black). Undeformed Unconformity
hite checkered line) separates underlying folded
Schwarzkalk and Schwarzrand beds (2
ed and imbricated Dassie beds. The g

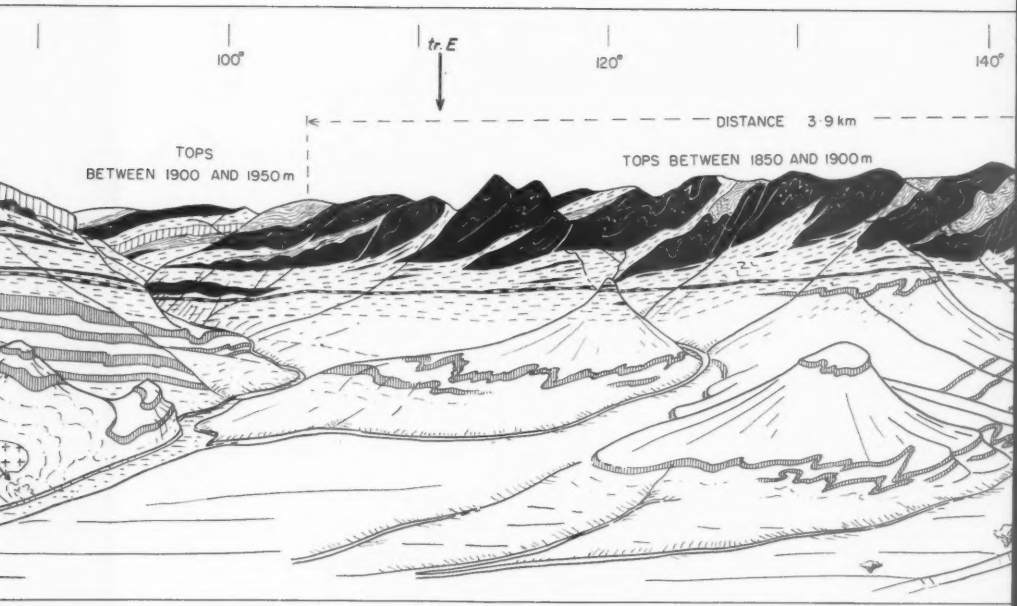

E" SHOWING IMBRICATED FOLDING OF DASSIE SERIES ABOVE

rand beds (2 and 3) from overlying intensely fold-
beds. The great dolomite thrusts (represented in black) override one another. They consist of tight
structures, and their dragging tails suggest considerabl

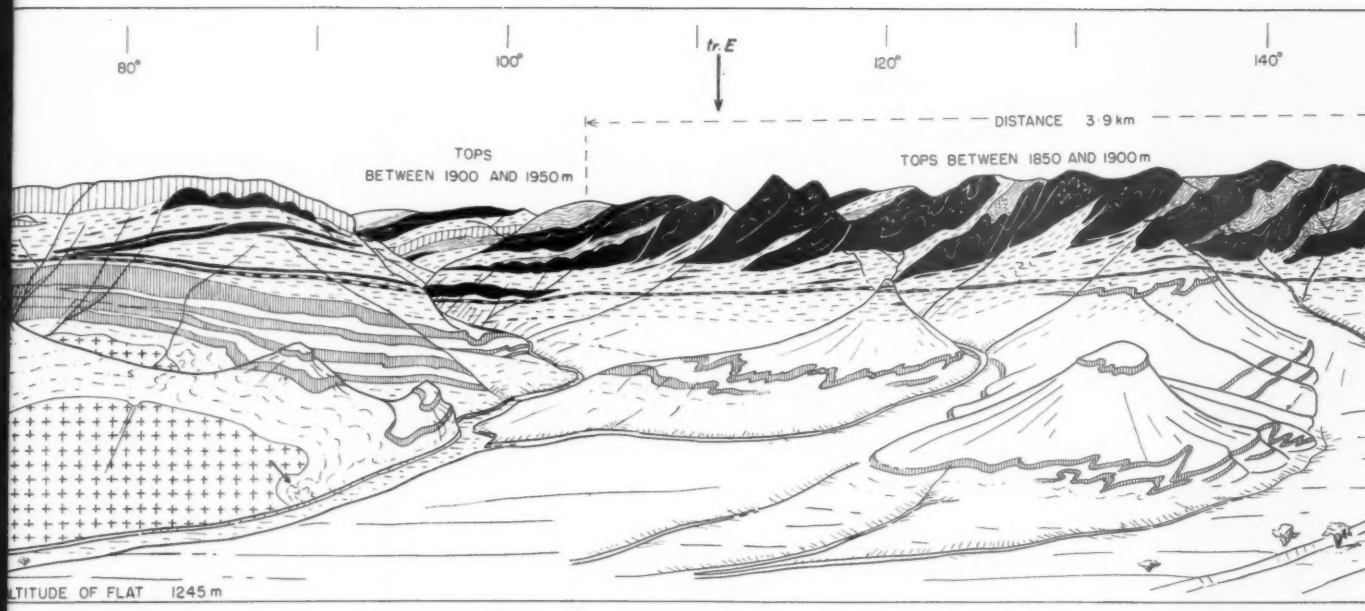

ARM "DIE VALLE" SHOWING IMBRICATED FOLDING OF DASSIE SERIES ABOVE UN

Schwarzkalk and Schwarzrand beds (2 and 3) from overlying intensely folded and imbricated Dassie beds. The great dolomite thrusts (represented in black) override one another. They consist of tightly packe structures, and their dragging tails suggest considerable displac

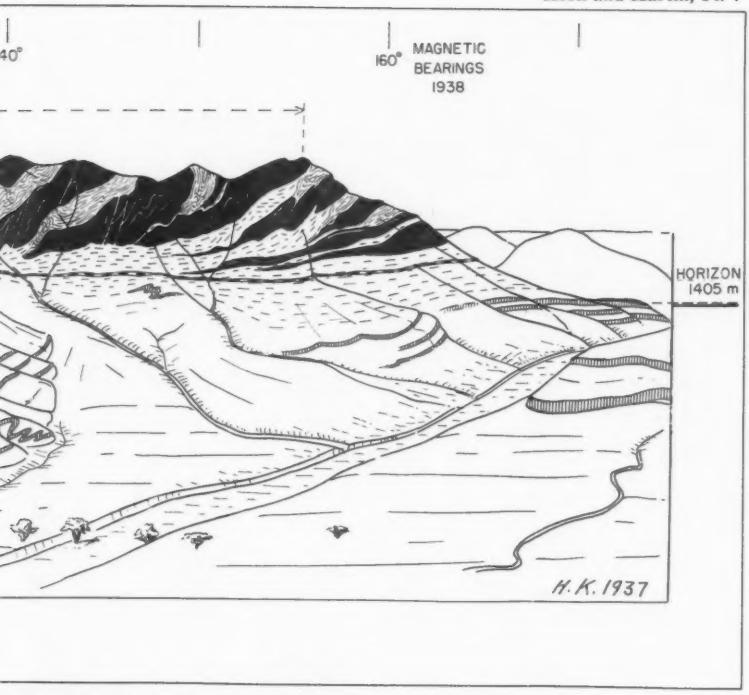

VE UNCONFORMITY DOLOMITE

ghtly packed anticlinal
rable displacement.

FIGURE
1, Pa
eratic bl
mite disi

cance o
hereafte

Struc

The r
is proba

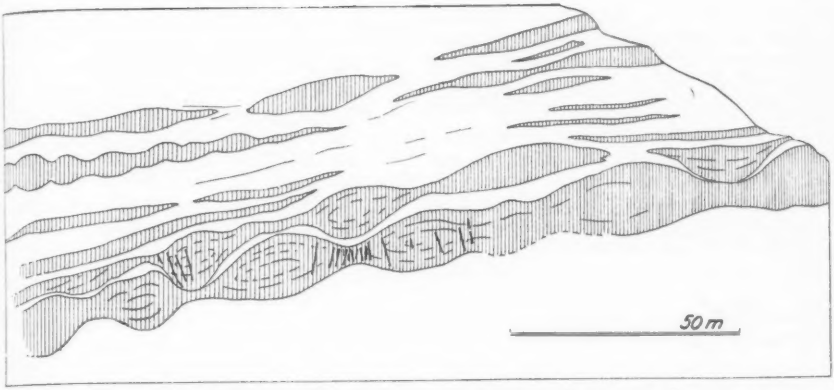

FIGURE 14.—DOLOMITE BANDS OF KUDU SERIES SHOWING BOUDINAGE STRUCTURE

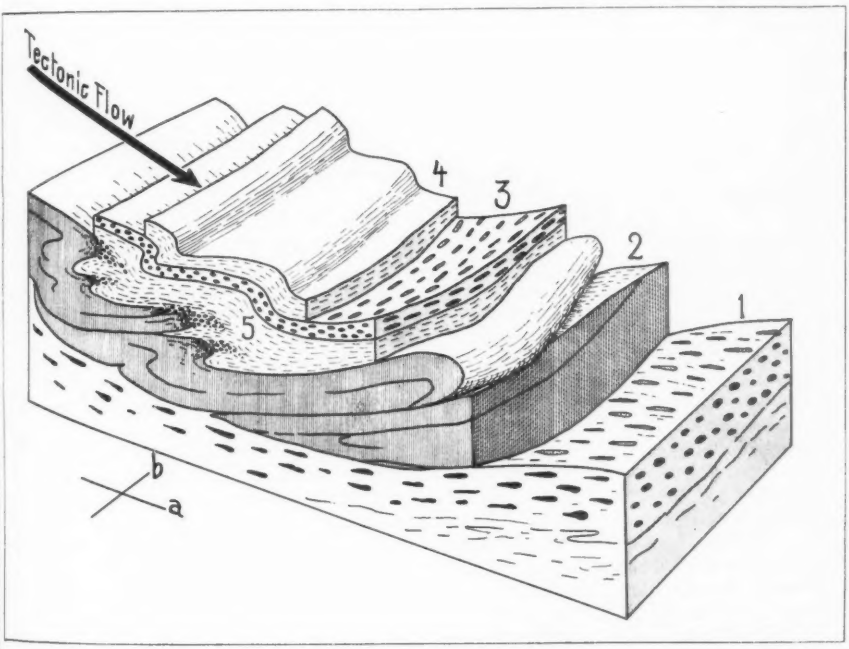

FIGURE 15.—DIAGRAM SHOWING TECTONIC RELATIONSHIP OF PAVIAN, KUDU, AND KLIPBOK SERIES

1, Pavian series, pebbles and boulders elongated in *a*; 2, Kudu series; 3–5, Klipbok series (3, conglomeratic blue limestone of Klipbok series, pebbles elongated in *b*; 4, shales and slates; 5, digitations of dolomite disintegrating into breccias).

cance of this phenomenon will be discussed hereafter.

Structure of Southeastern Mountain Border

The rectilinear trend of this mountain border is probably due to a fault in the basement; some faulting in this zone can be observed on farm Hauchabfontein. Above this fault zone the quartzite horizon of the Schwarzrand series has been torn away by the advancing Schwarzkalk series and overturned toward the south. It is locally overridden along a flat thrust plane

which is preserved in several localities (Pl. 6, *A*). There can be no doubt that the nappes once stretched even farther into the foreland, perhaps as far as the anticlinal zone of Achaub. Since they were underlain by the soft Schwarzrand shales the nappes eroded easily as far as the overturned quartzite. The scarp is thus primarily an erosion feature.

The basement fault which separates the Naukluft Basin from the main Nama Basin disappears northeast of Rokskeur. There have been no younger movements along this zone. The fault is of local significance only and does not extend across the continent, as Krenkel (1928) had thought.

Movement Pattern

The Naukluft Mountains owe their relief to erosion only. If erosion effects are disregarded the Naukluft area becomes a basin filled with intensely folded sediments (Pl. 6, *B*, profile *b*). There are no indications that the folded segment has ever been raised above its surroundings. On the other hand, there is much to suggest a connection between the folding and basin formation.

Within the Nama sea, the Naukluft Basin distinguished itself by the instability of its floor: early sedimentation already was related to a mild folding phase. The succeeding folding phase affected the Schwarzkalk and part of the Schwarzrand series. The distribution of folding in this phase shows its dependence on basin structure. In the Tsondab trough, a local depression, the Schwarzkalk series remained almost undeformed, whereas everywhere else it was intensely folded. It seems significant that deformation reaches its highest intensity on the slopes of the Steinfeld Range, where the basin floor is most steeply inclined. There the Schwarzkalk rocks behaved like a cloth, sliding down an inclined table top and piling into folds; thus folding is most intense where the inclination is greatest and least intense in the Tsondab trough where the inclination is smallest.

The few rootlike wedges of Schwarzkalk rocks in the basement are far too small to explain the intensity of folding or the overturning of folds (directed in all cases toward the deeper part of the basin) primarily by tangential shortening in the basement.

Two explanations suggest themselves: shearing off and folding by a *traineau écraseur*; or shearing off and folding by gravity gliding. The first alternative can be discarded for Schwarzkalk folding because it is the thin Unconformity dolomite that immediately overlies the deformed Schwarzkalk beds which were thus plainly truncated by erosion.

The best explanation seems to be that the Schwarzkalk series was folded in the process of gliding down into the basin. The shearing off was probably caused by movements of the floor connected with the pronounced subsidence that accompanied deposition of the Schwarzrand shales; at the same time these movements constricted the space on the flanks of the basin, loosening the sediments. Gliding became possible along argillaceous horizons.

The same sequence of events appears to have repeated itself a second and a third time. Renewed subsidence following deposition of the Unconformity dolomite led to filling of the basin with the sediments of the Zebra and Pavian series, the former representing the facies of the northwestern part. After the basin had been filled (with reef dolomites), renewed subsidence led to deposition of the purple shales of the Dassie (and Kudu?) series.

Lowering of the trough may have caused the sliding off and folding of the Zebra series; this assumption would explain the discordant axial trends of the Zebra series as opposed to those of the younger Dassie, Kudu, and Klipbok series. It would also explain the axial freedom and looseness of deformation in the Zebra series for this type of folding can hardly have taken place under the great load of the Dassie or Kudu series. The shales above the Unconformity dolomite acted as a glide horizon. Only gravity gliding can satisfactorily explain the intense folding above the undisturbed thin dolomite.

This deformation phase was restricted to the northwest slope of the trough and did not affect the facies area of the Pavian series.

The cycle (trough filling, renewed subsidence and folding) was repeated a third time for the Dassie, Kudu, and Klipbok series. The rocks of the Klipbok series provide evidence that folding started with renewed subsidence.

The broad tongue of the Kudu nappe rests directly in front of the highest part of the Nauchas Highlands. Within this tongue the fold axes form an arc, convex toward the south. The nappe reaches its most southerly point in the apex of the fold arc. This fold arc rests freely on the independently folded lower units and is separated from them by a practically undisturbed unconformity. The nappe arc can have attained this position only by movement under the influence of gravity, in the manner of a glacier tongue. In that case there should be a

relationship between the locus of farthest advance and the shape of the basin. That relationship exists. The apex of the fold arc lies above the deepest part of the basin (Fig. 12). Furthermore, the shape of the northern rim of the basin also appears to have influenced the movement. The base of the Nama has its steepest dip on the southern slopes of the Steinfeld range (Fig. 4). This steeply inclined slope points exactly to the apex of the fold arc. The elongated pebbles of the Pavian series and the lineations of many rocks conform to the same direction.

The connection between the movement of the nappe and the shape of the basin could not be closer. From the northern slope the nappe slid into the deepest part of the basin and advanced farthest toward the south below the steepest part of the rim. The steepest slope produced the greatest momentum: the influence of gravity seems evident.

Before they moved down, the strata composing the nappe were probably overlying the Nauchas Highlands. The base of the Nama is not preserved north of the Steinfeld range. Yet it must have existed above the highest granite peaks, which attain heights of 7200 feet. Hence the drop into the basin was at least 2600 to 3300 feet. The conditions for gravity gliding existed.

This explanation is based on the assumption that relative heights have not changed since the folding of the Nama; no post-deformation faults exist between the Naukluft Basin and the Nauchas Highlands. Younger faults occur only west of the escarpment. They are of post-Karroo age and are connected with the formation of the escarpment.

The threefold repetition of events indicates a fixed relationship between subsidence, sedimentation, and folding. After each stage of subsidence argillaceous sediments were deposited. These were followed by quartzites and limestones. The cycle was closed by deposition of dolomites, commonly reef dolomites, a typical shallow-water facies. This kind of succession is not very stable mechanically. It rests on the plastic shales literally as on clay. If such a succession is tilted through renewed subsidence of the trough and simultaneously shaken by small deep-seated movements and earthquakes, then it can easily be set into motion.

As sedimentation seems to mirror the movements of the basin, the question arises whether isostasy might have contributed to the repeated subsidences. The sediments of the Naukluft trough differ from geosynclinal sediments chiefly by their limited thickness. The accumulation preceding an increased rate of subsidence does not favor the assumption of isostatic control; if compression of the basement in the northern part of the basin (Fig. 4) is taken into consideration, then a connection with an orogenic phase seems indicated. Present knowledge suggests that the movements might have been connected with the latest phase of Proterozoic folding of the Damara belt, whose southern front approaches the northern rim of the Naukluft trough at Ababis to within 10 miles. The Naukluft Basin might therefore have been a foredeep, formed during the folding of the Damara system, and movement of the Nama rocks might have been triggered by thrusting and folding in the hinterland. More radioactive age determinations are needed to confirm or disprove this possibility.

Whether connected with a major orogeny or not, the combination of comparatively thin strata with folding of Alpine intensity is probably unique. It is easily explained by the gravity gliding hypothesis, which takes into account such special features as the "double unconformity", axial unconformities, and downward-facing folds; it seems impossible to satisfactorily explain this combination of features in any other way.

Internal Structures and Rock Deformation

The structural features related to deformation in the Naukluft range do not differ in principle from those in other folded belts. Argillaceous rocks commonly show intense cleavage. Cleavage planes are more or less parallel to the axial planes of the folds. Plate 5, figure 1 shows deformation along cleavage planes in a light limestone band between shales. The rock was stretched by movement parallel to the axial plane and compressed perpendicularly to it.

Pebbles of the Pavian series are elonged at right angles to the fold axes, and they conform to the cleavage planes. Figure 16 shows a dolomite block in the apex of a small fold. In this case anisotropic stress distribution has led to club-shaped deformation and to piercing of several strata. Dolomite pebbles are deformed in all cases along symmetrically disposed conjugate shear fractures and by tension fractures. Calcareous pebbles have undergone plastic deformation and recrystallization.

The orientation of elongated pebbles is different for the Pavian and for the Klipbok series. In the Pavian series, pebble elongation is in all cases at right angles to the fold axes. This

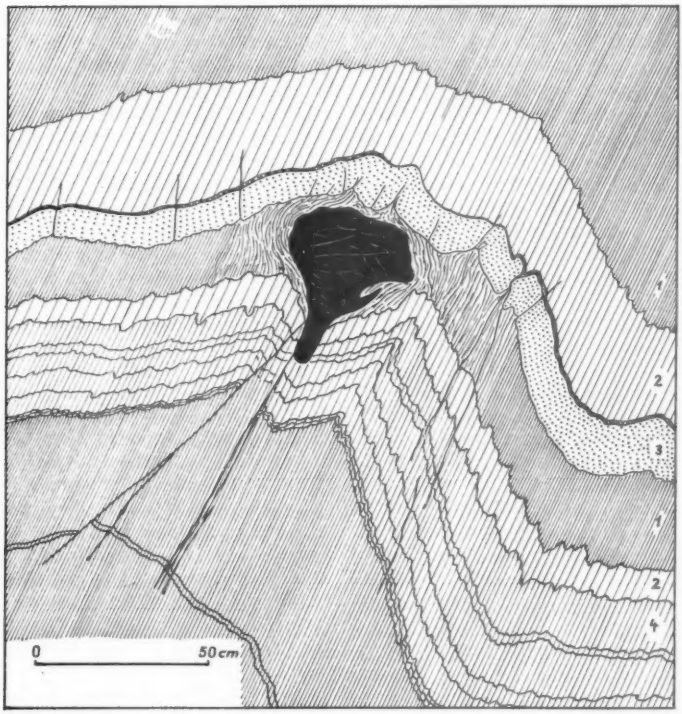

FIGURE 16.—DEFORMED DOLOMITE BLOCK IN SMALL ANTICLINAL FLEXURE

1, Soft shale; 2, arenaceous shale; 3, quartzite; 4, laminated shale. Anistropic stress distribution caused by a dolomite block in the apex of a fold just below the quartzite band has led to club-shaped deformation of this block and piercing of several strata.

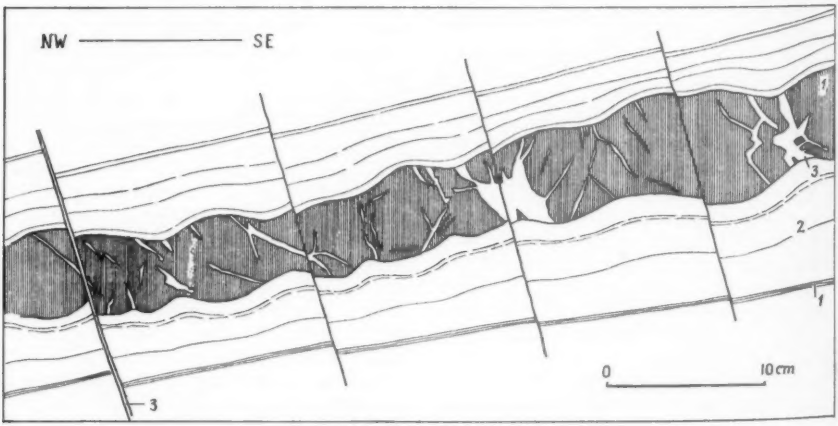

FIGURE 17.—SHALE BAND FRACTURED IN PLASTICALLY DEFORMED LIMESTONE

Shale has accommodated itself to plastic deformation of limestone by boudinage and with associated symmetrical calcite-filled fractures. 1, Shale; 2, laminated limestone; 3, calcite.

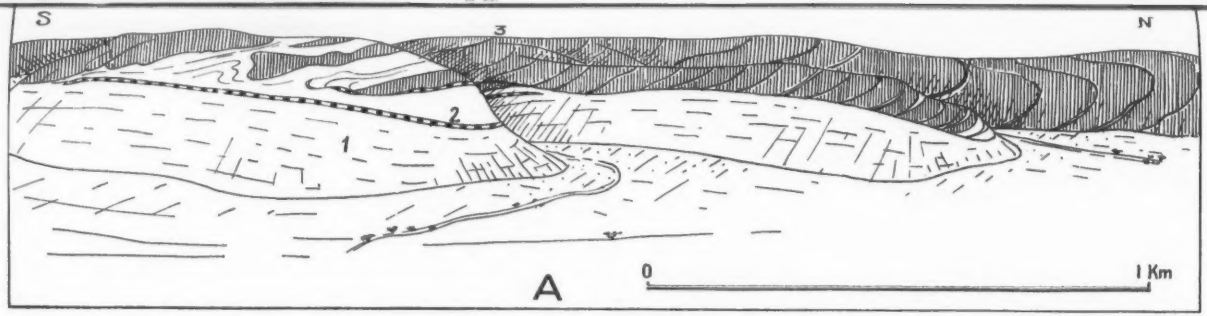

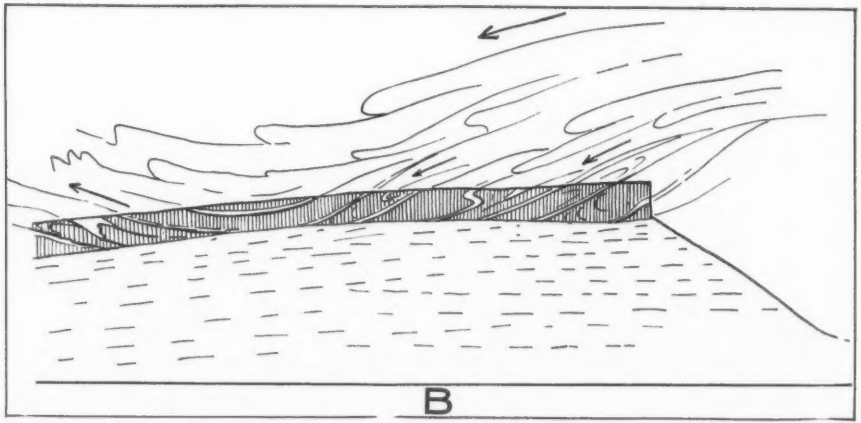

FIGURE 18.—STRUCTURE OF KUDU NAPPE

A is a sketch of a hillside at southern boundary of farm Nauzerus. The nappe here consists of southward-dipping dolomite slices which end abruptly at the base of the nappe. A few miles farther south the slices dip in the opposite direction and folding is once more apparent. 1, Slates of Pavian series; 2, unconformity dolomite; 3, dolomite of Kudu series. *B* interprets this structure as down-facing folds which have lost their apices by friction along the main movement plane. Orientation as in Figure 18, *A*. Total width about 15 km.

elongation corresponds to the *a* direction of Sander's terminology (Sander, 1948, p. 68).

In the Klipbok series, by contrast, pebbles are elongated parallel to the fold axes. The elongation thus corresponds to the *b* direction. In both cases a more or less pronounced lineation parallel to the axes of greatest elongation can be observed (Fig. 15).

There is thus a surprising difference of deformation style which must be fitted into the general movement pattern.

The Pavian series forms the floor over which the great Kudu nappe has moved. Under the great load of this *traineau écraseur*, the Pavian series has been rolled out and folded. It seems understandable that the fluid nature of this movement should produce stretching in the direction of flow.

The Klipbok series was folded under quite different conditions. It was riding on the back of the rather competent Kudu dolomite and was comparatively unconfined laterally. This movement produced its own characteristic internal deformation (elongation in *b*).

Pure limestones throughout show fully plastic, continuous deformation, more so than the dolomites and even the shales. Thin shale intercalactions are fractured along symmetrical conjugate calcite-filled fissures (Pl. 5, fig. 2). Thicker bands are stretched into boudinage structures and torn. It seems that shales become more competent if their water content is reduced by compression. Figure 17 and Plate 5, figure 3 show the extent of deformation, even in apparently little affected limestones. The pebbles embedded in the blue limestone of the Pavian series are elongated and oriented at right angles to the fold axes. The plastically deformed limestones are finely recrystallized. It is only in the thicker Schwarzkalk beds that deformation is more brittle. These rocks are considerably sheared and fractured, and the fractures are calcite-filled.

Thin quartzite bands alternating with shales are folded without being fractured. They are intensely puckered in many places. Thicker beds are, however, commonly sheared and covered with slickensides or brecciated along lines of flexure.

The dolomites are almost everywhere intensely sheared and brecciated. Even folds appearing perfectly continuous from a distance prove to be a mosaic of fragments when viewed more closely. Only a few thin dolomite bands are folded without being fractured.

Conjugate fracture systems in the Naukluft area generally show a high degree of symmetry which is attained only exceptionally in other folded areas. This symmetry is probably due to the great freedom of this unconstricted deformation.

Such phenomena fit well into the hypothesis of gliding under the influence of gravity with little confinement. The brittle deformation style of the shales, quartzites, and dolomites might suggest comparatively rapid folding, but lack of confinement would tend to produce similar structures, regardless of speed of deformation. The intimate connection between sedimentation and folding shown by the Klipbok series suggests slow movement.

Summary

The Naukluft Mountains are unique in many respects. A comparatively thin sedimentary succession has been intensely deformed in several phases. Folding phases and cycles of sedimentation are closely related, and both appear linked to discontinuous subsidence of the sedimentation trough.

Movement was most intense in the higher units. These transgressed the lower units as nappes. The intensity of tangential movement decreased downward, and the basement shows only a few, commonly steep, crush zones. The various tectonic units are structurally independent and selfcontained. An undisturbed unconformity exists between two of these. The uppermost nappes form a fold arc whose axial directions diverge to a greater or lesser extent from those of the lower units ("axial unconformity"). This flowage arc rests in front of the steepest slopes of the basin.

All the evidence seems to show that the sedimentary rocks have moved down one side of the basin, becoming folded in the process. Thus the Naukluft Mountains are an ideal example of deformation under the influence of gravity.

The unique style of folding is due to an unusual coincidence of several circumstances; conclusions arrived at here cannot, therefore, be applied directly to other folded areas.

However, the geology of the Naukluft area does indicate a great deal about the nature of rock deformation and sedimentation. More detailed studies in this exceptionally instructive and well-exposed area would add substantially to our fundamental knowledge of deforming processes and sedimentation.

References Cited

Cahen, L., 1954, Géologie du Congo belge: Liège, H. Vaillant-Carmanne, 577 p.

De Kock, W. P., 1934, The geology of the western Rehoboth: S. W. Africa Dept. Mines, Mem. No. 1, 136 p.

Gürich, G., 1930, Die bislang ältesten Spuren von Organismen in Südafrika: Compte Rendu 15th Internat. Geol. Congr., v. 2, p. 670–680

Haughton, S. H., 1929, Exhibition of fossils from the Nama system of South West Africa: Royal Society S. Africa Proc., May 15, 1929

— 1950, The age relationships of the Matsap Loskop, Waterberg and Nama systems: Geol. Society S. Africa Trans., v. 53, p. 205–208

Haughton, S. H., and Martin, H., 1956, The Nama system in South and South-West Africa: XX. Congreso Geologio Internacional, El Sistema Cámbrico, v. 1, p. 323–339

Holmes, A., and Cahen, L., 1955, African geochronology: Colon. Geol. Miner. Res., v. 5, p. 3–39

Kienow, S., 1955, Mechanische Probleme bei der Auffaltung der subvariszischen Vortiefe: Zeitschr. Deutsch. Geol. Ges., v. 107, p. 140–157

Krenkel, E., 1928, Geologie Afrikas, 2 Teil: Berlin, Gebrüder Borntraeger, 527 p.

Maack, R., 1924, Die Tsondab Wüste und das Randgebirge von Ababes in Südwestafrika: Berlin, Zeitschr. Deutsch. Ges. Erdkunde, No. 1–2, p. 13–29

Range, P., 1912, Geologie des deutschen Namalandes: Beitr. geol. Erf. d. Deutsch. Schutzgeb, v. 2, 104 p.

Richter, R., 1955, Die ältesten Fossilien Süd-Afrikas: Senckenbergiana, v. 36, No. 3–4, p. 243–289

Rimann, E., 1915, Geologische Untersuchungen des Bastardlandes in Deutsch-Südwestafrika: Berlin, Dietrich Reimer, 100 p.

Sander, B., 1948, Einführung in die Gefügekunde der geologischen Körper; Part I: Vienna, Springer Verlag, 215 p.

Schwellnus, C. M., 1941, The Nama tillite in the Klein Kharas Mountains, S.W.A.: Geol. Society S. Africa Trans., v. 44, p. 19–33

Geological Survey, Windhoek, South West Africa

Manuscript Received by the Secretary of the Society, December 23, 1957

Published Under the Government Printer's Copyright Authority No. 2335 of 24/7/56 of the Union of South Africa

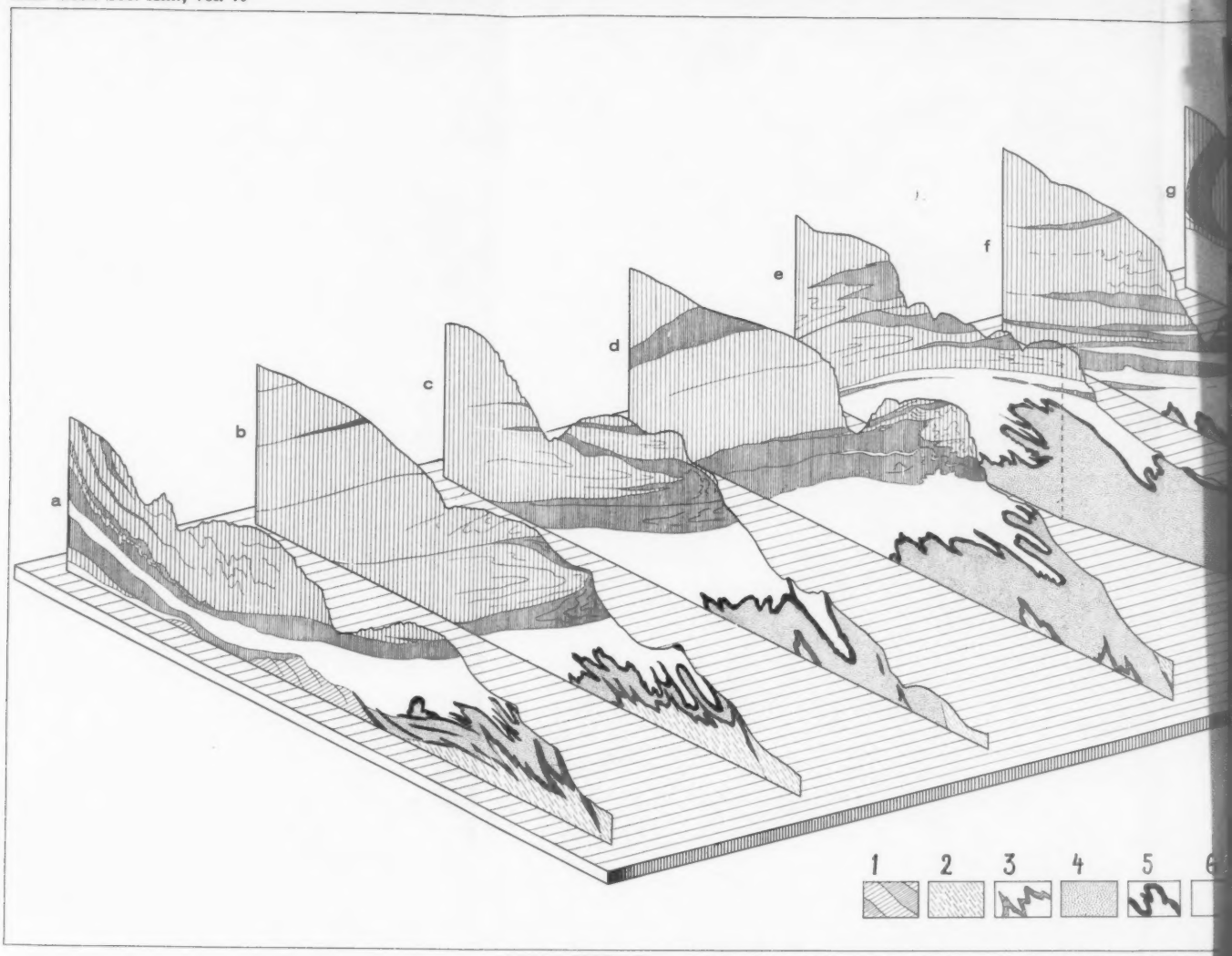

A. PROFILES OF SOUTHERN AND SOUTHWESTERN

1, Dolomite of southern facies of Pavian series; 2–5, Pavian series, northern facies (2, brown arenaceous slates; 3, blue conglomeratic limestone; 4, boulder lamina

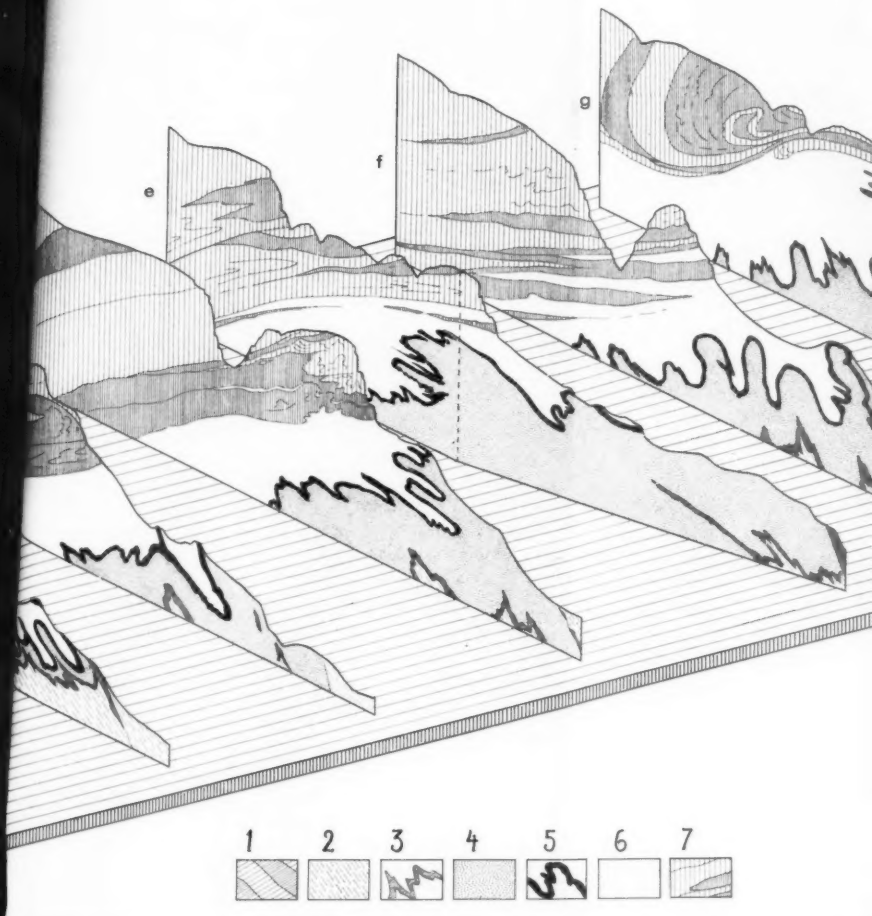

S OF SOUTHERN AND SOUTHWESTERN MOUNTAIN FA

outhern facies of Pavian series; 2–5, Pavian series, north-
own arenaceous slates; 3, blue conglomeratic limestone; 4, boulder slates; 5, white dolomite); 6
laminated limestone; 7, platy and ma

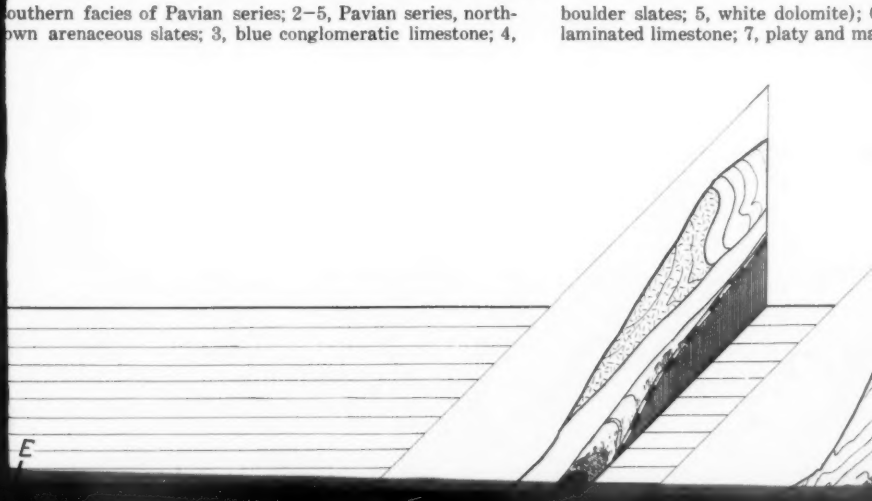

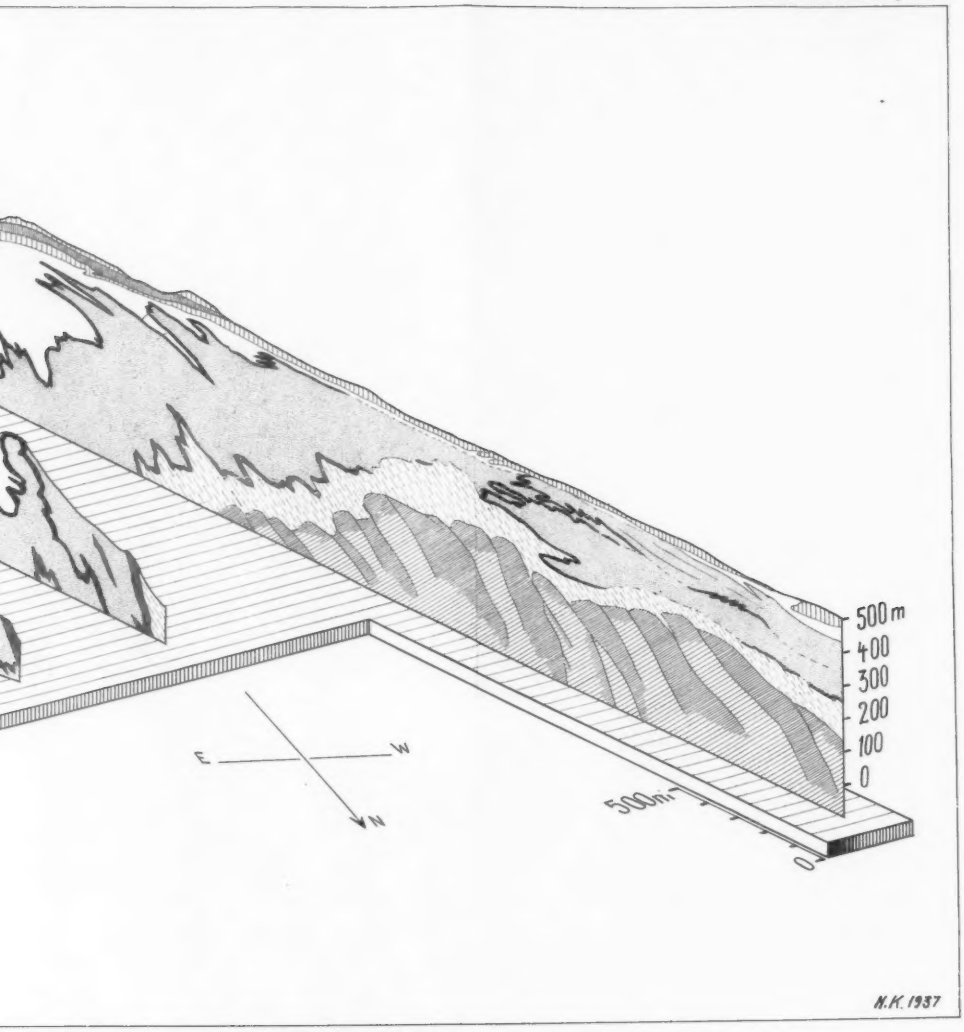

FACE, FARM BLÄSSKRANZ

ite); 6–7, Kudu series (6, purple slates and
nd massive dolomites).

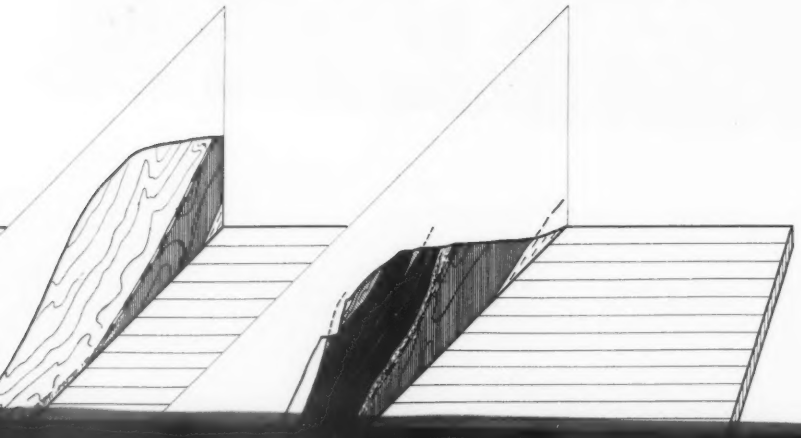

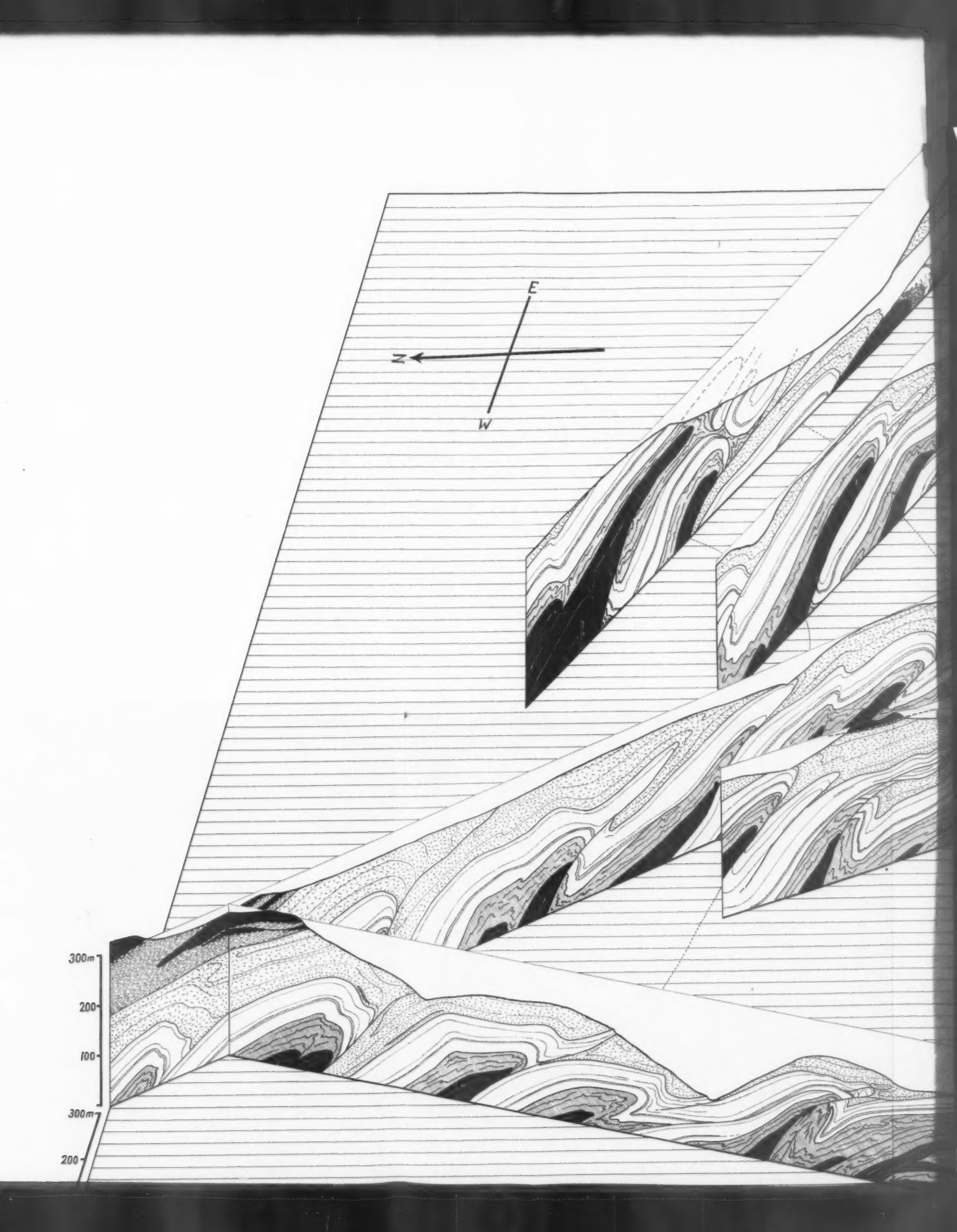
E
N
W
300m
200
100
300m
200

1, Dolomite of southern facies of Pavian series; 2–6, Pavian series, northern facies (2, brown arenaceous slates; 3, blue conglomeratic limestone; 4, lamil

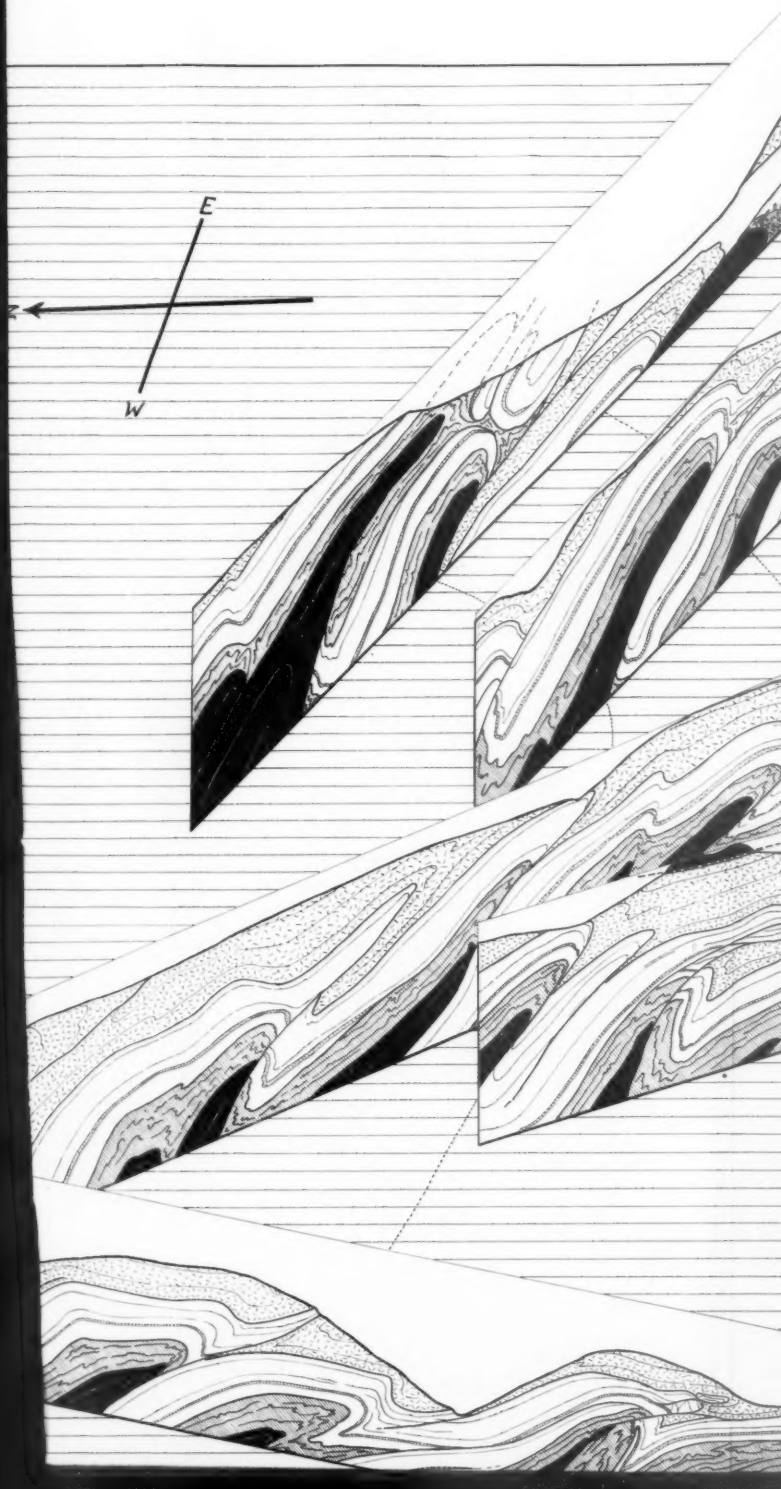

boulder slates; 5, white dolomites); 6–4, Kuddu series (6, purple slates and laminated limestone; 7, platy and massive dolomites).

Dassie series
8 White dolomite
7 Chert-banded dolomite
6 Thin-bedded quartzites and purple slates
5 Massive dolomite and red limestone

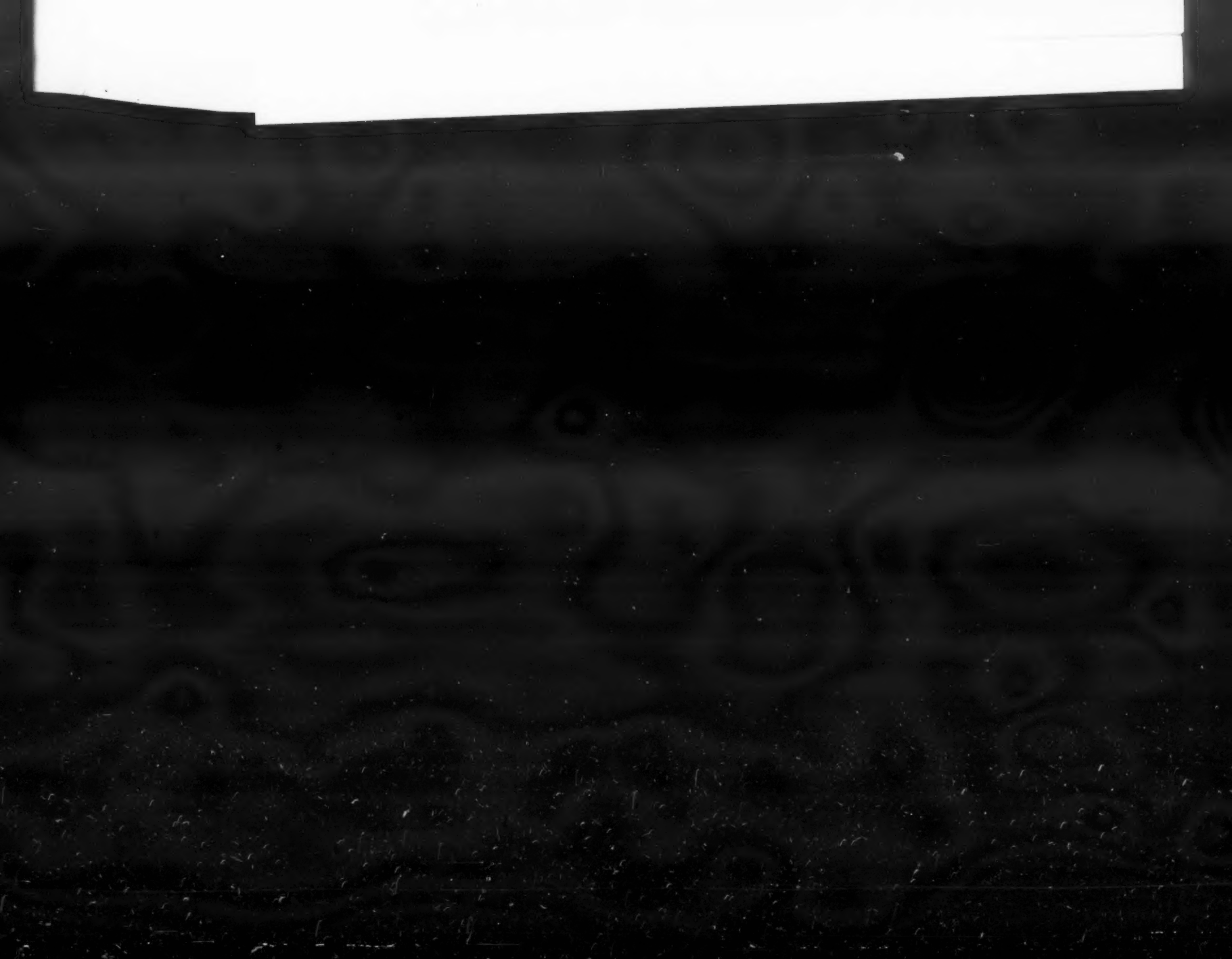

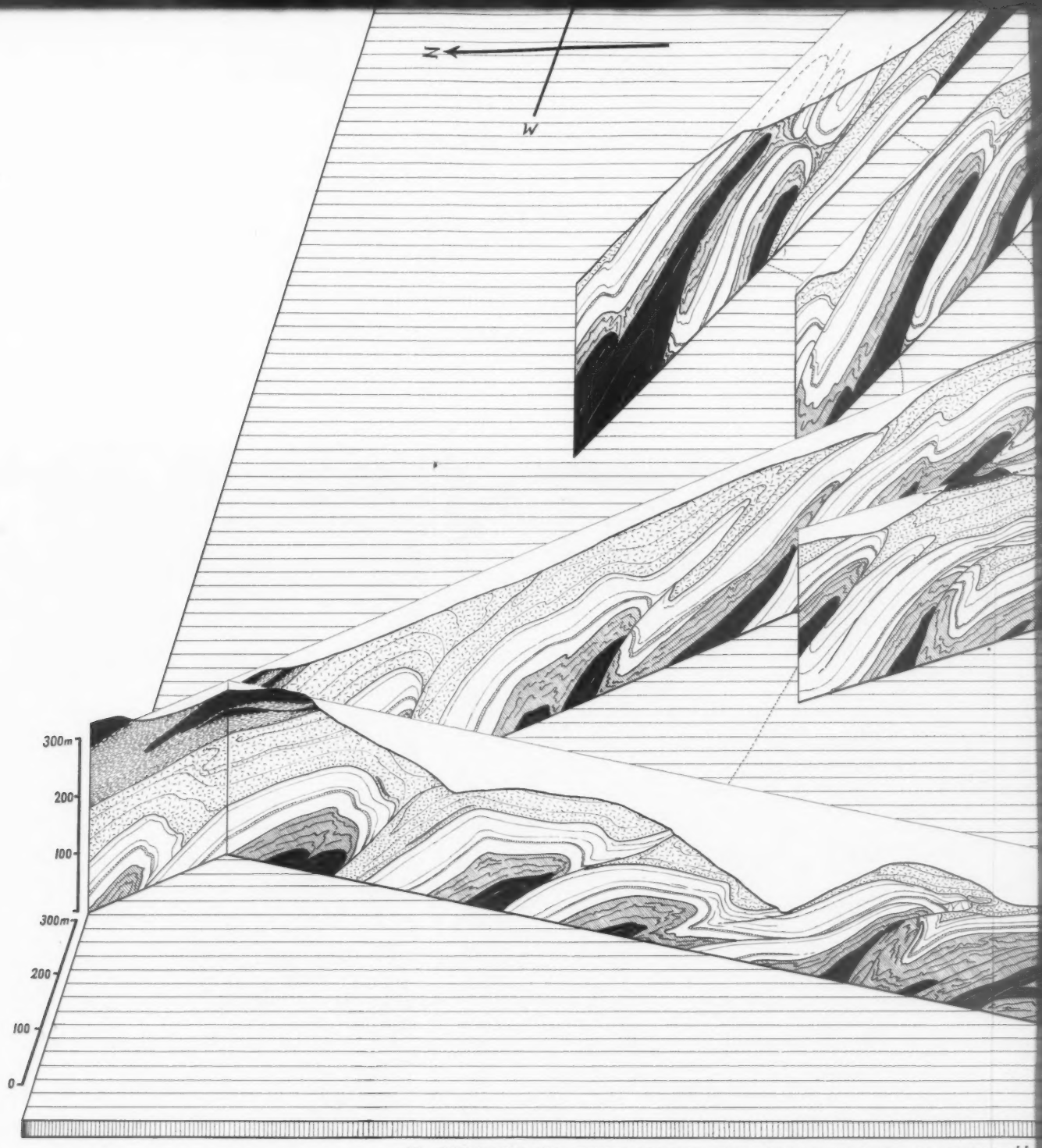

B. SECTIONS THROUGH FRONT RANGE, FARM BÜ

The Dassie nappe (its base on the Unconformity dolomite is shown only in the upper profiles) consists of imbricated digitations. Curving thrust planes and formation of digitations result from differential retardation by friction.

Dashed lines on the datum plane connect in the arcuate pattern of the whole structure basal bluish-purple slates (4) and lowest dol

PROFILES, FARMS BLÄSSKR

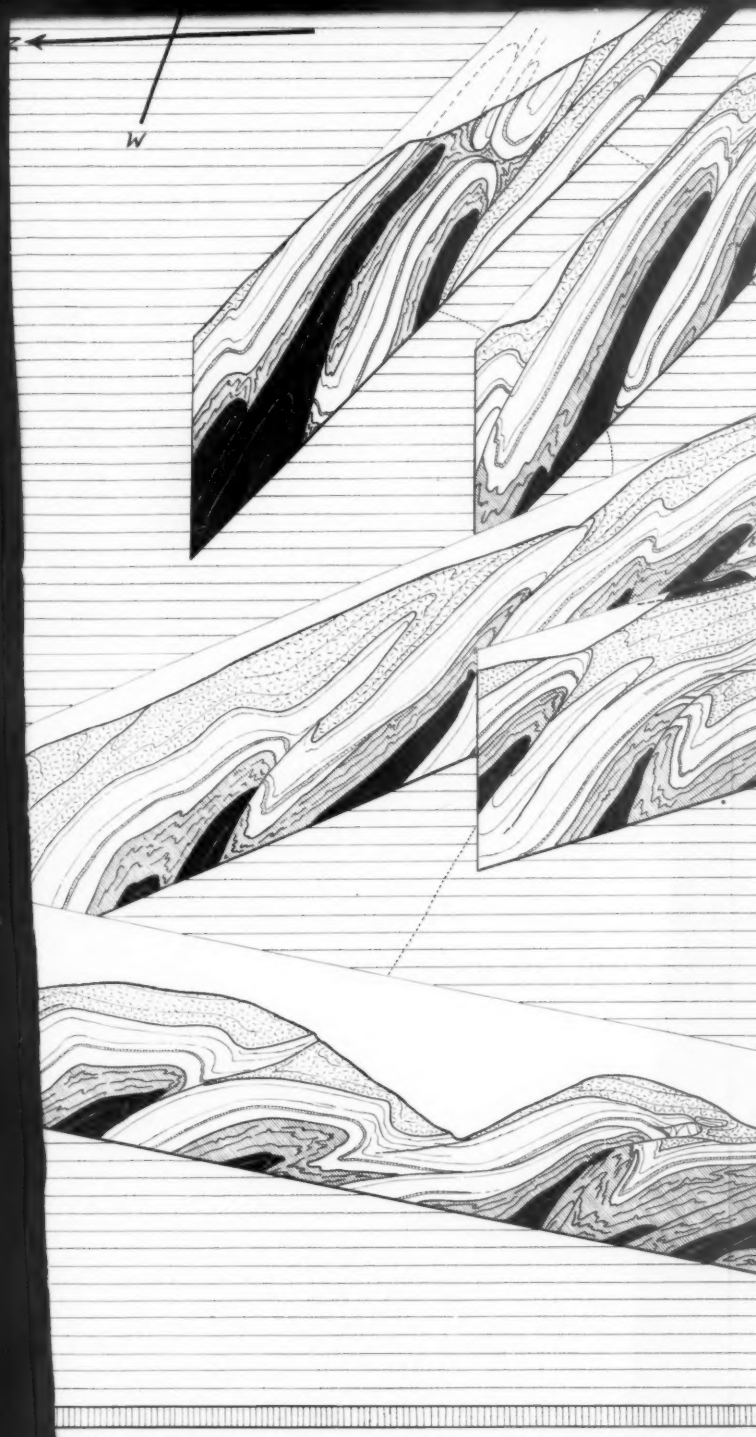

CTIONS THROUGH FRONT RANGE, FARM B

rmity dolomite is shown only in
gitations. Curving thrust planes
ferential retardation by friction.

Dashed lines on the datum plane connect
the arcuate pattern of the whole struct
basal bluish-purple slates (4) and lowest

PROFILES, FARMS BLÄSSE

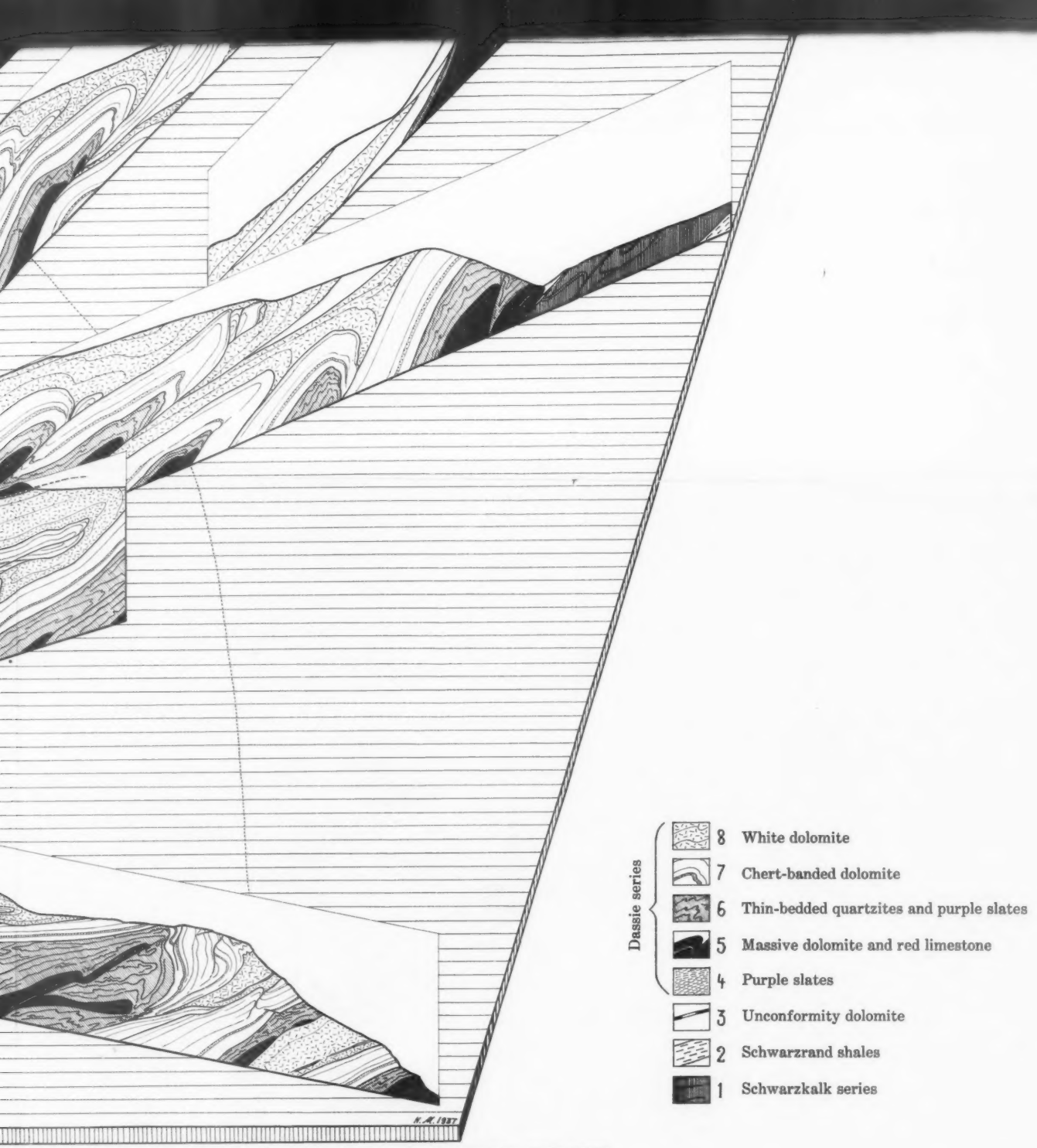

M BÜLLSPORT, NORTHEAST OF TSONDAB RIVER

onnect individual fold elements and show structure. A second, higher nappe with owest dolomite (5) appears at the extreme north end of the lowest section and as a small outlier on top of the small profile in the center.

SSKRANZ AND BÜLLSPORT

Introduct
Previous
Acknowle
Geology
Structure
Analysis
Summary
Reference

Figure
1. Index
Valle

Sinkin
don coun
of Tyron
Nittany
and dolo
anticline,
plunging
open to t
west by a
by Tusca
plunging

Close
Birmingh
cian and
the imag
of these
surrounde
requires
ing or by
ing. Ear
out-of-pla

BULLETIN OF THE GEOLOGICAL SOCIETY OF AMERICA
VOL. 70, PP. 1079–1088, 7 FIGS. AUGUST 1959

THRUST FAULTING IN SINKING VALLEY, BLAIR AND HUNTINGDON COUNTIES, PENNSYLVANIA

BY N. N. MOEBS AND R. B. HOY

ABSTRACT

Sinking Valley, Pennsylvania, is floored by Cambro-Ordovician limestone and dolomite which are folded into an asymmetrical anticline overturned to the northwest. Information obtained from diamond-drill cores indicates an extensive thrust fault, accompanied by subsidiary branching offsets, which has displaced the steeply dipping northwestern limb of the anticline about 2 miles.

CONTENTS

TEXT

	Page
Introduction	1079
Previous work	1080
Acknowledgments	1081
Geology of the Sinking Valley area	1082
Structures	1084
Analysis of drilling information	1085
Summary	1087
References cited	1088

ILLUSTRATIONS

Figure	Page
1. Index map showing location of Sinking Valley, Pennsylvania	1080
2. Generalized areal geology of Sinking Valley, Pennsylvania	1081
3. Structure sections of Sinking Valley, Pennsylvania, showing the interpretation of the authors	1082
4. Sections illustrating various hypotheses for the structure at Birmingham, Pennsylvania	1083
5. Generalized stratigraphy of Sinking Valley, Pennsylvania	1084
6. Geologic map of Sinking Valley showing diamond-drill-hole locations	1085
7. Diamond-drill-hole sections showing structure at Sinking Valley, Pennsylvania	1086

INTRODUCTION

Sinking Valley, located in Blair and Huntingdon counties, Pennsylvania, 2 miles southeast of Tyrone (Fig. 1), is the southwest end of Nittany Valley. Cambro-Ordovician limestones and dolomites are exposed in an asymmetrical anticline, over-turned to the northwest and plunging southwest (Figs. 2, 3). The valley is open to the northeast but enclosed to the southwest by a V-shaped range of mountains formed by Tuscarora sandstone extending around the plunging anticline.

Close to the Little Juniata River near Birmingham two exposures of Upper Ordovician and Silurian rocks have long challenged the imagination of geologists. The presence of these shale and sandstone formations, surrounded by older dolomites and limestones, requires considerable displacement by faulting or by a combination of faulting and folding. Earlier workers have explained the out-of-place formations either as a slice which has been thrust northwest from the overturned limb of a second anticline to the southeast or a graben exposed through a thrust sheet.

Diamond-drill cores from Sinking Valley disclose a first-order fault hitherto revealed only at the exposures near Birmingham. In the area of drilling, within 2 miles west and southwest of Birmingham, this fault separates Cambrian, Lower and Middle Ordovician limestone and dolomite from the underlying Upper Ordovician and Silurian shales and sandstones. The fault is of an unusual type: in a broad sense it is concentric with the surface of the earth. It involves movement on a domed surface that has no outcrop expression except by a happenstance of folding and erosion where the fault and the younger rocks are exposed in the fensters at Birmingham.

The information obtained from drill cores suggests an explanation for the structural relationships that appears to be more plausible than earlier hypotheses. A 2-mile movement

on the fault would explain the offset between the rocks of the Birmingham fensters and their counterparts to the northwest in the upper block consisting of Brush Mountain.

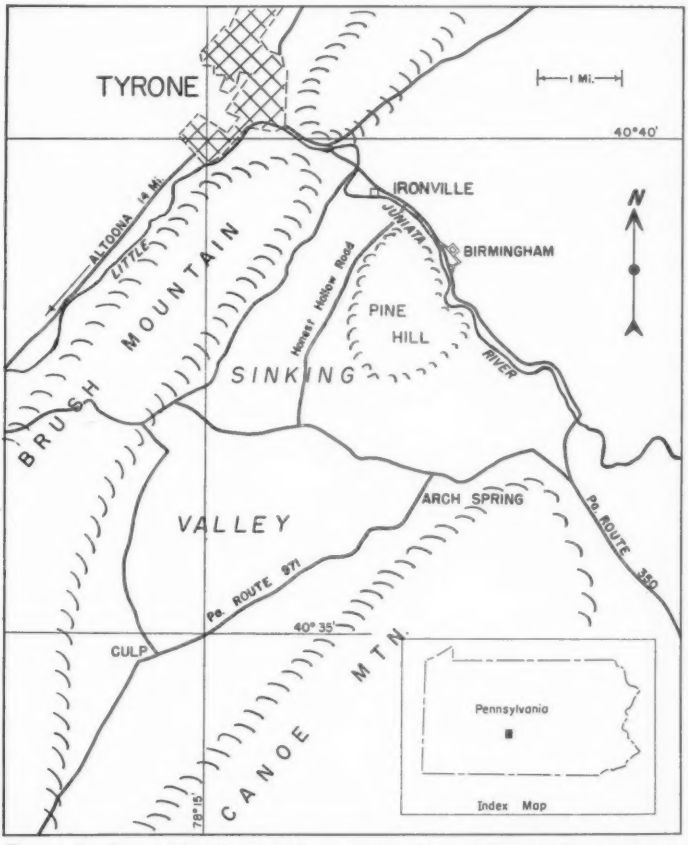

FIGURE 1.—INDEX MAP SHOWING LOCATION OF SINKING VALLEY, PENNSYLVANIA

PREVIOUS WORK

Rogers (1858, p. 503–504) was the first to note the presence of faulting at Birmingham. Platt (1881, p. 83–92) and Lesley (1885, p. 359–384) in published reports on Blair and Huntingdon counties, respectively, make no mention of a major fault at Birmingham. Butts (1918, p. 523–537) mapped the anomalous condition of younger rocks surrounded by older as emplaced by faulting.

The complex structures at Birmingham and vicinity have again more recently been studied by Butts *et al.* (1939, p. 75–78), who mapped two fensters, the first at Birmingham and the second about 1 mile northeast of Birmingham. Further work was done by Stose (*in* Butts *et al.*, 1939, p. 78), Zeller (1949, M.S. thesis, Pa. State Univ., p. 16–45), and Fox (1950, p. 162), who gave the name Knarr window to the second fenster northeast of Birmingham.

Figure 4 illustrates the structural hypotheses proposed by these men. Butts *et al.* (Sec. A) suggest that the Gatesburg formation in the upper block has been thrust from the southeast over the limestone of the Black River-Chazy groups with the Black River-Chazy to Tuscarora sequences northwest of the fault

"... having been strangely preserved and faulted downward on the northwest side. This interpretation involves the complete crushing out of the

southeast limb of an overturned anticline between Tyrone and Birmingham and the survival of a fragment of the overturned northwest limb of a second anticline lying southeast of Birmingham."

formations as a downfaulted segment of the Sinking Valley anticline, all these hypotheses require that younger rocks be thrust from the overturned northwest limb of a second anticline

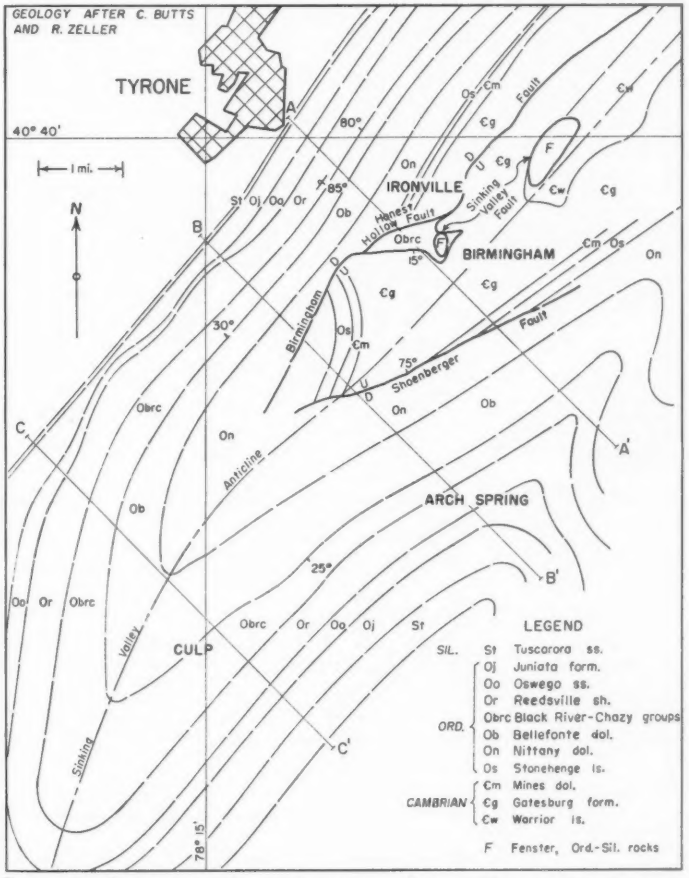

FIGURE 2.—GENERALIZED AREAL GEOLOGY OF SINKING VALLEY, PENNSYLVANIA

Stose (Sec. B) proposes a series of three southeastward-dipping and overlapping faults which converge at depth, exposing the younger rocks as a slice or horse contained between two of the thrust faults. Zeller (Sec. C) postulates three intersecting faults which thrust younger rocks to the northwest from the overturned northwest limb of the next anticline. Fox (Sec. D) interprets the exposure as representing folded formations in a graben which has been overridden by a thrust sheet. Except for the Fox interpretation, which explains the younger 4–5 miles southeast. As Butts et al. recognized (1939, p. 78), this idea is out of harmony with the fact that the Birmingham fault dies out within 2 miles to the southwest.

ACKNOWLEDGMENTS

The authors wish to express appreciation to the officials of The New Jersey Zinc Company for releasing the information for publication, and to W. H. Callahan, Manager of Exploration, who encouraged publication of the

data. A. H. Willman and D. L. Adair logged much of the core and contributed to the structural interpretation. Zeller's detailed map of the Birmingham area (1949, M.S. thesis, Pa. State Univ., p. 17) was used as a basis for projecting subsurface structures to that locality.

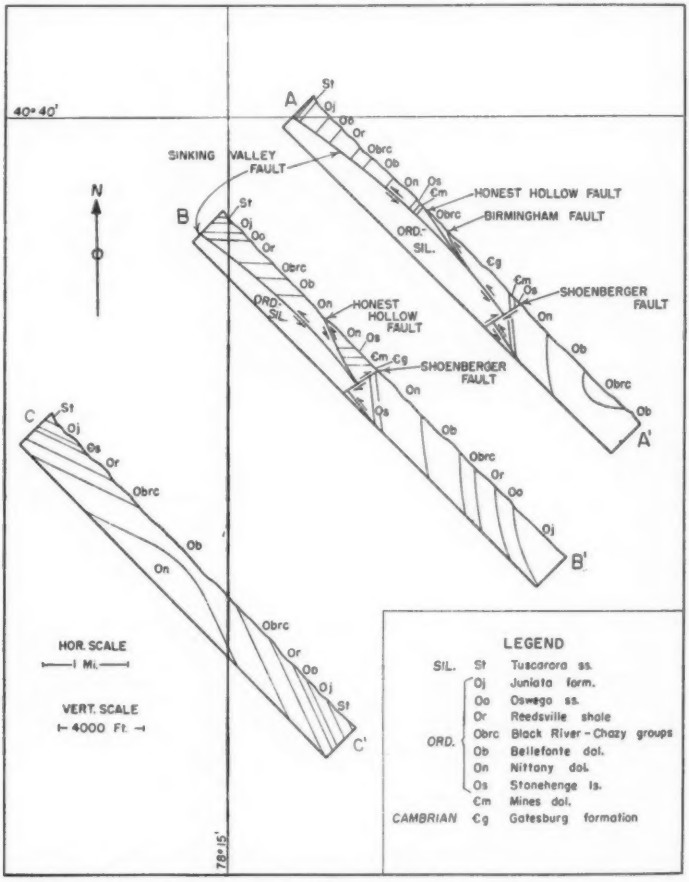

FIGURE 3.—STRUCTURE SECTIONS OF SINKING VALLEY, PENNSYLVANIA, SHOWING THE INTERPRETATION OF THE AUTHORS
(*See* Fig. 2 for location of sections)

GEOLOGY OF THE SINKING VALLEY AREA

The stratigraphy and the general structural relationships of the Sinking Valley area are described by Butts *et al.* (1939, p. 1–78). The formations are included in the Cambrian, Ordovician, and Silurian systems. The oldest formation is the Upper Cambrian Warrior limestone, exposed along the axis of the Sinking Valley anticline, extending northwestward from a point about a mile northeast of Birmingham. The youngest formation is the Silurian Tuscarora sandstone which forms the summits of the mountains that surround the valley (Fig. 2). The older units, up through the Ordovician Trenton group, consist mainly of dolomites with subordinate formations and members of limestone. The younger units, the Ordovician Reedsville shale, Oswego sandstone and the Juniata formation, consist of shale and sandstone. The thickness and general de

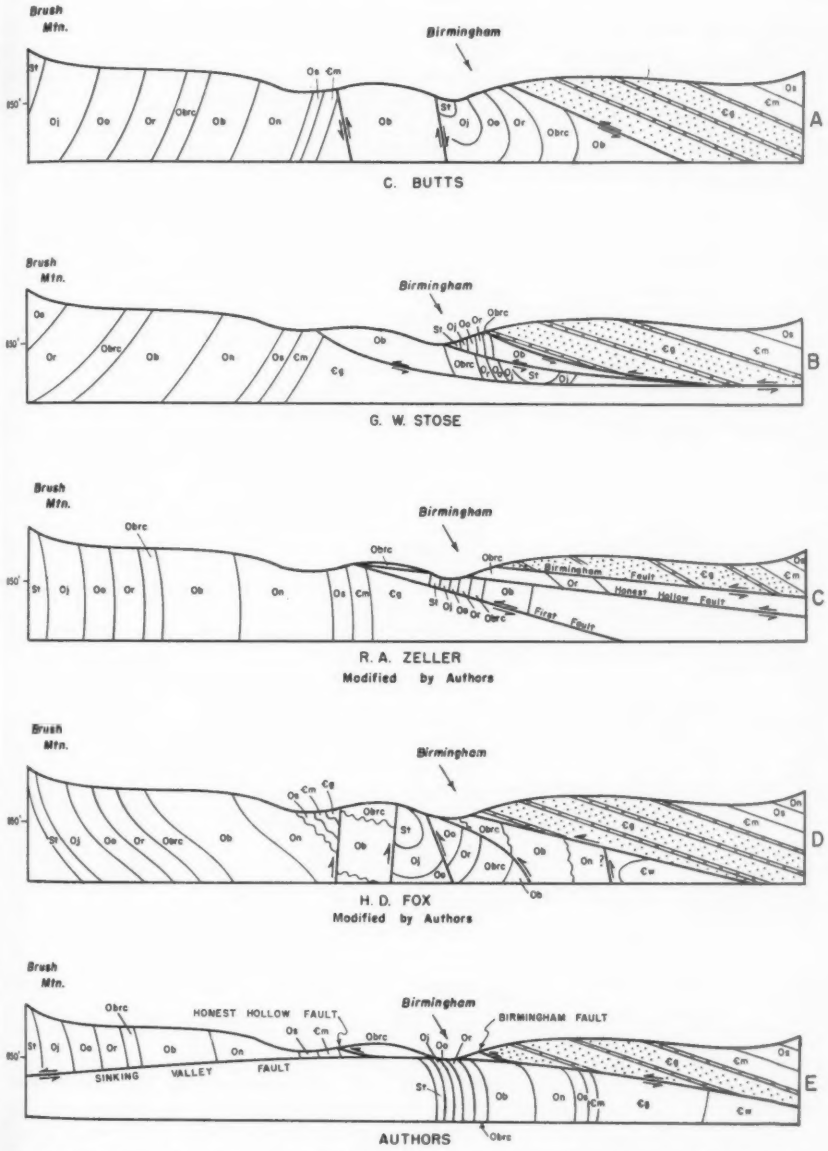

FIGURE 4.—SECTIONS ILLUSTRATING VARIOUS HYPOTHESES FOR THE STRUCTURE AT BIRMINGHAM, PENNSYLVANIA

Vertical scale exaggerated to show structural details. Length of section approximately 3.5 miles. For explanation of geologic symbols *see* Figure 3.

SYSTEM	FORMATION (GROUP)	THICKNESS IN FEET	GENERAL CHARACTER
SILURIAN	TUSCARORA QUARTZITE	400	sandstone and quartzite
ORDOVICIAN	JUNIATA FORMATION	1250	red shale, red, green, and gray sandstone
	OSWEGO SANDSTONE	800	thick-bedded gray sandstone, occasional red shale or sandstone
	REEDSVILLE SHALE	1250	calcareous olive-green shale and basal black shale
	(TRENTON GROUP)	400	thin-bedded dark limestone
	(BLACK RIVER-CHAZY GROUPS)	380	thick-bedded, dove-gray limestone
	BELLEFONTE DOLOMITE	1500	thick-bedded gray dolomite, occasional chert
	NITTANY DOLOMITE	1250	thick-bedded gray dolomite, occasional sandy beds
	STONEHENGE FORMATION	200	thin-bedded, argillaceous, lime and dolomite limestone
CAMBRIAN	MINE DOLOMITE	200	thick-bedded dolomite, abundant chert and oölites
	GATESBURG FORMATION	1750	thick-bedded dolomite, sandstone and sandy dolomite
	WARRIOR LIMESTONE	1200	thick- and thin-bedded gray limestone with siliceous shale partings

FIGURE 5.—GENERALIZED STRATIGRAPHY OF SINKING VALLEY, PENNSYLVANIA

scriptions of the formations are given in the columnar section (Fig. 5). Although the Trenton group limestones are shown on the columnar section they are similar in lithologic character to the Black River-Chazy limestones and for mapping purposes are included in the Black River-Chazy sequence.

STRUCTURES

Butts *et al.* (1939, p. 75–78) point out that the area is located on the summit and flanks of the Nittany arch, which is an anticlinorium extending for more than 80 miles northwestward. In cross section the arched form is modified by faults and minor undulations superposed on the major structures. The Sinking Valley anticline represents the southwest extremity of the apex of the arch (Fig. 2). It is asymmetrical, overturned to the northwest. It is complicated by faulting along its axis where the Birmingham fault thrusts older formations to the northwest (Fig. 2). The exposures of younger rocks at Birmingham and at the Knarr fenster a little more than a mile northeast of Birmingham (Figs. 2, 3) indicate

that additional faulting of considerable magnitude took place, but as Butts *et al.* (1939, p. 78) stated, "... no satisfactory explanation of the entire situation has yet been reached."

Nittany dolomite or Stonehenge limestone above. The rocks cored under the fault have been tentatively identified as Reedsville shale and Juniata formation on the basis of color

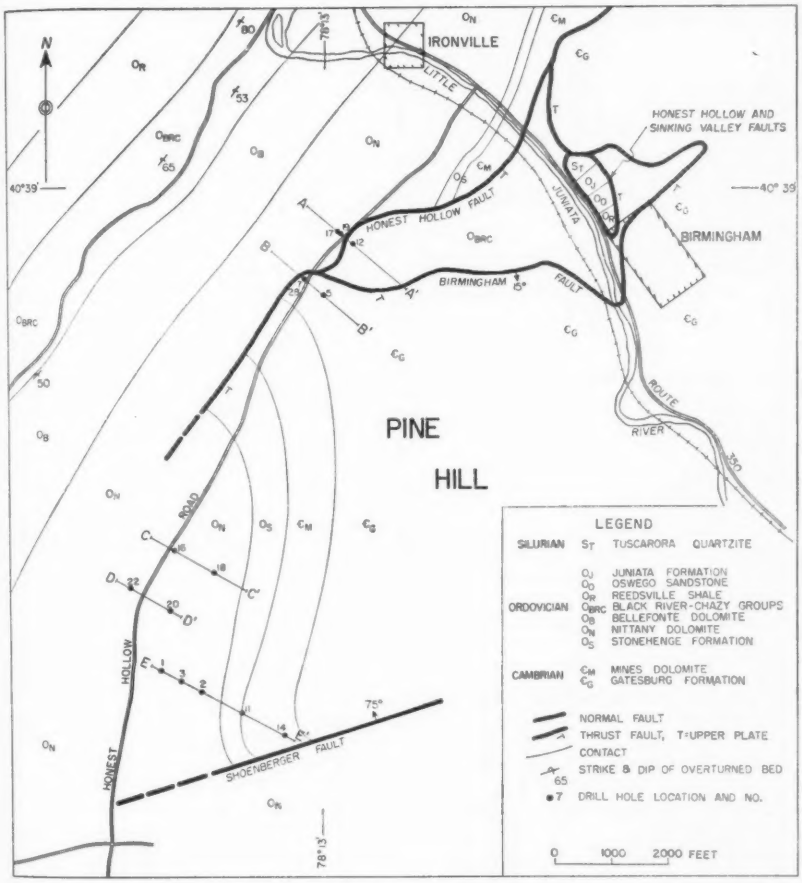

FIGURE 6.—GEOLOGIC MAP OF SINKING VALLEY SHOWING DIAMOND-DRILL-HOLE LOCATIONS

ANALYSIS OF DRILLING INFORMATION

A series of exploration holes drilled west and southwest of Birmingham in 1956 provided information revealing the existence of a gently arched fault under the area (Figs. 6, 7), which the authors named the Sinking Valley fault. Eight holes reached sufficient depth to penetrate the fault, which is evidenced by abundant fracturing and recementation, grooving, polishing, and abrupt change in stratigraphy. Each hole cored black shale or red and green sandstone and shale under the fault in contact with and composition. These rocks correspond to the two formations observed in the Birmingham exposures, which have been identified by Butts, Zeller, and others as Reedsville and Juniata.

Recognition of the Sinking Valley fault permits a relatively simple explanation for the presence of the younger rocks in the Birmingham area. The two exposures are fensters through an upwarped thrust fault which has an axis nearly coincident with that of the Sinking Valley anticline. A net dis-

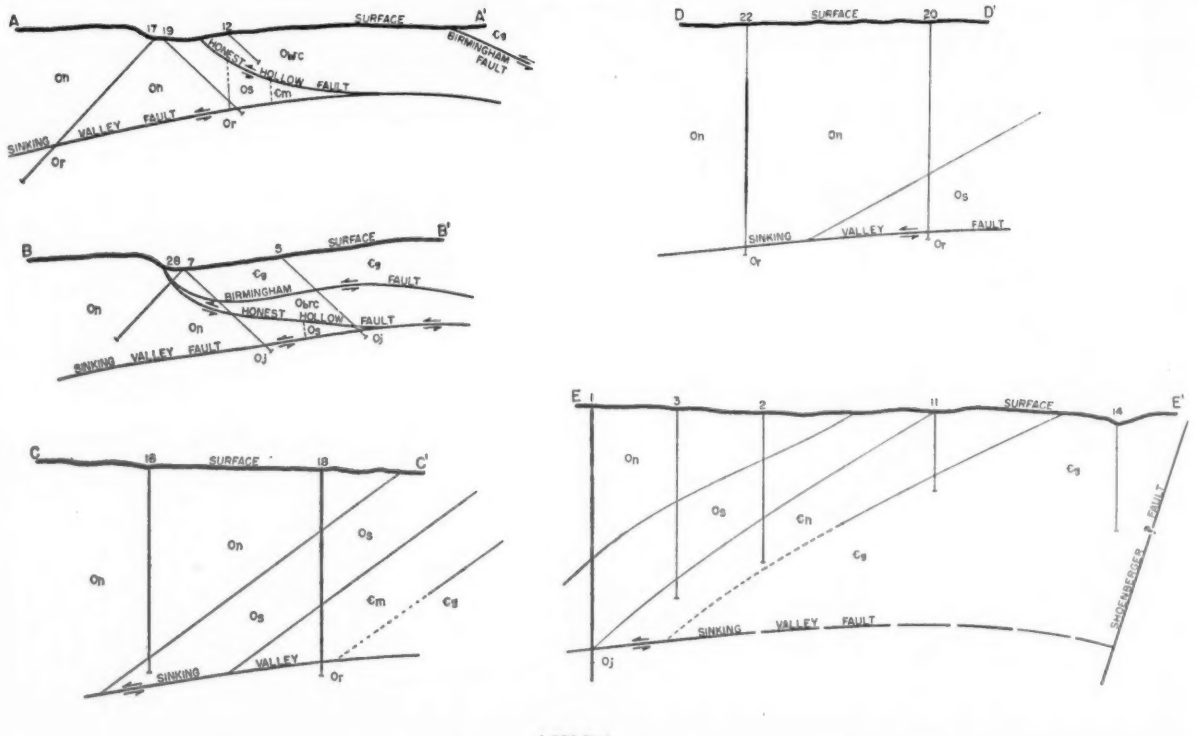

⊢300 Ft.⊣

FIGURE 7.—DIAMOND-DRILL-HOLE SECTIONS SHOWING STRUCTURE AT SINKING VALLEY, PENNSYLVANIA
For explanation of geologic symbols *see* Figure 3.

placement of 2 miles on the Sinking Valley fault would account for the position of the Tuscarora in the fenster relative to the Tuscarora of the upper block northwest at Brush Mountain (Fig. 4, sec. E). The other thrusts are lesser southeast-dipping branches of the main break. The Birmingham fault has relatively little displacement and can logically die out to the southwest as mapped by Butts *et al.* (1939, p. 78). The slice under the Birmingham fault, consisting largely of brecciated limestone, is probably the Black River-Chazy sequence, or possibly Stonehenge, in a horse dragged along between the Birmingham and the lower branch fault, which was recognized by Zeller (1949, M.S. thesis, Pa. State Univ., p. 19) and is here named the Honest Hollow fault. This slice has been thrust between the Gatesburg above and the Mines, Stonehenge, and Nittany below. The relatively large volume of limestone in the slice compared to the narrow trace of the Black River-Chazy sequence against the fault requires either that another thicker limestone unit is involved (for example, the Stonehenge) or that the Black River-Chazy sequence was intercepted where the dip is more gentle than indicated on the sections. Little is known regarding the structure of the under block. The strike component of the thrust offset may be so large that a gently dipping part of the structure is present under the Sinking Valley fault. Section A-A′ (Fig. 7) illustrates the Sinking Valley fault below and the Honest Hollow fault branching therefrom to the surface, overlain by the Black River-Chazy sequence, and, near A′, the Birmingham fault overlain by Gatesburg. Section B-B′ (Fig. 7) is similar, except that it illustrates the manner in which the Black River-Chazy block pinches out where the Honest Hollow and Birmingham faults rejoin near the surface.

Comparison of sections shows that the trace of the Sinking Valley fault becomes progressively deeper to the southwest, which indicates that the "arch" of the fault, like the axis of the anticline, plunges southwest. The fault also dips northwestward from the fensters without causing any recognized stratigraphic breaks; it must continue subsurface under the Bald Eagle Valley and, unless it steepens or dies out along bedding, under the Allegheny Plateau.

This type of fault, having no apparent surface expression except of accident of erosion at the fensters, is unusual but not unique, because Rodgers described (1950, p. 680) and illustrated (p. 678, Fig. 3) an almost identical fault in the Sequatchie anticline area of Tennessee. He states:

> "If they are windows, they have been eroded through a thrust fault that disappears northwestward, its displacement having been taken up in the arching along the Sequatchie anticline and the folds farther northwest."

Hayes (1891, p. 141–152) was the first to describe low-angle thrust faults in the southern Appalachians of great lateral displacement with the fault surfaces commonly warped. Rodgers (1949, p. 1649) noted that faults such as Hayes described have been found in many parts of the southern and northern Appalachians, whereas in the folded middle Appalachians, where the structure is simpler, large low-angle faults have nowhere been recognized. Rodgers was notably perceptive when he stated,

> "... the faulted area on the Nittany anticline at Birmingham, Pennsylvania, ... strongly suggests low-angle faulting to a geologist who has worked among the low-angle thrust faults of east Tennessee."

Stearns (1955, p. 620–625) describes a number of low-angle thrust faults in the Cumberland Plateau of Tennessee. These differ from the Sinking Valley fault in that they commonly show a low angle of faulting relative to bedding, and the beds above the fault planes are characteristically crushed, whereas at the Birmingham fenster the rocks below, as well as above, the Sinking Valley fault are intensely crushed and thinned, and the angle of faulting relative to the bedding is large.

No new information has been revealed regarding the Shoenberger fault (Fig. 6, Fig. 7, sec. E-E′), as drill-hole 14 did not reach sufficient depth to penetrate its projected trace.

Summary

Geological analysis of subsurface information revealed by diamond drilling in Sinking Valley provides a more simple explanation than those previously proposed for a complex fault pattern. Exposures of younger shales and sandstones near Birmingham are revealed in fensters through a thrust fault containing older dolomites and limestones in the upper block. The thrust is arched along an axis closely coinciding with the axis of the Sinking Valley anticline and, like the anticline, plunges southwest. The main fault, named the Sinking Valley fault, has a net displacement of 2 miles. The fault dips gently northwest from Birmingham under

For explanation of geologic symbols see Figure 3.

Brush Mountain and, presumably, continues at depth until it dies out. Although the major thrust is unusual in being without apparent surface expression except at the fensters a similar fault has been described by Rodgers in Tennessee.

Two faults, named the Honest Hollow and the Birmingham, are located in the immediate vicinity of Birmingham. These dip southeast and are branches from the main thrust. They join each other in both directions along strike, enclosing an irregular lens-shaped horse consisting largely of broken and brecciated Black River-Chazy limestones.

References Cited

Butts, C., 1918, Geologic section of Blair and Huntingdon counties, central Pennsylvania: Am. Jour. Sci., v. 46, p. 523–535

Butts, C., Swartz, F. M., and Willard, Bradford, 1939, Geology and mineral resources, Tyrone quadrangle: Pa. Geol. Survey 4th ser., Topog. and Geol. Atlas Pa. 96, 118 p.

Fox, Harold D., 1950, Structure and origin of two windows exposed on the Nittany Arch at Birmingham, Pennsylvania: Am. Jour. Sci. v. 248, p. 153–170

Hayes, C. Willard, 1891, The overthrust faults of the southern Appalachians: Geol. Soc. America Bull., v. 2, p. 141–154

Lesley, J. P., 1885, The Little Juniata section and Warrior's Mark, p. 359–384, *in* White, I. C. The geology of Huntingdon County, Pennsylvania: 2d Pa. Geol. Survey Rept. T3, 471 p.

Platt, F., 1881, The geology of Blair county, Pennsylvania: 2d Pa. Geol. Survey Rept. T, 311 p.

Rodgers, John, 1949, Evolution of thought on structure of middle and southern Appalachians: Am. Assoc. Petroleum Geologists Bull. v. 33, p. 1643–1654

—— 1950, Mechanics of Appalachian folding as illustrated by Sequatchie anticline, Tennessee and Alabama: Am. Assoc. Petroleum Geologists Bull., v. 34, p. 672–681

Rogers, H. D., 1858, The geology of Pennsylvania VI: 1st Pa. Geol. Survey, 568 p.

Stearns, Richard G., 1955, Low-angle overthrusting in the central Cumberland Plateau, Tennessee: Geol. Soc. America Bull. v. 66, p. 615–628

The New Jersey Zinc Company, R.D. 1, Central Valley, Pa.; Earth Sciences Dept., Stanford Research Institute, Menlo Park, Calif.

Manuscript Received by the Secretary of the Society, July 24, 1958

BULLETIN OF THE GEOLOGICAL SOCIETY OF AMERICA
VOL. 70, PP. 1089–1118, 12 FIGS. AUGUST 1959

TURBIDITES IN FLYSCH OF THE POLISH CARPATHIAN MOUNTAINS

By S. Dzulynski, M. Ksiazkiewicz, and Ph. H. Kuenen

Abstract

The Polish Carpathian Mountains are occupied for the greater part by rocks of the flysch type, in which graded bedding with the usual accompanying sole markings and other features of turbidites are ubiquitous. For several years Polish geologists have successfully applied the concept of turbidity flow to explain features formerly thought to be conflicting. This paper deals with paleogeographic problems and summarizes results so far attained by numerous measurements of current direction. A few separated troughs persisted throughout the Cretaceous and Paleogene sedimentary history. Each of these oblong basins had its separate history in which location and direction of supply varied greatly with time. Most units show a consistent system of transport. Dominantly lateral supply is obvious in some cases. In others the measurements indicate a distant supply and from thence longitudinal transport in the flysch trough with or without local coarse supply from the sides. However, evidence, mainly paleogeographic, strongly suggests that local cordilleras between or flanking these troughs acted as the main source. Continued field work may throw light on this controversial topic which occurs in many other geosynclines that contain turbidite formations.

A number of sedimentological problems are examined on the basis of evidence mainly from Poland: upper margins of graded beds, suspended currents, convolute lamination, doubtful turbidites, glauconite in turbidites. A few new sole markings are named and described.

CONTENTS

TEXT

	Page
Introduction	1089
Acknowledgments	1090
Paleogeography	1090
Tectonics and stratigraphy	1090
Features of the Carpathian flysch	1094
Some paleogeographic conclusions	1096
Alternative interpretations	1107
Turbidity currents	1110
Introductory remark	1110
Upper margin of graded beds	1110
Suspended currents	1112
Convolute lamination	1112
Doubtful turbidites	1113
Glauconite in turbidites	1114
Sole markings	1115
Selected bibliography	1117

ILLUSTRATIONS

Figure	Page
1. Tectonic map of the Polish Carpathian Mountains	1091
2. Two cross sections through the Polish Carpathian Mountains	1092
3. Current directions	1099
4. Paleogeography of the Carpathian area during the Cenomian and Turonian	1101
5. Current directions in the Pasierbiec sandstone in the Skawa and Raba valleys	1102
6. Current directions during the sedimentation of the Krosno, Magura, and Podhale beds	1103
7. Current directions during the sedimentation of the Middle and Upper Krosno beds in the eastern part of the Polish Carpathian Mountains	1104
8. Paleogeography of the Carpathian area during the latest Eocene and Oligocene	1105
9. Diagrams illustrating current directions and bottom slopes in the flysch troughs	1109
10. Three soles with prod casts	1115
11. Bounce cast with cast of a small plateau at the downcurrent end	1116
12. Skip cast and prod cast at the bottom	1117

TABLES

Tables	Page
1. Stratigraphy of autochthonous flysch and the Klippen and Magura nappes	1093
2. Stratigraphy of the Silesian nappe	1094
3. Stratigraphy of the Skole nappe	1095

Introduction

The Carpathian Mountains are uncommonly rich in rocks usually referred to as flysch. This ill-defined term as used here means: thick series of regularly bedded marine geosynclinal sedimentary rocks showing alternation of shales or marls with dark sandstones (graywacke-like rocks), usually poor in fossils but rich in organic and inorganic sole markings (= hieroglyphs).

In this paper units containing fragmental calcarenites instead of sandstones are also included. Nearly all flysch units show some graded bedding, and in many cases this structure is common or even predominant.

In Poland the Carpathian Mountains are built up almost entirely of flysch rocks over their whole length of 300 km. Ksiazkiewicz spent 30 years on the study of stratigraphic and structural problems of this area. Over a period of 50 years the application of the concept of nappes has brought a revolution in the understanding of the structural features. Three main nappes and several smaller units can be distinguished; each has its own complications (Figs. 1, 2).

In spite of scarcity of fossils diligent search has brought to light ample evidence on which to found a general stratigraphy, and for many units a more refined subdivision can be given (Tables 1–3).

Understanding of the paleogeography and sedimentation has lagged far behind. The sources from whence the sedimentary material was derived remained in doubt, although large neighboring areas can be excluded because they were submerged most of the time. Pebble composition proved to be of little help, because many of the rock types encountered are not known from the vicinity *in situ*. A few conglomeratic formations show gradual changes in thickness over wide areas and thus provide some indication of the direction of transport. But the paleogeography within the geosyncline remained mostly guesswork. The sands and coarser material were taken to prove shallow water. However, they are interbedded with shales and marls which show distinct indications of deep-water origin such as flat lamination, only pelagic fauna and agglutinating Foraminifera, and a profusion of undisturbed organic hieroglyphs. The environment of deposition remained in doubt because of the conflicting evidence for deep and shallow water.

This deadlock now appears to have been overcome by adoption of the concept of turbidity flow. For 6 years Ksiazkiewicz and his pupils have been applying the ideas and methods advocated by Kuenen in connection with graded rock series. The inorganic sole markings, the slump structures, the types of bedding, the internal lamination and lineation, and the ripple mark have all been examined with care. All features characterizing presumably resedimented strata have been discovered in the present area, and some new types have been recognized. The directions of supply deduced from these features have been regionall mapped in several flysch units in various area

The data on environment and paleogeog raphy that can thus be ascertained are still fa from complete, and at least 6 years will be re quired to finish the first survey. However, th results already obtained are so enlightening an promise such a stride forward in understandin the history of a geosyncline that a new phase i Carpathian geology appears to have bee entered. Hence, an interim report on the pre liminary findings is well warranted.

Kuenen's visit to the area under the guidanc of Dzulynski and Ksiazkiewicz provided a opportunity for reviewing present results an principal problems and for a comparison wit other turbidite formations. The new data an the exchange of ideas helped to throw light o some problems of general interest for all tu bidite formations.

The first part of this paper is devoted t paleogeography in an attempt to show how th new data can be used to advantage. Whe source areas for various formations are sought conflicting evidence is encountered in som cases, and this difficulty has not yet bee solved. In the second part of this paper a num ber of problems concerning turbidites and th mechanism of turbidity flow are reviewed.

We hope that this summary may prove in teresting to geologists unable to visit th Polish Carpathian Mountains and that it may stimulate fruitful application of the concept o turbidity currents in other regions.

Acknowledgments

We wish to thank the Polish Academy o Science for inviting Kuenen to spend 18 day in Poland as their guest, and the Polish Geo logical Survey for providing transportation We are also much indebted to A. Radomski an E. ten Haaf for their generous permission to us unpublished data.

Paleogeography

Tectonics and Stratigraphy

South of the Polish flysch Carpathian Moun tains lie the Tatra Mountains constituted by massif of granites and folded Triassic to Middl Cretaceous sediments. This massif is sur rounded by a transgressive envelope of th Podhale flysch of mainly Eocene age, folde but not overthrust. The present breadth in th north is 15 km. Along the northern margin o

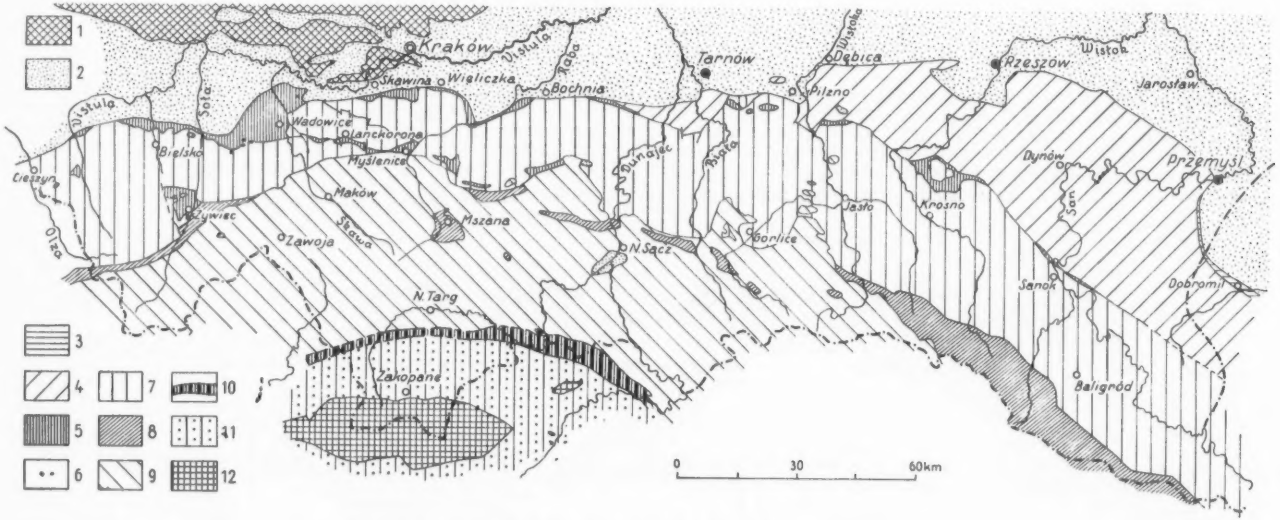

FIGURE 1.—TECTONIC MAP OF THE POLISH CARPATHIAN MOUNTAINS

1—Foreland; 2—Miocene of the foredeep and in transgression on the Carpathian Mountains; 3—Marginal zone; 4—Skole nappe; 5—Sub-Silesian nappe; 6—External Klippes; 7—Silesian nappe; 8—Fore-Magura zone (Dukla folds, for example); 9—Magura nappe; 10—Internal Klippen zone; 11—Podhale flysch; 12—Pre-Eocene nappes of the Tatra Mountains

FIGURE 2.—TWO CROSS SECTIONS THROUGH THE POLISH CARPATHIAN MOUNTAINS

Upper cross-section, through western part: M_1—Folded Miocene; M_2—Nonfolded Miocene; a—Lower Cretaceous of the Sub-Silesian nappe; b—Upper Cretaceous of the Sub-Silesian nappe; c—Paleogene of the Sub-Silesian nappe; k_1—Lower Cretaceous of the Silesian nappe; k_2—Upper Cretaceous of the Silesian nappe; p—Paleogene of the Silesian nappe; 1—Cretaceous of the Magura nappe; 2, 3—Paleogene of the Magura nappe. Lower cross-section through eastern part: 1—Lower Cretaceous; 2—Upper Cretaceous of the Skole nappe; 3—Upper Cretaceous of the Dukla folds and Magura nappe; 4—Upper Cretaceous of the Sub-Silesian nappe; 5—Upper Cretaceous of the Silesian nappe; 6—Eocene beds in all units; 7—Krosno beds; 8—Magura sandstone; 9—Miocene of the Foredeep.

this unit runs a narrow belt of intensely thrust and crushed Jurassic and Cretaceous rocks called the Pieniny Klippenzone. It consists mainly of limestones and marls followed by flysch members containing conglomerates, sandstones, and shales.

Excepting minor thrust units the major part of the Polish Carpathian Mountains is occupied by three great nappes of Cretaceous and Paleogene flysch: the inner Magura nappe, the Silesian nappe, and in the northeast the Skole nappe (Fig. 1). The average combined breadth of these nappes is 75 km. A belt 5–90 km wide of autochthonous Miocene rocks occurs toward the foreland; it is mainly of marine origin but otherwise somewhat resembles the Alpine Molasse. For the three nappes the minimum proven amount of overthrusting is 23, 26, and 8 km respectively. The actual amount may be much greater.

TABLE 1.—STRATIGRAPHY OF THE AUTOCHTHONOUS FLYSCH AND THE KLIPPEN AND MAGURA NAPPES
T—turbidites; F—fluxoturbidites; TF—mixed or intermediate

TATRA MOUNTAINS AND PODHALE AREA

Middle and Upper Eocene, probably also Oligocene	Podhale flysch, 3000 m (coarser toward the top, shaly toward the base) Nummulitic limestones Basal conglomerates	T
Triassic to Middle Cretaceous Pre-Triassic	Folded and thrust older beds Crystalline basement	

KLIPPEN SERIES

Paleogene	Magura sandstone Hieroglyphic beds Locally coarse sandstones	T, partly F T F?
Senonian	N—Red marls; S—Jarmuta sandstones and conglomerates	T
Turonian-Cenomanian	Sandstones Red and green marls, in conformity on older, Neocomian and Jurassic rocks	T

MAGURA NAPPE

		N		S	
Paleogene	Oligocene	Magura sandstone 1500 m	T	Magura sandstone 2000 m	T, partly F
	Eocene	Submagura beds 300 m	T	Hieroglyphic beds 200 m	T
		Red shales 300 m		Pasierbiec sandstone 200 m	TF
		Ciezkowice sandstone 200 m		Lacko marls 200 m	
	Paleocene		TF?	Red shales 200 m	
	Senonian	Inoceramian beds 1000 m	T	Inoceramian beds	T
	Turonian	?		?	

Each of these tectonic units is either divided into flatly thrust sheets, as in the western part (Fig. 2, upper cross section), or is intensely folded into a number of steep anticlines and synclines, which is characteristic of the tectonics of the eastern part of the Polish Carpathian Mountains (Fig. 2, lower cross section). Many exposures show overturned strata. In spite of this the degree of dynamic metamorphism is slight, so that primary sedimentary features are excellently preserved. The number of exposures is disappointing.

Tables 1, 2, and 3 show the recognized members and their estimated thickness. For greater

TABLE 2.—STRATIGRAPHY OF SILESIAN NAPPE
T—turbidites; F—fluxoturbidites; TF—mixed or intermediate

SILESIAN NAPPE

		Western part		*Eastern part*	
Paleogene	Oligocene	Krosno beds 600 m	T, some TF	Krosno beds > 2000 m	T, some F
	Eocene	Menilite beds 150 m		Menilite beds 300 m	
		Red shale, Hieroglyphic beds 300 m	T	Red shale, Hieroglyphic beds	T
		Ciezkowice sandstone 150 m	F		
	Paleocene	Upper Istebna beds 300 m	F	Upper Istebna beds 80 m	F
Cretaceous	Senonian	Lower Istebna beds 1000 m	T, F	Red shale or marls 50 m	
	Turonian			Red shale or marls 50 m	
	Cenomanian-Albian	Godula beds 2000 m	T	Godula beds 0–200 m or red shale 50 m	T
	Albian (lower)	Mikuszowice silex < 50 m	T		
		Lgota beds 300 m	T, partly F	Lgota beds 300 m	T
	Aptian	Wernsdorf shale 200 m		Wernsdorf shale or	
	Barremian			Grodischt sandstone	TF
	Hauterivian	Grodischt sandstone 50 m	TF		
	Valanginian	Upper Cieszyn shale 300 m	T	Upper Cieszyn shale	T
	Berriasian	Cieszyn limestone 200 m	T		
		Lower Cieszyn shale 200 m			
Tithonian		Stramberg limestone			

SUB-SILESIAN NAPPE
(Because of tectonic reduction thickness cannot be estimated.)

Paleogene		Krosno beds Menilite beds Variegated shales and marls	T
Cretaceous	Senonian Turonian	Variegated or grey marls *ca.* 150 m	
	Cenomanian	Variegated shales	
	Albian Aptian	Gaizes, silex, sandstones	T
	Barremian Hauterivian	Grodischt sandstone	T
	Valanginian	Upper Cieszyn shales	T

detail the reader is referred to the publications of Swidzinski (1947) and Ksiazkiewicz (1956).

Features of the Carpathian Flysch

The flysch units of the Polish Carpathian Mountains together form nearly 6000 m of deposits, a large part of which is built up typical flysch rocks. This series is well differe tiated both vertically and laterally, and near every stratigraphic unit is represented by least two facies.

Two chief types of sediments can be disti guished within the Carpathian flysch. The ma

body is represented by typical turbidite units. A subordinate part, totalling about 15 per cent in thickness and even less in areal extent, is

TABLE 3.—STRATIGRAPHY OF SKOLE NAPPE

T—turbidites; F—fluxoturbidites; TF—mixed or intermediate

SKOLE ("SKIBA") NAPPE

Paleogene	Oligocene	Krosno beds *ca.* 1000 m	T
	Eocene	Menilite shale + Kliwa sandstone 200 m	F?
		Hieroglyphic beds 200 m or Popiele marls	T
		Red shales 150 m	
	Paleocene	Babica clays and conglomerate (locally) 150 m	T, TF
Cretaceous	Senonian	Baculite marls	
	Senonian-Turonian-Cenomanian	Inoceramian beds	T
	Albian	Siliceous marls	
		Red and green marls	
	Barremian-Aptian	Black shales	

MARGINAL ZONE

Middle Miocene	Clays and sands	
Lower Miocene, partly Oligocene?	Sloboda conglomerates	
Oligocene	Saliferous clays	
	Krosno beds	T
	?	

formed of rocks that are of somewhat similar appearance but are of more doubtful origin.

To the first type belong: the Teschen, Jarmuta, Godula, and Inoceramian beds and most of the Lgota beds in the Cretaceous; the Hieroglyphic beds, Podhale flysch, Magura sandstone, and most of the Krosno beds in the Paleogene.

The second type is represented mainly by the Paleogene Ciezkowice sandstone and Upper Istebna beds, and by the Cretaceous Lower Istebna beds and Lower Lgota sandstones. Some types, such as the Grodischt sandstone, Pasierbiec sandstone, Lower Krosno beds, and some subtypes of Magura sandstones, may be regarded as intermediate forms between the two types.

The first type displays all the features known from other areas where evident turbidite formations are developed. It consists of sandstones and, in a few places, conglomerates alternating with shales or marls. In some cases detrital limestones take the place of the sandstones. The sandstones are muddy, evenly bedded, more or less distinctly graded, and of moderate thickness, *i.e.*, hardly exceeding 2 m, and normally much thinner (0.1–0.5 m). The lower surface is always sharply marked and in most places exhibits a profusion of sole marks (hieroglyphs). Small-scale current bedding and horizontal lamination are plentiful in these beds, in the fine-grained upper parts. In many beds, especially in the Inoceramian, Submagura, and Krosno beds, there is a fine display of convolute lamination. Flute casts, as well as organic hieroglyphs, are very numerous. Many of the latter are postdepositional, but several are predepositional.

The second type of flysch is described elsewhere in this paper, and the name "fluxoturbidite" is proposed. It is transitional between true turbidites and pure slides, because it shows a mixture of features characteristic of the two mechanisms of transport.

There are also numerous indications of slumping in the Carpathian flysch, and nearly every stratigraphic unit contains beds distorted or disrupted by submarine sliding. In other cases the reworking has gone much further, and the resulting deposits consist of clay or silt mixed with pebbles and blocks. Such beds occur in several members of the flysch sequence; they are particularly common in the Upper Istebna and Babica beds (Paleocene). The thorough mixing of pebbles and boulders with clay and their chaotic arrangement signify that these beds were formed by true subaqueous mud flows. By the regional occurrence of such deposits within the Babica clays these slumps can be traced at least 30 km from the presumed source. This indicates extreme mobility for such mud slides, and depths far exceeding neritic must have been attained at the far end.

Flyschlike calcareous units occur, and the Teschen limestones have always been regarded as a type of "flysch" by Carpathian geologists. These rocks provide a fine example of a calcareous turbidite formation. Many of the limestones are excellently graded from gravel sizes

through algal and echinoderm sand-sized fragments to a fine-grained limestone. Flute casts, load casts, current-ripple lamination, horizontal lamination, much convolution, tracks, and burrows are other features of these beds; they differ from normal turbidites only in the chemical nature of the particles. Hence, there does not appear to be any valid reason for excluding them from the definition of flysch, as some authors do.

Directional features are plentiful in the Carpathian flysch and together with facies analysis provide abundant material on which to base paleogeographic reconstruction (Ksiazkiewicz, 1958a). Nearly every unit in good exposures exhibits sufficient features (sole markings or current bedding) for determining the main direction of transport. More than 1000 measurements have already been made, but for several units the picture is still far from complete, and the absence of measurements in adjoining areas beyond the Polish frontiers hampers attempts at paleogeographic conclusions.

The following is a summary of what has already been ascertained.

The Teschen limestones and shales exhibit features pointing to a transport from the northwest, the Grodischt sandstones from the southwest or southeast, the Lgota beds from the southwest; but certain incorporated coarse-grained sandstones came from the northwest. The Godula and Istebna beds were supplied from the southwest, and the same direction is shown in the Ciezkowice sandstone (Koszarski, 1956) and in the Hieroglyphic beds of the Silesian zone. The Inoceramian beds of the Skole zone show a supply of the material from the northwest, whereas the Inoceramian beds of the Dukla and Magura zones were deposited by currents flowing mainly from the east or southeast. The Magura sandstones were deposited by currents coming from the northeast, according to measurements by Ksiazkiewicz (1958b) and by W. Sikora and K. Zytko (Unpublished) in the area south of Zywiec. The youngest member of the Carpathian flysch, the Krosno beds, shows directional features pointing mainly to flow from the west, although in the most western area and in the extreme east opposite directions may be noted.

Some Paleogeographic Conclusions

Considerable changes in the shape of the basins and the points of supply have occurred during the sedimentary history because of orogenic activity and presumably also as a result of migration of river mouths. Hence each successive formation must be regarded separately but in conjunction with other deposits of the same age.

Throughout the geosynclinal period two troughs, the Main and the Magura, ran parallel to each other and to the axis of the Carpathian Mountains and were separated by a ridge that was sometimes above and sometimes below sea level.

In Middle Eocene times a third trough, that of Podhale, developed by subsidence in the south on the site of the previously folded mountain range. These troughs were fed from various points and at times from entirely different sources. Current directions were altered, even reversed, and the great changes in sedimentary materials and processes thus brought about led to the production of distinctive types of flysch. These types had been recognized previously and given different names.

Thus the application of the concept of turbidity currents promises to lend more meaning to the present collection of more or less disconnected data. Instead of an apparently arbitrary occurrence of contemporaneous but different rock types of variable thickness in a haphazard sequence, a picture is now evolving of interrelated phenomena taking place in a logical sequence. However, many details must still be investigated, and evidence on some major problems is conflicting.

The most unexpected result of mapping current directions in turbidites has been the indication of the strong predominance of longitudinal or sublongitudinal transport in the flysch troughs. As Kuenen pointed out (1957), this tendency has already been observed in several other regions: in Wales (Kuenen, 1953; Kopstein, 1954) and more spectacularly in the Apennines (ten Haaf, 1957; 1959). This rule has also been established by the work in Poland (Dzulynski and Radomski, 1955) for the Podhale trough and by Ksiazkiewicz (1956) for the Main and Magura troughs. Apparently longitudinal transport is also dominant in the Rumanian Carpathian Mountains (Patrulius, personal communication) and the Caucasus (Vassoevich, personal communication).

The large number of observations recently made in the Polish Carpathian Mountains tends to confirm this general rule. More or less arbitrary deviations from the longitudinal direction or a significant number of additional oblique current directions are found in some units, but even a dominantly transverse system is encountered in one or two instances.

Three explanations can be offered to account for these findings. One is that currents came in transversely from the coastal zones of the geosyncline but on reaching the axial region of the trough turned in one or the other direction, according to the slope of the basin axis (Ksiazkiewicz 1956, p. 387; 1958a).

This view tries to combine the testimony of the indicated current directions with the presumed paleogeographic picture, even if the latter is somewhat doubtful or obscure. Whenever the two are not in harmony more weight is given to the paleogeographic evidence. The reasoning is that upstream from the point of observation the direction of the currents may have been curved. This manner of explaining the situation is referred to below as the "paleogeographic view".

The opposite view was expressed by Kuenen (1957b) who advocated that current evidence is a reliable guide, especially where the measurements are dominantly longitudinal. Divergent measurements in a few places are then attributed to a tectonic disturbance, faulty observation, or local contemporaneous tilting of the trough floor. This reasoning is based on theoretical considerations favoring longitudinal transport. The new data include unequivocal evidence of lateral supply, which shows that this view is too dogmatic for general application.

A third possibility is that the measured directions form a more trustworthy guide than paleogeographic evidence. If the latter points to supply from the sides but is contradicted by longitudinal current directions without a sufficient number of transverse or oblique current directions, it is assumed that the paleogeographic evidence is not reliable. The reasoning is that transverse currents cannot have been active without leaving as good sole markings as they did after they turned lengthwise in the trough. This manner of explaining the situation where evidence is conflicting is referred to here as the "current view". If this reasoning is accepted more sediment can be attributed to large deltas that had extrageosynclinal sources and is probable according to the paleogeographic view.

Before we attempt to choose between these two views the evidence now available for a number of units will be treated separately. For given units the source areas will be discussed according to the two possibilities. The two figured paleogeographic reconstructions of the Polish Carpathian geosyncline (Figs. 4, 8) are based on the paleogeographic view and thus represent the more orthodox approach.

(1) LOWER LGOTA SANDSTONE (ALBIAN): These beds are about 200 m thick. In the western part of the Carpathian Mountains current bedding and flutings point to a source situated in the area now located somewhere south or southwest of Kraków, presumably on the northern shore of the geosyncline. It is clear that the material came from an external source and not from an internal region of the geosyncline. At the beginning of the Albian a fairly large land area north and northwest of the geosyncline extended to Central Poland. Distribution of Albian and Cenomanian sedimentary rocks indicates that during the Albian the sea invaded the axial zone of the Middle European basin which extended through Germany and Poland. To the south it left a vast land area that was not submerged until during the Cenomanian. Hence in this case the current view appears to be applicable, because it is not in conflict with the paleogeographic picture. Possibly a river drained the northern bordering land and supplied the sediment of the Lower Lgota beds to the trough somewhere in the west.

(2) GODULA BEDS (UPPER ALBIAN-CENOMANIAN-TURONIAN): These beds are 2000 m thick in the west but wedge out to the east and northeast. The direction of flow was from the west, mainly the southwest (Fig. 3). Toward the west, north, northeast, and east the Godula beds are replaced by shaly deposits, mainly red clays. According to the paleogeographic view it is improbable that the material for the Godula beds came from an external source in the north because of the presence of shales on that side of the basin. This points to a supply from an area situated within the geosyncline. If one assumes lateral supply this source must have been a land area situated southwest or south of the basin in which the Godula beds were deposited. This land area supplied sand which was carried on a slope of the sea floor to the east and northeast. The grain size does not diminish in the direction of flow, which indicates that several points furnished sand along the coast of this land area. The greatest thickness in the west indicates that the main supply points were situated in the western part of the presumed land area, named Silesian Cordillera by Ksiazkiewicz (1956).

The presence of glauconite seems to argue against the supposition that a river delta was supplying material to the Godula beds. Although possibly glauconite formed in the foresets of the delta, it is more probable that small

rivers flowing from the land area supplied sand and clay to the littoral fringe, and that the glauconite was formed in the coastal zone, where sedimentation was slower. This extensive source all along the coast indicates that the sediment must have entered the trough laterally.

The gradual decrease in thickness to the east can perhaps be accounted for more logically on the basis of the current view. All sedimentary matter then is assumed to have come from the southwest from an area beyond the Silesian Cordillera (Fig. 4), where the paleogeography is still obscure. The observed current directions also favor this view. But the Godula beds thin toward the west also (Ksiazkiewicz, 1956, Fig. 2). Investigations west of the frontier are urgently needed to throw more light on this problem.

South of the presumed Silesian island lay another flysch trough (Magura trough). The postulated land area furnished little sediment to this trough. Probably the lowest part of the Inoceramian beds was deposited in this trough at the same time as the Godula beds in the Main trough. Flow direction in these beds is mainly from the east and southeast (Ksiazkiewicz, 1958a), and only a small supply from the north can be assumed according to direction measurements. Possibly this can be explained by assuming that the main runoff was directed to the north.

This would signify a steep southern slope for the source area. Actually, coarse-grained sandstones containing abundant glauconite, feldspar, and biotite, the so-called biotite facies (Ksiazkiewicz, 1956, Fig. 3), occur in the Inoceramian beds of the Magura zone in Silesia near the northern margin of the trough.

A paleogeographic reconstruction of the region applicable to the Cenomanian-Turonian can be made for most of the time during which the Godula beds were being deposited (Fig. 4). The result does not point to an external source, as most of the area which lies in the upcurrent continuation from the measured directions of flow was submerged. A larger part of this area, *i.e.*, the Sudeten Mountains and the Bohemian massif, is still covered by Cenomanian sandstones and Turonian marls.

This review shows that the evidence for the source area of the Godula beds is mainly in favor of the paleogeographic view.

(3) INOCERAMIAN BEDS: Two belts of Inoceramian beds occur in the Carpathian Mountains; the northern belt was formed in the northeastern part of the Main trough, the southern in the Magura trough. These belts
not strictly coeval: the northern belt represe
Cenomanian-Turonian-Senonian deposits, a
in the southern belt the Inoceramian beds
mainly Senonian, although their lower part m
belong to the Turonian. The presence of
Cenomanian in the southern belt is doubtful
considerable part of the Inoceramian beds
both areas was deposited at the same time
the Godula beds.

In the Polish Carpathian Mountains
Inoceramian beds of the northern belt, now
cluded in the Skole nappe, show a persist
direction of current from the west-northwe
According to the current view this evide
indicates that the source area was somewh
east of Kraków, and that the land that f
nished material to the Inoceramian beds
now deeply buried below the Miocene of
foredeep and the cover of the Carpathi
nappes.

The paleogeographic evidence presents di
culties, however. Boreholes provide some
sight into the nature of this presumed sou
area. Paleozoic and even crystalline rocks h
been found; all have Jurassic cover, and so
have Cretaceous cover. This cover consists
Cenomanian conglomerates and sandstones
lowed by Turonian and Senonian limesto
and marls. This indicates that the whole fo
land area limiting the geosyncline from
north was submerged. Hence this evide
points to a source area situated along
northern margin of the geosyncline. If
paleogeographic view is followed and we t
into account only the proven distance of
marginal thrust of the Carpathian nap
(about 10 km), then the source area is a v
limited area at the border of the Carpath
geosyncline and does not have overlying Ce
manian and Turonian sedimentary rocks (F
4). Very much the same picture can be rec
structed for the Senonian: neither a large l
area nor space for a large delta-building ri
is available in the paleogeographic reconstr
tion. This holds even if the amount of thrust
the Carpathian margin was much greater,
that the present border of the Carpath
flysch was pushed back not 10 km but a
dozen km. Most of the area bordering the C
pathian geosyncline from the north was in
dated during the Late Cretaceous, and onl
limited area was left as the presumable sou
area for the Inoceramian beds of the Si
zone. Possibly this area formed a marginal z
that had a strong uplifting tendency. It

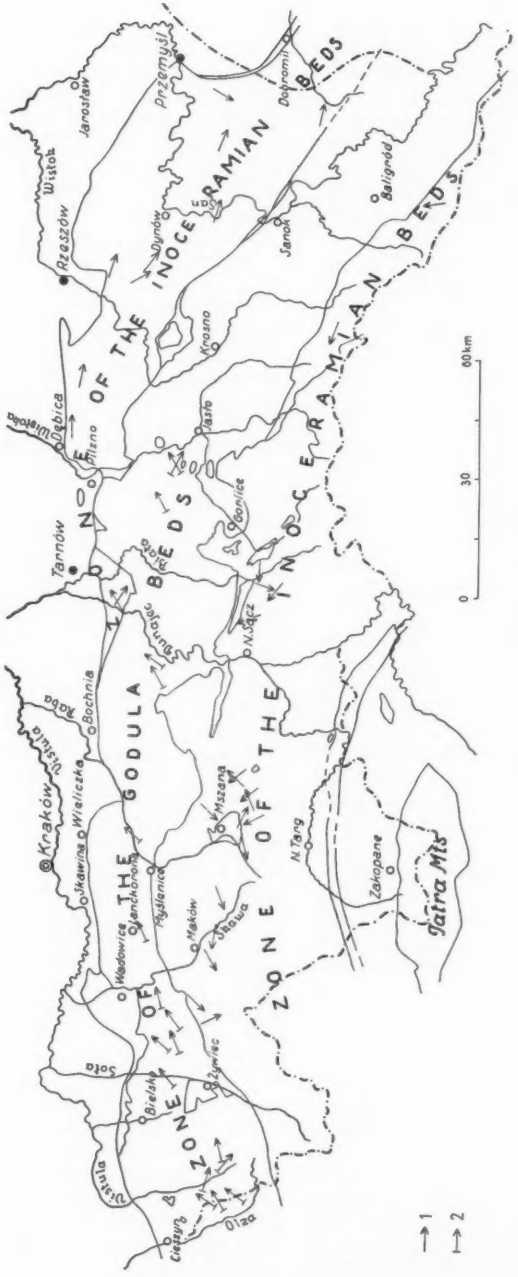

FIGURE 3.—CURRENT DIRECTIONS
1—Inoceramian beds; 2—Godula beds

probably built of crystalline rocks, covered by Devonian and Carboniferous sediment, in which the highest member was formed by not very coherent Coal Measure sandstones. These could have been reworked by small rivers and marine abrasion to supply the sand of the Inoceramian beds. Numerous occurrences of coal fragments and blocks seem to corroborate this assumption.

Again the evidence for the Inoceramian beds is somewhat conflicting. Paleogeography indicates a narrow marginal belt as source, whereas the current directions, volume, and uniformity of the beds would harmonize better with a wide source area supplying sediment to the western end of the trough.

The Inoceramian beds of the southern zone, occurring today in the Magura nappe and Dukla folds, exhibit flute casts, pointing to a main supply from the east and southeast, with a subordinate addition from the north, obviously from the Silesian cordillera. According to the paleogeographic view this might represent the main source area for the western end of the trough. Nevertheless an important source area farther east also must be assumed; presumably it is in the southeast in the region situated outside the Polish Carpathian Mountains, somewhere in the vicinity of the internal Klippen zone. However, this zone itself was well below sea level during the Cenomanian and Turonian, as shown by the occurrence of foraminiferal marls. South of this sea a vast land area probably emerged soon after the Albian. The presence of this land is postulated on the ground that Albanian sedimentary rocks are the youngest rocks in the folded sequence of the Tatra Mountains and other internal ranges of the Carpathian Mountains. No Upper Cretaceous beds are known in this area, although littoral deposits of Senonian age occur at its periphery. But there is no indication whatsoever that this land area furnished material to the trough fringing it in the north before the Senonian. According to paleogeographic evidence the only land area that could furnish sand to the southern Inoceramian zone was the prolongation of the Marmaros massif, itself well submerged at the time in question. The submergence is proved by abundance of marine deposits of Late Cretaceous age within and near the massif. Again we look in vain on the paleogeographic map for a land of considerable size at the border of the geosyncline (Fig. 4) and are led to postulate an island of modest dimensions that could deliver enormous volumes of quartz sand and clay without much feldspar.

For the Senonian a similar picture is eviden
In the Klippen zone the Jarmuta beds we
derived presumably from a land area borderin
the geosyncline on the south. These beds are
limited extent, however, and the main mass
the Senonian Inoceramian beds of the Duk
and Magura units must have had a differe
source area. Tentatively we assume that t
prolongation of the Marmaros cordillera nor
of the Klippen zone functioned as source are

According to the current view the source are
for all the Inoceramian beds of the Magur
trough was in the southeast either in the Ma
maros cordillera or some other unspecifie
land mass.

(4) MIDDLE EOCENE DEPOSITS: During Midd
Eocene argillaceous deposits dominated in t
Main trough, whereas mainly coarse-graine
beds were accumulating in the Magura troug
This period has been selected for considerati
not because of great thickness of deposit
beds, but because it offers an example of tran
verse current directions.

In the Magura trough three types of sed
ments were deposited at this time: (1) coars
grained Pasierbiec sandstone up to 200 m thic
(2) fine-grained hieroglyphic beds, (3) mar
The hieroglyphic beds have flutings from t
east and northeast; hence they indicate long
tudinal flow. Although this trend has be
followed for about 200 km, no appreciab
change in grain size or current direction h
been found. The Pasierbiec sandstone sho
directions generally from the north. Ksiazki
wicz studied this problem within a large ar
in the region north of Babia Góra and arou
Rabka. Although the results are incomple
(Fig. 5) they show fairly well that flut
directions in the extreme western part of t
investigated area deviate slightly toward t
west; in the eastern part they deviate towa
the east, so that a fan-shaped arrangeme
results. It is not known how they beha
farther east and farther west, but the Pasierbi
sandstone thins in these directions and dis
pears and is replaced by the hieroglyphic be
or marls (Fig. 5, inset). The Pasierbiec san
stone presents the best example discovered
far in the Carpathian flysch of grain size dim
ishing in the direction of flow. Not only do
conglomerates disappear in the down-curre
direction, but coarse grain in the sandsto
gradually gives way to finer grades, and at
same time the amount of fine grains of gl
conite increases.

(5) KROSNO BEDS (UPPERMOST EOCENE A
OLIGOCENE): The directions of turbidity c

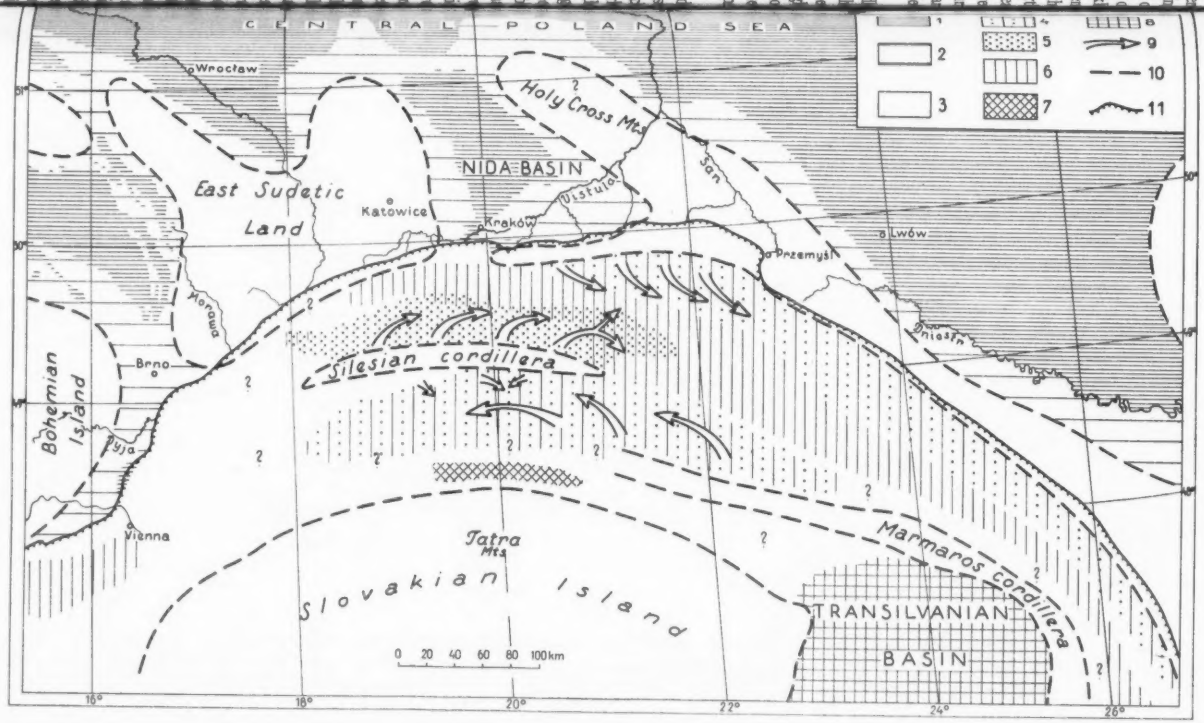

FIGURE 4.—PALEOGEOGRAPHY OF THE CARPATHIAN AREA DURING THE CENOMANIAN AND TURONIAN

1 and 2—epicontinental area: 1—Marine deposits at the surface or below; 2—Marine deposits probably removed by erosion; 3—land areas; 4–8—geosynclinal area (before the compression of the geosyncline): 4—Inoceramian beds; 5—Godula beds; 6—Variegated, mostly red shales; 7—Variegated marls; 8—Sediments in the Transylvanian basin; 9—Current direction; 10—Approximate boundary between land and sea; 11—Present margin of the Carpathian Mountains.

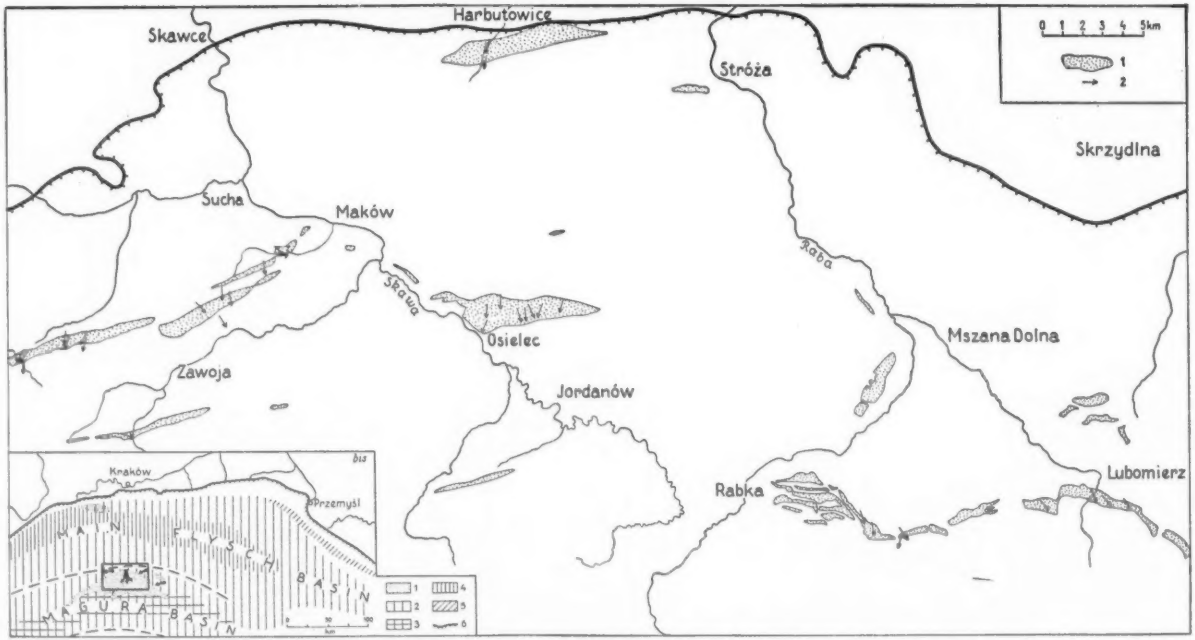

FIGURE 5.—CURRENT DIRECTIONS IN THE PASIERBIEC SANDSTONE IN THE SKAWA AND RABA VALLEYS

Sandstone occurrences based on maps of Swiderski in the eastern part, and of Ksiazkiewicz in the westernpart.
1—Pasierbiec sandstone; 2—Current directions; Thick line—margin of the Magura nappe
Inset: sediments in the Carpathian flysch geosyncline in the Middle Eocene. 1—Sandstones; 2—Thinbedded sandstones and shales; 3—Lacko marls; 4—Variegated shales and marls; 5—Popiele marls; 6—Margin of the Carpathian Mountains. Rectangle denotes the area of the larger map.

Inset: sediments in the Carpathian flysch geosyncline in the Middle Eocene. 1—Sandstones; 2—Thinbedded sandstones and shales; 3—Lacko marls; 4—Variegated shales and marls; 5—Popiele marls; 6—Margin of the Carpathian Mountains. Rectangle denotes the area of the larger map.

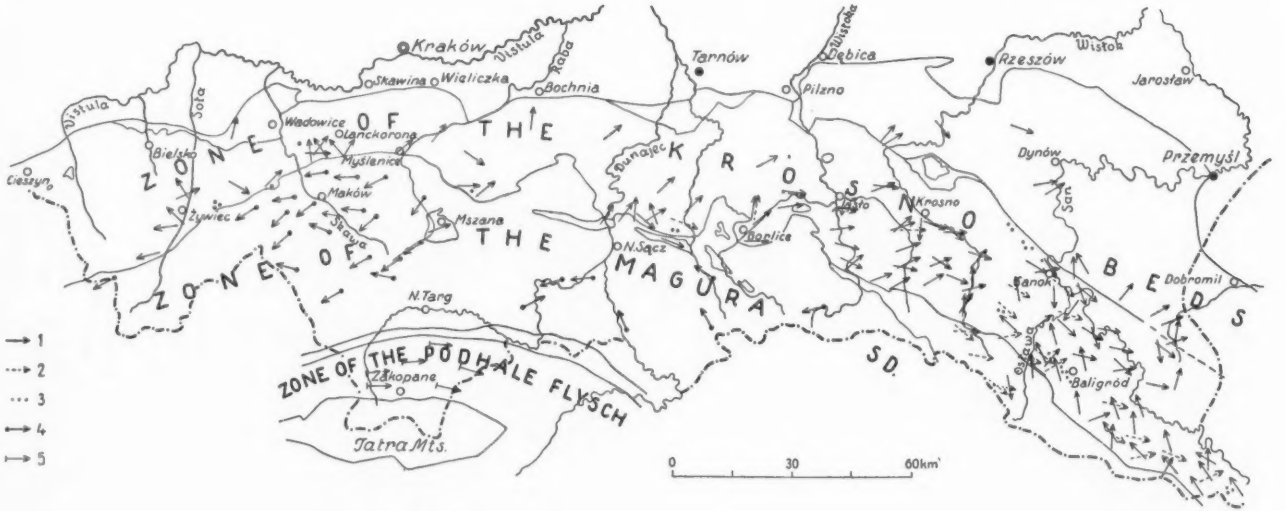

FIGURE 6.—CURRENT DIRECTIONS DURING THE SEDIMENTATION OF THE KROSNO, MAGURA, AND PODHALE BEDS

1—Current directions in the Krosno beds, in the eastern part of the map only in thick-bedded sandstones of the Lower Krosno beds; 2—Current directions in thin-bedded sandstones of the Lower Krosno beds in the eastern part of the map; 3—Exotic blocks in the Krosno beds; 4—Current directions in the Magura sandstone; 5—Current directions in the Podhale flysch (after Radomski)

rents in the lower part of the Krosno beds, synthesized from the data collected by Ksiazkiewicz in the western Polish Carpathian Mountains and Dzulynski and Slaczka in the to have contributed sediments to the Godu and Istebna beds referred to above. In t Krosno beds the current directions favor tran verse supply, and a less ambiguous pictu

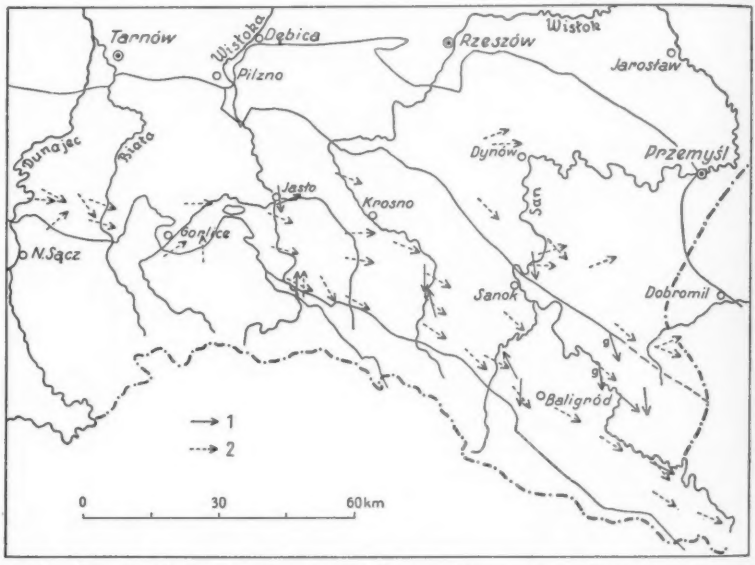

FIGURE 7.—CURRENT DIRECTIONS DURING THE SEDIMENTATION OF THE MIDDLE AND UPPER KROS BEDS IN THE EASTERN PART OF THE POLISH CARPATHIAN MOUNTAINS

In the western part current directions are the same as in the Lower Krosno beds: 1—thick-bedded san stones; 2—thin-bedded sandstones; g—glauconite sandstones

middle and eastern Polish Carpathian Mountains, are shown in Figure 6.

The distribution of current directions implies the existence of at least three source areas contributing sediments to the Krosno trough.

The first source area was situated south of the Main flysch trough somewhere in the area between the Sola and Wisloka rivers. Measured directions are mainly transversal and rather variable. Hence it may be assumed for both the current view and the paleogeographic view that turbidity currents came off the southern border of the trough and tended to fan out on the trough floor. Some currents appear to have continued toward the western and eastern parts of the Main flysch trough. (*See* Fig. 8.) The material becomes progressively finer-grained away from this source. Therefore the sandy facies in the lower part of the Krosno beds is largely limited to the zone along the present margin of the Magura.

This source probably can be identified with the same postulated land area that is supposed

evolves than for the Godula beds with the longitudinal currents.

The second source possibly coincided wit the Marmaros Massif. The eastern part of t Central Depression has been nourished large from this area. The currents which came fro this source could reach the region of the Oslaw river from the southeast and deposited thic bedded sandstones.

The third source area that contributed sed ments to the Krosno beds developed southwe of Przemysl as a ridge in the beginning of t Oligocene and divided the Main flysch trou into two basins. (*See* Fig. 8.)

The influence of this latter source seems to b less conspicuous in the southern basin than the northern one. This comparatively sm influence on the southern basin may be due the smaller supply or to the removal of t northern margin of the Krosno beds by erosio Possibly both factors played a part and t gether account for the more restricted occu

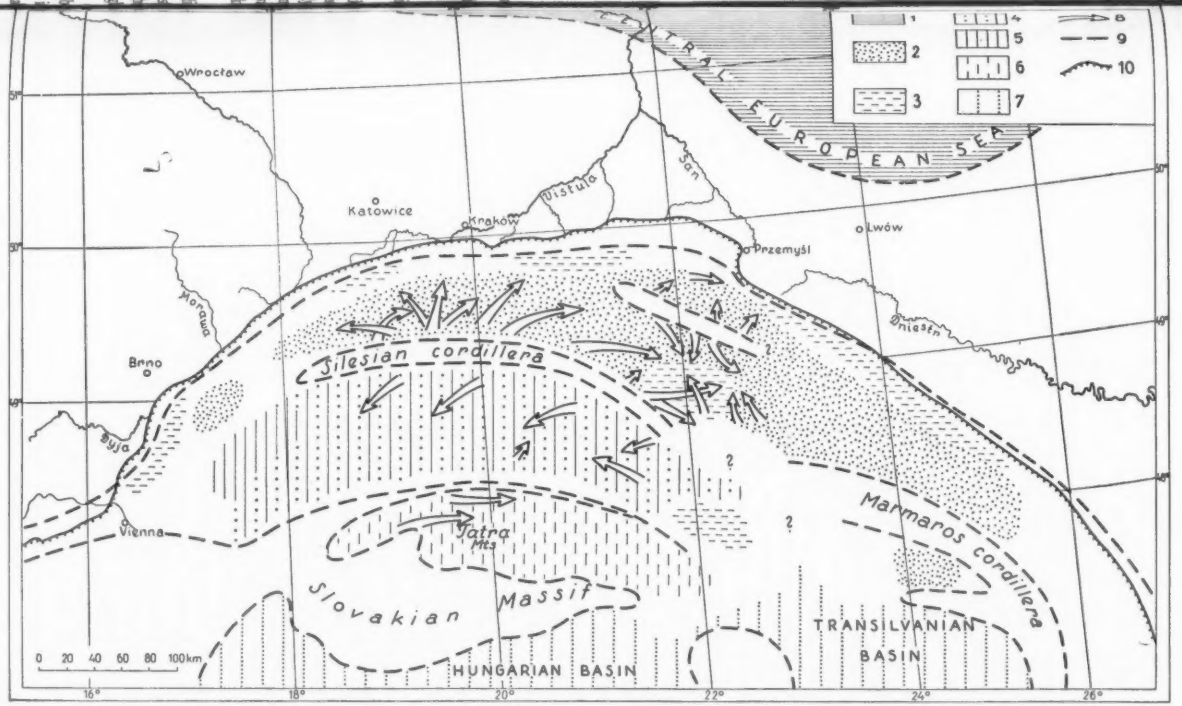

FIGURE 8.—PALEOGEOGRAPHY OF THE CARPATHIAN AREA DURING THE LATEST EOCENE AND OLIGOCENE

1—Epicontinental sea in Central Poland; 2-6—Geosynclinal area (before the compression of the geosyncline): 2—Krosno beds in sandy facies; 3—Krosno beds in marly facies; 4—Magura sandstone; 5—Magura sandstone replaced by shales; 6—Podhale flysch; 7—Sediments of internal basins; 8—Current directions; 9—Approximate boundary between land and sea; 10—Present margin of the Carpathian Mountains.

rence of sandstones in the southern basin laid down by currents from the north.

Figure 8 indicates that large quantities of sand were deposited near the source areas discussed. These sandy facies seem to surround the area south of Krosno and Sanok where the Krosno beds attain a thickness of about 3000 m. The proportion of marly shales to sandstones in this area is greater than in the surrounding regions, and the thick-bedded sandstones are less conspicuous. Possibly this "marly facies" corresponds to the central part of the basin where the currents from various sources met. The turbidity currents had probably lost most of their sandy load before reaching the distant central part of the trough. Only exceptionally strong currents could deposit large quantities of sand in this area. A large amount of this marl may have settled from currents which became ponded in the deepest part of the trough.

Farther to the east from the area occupied by the marly facies a remarkable situation was discovered that is unique as far as present knowledge goes. In this part of the geosyncline the thick-bedded, coarse-grained sandstones are interstratified in a sequence 300 m thick with fine-grained and thin-bedded sandstones displaying convolute structures. The former were laid down by currents from the southeast or south and the latter from the southwest to northwest (Dzulynski and Slaczka, 1958).

This relation is encountered over a region more than 50 km long in the upper part of the Lower Krosno beds. If a horizontal floor is postulated to account for opposing directions of flow two difficulties arise: (1) How could this delicate balance be maintained during accumulation of a column of sediment 300 m thick? (2) What was the driving force that carried the currents so far on a horizontal bottom? Clay and silt can be carried great distances merely by the spreading of a cloud, as indicated by findings in the present oceans, but this is not a very satisfactory suggestion for sand. A slow marine current flowing toward the southeast up a longitudinal slope could produce this situation, but no shales of pelagic origin would have been deposited.

The observations hitherto discussed pertain to the lower part of the Krosno beds. During the sedimentation of the Middle Krosno beds the conditions in the Carpathian geosyncline underwent some changes. The sandstones became finer-grained, and their thickness decreased. Over vast areas fine-grained sandstones with convolute structures were deposited. Whereas in the western Carpathian Mountains no distinct change in the direction of currents between the lower and middle part of the Krosno beds was observed, the conditions in the Central Depression underwent a change. (*See* Fig. 7.) The influence of the Marmaros source area decreased gradually, and the currents that came from the northwest or west (longitudinal transport) became predominant.

Figure 7, synthesized from the data collected by Dzulynski and Slaczka (1958), represents the directions of turbidity currents in the eastern part of the Polish Carpathian Mountains during deposition of the Middle and Upper Krosno beds. Although longitudinal transport is indicated, measured directions show that the source area north of Sanok still contributed sediments on both sides into the southern and northern basins. In the first basin large inclusions of thick-bedded glauconite sandstones were deposited. The soles of these poorly graded fine-grained sandstones exhibit large flute casts up to 1 m long and 50 cm wide.

Before current measurements were initiated the paleogeographic reconstructions of source areas were based on the facies and the distribution of exotic boulders. Several suggestions set forth by previous authors have been confirmed by the present sedimentological investigations based on entirely different methods. The Marmaros Massif as a source area for flysch rocks had been recognized long ago. Wdowiarz (1953) on the basis of the occurrence of exotic boulders found by him and Gawell in the Krosno beds suggested the existence of small land areas north of Sanok in the Oligocene.

In Figure 6 the distribution of exotic boulders is shown by black dots.

(6) MAGURA SANDSTONE: Current directions in this unit have been mapped by Ksiazkiewicz in some detail within the area between Wadowice and Mszana and to the southwest (Fig. 6). The prevalent direction here is from the north to east. Cursory observations in other areas show similar directions with some minor exceptions. It seems now well established that most of the Magura sand came from the northeast and that an inflow from the south is indicated only south and east of Nowy Sacz.

If this situation is to be explained on the basis of the paleographic view, then possibly the Magura sandstone had its main source in the area situated north of the Magura trough, i.e. in the Silesian cordillera. The eastern part of this area, however, supplied most of the sand to the Magura trough; the western part of the

land area furnished materials in the opposite direction to the northern trough in which the Krosno beds were being deposited (Fig. 8).

The difference in lithology between the Krosno and Magura sandstones must then be attributed to contrasts between these two parts of the common source area.

If the current view is applied the measured directions point to supply for the Magura sandstone somewhere in the east. The difference in lithology between Krosno and Magura sandstones is thus more readily accounted for, as they are assumed to be derived from widely separated sources.

Current directions are sublongitudinal with regard to the general strike of beds, and no differences in grain size downcurrent can be noted. Farther away in the direction of flow the Magura sandstones pass into the shaly facies (Zlin beds of Czechoslovakian geologists) in Moravia.

A smaller part of the Magura sandstone can be attributed to a source situated to the south or southeast on the strength of some currents directed northward. Further research is needed to find out whether this source was connected with the Klippen zone or with the prolongation of the Marmaros zone.

(7) PODHALE FLYSCH: This unit has been investigated recently by Radomski (1957), who found that the predominant direction of turbidity currents was from the west. The longitudinal transport is well displayed, except for some deviations from this direction along the northern margin of the Podhale flysch.

In the case of the Podhale flysch the current view seems to account satisfactorily for the data gathered. A land mass adjoining the basin on the southwest was of sufficient extent to provide a large amount of sediment (Fig. 8). The existence of this land is based on the disappearance of the flysch toward the west, and on the differences between the Magura flysch of the external zone and the internal Podhale flysch. No transitional zone was found between them. Radomski assumed that somewhere in the west a river mouth supplied sands to the end of the basin.

The geanticlinal belt north of the present Podhale region appears to have contributed sediment to the trough, because exotic boulders are scattered along this northern margin of the Podhale flysch, and numerous deviations from the general current direction occur. However, Radomski followed the paleogeographic view and assumed a supply from the north and probably also from the south in addition to a source in the west.

Alternative Interpretations

An attempt can now be made to assess the merits of the two alternative interpretations when applied to the units discussed.

The original geography of the flysch troughs cannot be reconstructed accurately. Even before orogeny died out the slopes may have been upwarped and stripped of their sedimentary cover. Denudation and tectonic cover have caused further changes. Therefore the question of whether current directions coincided with the trough axis can be answered only roughly, and part of the evidence for currents from the side may now be missing.

The case for the paleogeographic view is obvious. It is assumed that the paleogeographic situation is fairly well known and that uncertainties as to tectonic reconstructions or dating of events and distribution of sea, land, and other features are relatively small and do not allow significant alterations to accommodate extensive source areas that are not shown on the paleogeographic maps (Figs. 4, 8).

In some cases this point of view indicates supply from the sides of troughs in which the measured current directions give no evidence or only slender evidence for this conclusion (*e.g.*, Godula beds in the western part of the Main trough, Inoceramian beds in the Skole nappe, and the Magura sandstone in the western Magura trough).

To account for the fact that the currents left no evidence of transverse supply, it must be assumed that the lateral direction was developed in the marginal parts of the trough that have been uplifted and destroyed and/or that the currents did not start to deposit turbidites until they had turned lengthwise in the troughs. As stated above the big arrows in Figures 4 and 8 are drawn according to the paleogeographic view.

An advantage of this reasoning is that the distances of transportation one has to assume are smaller than for the current view. For beds that show longitudinal directions but are composed of thin current-bedded and laminated beds (Godula, Inoceramian, Hieroglyphic, Upper Lgota beds and Teschen shales), a required distance of 100–150 km is more easily accepted than twice that amount necessary in the case of the current view. The intercalation of conglomeratic beds in a few places is also an indication of a near-by source.

In many coarse-grained sandstones nummulites, bryozoa, and lithothamnia occur in great profusion. These are shallow-water organisms but not from a delta environment. It is more probable that they were carried down from shallow coastal water rather than from a delta.

The case for the current view can be based on several arguments:

(1) Two examples can be given of obvious lateral supply based on composition and current measurements. In the Podhale flysch (Fig. 6) some horizons contain coarse material that came from the north into a trough supplied by currents from the west. The Lgota sandstone shows a southwesterly supply. But at Kalwaria there occurs a coarse variety containing angular coal fragments supplied from the north. Two other examples of transverse current directions, Pasierbiec sandstone and Lower Krosno beds in the western Main trough, are both linked with a downcurrent decrease in grain size. To a certain extent this is also the case for the lateral supply from the southern border of the Skole nappe. Hence, the available data indicate that lateral supply leaves abundant evidence in the shape of measurable current directions.

(2) Generally grain size does not decrease along the current direction where it is longitudinal. This might be accounted for by supply from the side, but lack of horizontal grading is also found where longitudinal transport has to be assumed even according to the paleogeographic view. This holds even where 100–200 km appear to have been covered.

(3) In several flysch units the thickness of the formation decreases downcurrent, but with uniform lateral supply it should increase. The lateral supply would have to show a strong downcurrent decrease in all these cases, but the observed uniform grain size does not support a number of separate lateral sources decreasing in volume downcurrent.

(4) Some flysch units are remarkably uniform in composition and lack the rapid horizontal variation in mineralogy and grain size one would expect in the case of detritus carried from the sides and coming from a rising cordillera, at least after the sedimentary cover had been stripped off.

(5) For the paleogeographic view it is assumed that if a sandy flysch is separated from a coast by red clays or other fine-grained deposits, it must have been provided from elsewhere. However, the possibility must be admitted that turbidity currents can transport sand through a submarine valley across an area of clay deposition. This by-passing took place in present oceans during the Ice Age when coarse sediment was transported down submarine canyons to the ocean floor.

(6) According to the paleogeographic view lateral supply can have taken place without leaving evidence in the measurable current directions. The explanation offered is that longitudinal transport was confined largely to the central parts of the troughs and that its present predominance is a result of the destruction of former lateral slopes. But in an oblong basin the lateral slopes must be much steeper than the pitch of the trough axis. Otherwise the basin would have to be round. If this pitch can direct the currents, the steeper lateral slopes must have done so even more markedly. The preserved trough floor with parallel currents must have had a flat cross section with a slight longitudinal pitch; otherwise the currents would have run obliquely or only down the axis of the central depression (Fig. 9). An occasional lateral current in such a flat-floored basin cannot start to turn lengthwise until it has reached the bottom of the trough wall. It can then be deviated by the pitch, but only gradually. Even if the currents did not start to deposit until they had turned to a longitudinal direction, they must have formed flutings in oblique directions. The whole breadth of the trough floor should contain the evidence of transverse currents in the shape of sole markings, if not as current bedding. This evidence would remain after the margins had been upwarped and destroyed.

In the case of major supply from the side, the currents coming off the lateral slope should fan out and start dropping part of their load. The floor will be built up by successive deposits until it has a slight transverse slope to the opposite side. A stabilized condition is then attained, and the currents will spread obliquely across the floor by gradually turning to the longitudinal direction. All this fan-shaped and oblique flow should be recorded in flutings because they are formed in the central parts of the trough. The currents coming from higher up should tend to pass along the opposite side of the trough in consequence of this transverse slope. In other words the sediment on the trough floor should characteristically contain evidence of directions fanning at least 120° away from all the points where currents arrive from the lateral slope. More centrally oblique directions should prevail, and on the opposite side longitudinal directions should dominate. The Krosno

beds in the Main trough appear to conform fairly well to this deduced pattern and to have come off the Silesian cordillera or a raised trough rim in the south composed of older flysch rocks.

trough could not be reached in the latter case. The Pasierbiec beds and the Lower Krosno beds in the Main trough are transverse and show wedging. This may indicate turbidity currents of smaller volume than those that ran

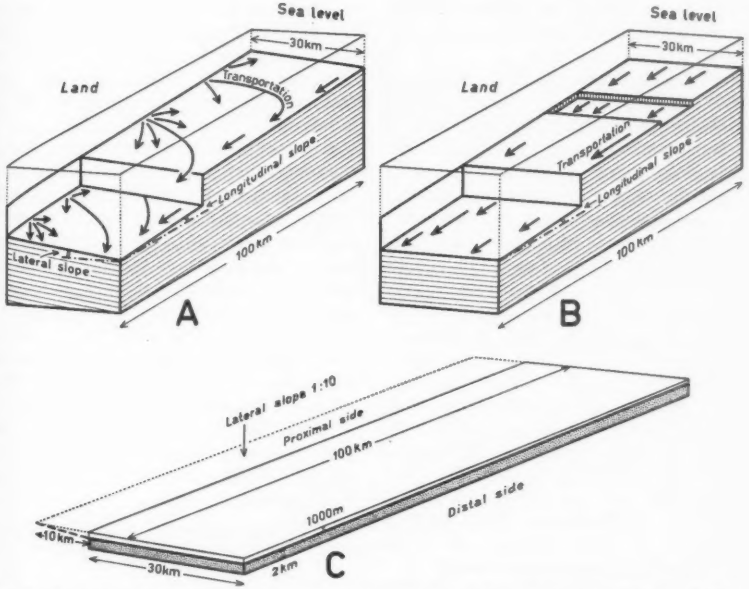

FIGURE 9.—DIAGRAMS ILLUSTRATING CURRENT DIRECTIONS AND BOTTOM SLOPES IN FLYSCH TROUGHS
Case A of lateral supply and case B of longitudinal supply. Both appear to occur and are indicated by combined paleogeographic and sedimentological evidence. However, in some units dominantly longitudinal currents are measured, although paleogeography favors lateral supply. C. True-scale diagram of a normal flysch trough.

If the situation shown in Figure 9, *A* is translated to normal scale for a flysch trough (Fig. 9, *C*) one realizes better how improbable is the postulate of dominantly transverse currents, where sole markings show almost exclusively longitudinal directions.

(7) A further difficulty is connected with the size of the individual beds. If a current is to reach the opposite side of a trough floor a few dozen kilometers broad, then turn downslope and continue for an even greater distance along the trough, its deposit must cover an area of many hundreds of square kilometers. The volume of many such beds must be of the order of 1000 cu. km. If small streams and coastal erosion supply the flysch sediment, it is hard to imagine how such enormous volumes can be set in motion to form a single turbidity current. Smaller slides would form either very thin beds or thick beds on a small area. The opposite side of the longitudinally. If the current view is correct and a single delta is being formed reaching into deeper water, then an occasional slide might set a large volume of sediment in motion.

(8) The horizontal grading of beds showing transverse current directions can be accounted for more satisfactorily by the current view. The volume of turbidity currents coming down lateral slopes must be small compared to the main longitudinal currents. These small currents will not reach far, and their deposit will show distinct decrease in grain size away from their source, especially if they contain coarse sand and gravel. If longitudinal currents have developed from lateral ones they should behave the same way, but actually they produce very little horizontal grading.

(9) For the paleogeographic view a Silesian Cordillera is assumed situated between the western parts of the Main and Magura troughs.

It provided the sediment for the Godula and for the Krosno beds in the north but also for a part of the Inoceramian and for most of the Magura sandstone to the south. This island and the southern slope of the Main trough have since been covered by the Magura nappe composed of the central part of the Magura trough, and the northern slope of the latter has also been eroded.

A difficulty arises when the total volume of sediment is compared to the size of this island. About 1500 m in the north and 2000 m in the south cover a combined area 5 or 6 times that of the island in Figure 4. This would mean 10,000 m of denudation. Because feldspar and gravel are not abundant in the turbidites this sediment cannot have been derived from basement rocks but must all have been available as friable sandstone and unconsolidated shale, presumably Carboniferous. The island must be twice or three times the area shown in Figure 4.

In this manner one is forced to assume a central massif 50 km wide and a later overthrusting of that amount, plus the proven overthrust of 25 km, which is entirely flysch over flysch. There is hardly space below the Magura nappe to accommodate this hypothetical land.

For the current view the difficulty is greatly reduced because not much more than 600 m of Krosno beds in the Main trough need be attributed to the island between the troughs.

(10) In a recent paper Kuenen (1957b) pointed out that in the past it was an axiomatic assumption that detrital sediment in geosynclinal troughs had been carried in from the side provided by a rising geanticline undergoing denudation. According to recent sedimentological work at sea, islands like Trinidad and Tobago have remarkably little influence on the sediment accumulating in their surroundings. An island of only a few thousand square kilometers probably could not produce a rapid supply of sand during a long period. Only gravel and boulders might be delivered to the submarine slopes in profusion. It is reasonable that a powerful and prolonged supply of sand must be attributed in most cases to weathering of a wide area of subdued relief and that large rivers draining this surface bring the sand to the sea. However, rivers can easily be barred from entering a geosynclinal trough laterally by the flanking geanticlines. Hence they tend to reach in from the ends. Kuenen compared this picture to present-day land-locked trenches and found that supply from the end is the rule. In cases where a river managed to reach a trough in the middle the sediment should travel longitudinally in opposite directions toward the ends of the geosyncline.

This reasoning indicates a construction in which sand and clay tend to be supplied at the end of a trough. The longitudinal flow found commonly in flysch sediments can thus be satisfactorily accounted for. Before the concept of turbidity flow had provided an explanation for transportation of detrital sediment for long distances on submarine slopes the suggested paleogeographic picture could not have been entertained.

It would be premature to assess the value of these arguments favoring the current view and to weigh them against the opposing paleogeographic evidence. A large body of data still has to be gathered by continuing the present research, and these investigations should also be extended to adjoining parts of the Carpathian Mountains.

The same controversial problem is encountered in many other geosynclines with turbidite formations. In each case there are differences according to local circumstances, but results obtained in one area should prove useful to understanding the paleogeography of others. Kuenen (1958) reviewed some general aspects of this topic.

Turbidity Currents

Introductory Remark

The problems reviewed here concerning turbidity currents and their deposits pertain not only to the Carpathian Mountains but to all basins containing resedimented deposits, but the data gathered in Poland are here used to throw light on these topics.

Upper Margin of Graded Beds

The impression gained by Kuenen from the examination of many turbidite formations is that most graded beds end upward more or less abruptly in sand or silt sizes and are sharply marked off from the overlying pelagic clay or marl. Dzulynski and Ksiazkiewicz, however, found a gradual transition in many places. Ksiazkiewicz noticed in some cases that a turbidite is covered by barren clay a few centimeters thick, even in localities where there follows a stratum relatively rich in pelagic or benthonic Foraminifera. This indicates that the lower part was deposited much more rapidly than the upper, truly pelagic part. This observation should be held in mind when collecting

fossils, because the shales of most turbidite series are extremely poor in organic remains.

Observations in the Krosno beds reveal several types of transition from sandstone to the overlying shale.

(1) If current bedding occurs in the upper part of the bed, the dip of foreset laminae may decrease gradually upward until it passes into fine horizontal lamination, which becomes finer as grain size decreases in each subsequent lamina. The lamination disappears imperceptibly into the pure shale.

(2) In cases where the upper part of the bed shows lamination but no current bedding the same relation to the overlying shale may occur.

(3) The third type of transition results from simple and gradual decrease in grain size of sand and silt particles, and the sandstone merges into the pure shale. This case presents the ideal type of graded bedding. The existence of such a continuous transition from sandstone to shale has been described from the Carpathian flysch by Ksiazkiewicz (1954a).

(4) In very poorly graded or nongraded sandstones composed of grains of approximately equal size the transition may be accomplished by continuous increase of clayey matter, and the sandstone passes gradually into pure shale.

Sandy mud flows in the Passage beds pass continuously into the pure shale in the manner described above. (*See* Dzulynski, Radomski, and Slaczka, 1957.)

Radomski found in the Podhale flysch that if the transition from sandstone to shale is continuous the lower part of the latter contains angular grains of sand identical to those in the sandstone layer, whereas in the upper part of the shale a few well-rounded grains occur. The latter seem to be derived from beach dunes and were carried to sea by wind. The part of the shale in which these well-rounded grains occur may be considered a true pelagic deposit.

The scarcity of hieroglyphs on the top surfaces may also be attributed to a comparatively rapid covering of recently deposited sand by clay (Dzulynski and Kinle, 1957).

The cases described above indicate that in many instances the lower part of shales do not represent true pelagic sediments but resulted from slow dilute turbidity currents, as was suggested by Crowell (1955). However, the deposition of a few centimeters of clay from a turbidity current is difficult to account for at first sight.

A current sufficiently slow to deposit clay should be very dilute, and in that case only an extremely small thickness could be deposited from it.

A very rough estimate for the maximum thickness of dispersed clay that could be deposited by a current on top of the silty part can be made as follows. Assuming that the floccules settle at a rate of 0.006 cm per second (equivalent to quartz spheres of 0.01 mm diameter) in the salt water, and that the upward component of turbulence is 10 per cent of the horizontal velocity, then these floccules would be significantly retarded in settling when carried in a current flowing faster than 0.06 cm per second at the bottom, or 0.2 cm per second as an average. To be on the safe side it is assumed that 1 cm per second or 5 times this velocity is the maximum at which some deposition can still take place. At higher speeds all such flocculated clay is kept in suspension. Taking the bottom slope as $\frac{1}{1000}$ and the hydraulic mean depths as 110 cm the density follows from the formula (*see* Kuenen, 1952):

$$\text{velocity} = C\sqrt{d \times s \times \text{hmd}}$$

$$1 = 400\sqrt{d \times \frac{1}{1000} \times 110}$$

$$d = 0.000\,056.$$

In this current, which is $2\frac{1}{2}$ m thick, there should be about 0.014 gr of clay above each square centimeter of bottom area. Only an imperceptible film of clay could be deposited from so dilute a cloud. Hence, probably any measurable thickness of clay deposited by a turbidity current, other than that caught between larger grains, must be accounted for by some other mode of deposition.

It may be inferred that beds ending upward in sand or silt sizes were deposited from currents that have tails containing small amounts of fine clay. This load caused a velocity too high for clay to be deposited.

For the beds passing upward into lutite with or without an admixture of silt or fine sand two possible explanations can be offered. One is that the turbidity current became ponded in the lowest part of the basin and that the bed was deposited below the surface of the mud cloud. If this is the case the thicker beds, presumably deposited by larger currents forming deeper ponds, should show a more pronounced tendency to grade up into the lutite than the thin beds. At a given locality the beds may have been deposited below the level of ponding for voluminous currents but above the level and

therefore outside the area of a stagnant cloud produced by a minor flow.

Significant evidence on this problem is given by the regional distribution of formation thicknesses. The Godula beds in the western part of the Silesian Carpathian Mountains are 2000 m thick and contain about 1000 m of shale. Current directions show that transportation came from the west and continued eastward as far as turbidites are found. In the eastern part of the western Carpathian Mountains between Wadowice and Myslenice, the thickness is 700 m, and in the middle Carpathian Mountains in the Jasto area some turbidites occur, but their thickness is only 300 m with the same sand/shale ratio. East of Jasto only a few meters of red shales represents the same length of time. These red shales were probably deposited above the level of ponded currents and may be equated with the red clay discovered in the present Atlantic Ocean on hills emerging from abyssal plains of calcareous silts.

But the gradual downcurrent dwindling of the total thickness of shale in the Godula beds is strong evidence against a significant ponding of clay clouds at the far end.

The same conclusion can be drawn from the Istebna beds. In the western Silesian Carpathian Mountains these rocks are 1500 m thick, of which 20 per cent or 300 m is shales. In the Wadowice area 1000 m contains 20–25 per cent (= 250 m) shale. In the Krosno area the thickness is 500 m, west of Sanok 70 m with 50 per cent shale (= 35 m), and farther east about 25 m of red marls.

The absence of significant ponding in these formations does not prove that it has never played a part. During deposition of other units the currents may have succeeded in carrying larger amounts of turbid water to the lower ends of slopes because these slopes were smaller.

The thickness of the red shales and of the truly pelagic clay in distal parts of the basins is less than that of the pelagic part of the shales found closer to the origin of the currents. This shows that the clay reaching the bottom by diffusion and transportation in higher levels decreases in amount away from the source of the sand. One can easily imagine a delta contributing both sand and clay to the basin. This type of distribution implies that the basin waters were not stirred by powerful circulating currents and suggests poor ventilation of bottom waters. The scarcity of benthonic fossils could be accounted for in the same way.

Closer inspection of the shales between the turbidites in many cases reveals some lamination. This structure could be the result of occasional dilute, slow turbidity currents carrying and depositing fine silt and flocculated clay.

If ponding had only a very restricted influence on the deposition of clay in some units, another explanation is required for the shaly top of their turbidite beds. The most probable explanation is that a certain amount of clay is carried in the form of faecal and pseudofaecal pellets and as small chips and crumbs derived from unconsolidated and slightly compacted clay beds. Such pieces could settle from a much faster—that is to say a much more heavily loaded—current than minute floccules. Depending on their size and density these particles would be deposited with sand, or silt, or afterwards from the tail of the current. Their originally granular nature would not show up after the later compaction.

Suspended Currents

Dzulynski and Radomski (1955) suggested that turbidity currents may lose contact with the bottom on a slope and continue "in suspension". In normal marine waters such a current would have to be extremely dilute and unable to carry anything but the finest clay. However, in a basin that contains fresh or brackish water at the surface and high salinity at depths somewhat more favorable conditions prevail. But as the interface between stagnant water masses of differing density is horizontal, there is no slope to drive a turbidity current spreading out between them. Hence, the velocity will be very small and the carrying power insignificant.

Convolute Lamination

Possibly convolute lamination is partly due to sliding. The occurrence of these structures with the anticlines removed and an upper, separately convoluted stratum replacing them, could be accounted for in this manner. The downcurrent overturning of the anticlinal crests also suggests slip after deposition. But there are serious objections to this view as a general explanation of convolute bedding. In experimental currents the deposit is at maximum mobility while being built up; waves run along the surface of the newly forming bed. In the course of a minute or less, compaction causes the bed to contract to half its thickness, and the hydroplasticity is gradually much reduced even while the tail of the current is still sweeping along the bottom. As the pull of gravity remains constant, but the current drag and

mobility diminish, it is illogical to suppose that a tendency to slide will increase. Hence, sliding will not affect a bed after it has been laid down if no abnormal circumstance acts as a trigger. Then if sliding were to set in when the deposition is complete, for instance in consequence of an earthquake, the movement should not stop again after a slight displacement but should continue until a true, normal slump had developed.

However, the strong downcurrent overturning of convolute anticlines in many beds may be due to the combined action of current drag, gravity, and wandering of ripple crests with the current.

Kuenen (1953b) attributed convolute lamination to deformation of the extremely hydroplastic deposit *in statu nascendi*, seeking the main cause in hydrodynamic pressures during rippling. A test of this explanation is that the current velocity belonging to rippling (between 60 and 30 cm/sec.) should fit grain sizes in convoluted beds. According to ten Haaf's (1956) measurement, the larger grains in most convoluted beds are between 0.1 and 0.06 mm. Quartz grains of these sizes sink at 1 and 0.3 cm/sec. respectively. These should tend to drop out gradually from currents 50–100 times as fast, because the upward component of turbulence is a tenth of the horizontal velocity. Both values decrease just along the bottom. This gives 50–100 cm/sec. for the larger size and 15–30 cm/sec. for the smaller, in good agreement with rippling velocities.

Dzulynski and Slaczka (1958) observed the following relation between convolute structures and current bedding in the Krosno beds. As has been found elsewhere, certain beds with convolute structures display in their lower parts current bedding which in many cases is undeformed or only slightly disturbed by convolutions. This lamination shows through on the soles of such sandstones in the Krosno beds so that they display a curious pattern, just visible in oblique lighting, composed of parallel bands of crescentic zigzags, all with the convexity facing upcurrent[1], as proved by other current indicators (Fig. 12). Such an arrangement suggests that first barchanlike (= crescentic) ripples developed on the muddy bottom. The depressions between the crests of these dunes tend to coincide with broad synclines of the longitudinal convolute bedding, and the "wings" of closely pressed barchans coincide with narrow anticlines.

In sections that have incipient convolutions these "wings" and the crests of the barchanlike structures are inclined toward the depressions.

In rare places where ripple marks are found on the top surfaces of the sandstone beds they do not resemble barchans. Their convex sides are directed downcurrent as in linguoid ripples. This is also the shape of ripple marks developed on marls which have left their counterparts on the soles of some sandstones—a rare phenomenon.

Doubtful Turbidites

In studying well-exposed sedimentary formations there is generally no great difficulty in deciding whether or not one is dealing with turbidites. One may find the combination of a thick series consisting of a regularly stratified alternation of clay or marl with graded granular beds of dark sandstones (graywackes) or calcarenites, abundant current sole markings, organic hieroglyphs, current-ripple lamination and convolute lamination, slump structures, clay pebbles, load casts, a scarcity of benthonic fossils, and no influence of surface phenomena. This is evidently a resedimented formation deposited in quiet deep water. In other places, since all the typical features are missing turbidity-current action did not take place. Even where only one or two of the characteristics of resedimentation are found it is usually obvious that the environment was shallow and that transport was by superficial forces. However, many of the formations do not present such clear evidence.

For instance, thick series of shales or marls regularly alternate with limestones or marly limestones and show faunistic evidence of pelagic origin but lack all features associated with the action of turbidity currents. In these cases chemical precipitation is indicated. The same may be suggested for aphanitic limestones intercalated between normal sandy flysch rocks.

In most turbidite formations a few conglomerates are found; some are sandy, but most show shaly matrices containing pebbles or boulders which are not in direct contact with each other. These can be confidently attributed to slides. In the Polish Carpathian Mountains they can be traced in the direction of movement for 30 km at least—the Babice conglomerates, for instance. Although the thickness diminishes the boulder size undergoes only slight reduction over this distance. In the Kulm

[1] Similar structures were found by Wood and Smith (1958, p. 169) in the Aberystwyth grits.

of central Germany (Edertal) obvious slide conglomerates pass laterally into coarse-graded beds that decrease in thickness and grain size as they are traced away from the source. In this latter case the slides appear to have generated powerful turbidity currents.

A more difficult case is presented by the Flözleeres of Sauerland. Since an earlier visit (Kuenen and Sanders, 1956) Kuenen has had opportunity for some additional observations and discussion in the field with several colleagues. However, the following remarks are merely tentative.

The lower part of this graywacke-shale formation shows much graded bedding, and the finer-grained parts of the beds show horizontal lamination. Although features indicative of current directions are scarce, nothing indicates the irregular deposition characteristic of tidal and coastal waters. But at higher levels in the sequence one is less and less reminded of typical turbidites. The bedding becomes less regular, and there are slump structures and local erosional gaps, either washouts or slideouts. The shale is more sandy, and at some exposures coarse-grained sands occur in very thin beds or as separated ripple crests on a lamination plane in the shale. Still higher the autochthonous productive Carboniferous begins. This transition appears to take place over a wide area more or less simultaneously. Hence, one can suggest as a working hypothesis that a wide basin was gradually filled up to sea level. Turbidity flow formed the main mechanism of transport, but bottom slopes were too slight to produce full-fledged turbidity currents.

A different type of sedimentation is encountered amidst normal turbidites in many places. In this type the grain size is large, and the beds tend to be less muddy. The bedding is thick and rather irregular, and the shales between are silty to sandy and thin or even absent. Current sole markings are scarce, load casting is more common, and coarse current bedding of somewhat variable direction is encountered. Indications of slumping are found, and grading is absent, repetitive, irregular, or even inverted, and irregular lenses of coarser grain occur in a few places inside the beds. These sandstones may occur as large lenses between normal flysch or shales. In other cases the material or the direction of supply contrast with those of the normal surrounding flysch of the same age.

Because characteristics of deposition from turbidity currents appear to be mixed with evidence for sliding, we propose to call this kind of bed a "fluxoturbidite". As with the term turbidite it is intended as a short way to express what kind of origin the author assumes (as eolianite, tillite). In case of doubt one can use a petrographic description.

These abnormal properties appear to indicate: (1) a powerful supply forming thick beds and leaving no time for the accumulation of clay, and/or (2) a steep slope producing slides and not allowing the deposition of mud but only of sandy or silty clays, (3) a short distance to the origin, so that the material was not spread out into thin beds covering wide areas, coarse material had not been dropped on the way, and turbidity currents had not succeeded in sorting the materials to produce regular grading, (4) instead of the usual longitudinal supply this material can have been introduced from the side.

In some cases all these conditions may have been combined; in others either one or the other may have predominated. Hence, the abnormal features also vary in distinctness from case to case. In some instances most features are normal, and only one or two of the unusual characteristics occur.

We suggest that the cause for this abnormal type of flysch can be either a deepening of the basin and steepening of the slope, or a quickening of the supply, or a change in position of the supply, for instance the building of a new delta.

But whatever the cause, the mode of transport has changed. Instead of a well-mixed turbulent turbidity current carrying almost the entire load in suspension, one can imagine a turbidity current in which most of the sand and gravel moves in a watery slide along the base. The current is too poor in clay to raise this load in suspension, and the slope is too steep for the load to come to rest until it has spread out in a layer.

A true turbidity current can be likened to a dry avalanche, and a normal slump is the equivalent of a wet avalanche remaining in contact with the ground. We believe that an intermediate type of movement is also possible and suggest that the resulting deposit be called a fluxoturbidite.

Glauconite in Turbidites

Kuenen was kindly shown exposures of the Cretaceous flysch of the Lainbach in Bavaria, by Doctor Zeil who is mapping this area and wishes to reserve his opinion on the nature of these rocks. For geologists who have accepted the hypothesis of turbidity currents there can be little doubt that the flysch in question is

built up mainly of typical turbidites. Within this flysch there occur a few quartzitic beds up to about 1 meter thick that have 20 per cent glauconite and hardly any clay. As they show graded bedding, flute casts, load casts, convolute lamination, and regular bedding alternating with green shale there is a strong case for considering them turbidites. The scarcity of clay and the high percentage of glauconite can be interpreted as evidence for shallow water and winnowing action. Possibly the glauconite is secondary.

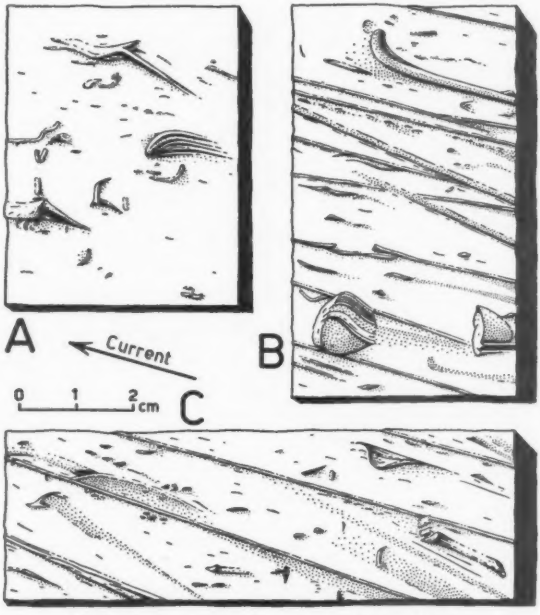

FIGURE 10.—THREE SOLES WITH PROD CASTS
A—Lower Menilite beds; B and C—Beloweza beds

Glauconite in the Pasierbiec and Submagura beds described above is undoubtedly a resedimented constituent of typical turbidites, because Ksiazkiewicz (1954a, p. 443) noted that the glauconite is graded and that its size is roughly similar to that of the surrounding quartz grains. It is even adapted to the horizontal grading noted in the Pasierbiec sandstone beds.

As the percentage of glauconite is no less than 12, it follows that under favorable circumstances a turbidity current can become charged with a significant admixture of this mineral. Although the percentage in the Bavarian rocks is even higher this can no longer be used as argument against resedimentation by turbidity currents. Moreover, low percentages of clay characterize many other obvious turbidites. Thus the features of the Bavarian glauconite beds do not argue against their being turbidites; it would be extremely difficult to account for the emplacement by any other mechanism. Here, as in most cases, no exact figure for the depth can be given other than that the environment was below the reach of wave action and tidal or wind-generated currents.

Sole Markings

GROOVE CASTS: Dzulynski and Radomski (1955) illustrated markings which they attributed to chunks of mud being cast against the bottom by turbidity currents. Kuenen (1957a) later took partial exception to this explanation. The comparatively steep, short scarplets shown in some instances, are evidently due to small faults. The mud pebbles found at their base have presumably been caught in the shelter thus provided and were the result, not the cause, of the grooving. The part played by mud pebbles in scratching the bottom is probably greater than Kuenen allowed. Possibly more

compacted, firmer clay beds have been torn up and incorporated in turbidity currents in certain areas. The higher density would allow such pieces to hit the bottom more easily than soft, low-density mud pebbles. Moreover, the firmer consistency would allow them to retain jagged edges that would scratch the bottom more efficiently than could a soft piece of mud. We suggest that much flysch is derived from the resedimentation of earlier flysch only partly consolidated when it was raised and attacked by erosion and slumping.

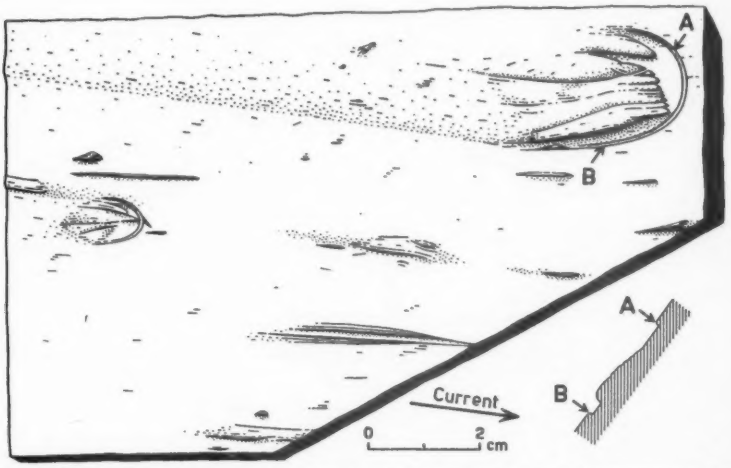

FIGURE 11.—BOUNCE CAST WITH CAST OF A SMALL PLATEAU AT THE DOWNCURRENT END
Krosno beds, Rymanov

Vassoevich (1953) explained groovings as due to sliding of deposited sandstone layers over the muddy bottom and proposed the term "olistoglyphs" for the structures discussed. Later Kuenen (1957a) described this mechanism from experimental slumps.

Slide marks described by Kuenen from soles may also occur within the sandstone beds, provided these latter are composed of two or more distinct layers of sand deposited one upon another without shale intercalation. Such slide marks undoubtedly of sedimentary origin have been found in the Krosno beds and seem to be a common feature within some thick-bedded, composite sandstones.

In a recent paper, Kuenen (1957a) listed a number of sole markings found in many places in turbidite series. A few additional types, one of which is very common in the Carpathian Mountains and probably also elsewhere, are added here:

(1) PROD CASTS: Prod casts, a common kind of sole marking, consist of short ridges, parallel to the current, which deepen gradually downcurrent and end abruptly; in many cases the ridges curve slightly sideways at the downcurrent end (Fig. 10). Other prod casts look as if they had fallen over sideways, when held with the sole upward. Obviously, however, the filled-in hollow cannot have "fallen" upward. The length ranges between a few millimeters and 20 cm. Width and depth are seldom more than 1 cm. Most show parallel striation. They look much like the upcurrent halves of short groove casts. The ridge is a casting of a groove, evidently produced by an object prodding into the soft bottom as it was borne along by the current and then wrenched out again. Therefore the name prod cast is suggested. Presumably the object was oblong and turned over lengthwise or veered around as resistance increased or toppled sideways cutting an oblique furrow like a plough. The object may have been a stick, a fragment of shale, or fish bone, or something similar. In most cases the impactor has disappeared downcurrent, but in rare instances a hard object is found in the end of such a ridge. This need not be the impactor itself, for some foreign object could have been caught in such a groove.

(2) BOUNCE CASTS: From the Carpathian flysch Dzulynski and Radomski (1955) described rather small ridges, on the soles of sandstones, ranging up to 5 cm in length and somewhat less in width and running parallel to the current direction. Wood and Smith (per-

sonal communication) proposed the term "bounce cast" for these features.

These short grooves were presumably produced by objects grazing against the bottom and rebounding, leaving behind a shallow groove fading out gradually at both ends. Longer bounce casts and short groove casts are very similar.

Bounce casts, which fade out gradually at both ends, give only a current lineation. Prod casts provide good current indicators because of the deep downcurrent end. However, they must not be confused with flute casts that have the deep end upcurrent.

A special type of bounce cast is those that have a crescentic depression at one end. This depression is a counterpart of a small arcuate ridge produced by objects brushing against the bottom and heaping the mud in front of them. The crescentic ridge (depression on the soles of sandstones) is developed in the place where the object touching the bottom was lifted again and carried away by the current.

In very rare cases the impact caused a crescentic fault in the mud running around the downcurrent end at a small distance. It divided a plateau with the bounce mark raised 1 mm above the unaffected surface. In the cast it forms a depressed area (Fig. 11).

(3) SKIP CASTS: A third kind of marking shows a linear arrangement like a dashed line in some instances in a long series. This suggests that the object carried by the current touched the bottom many times. We suggest the name "skip cast". The size of these casts is greater in some cases than that of normal bounce or prod casts. They tend to show crescentic depressions.

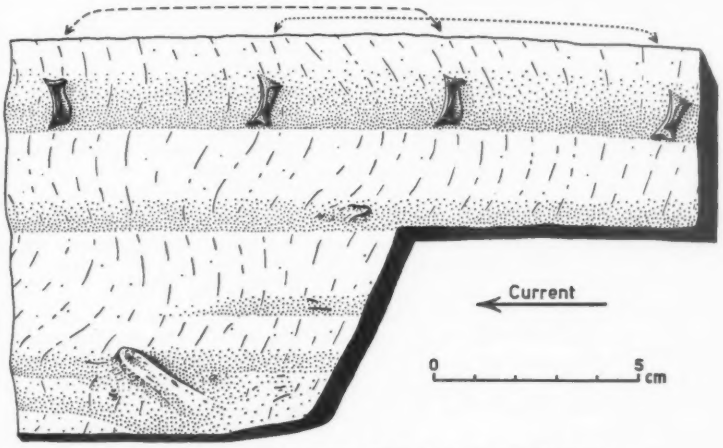

FIGURE 12.—SKIP CAST AND PROD CAST AT THE BOTTOM
The alternate shapes of the skip cast are alike, and the moving object was evidently turning over and over as it went along Krosno beds, Rudowka Rymanowska.

In the Krosno beds many skip casts usually 4–10 cm in length have been found. Possibly the moving object was a tree trunk or some other plant remains.

Some instances of skip casts may have been produced by fishes. They resemble tracks which are attributed to fishes brushing against the bottom. (*See* Abel, 1935, p. 192, Fig. 165.) In most cases the inorganic origin of the casts discussed is beyond doubt. The arrangement of these marks is consistent with other current structures; the casts (Fig. 12) are good current indicators and have been used for this purpose in the Krosno beds by Dzulynski and Slaczka (1958).

(4) CRESCENTIC FLUTE CASTS AROUND SHALE PEBBLES: Rich (1950) remarked on the occurrence among the Silurian sole markings at Aberystwyth of crescentic flutings. Polish geologists have discovered several cases in which a shale pebble remains to show that the origin was correctly inferred by Rich.

SELECTED BIBLIOGRAPHY

Abel, O., 1935, Vorzeitliche Lebensspuren: Jena, Verlag G. Fischer, 644 p.

Birkenmajer, K., 1956, Sedimentary characteristics of the Jarmuta beds (Maestrichtian) in the

Pieniny Klippen belt: Acad. Pol. Sci. Bull., v. 6, p. 730–735

Bukowy, S., 1956, Observations on the sedimentation of the Babica clays: Acad. Pol. Sci. Bull., v. 4, p. 631–635

Carozzi, A., 1955, Nouvelles observations microscopiques sur les dépôts de courants de turbidité du Malm de la Nappe de Morcles en Haute-Savoie: Inst. Natl. Genevois Bull., v. 58, p. 1–31

Crowell, J. C., 1955, Directional-current structures from the Prealpine flysch, Switzerland: Geol. Soc. America Bull., v. 66, p. 1351–1384

Dzulynski, St., and Kinle, St., 1957, Problematic hieroglyphs of probable organic origin from the Beloveza beds: Soc. Géol. Pologne Annales, v. 26, p. 266–269

Dzulynski, St., and Radomski, A., 1955, Origin of groove casts in the light of turbidity current hypothesis: Acta Geol. Polonica, v. 5, p. 47–66

—— 1957, Clastic dikes in the Carpathian flysch: Soc. Géol. Pologne Annales, v. 26, p. 226–263

Dzulynski, St., and Slaczka, A., 1958, Directional structures and sedimentation of the Krosno beds: Soc. Géol. Pologne Annales, v. 28, fasc. 3–4, p. 205–260

Dzulynski, St., Radomski, A., and Slaczka, A., 1957, Sandstone whirl-balls in the silts of the Carpathian flysch: Soc. Géol. Pologne Annales, v. 26, p. 108–124

Haaf, E. ten, 1956, Significance of convolute lamination: Geologie en Mijnbouw, v. 18, p. 188–194

—— 1957, Tectonic utility of oriented resedimentation structures: Geologie en Mijnbouw, v. 19, p. 33–35

—— 1959, Graded beds of the northern Apennines: Univ. Groningen, Thesis, 96 p.

Kopstein, F. P. H. W., 1954, Graded bedding of the Harlech Dome: Univ. Groningen, Thesis, 97 p.

Koszarski, L., 1956, Observations on the sedimentation of the Ciezkowice sandstone near Ciezkowice (Carpathian flysch): Acad. Pol. Sci. Bull., v. 4, p. 393–398

Ksiazkiewicz, M., 1954a, Graded and laminated bedding in the Carpathian flysch: Soc. Géol. Pologne Annales, v. 21, p. 399–449

—— 1954b, Evolution of the Carpathian flysch geosyncline: 19th Int. Geol. Cong. Comptes Rendues, sec. 13, t. 14, p. 9–15

—— 1956, Geology of the Northern Carpathians: Geol. Rundschau, Band 45, p. 370–411

—— 1958a, Sedimentation in the Carpathian flysch sea: Geol. Rundschau, Band 47, p. 418–425

—— 1958b, Stratigraphy of the Magura series in the Sredno Beskid (Carpathians): Inst. Geol. Biul. 135, Warszawa, p. 43–96

Kuenen, Ph.H., 1952, Estimated size of the Grand Banks turbidity current: Am. Jour. Sci., v. 250, p. 874–884

—— 1953a, Significant features of graded bedding: Am. Assoc. Petroleum Geologists Bull., v. 37, p. 1044–1066

—— 1953b, Graded bedding with observations on lower Paleozoic rocks of Britain: K. Nederl. Akad. Wetens. Afd. Natuurk, r. 1, v. 20, 47 p.

Kuenen, Ph.H., 1956a, The difference between sliding and turbidity flow: Deep-sea Research, v. 3, p. 134–139

—— 1956b, Problematic origin of the Naples rocks around Ithaca, N. Y.: Geologie en Mijnbouw, v. 18, p. 277–283

—— 1957a, Sole markings of graded graywacke beds: Jour. Geology, v. 65, p. 231–258

—— 1957b, Longitudinal filling of oblong sedimentary basins: K. Nederl. Geol. Mijnb. Gen. Verh., Geol. Ser., v. 18, p. 189–195

—— 1958, Problems concerning source and transportation of flysch sediments: Geologie en Mijnbouw, v. 20, p. 329–339

—— in press, Turbidity currents a major factor in flysch deposition: Ecolog. Geol. Helvetia

Kuenen, Ph.H., and ten Haaf, E., 1956, Graded bedding in limestones: K. Nederl. Akad. Wetens., Proc., Ser. B, v. 59, p. 314–317

Kuenen, Ph.H., and Sanders, J. E., 1956, Sedimentation phenomena in Kulm and Flözleeres graywackes, Sauerland and Oberharz, Germany: Am. Jour. Sci., v. 254, p. 649–671

Kuenen, Ph.H., Faure-Muret, A., Lanteaume, M., et Fallot, P., 1957, Observations sur les flysch des Alpes Maritimes françaises et italiennes: Soc. Géol. de France Bull, Ser. 6, v. 7, p. 11–26

Natland, M. L., and Kuenen, Ph.H., 1951, Sedimentary history of the Ventura Basin, Calif. and the action of turbidity currents: Soc. Econ. Paleontologists and Mineralogists Special Pub. no. 2, p. 76–107

Obuchowicz, Z., 1957, Introductory investigations on the division into horizons of the Krosno beds (Oligocene) of the Central Depression: Serv. Géol. Pologne Bull., v. 116, p. 128

Radomski, A., 1957, Remarks on the sedimentation of the Podhale flysch: Soc. Géol. Pologne Annales, v. 26, p. 132–145

Rich, J. L., 1950, Flow markings, groovings and intrastratal crumplings as criteria for recognition of slope deposits, with illustrations from Silurian rocks of Wales: Am. Assoc. Petroleum Geologists Bull., v. 34, p. 717–741

Swidzinski, H., 1947, Stratigraphical index of the northern flysch Carpathians: Serv. Géol. Pologne Bull., v. 37, p. 1–128

Vassoevich, N. B., 1953, O nekatorych flysevych teksturach (On some structures in the flysch): Trudy Lvovskogo Geol. Obscestv., v. 3, p. 17–85

Wdowiarz, St., 1953, Geology of Grabownica fold (Polish with Russian summary): Serv. Géol. Pologne Bull., v. 120, p. 1–80

Wood, A., and Smith, A. J., 1958, The sedimentation and sedimentary history of Aberystwyth Grits: Geol. Soc. London Quart. Jour., v. 114, p. 163–195

LABORATORY OF GEOLOGY AND POLISH ACADEMY OF SCIENCE, KRAKÓW, POLAND; JAGELLONIAN UNIVERSITY OF KRAKÓW AND GEOLOGICAL SURVEY OF POLAND, KRAKÓW, POLAND; UNIVERSITY OF GRONINGEN, NETHERLANDS

MANUSCRIPT RECEIVED BY THE SECRETARY OF THE SOCIETY, MARCH 17, 1958

Short Notes

BULLETIN OF THE GEOLOGICAL SOCIETY OF AMERICA
VOL. 70, PP. 1119-1126, 2 FIGS. AUGUST 1959

CHEMISTRY OF GRANOPHYRES FROM WICHITA LOPOLITH, OKLAHOMA

BY WARREN HAMILTON

The Wichita Mountains of southwestern Oklahoma expose the upper part of a large lopolith of late Precambrian or Early Cambrian age. A thick sheet of many masses of red granophyre and allied granite and rhyolite overlies gabbro and anorthosite; the red rocks dominate the present exposures. A summary of the field relations and petrography of the Wichita rocks has been published (Hamilton, 1956).

The red rocks of the Wichita lopolith are dominantly granophyres, composed of micrographically intergrown quartz and microperthite. Albite, biotite, hornblende, augite, chlorite, and magnetite are present in generally minor amounts. Subordinate to the granophyres are granites and rhyolites that have the same distinctive mineralogy and have widespread granophyric facies; rocks texturally intermediate between the three types are widespread, and granites, granophyres, and rhyolites are presumably identical chemically.

For new analyses of Wichita granophyres are given in Table 1, together with three analyses published previously. Three of the new analyses are of very leucocratic granophyres, with less than 1–2 per cent of accessory minerals, and the fourth has about 5 per cent of accessory minerals. (Most of the Wichita granophyres are leucocratic, but no analyses were made of the rocks with a higher content of accessory minerals.)

The silicic rocks of the Wichita lopolith are strongly alkaline. Relative to calc-alkaline rocks, they are low in Al_2O_3 and CaO and high in iron. The molecular proportion of Al_2O_3 is about equal to or is less than the total of CaO and alkalis. In only one analysis (Table 1, col. 7) is Al_2O_3 less than the sum of K_2O and Na_2O, and the alkalis in this old analysis by Fairchild look suspiciously high—but uncommon granophyres in the Wichita Mountains, not included in these analyses, carry aegirine or riebeckite, and such rocks are clearly peralkaline.

Microperthite is the sole feldspar in some of the Wichita Mountain rocks, but generally it is accompanied by a little albite in discrete crystals. The albite is microantiperthitic in some rocks. So pervasively clouded is the feldspar that optical identification is difficult, and in one analyzed specimen even the distinction between albite and microperthite could not be made for many grains. The bulk compositions of the feldspars were calculated by subtracting assumed compositions of the modal accessory minerals from the analyses. The resulting calculated feldspars are listed in Table 1 and plotted in Figure 1; as the rocks are leucocratic, errors in assumed accessory-mineral compositions could have little effect on these values. The microperthites carry subequal amounts of albite and orthoclase, and at most a few per cent of anorthite. Three of the four specimens analyzed have surpluses of about half a per cent each of Fe_2O_3 and of Al_2O_3 remaining after this calculation of feldspar and modal accessories.

Burwell (1956, p. 18) listed seven similar analyses of feldspar from granophyres and granites of the Wichita Mountains, and the average of these is given in Table 2. He did not describe methods of separation or mineralogic character of the feldspars, but the subequal Or and Ab and the minor An are clearly indicated. The calculated surpluses of Fe_2O_3 and Al_2O_3 are comparable to those of Table 1.

Although now unmixed in most specimens, the bulk composition of the microperthite suggests initial crystallization in the tolerant sanidine lattice. MacKenzie and Smith (1956) found sanidine cryptoperthite in a number of granophyres, and Smith, MacKenzie, and Emeleus (1957) reported all intermediate forms in the unmixing reactions sanidine → two sanidines (or sanidine plus anorthoclase) → orthoclase-(low) sodic plagioclase → microcline-sodic plagioclase perthite. They believe that the degree of exsolution and reformation reflects primarily the slowness of cooling.

The feldspars are pink to brownish red, clouded by clay(?) and specks of hematite. Examples of the specific distribution of clouding

TABLE 1.—CHEMICAL AND MINERALOGIC COMPOSITION OF GRANOPHYRES FROM WICHITA LOPOLITH, OKLAHOMA

	1	2	3	4	5 av. 1–4	6	7	8	9 av. 1–8
Major-Element Analyses (Weight per cent)									
SiO_2	77.58	71.72	77.24	76.52	75.8	73.61	74.14	76.79	75.4
Al_2O_3	11.75	12.54	11.82	12.10	12.1	11.97.	12.97	12.35	12.2
Fe_2O_3	.90	2.63	1.33	.99	1.5	2.34	1.07	0.90	1.5
FeO	.07	1.51	.17	.45	.5	1.51	1.20	0.43	0.8
MgO	.06	.53	.11	.14	.2	.19	tr.	0.03	0.15
CaO	.29	1.25	.11	.40	.5	1.38	.48	0.51	0.6
Na_2O	3.34	3.87	3.43	3.60	3.6	3.76	4.61	4.23	3.9
K_2O	5.32	4.24	5.16	5.03	4.9	4.32	5.30	4.31	4.8
H_2O-	.07	.21	.06	.07	.1	.32	.12	0.04	0.1
H_2O+	.20	.35	.14	.11	.2	.35	.19	0.15	0.2
TiO_2	.14	.49	.15	.14	.2	.46	.25	0.08	0.2
CO_2	.03	.04	.02	.03	.03	—	—	—	0.03
P_2O_5	.01	.09	.02	.02	.03	.15	tr.	0.00	0.04
MnO	.01	.10	.03	.03	.04	.09	.03	0.01	0.04
	99.77	99.57	99.79	99.63		100.51	100.36	99.83	
Minor-Element Analyses (Weight per cent)									
Ba	0.007	0.15	0.07	0.07	....	*with* 0.04 (BaO)	....	...	...
Be	.0007	.0003	.0003	.0003	0.0004	.....			
Ce	.03	.03	.03	.03	.03				
Co	<.0005	.0005	<.0005	<.0005	<.0005				
Cr	.0001	.00015	.0001	.0001	.0001				
Cu	.0003	.0007	.0003	.0007	.0005				
Ga	.003	.0015	.0015	.003	.002				
La	.015	.015	.015	.015	.015				
Mo	<.0005	.0005	<.0005	<.0005	<.0005				
Nb	.007	.007	.007	.007	.007				
Nd	.015	.015	.015	.015	.015				
Pb	.0015	.0015	.0015	.0015	.0015				
Sc	<.0005	.0007	<.0005	<.0005	<.0005				
Sn	<.001	.001	.0015	<.001	.001?				
Sr	.0003	.015	.0015	.0015	.005	0.02 (SrO)			
V	<.001	.001	<.001	<.001	<.001				
Y	.007	.007	.007	.007	.007				
Yb	.0015	.0015	.0007	.0007	.001				
Zr	.03	.07	.03	.015	.03				

(*Table continued on page* 1122)

Explanation of Table 1

Columns 1–4, new analyses by V. C. Smith, supervised by Lee C. Peck (major oxides); and by J. C. Hamilton (minor elements), both of U. S. Geological Survey, Denver, 1958. Minor elements not listed are present only in amounts below threshold sensitivity of semiquantitative spectrographic analyses, which are made by the rapid visual-comparison method; the same logarithmic-third class intervals would probably be assigned in about 60 per cent of the cases by quantitative methods.

1. Pale-red (10 R 6/3) granophyre, with .5–1 mm bipyramids of quartz and a few phenocrysts of microperthite in finely micrographic quartz and microperthite. The orthoclase phase of the microperthite is uniformly darkly cloudy. Quartz is clear and unstrained; micrographic elements are rods from <0.01 mm to 0.5 mm in diameter. The 0.5-mm anhedra of fluorite are intergrown with leucoxene and magnetite, the latter considerably altered to hematite. Hilltop outcrop 2.35 miles N. 25° E. from highway intersection at southwest corner of Cache; for photomicrograph, *see* Hamilton (1956, Pl. 1, fig. 5). Bulk specific gravity 2.54. Field no. WM-1; lab. no. D-1510.

2. Pale reddish-brown (10 R 5/4) granophyre, with big (to 5 mm) euhedral phenocrysts of microperthite and albite in a groundmass that is partly aplitic and partly micrographic. Little quartz is apparent without use of a hand lens. Most of the feldspar of both phenocrysts and micropegmatite is darkly clouded, but much is only partly clouded; clouding may be anywhere: cores, rings, rims, or ends in phenocrysts, or blotches. Some phenocrysts have dark subhedral rings between clear rims and irregularly clouded cores. Of the feldspar, about one-sixth is identifiable as albite, partly with chessboard texture, and one-quarter as microperthite; the remainder is too altered to permit recognition. Quartz forms tiny bipyramids but is mostly in micrographic intergrowths. Thin quartz stringers and blebs cut some of the feldspars. The anhedral magnetite and hornblende (green, $Z \wedge c \sim 20°$, $-2V \sim 80°$) are in granular aggregates, and many of the individual hornblende crystals contain cores of augite made partly opaque by leucoxene. Broken rock, southwest part of summit of Mt. Scott; for photomicrograph, *see* Hamilton (1956, Pl. 2, fig. 1). Bulk specific gravity 2.65. Field no. WM-9; lab. no. D-1511.

3. Light reddish-orange (10 R 7/6) granophyre, with both the 2-mm euhedral feldspars and the 1-mm quartz bipyramids rimmed and surrounded by micropegmatite. The host-feldspar phase is much more clouded than the exsolved phase in both the dominant microperthite and the subordinate albite-antiperthite. Some big feldspars are of soda-orthoclase ($2V \sim 90°$), little altered or exsolved. Baveno and Manebach twins are common in all three types of feldspar. The cloudy alteration of the feldspar is very irregular and in the uniform soda-orthoclase crystals is nearly restricted to the local areas of microperthite. The quartz bipyramids, unlike the feldspar phenocrysts, are slightly corroded. The green biotite is partly chloritized and occurs variously as tiny granules aggregated with magnetite, as thick ragged 0.1-mm anhedra, and as isolated tiny flakes. The 0.1-mm granules of magnetite are mostly clustered, and many have hematitic rims. Hematite also occurs as thin seams and as the lining of the numerous tiny cavities. Highway cut, 0.7 mile south of Lugert (the host granophyre, not the granite dike at this locality); for photomicrograph, *see* Hamilton (1956, Pl. 2, fig. 2). Bulk specific gravity 2.56. Field no. WM-24A; lab. no. D-1512.

4. Dark orange-pink (10 R 6/4) granophyre, with 3-mm euhedral feldspars rimmed and surrounded by micropegmatite. Some of the discrete crystals of albite are intergrown with the phenocrysts, and some are in micropegmatite. The potassic phase of the microperthite is mostly orthoclase, but locally microcline; as the albite is grid-twinned and both feldspars are clouded, microcline and albite may have been confused in part. The micropegmatitic quartz rods are mostly rounded, giving an unusual granular appearance to the intergrowths. Feldspar phenocrysts are clouded only along poorly defined zones, generally not parallel to cleavages; the micropegmatitic feldspar is much but variably clouded. The quartz phenocrysts are rounded equants, probably resorbed bipyramids, and some of these contain zigzag zones strewn with minute prisms of green amphibole(?). The biotite is of two types, occurring separately: unaltered olive-gray anhedra, and dark-green greatly altered poikilitic grains with rims and interlaminae of magnetite and hematite. The numerous relatively large stubby prisms of zircon are aggregated with the granular magnetite. Road cut, west side of Altus Reservoir, just north of Quartz Mountain State Park picnic area. Bulk specific gravity 2.59. Field no. WM-26; lab. no. D-1513.

5. Average of 1–4

6. Granophyre, west of Mt. Sheridan, quoted from Taylor (1915, p. 21). Analysis by George Steiger.

7. Granite or granophyre, from within a few miles of town of Granite, quoted from Taylor (1915, p. 21). Analysis by J. G. Fairchild. The alkalis appear to be too high in this analysis.

8. Granophyre, 9 miles east of Lugert, quoted from Merritt (1958, p. 43). Analysis by D. Thaemlitz, Univ. of Minnesota.

9. Average of 1–4 and 6–8

TABLE 1—*Continued*

	1	2	3	4	5 av. 1–4	6	7	8	9 av. 1–8
				Modes (Volume per cent)					
Quartz	38.5	35.2	38.2	35.0	37				
Microperthite	60.7	59.2	54.8	61.3	61				
Albite	....		5.7	2.0					
Biotite	tr.	.....	.5	1.0					
Hornblende		2.0	....	tr.	1				
Augite		1.1		....					
Magnetite + ilmenite + hematite	.3	1.8	.5	.7	1				
Sphene + leucoxene	.2	.3	tr.						
Fluorite	.2	tr.		tr.					
Zircon	tr.	tr.	tr.	tr.					
Apatite	tr.	tr.	tr.	tr.					
Muscovite		tr.							
Chlorite		.2	.2						
Calcite		tr.							
Epidote		tr.							
				Calculated Relationships					
Molecular proportions relative to (CaO + Na_2O + K_2O) = 100									
CaO	4.5	17.2	1.8	6.0	8	18.7	6.2	7.4	8.6
Na_2O	46.6	48.2	49.3	49.0	48	46.3	53.4	55.4	50.5
K_2O	48.9	34.7	48.8	45.0	44	35.0	40.4	37.2	40.9
Al_2O_3	99.8	94.8	103.5	100.1	99	89.5	91.4	98.3	96.1
Calculated bulk feldspar composition, after allowance for modal accessories, in weight per cent									
An	0	3.9	0.2	2.4	2				
Ab	47.2	54.0	48.6	49.7	50				
Or	52.8	42.1	51.2	47.9	48				
Surplus after chemical calculations of modal minerals, in weight per cent									
Al_2O_3	+0.6	+0.6	+0.4	+0.1	+0.4				
Fe_2O_3	+0.5	+0.6	+0.5	0	+0.4				

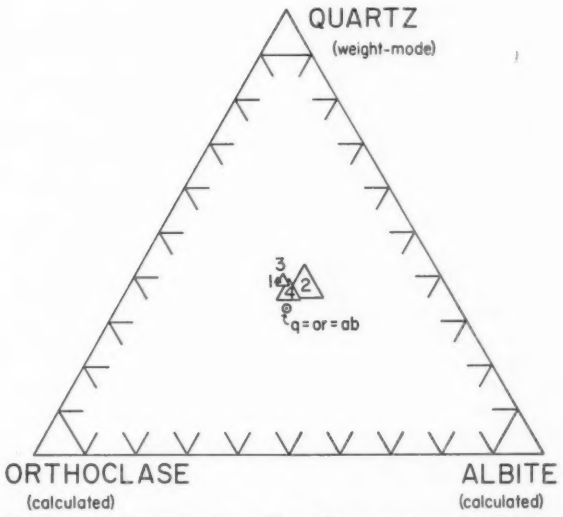

FIGURE 1.—MINERALOGIC COMPOSITION OF FOUR GRANOPHYRES FROM WICHITA LOPOLITH
Sizes of small triangles indicate totals of all other minerals. Numbers refer to columns of Table 1.

TABLE 2.—COMPOSITION OF FELDSPAR FROM RED ROCKS OF WICHITA LOPOLITH

	1	2		3
SiO_2	66.7	2.4	Ab	51.9
Al_2O_3	19.0	0.4	Or	45.5
Iron as Fe_2O_3	0.7	0.7	An	2.6
MgO	0.1	0.1		
CaO	0.5			100.0
Na_2O	5.9			
K_2O	7.3			
H_2O	0.1	0.1		
TiO_2	0.1	0.1		
	100.4	4.6		

1. Average of seven similar analyses by T. E. Hamm, from Burwell (1956, p. 18).

2. Excesses remaining after calculation of theoretical feldspars of column 3.

3. Ideal feldspar composition calculated by allotting all CaO, Na_2O, and K_2O of column 1 to feldspar; in weight per cent.

material are given in the descriptions of Table 1; it is pervasive in some rocks but variably distributed in others. Host-phase feldspar is much more clouded than the exsolved phase, and much of the nonperthitic feldspar (soda-orthoclase or albite) is unclouded. The clouded areas make blotchy patterns, or crudely oriented zones *not* parallel to cleavage, or zones (cores, rims, rings, often subhedral) with all degrees of sharpness within feldspars. Quartz is not clouded. This distribution suggests that much of the clouding matter formed before exsolution of microperthite, and that the hematite may represent ferric iron, variably migrated, initially within the feldspar lattice in the normal position of aluminum. The alteration to clay(?) must have been accompanied by selective removal of alkalis, so that primary alkali:alumina ratios would have been higher than the present ones.

Semiquantitative spectrographic minor-element analyses are also listed in Table 1. Some of the elements reported show variations that are probably significant when the three analyses of very leucocratic granophyres (1, 3, 4) are compared with the more mafic, although still leucocratic, rock (2). Strontium appears to vary, as expected, with calcium, although the amounts reported are surprisingly low. Cobalt, chromium, molybdenum, scandium, tin(?), vanadium, and, oddly, zirconium appear to vary with dark-mineral content, but the data are inconclusive.

Lithium, rubidium, and cesium are among the trace elements not detectable by semiquantitative methods in the Wichita granophyres. Horstman (1957, p. 24) analyzed 12 samples of

Wichita Mountains rocks—about half of them granophyres?—for Rb and Cs, and several of these for Li. He found a nearly constant K/Rb ratio of about 220, with amounts of Rb of 0.01–0.02 per cent. Most of the samples had Cs in less than threshold (0.0002 per cent) amounts, but several had about 0.001 per cent. Lithium values found were 0.001–0.005 per cent.

G. R. Tilton and coworkers have made many absolute-age determinations of Wichita Mountains rocks by lead, uranium, and thorium isotope ratios of zircons (from the same pegmatites as those analyzed previously by the Larsen lead-alpha method: Larsen, Waring, and Berman, 1953) and by potassium-argon and strontium-rubidium ratios in biotite in granophyre (from near the locality of specimen 4 of this paper). These many determinations indicate an age of about 520 ± 30 million years (Tilton, Davis, Wetherill, and Aldrich, 1957, p. 364), or very late Precambrian or Early Cambrian. All determinations are within the range 480–550 million years. In the north part of the Wichita Mountains, Upper Cambrian sedimentary rocks rest on granophyric rhyolite; anorthosite and overlying granophyre are brought up against these rocks from the south on later Paleozoic faults. The rhyolites may represent the little eroded upper crust of the complex, and the lopolith may be of extrusive rather than intrusive origin.

The granophyres of the Wichita lopolith are similar to those of other big lopoliths and are strikingly unlike calc-alkaline granites and rhyolites in composition (Fig. 2). The lopolithic rocks have high iron and low CaO and Al_2O_3, and are mostly clustered within a narrow compositional range. Another paper will discuss these and other group characteristics of the silicic differentiates of lopoliths and will present evidence that strongly reinforces the conclusion of R. A. Daly that lopoliths are extrusive complexes.

In my 1956 paper, I emphasized the complete dissimilarity in petrology and mode of formation between the "granites" of the Wichita and Arbuckle Mountains, 90 miles apart. The Wichita rocks are the granophyres of the cap of a lopolith; the Arbuckle rocks are calc-alkaline quartz diorites to granites of a composite batholith. So entrenched is the notion that the rocks of these two areas are chronologically and tectonically correlative that it continues to appear in print. Accordingly, I call attention to the strontium-rubidium age determination published recently by Davis, Tilton, Aldrich, and Wetherill (1958, p. 180) of 1360 million years for biotite from the Arbuckle Mountains. This is considerably older than the 940-million-years lead-alpha determination reported in my 1956 paper, made on a specimen probably from the same locality but certainly indicates the complete dissociation between the Wichita and Arbuckle basement provinces.

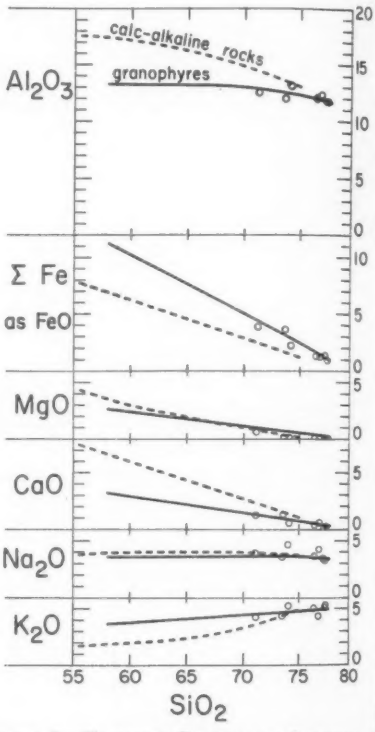

FIGURE 2.—VARIATION DIAGRAM OF ANALYSES OF GRANOPHYRE AND GRANITE FROM WICHITA LOPOLITH

Solid lines illustrate general trends in granophyres and allied silicic differentiates of Wichita, Duluth, Sudbury, and Bushveld lopoliths. Dashed lines illustrate trends in calc-alkaline volcanic rocks of Aleutian Islands (Quaternary), volcanic rocks of San Juan Mountains, Colorado (Tertiary), and batholithic granitic rocks of western United States (Mesozoic).

References Cited

Burwell, A. L., 1956, Potash agstone from Oklahoma: Okla. Geol. Notes, v. 16, p. 12–23

Davis, G. L., Tilton, G. R., Aldrich, L. T., and Wetherill, G. W., 1958, The age of rocks and minerals: Carnegie Inst. Washington Year Book no. 57, p. 176–181

Hamilton, Warren, 1956, Precambrian rocks of Wichita and Arbuckle Mountains, Oklahoma: Geol. Soc. America Bull., v. 67, p. 1319–1330

Horstman, E. L., 1957, The distribution of lithium, rubidium, and caesium in igneous and sedimentary rocks: Geochim. Cosmochim. Acta, v. 12, p. 1–28

Larsen, E. S., Jr., Waring, C. L., and Berman, Joseph, 1953, Zoned zircon from Oklahoma: Am. Mineralogist, v. 38, p. 1118–1125

MacKenzie, W. S., and Smith, J. V., 1956, Alkali feldspars in igneous rocks: Carnegie Inst. Washington Year Book no. 55, p. 195

Merritt, C. A., 1958, Igneous geology of the Lake Altus area, Oklahoma: Okla. Geol. Survey Bull. 76, 70 p.

Smith, J. V., MacKenzie, W. S., and Emeleus, C. H., 1957, Variation of alkali feldspars in igneous rocks (Abstract): Geol. Soc. America Bull., v. 68, p. 1796–1797

Taylor, C. H., 1915, Granites of Oklahoma: Okla. Geol. Survey Bull. 20, 108 p.

Tilton, G. R., Davis, G. L., Wetherill, G. W., and Aldrich, L. T., 1957, Isotopic ages of zircon from granites and pegmatities: Am. Geophys. Union Trans. v. 38, p. 360–371

U. S. Geological Survey, Federal Center, Denver, Colorado

Manuscript Received by the Secretary of the Society, February 28, 1959

Publication Authorized by the Director, U. S. Geological Survey